ISTANBUL TECHNICAL UNIVERSITY ★ GRADUATE SCHOOL OF SCIENCE ENGINEERING AND TECHNOLOGY

THE PRODUCTION OF QUALITY FUELS FROM THE CO-COMBUSTION OF ORIGINAL, PYROLYSED LIGNITE AND TORREFIED, PYROLYSED, ORIGINAL BIOMASS BLENDS

M.Sc. THESIS

Ayşen ÇALIŞKAN SARIKAYA

Department of Chemical Engineering

Chemical Engineering Programme

DECEMBER 2017

ISTANBUL TECHNICAL UNIVERSITY ★ GRADUATE SCHOOL OF SCIENCE ENGINEERING AND TECHNOLOGY

THE PRODUCTION OF QUALITY FUELS FROM THE CO-COMBUSTION OF ORIGINAL, PYROLYSED LIGNITE AND TORREFIED, PYROLYSED, ORIGINAL BIOMASS BLENDS

M.Sc. THESIS

Ayşen ÇALIŞKAN SARIKAYA
(506141028)

Department of Chemical Engineering

Chemical Engineering Programme

Thesis Advisor: Prof. Dr. Hanzade HAYKIRI-AÇMA

DECEMBER 2017

ISTANBUL TEKNİK ÜNİVERSİTESİ ★ FEN BİLİMLERİ ENSTİTÜSÜ

ORİJİNAL, PİROLİZ EDİLMİŞ LİNYİTLER İLE ORİJİNAL, TOREFİYE VE PİROLİZ EDİLMİŞ BİYOKÜTLE KARIŞIMLARININ BİRLİKTE YAKILMASI İLE KALİTELİ YAKIT ÜRETİMİ

YÜKSEK LİSANS TEZİ

Ayşen ÇALIŞKAN SARIKAYA
(506141028)

Kimya Mühendisliği Anabilim Dalı

Kimya Mühendisliği Programı

Tez Danışmanı: Prof. Dr. Hanzade HAYKIRI-AÇMA

ARALIK 2017

Ayşen ÇALIŞKAN SARIKAYA, a M.Sc. student of İTU Graduate School of Science Engineering and Technology student ID 506141028 successfully defended the thesis/dissertation entitled "THE PRODUCTION OF QUALITY FUELS FROM THE CO-COMBUSTION OF ORIGINAL, PYROLYSED LIGNITE AND TORREFIED, PYROLYSED, ORIGINAL BIOMASS BLENDS", which she prepared after fulfilling the requirements specified in the associated legislations, before the jury whose signatures are below.

Thesis Advisor :	**Prof. Dr. Name SURNAME** İstanbul Technical University	.....
Jury Members :	**Prof. Dr. Name SURNAME** Istanbul Technical University	.....
	Prof. Dr. Name SURNAME ..... University	.....
	Prof. Dr. Name SURNAME ..... University	.....

Date of Submission : 17 November 2017
Date of Defense : 13 December 2017

To my spouse and parents,

FOREWORD

I would like to express my special thanks to my advisor Prof. Hanzade AÇMA, for all her support, guidance and encouragement with her vast and valuable knowledge at every stage of this study. Her enthusiasm and tenacity has left a deep impression on me. During my study she always motivated me to do my best and assisted me with a full patience all the time when I needed.

My appreciation also goes to Prof. Serdar YAMAN for his supports and Ayşen AKTÜRK for her helps throughout the analyses.

Finally, I express my deepest appreciation to my beloved spouse Rıza Anıl SARIKAYA and my parents for their endless love and support.

November 2017

Ayşen ÇALIŞKAN SARIKAYA
(Chemical Engineer)

TABLE OF CONTENTS

Page

ABBREVIATIONS

AS	**:** Australian Standards
ASTM	**:** American Society for Testing and Materials
B/D	**:** Borchardt and Daniels
BS	**:** British Standards
DSC	**:** Differential scanning calorimetry
DTA	**:** Differential thermal analysis
DTG	**:** Differential thermogravimetric
GHG	**:** Greenhouse gas
HGI	**:** Hardgrove grindability index
IGCC	**:** Integrated gasification combined cycle
ISO	**:** International Organization for Standardization
OECD	**:** The Organisation for Economic Co-operation and Development
PTFE	**:** Polytetrafluoroethylene
SEM	**:** Scanning electron microscopy
TGA	**:** Thermogravimetric analysis
UK	**:** United Kingdom
UNFCCC	**:** United Nations Framework Convention on Climate Change
US	**:** United States
USA	**:** United States of America

SYMBOLS

°C	**:** Celcius
°F	**:** Fahrenheit
µm	**:** Micrometer
Btu	**:** British Thermal Unit
cal	**:** Calory
cm	**:** Centimeters
Ea	**:** Activation energy
g	**:** Grams
GW	**:** Gigawatts
ha	**:** Hectar
in	**:** Inches
J	**:** Joule
K	**:** Kelvin
k	**:** Specific rate constant
kcal	**:** Kilo calory
kg	**:** Kilogram
Ktoe	**:** Kiloton of oil equivalent
lb	**:** Pounds
min.	**:** Minutes
mL	**:** Mililiter
mm	**:** Milimeter
MPa	**:** Megapascal
Mt	**:** Million tonnes
Mtce	**:** Million tonnes of coal equivalent
$MtCO_2e$	**:** Million tonnes of CO_2 equivalent
MTEP	**:** Million tonnes of equivalent petrol
MW	**:** Megawatts
MWe	**:** Megawatts electric
MWth	**:** Megawatts thermal
n	**:** Reaction order

ϕ **:** Stoichiometric factor

R **:** Universal gas constant

s **:** Second

T **:** Temperature

t **:** Time

TEP **:** Tonnes of equivalent petrol

wt% **:** Weight percent

Z **:** Pre-exponential factor

α **:** Fractional conversion

LIST OF TABLES

Page

LIST OF FIGURES

Page

THE PRODUCTION OF QUALITY FUELS FROM THE CO-COMBUSTION OF ORIGINAL, PYROLYSED LIGNITE AND TORREFIED, PYROLYSED, ORIGINAL BIOMASS BLENDS

SUMMARY

Rapid increase in global greenhouse gas emissions (GHG) that is particularly produced by fossil fuel consumption has alarmed the world to focus on renewable energy sources and developing technologies that cause nearly zero emission. With 459 $MtCO_2e$ in 2013, Turkey is one of the top emitting countries in Europe due to the fact that the country's energy demand is increasing in parallel with population growth and industrialization. Turkey is almost lack of oil and large natural gas reserves and therefore depends on foreign energy sources. In order to decrease the share of imported resources in energy generation, strategies for securing energy supply and sustainable development were settled. Since the lignite coal is the major national fuel resource in Turkey, consumption of domestic coal was pointed out as the main goal by Turkish Energy Ministry and supported by government incentives.

Co-combustion of coal and biomass renders possible utilization of Turkish lignites. Since Turkey is rich in young lignite deposits of which calorific value is quite low for an efficient and sustainable energy production, biomass addition to lignite has been marked as a reasonable solution to decrease foreign energy dependency of the country by increasing national primary energy production. Moreover, regarding to environmental concerns for increasing GHG emissions, co-combustion of biomass and lignite blends seems reasonable to prevent over-consumption of coal and diminish pollutant emissions thanks to the carbon neutral nature of biomass.

Biomass addition to coal prior to burning has many justifiable reasons. Ash deposition and fouling on hot surfaces are commonly encountered problems when biomass is combusted alone and can be eliminated or decreased by co-firing of biomass/coal blends. Furthermore, emitted CO_2 by burning of biomass is captured during photosynthesis that prevents greenhouse effect thanks to the fixation of atmospheric CO_2. Many types of biomass species contain alkaline and alkaline earth elements in their composition that enable to capture released SO_2 from combustion of coal, rich by sulfur content. On the other hand, undesirable effects of potassium that is one of the important element in most biomass materials, can be diminished as potassium reacts with sulfur coming from coal in the blend.

Agricultural potential of Turkey that can be used as renewable energy source is substantial and has to be benefited due to its numerous advantages. According to the studies carried out by Forest and Water Affairs Ministry in 2002 to determine Turkey's biomass potential, Rhododendron was indicated as one of the suitable biomass species that can be used for energetic purposes. Hybrid poplar and ash-tree are also two of the most rapid growing woody biomass species along with their high economic value. Hence, these biomass materials were selected in this study to blend

with Afsin-Elbistan (AE), Adıyaman-Gölbaşı (AG) and Çorum-Dodurga (CD) lignites which are used in many lignite-fired power stations in Turkey. Particularly, AE lignite is the most important domestic primary energy source in Turkey with a reserve of 3.4 billion metric tonnes. Since these lignites have low fixed carbon, low calorific value, high ash and sulfur contents, combustion of lignite leads to serious problems that are needed to be handled. Thus, blending of low rank coal and energetically important biomass materials for co-combustion processes enables to compensate undesirable characteristics of both biomass and lignites.

In order to improve fuel characteristics of coal and biomass, thermochemical conversion methods such as pyrolysis, carbonization, gasification and liquefaction are applied. The aim of this study is to produce high quality fuel from co-combustion of the blends made of original, pyrolysed lignite samples and original, torrefied, pyrolysed biomass samples. Since understanding of the physical and chemical structure of lignite coal and biomass during thermal processes is essential for the design purposes and optimization of present conversion systems, burning test of the blends were performed using a thermogravimetric analyzer up to 900°C with a heating rate of 40°C/min under dry air atmosphere. Burning characteristics of the parent and blend fuels were determined from the TGA, DTG, DTA and DSC profiles obtained as an output of the thermal analyses experiments. Torrefaction of biomass samples at 200°C and pyrolysis of both biomass and lignite samples at 400°C and 750°C, respectively were carried out in the horizontal tube furnace under nitrogen atmosphere to prepare different types of blends that contain 10 wt% biomass and 90 wt% lignite. Proximate and ultimate analyses, calorific value measurements and SEM analyses were applied to parent fuels only excluding thermal analyses which was conducted for both parent and blend fuels in order to assess the co-combustion behavior of the blends and determine synergistic effects between biomass and lignites.

Moreover, in order to obtain a deep information about the thermal decompositions and burning processes of the parent and blend fuels, kinetic study was carried out by applying the Borchardt & Daniels (B&D) kinetic analysis method. Kinetics parameters such as reaction order, heat of reaction, activation energy, and pre-exponential factor were calculated from the data obtained during a single linear heating rate scan and results were discussed.

ORİJİNAL, PİROLİZ EDİLMİŞ LİNYİTLER İLE ORİJİNAL, TOREFİYE VE PİROLİZ EDİLMİŞ BİYOKÜTLE KARIŞIMLARININ BİRLİKTE YAKILMASI İLE KALİTELİ YAKIT ÜRETİMİ

ÖZET

Çoğunlukla fosil yakıtlar tarafından üretilen sera gazlarının salınımındaki hızlı artış, dünyayı alarma geçirerek yenilenebilir enerji kaynaklarına ve neredeyse sıfır emisyon sağlayan gelişen teknolojilere odaklanmaya itmiştir. 459 $MtCO_2e$ düzeyindeki salınım miktarıyla Türkiye Avrupa'nın en çok sera gazı üreten ülkelerinden biridir. Bu rakamın arkasındaki en büyük sebep hızla gelişen nüfus ve endüstrileşmeyle ortaya çıkan enerji talebidir. Türkiye, milli petrol ve doğalgaz rezervlerine sahip olmamasından dolayı enerjide dışa bağımlı bir durumdadır. 2013 yılı verilerine göre Türkiye'nin yerli enerji üretimi toplam birincil enerji arzının yalnızca %26.5'ini karşılamakta olup enerji ihtiyacının %72.3'ü ithal yakıtlardan karşılanmaktadır. Enerji üretiminde kullanılan ithal kaynakların payını azaltmak için enerji arzını koruyacak stratejilere ve sürdürülebilir gelişmeye yatırım yapılmalıdır. Linyit kömürünün Türkiye'nin en büyük yerli enerji kaynağı olmasına rağmen enerji üretimindeki payı %38'dir. Bu nedenle, yerli kömürün kullanımı Türkiye Cumhuriyeti Enerji ve Tabii Kaynaklar Bakanlığı tarafından bir numaralı hedef olarak belirlenmiş ve hükümet tarafından desteklenmektedir.

Kömür ve biyokütlelerin birlikte yakılması Türkiye linyitlerinin değerlendirilmesini sağlamaktadır. Türkiye'nin verimli ve sürdürülebilir enerji üretimi için çok yetersiz kalorifik değere sahip genç linyit yatakları bakımından zengin olmasından dolayı, linyitin biyokütle ile karıştırılarak yakılmasının yerli birincil enerji üretimini arttırarak ülkenin enerjide dışa bağımlılığının giderilmesi için uygun bir çözüm olduğu düşünülmektedir. İlaveten, sera gazı emisyonlarının yol açacağı çevresel sıkıntılar göz önünde bulundurulduğunda, linyit ve biyokütle karışımlarının birlikte yakılması ile aşırı linyit kullanımını azaltması ve biyokütlenin sıfır karbon doğası gereği emisyonları azaltması sebebiyle bu önerinin uygun olacağı düşünülmektedir. Sera gazı salınımını azaltmaya yönelik yapılan çalışmalar, elektrik üretiminin sadece %1'inin biyokütleden sağlanmasıyla yılda 60 Mt CO_2 gazı salınımının önlenebileceğini göstermektedir.

Kömürün biyokütle ile karıştırılarak termik santrallerde yakılmasının pek çok açıklanabilir sebebi bulunmaktadır. Biyokütlenin yalnız yakılması sırasında sıkça gözlemlenen kül birikimi ve sıcak yüzeylerdeki aşınma biyokütle/kömür karışımlarının beraber yakılmasıyla ortadan kaldırılabilir veya en azından azaltılabilir. Ayrıca, bu yöntem ile biyokütlenin yanması sırasında ortaya çıkan CO_2, fotosentez ile tekrar yakalanarak sera etkisi giderilmektedir. Birçok biyokütle tipi içerdiği çeşitli alkali ve toprak alkali elementler ile kükürtçe zengin kömürün yanması sırasında ortaya çıkan SO_2'nin tutulmasına olanak sağlar. Aynı zamanda, biyokütle bünyesindeki önemli bir element olan potasyumun istenmeyen etkilerinin

giderilmesi, potasyumun kömürden gelen kükürt ile reaksiyona girmesiyle azaltılmaktadır.

Türkiye'nin yenilenebilir enerji kaynağı olarak kullanılabilecek potansiyel zirai alanları çok fazla olduğundan, bu alanlardan barındırdığı pek çok avantaj nedeniyle olabildiğince yararlanmak gerekmektedir. Türkiye'nin biyokütle potansiyeli yaklaşık olarak 8,6 milyon tona eşdeğer petrol (MTEP) ve var olan biyokütlelerden elde edilebilecek biyogazın miktarı 1,5-2 MTEP olarak bilinmektedir. Türkiye Cumhuriyeti Orman ve Su İşleri Bakanlığı tarafından 2002 yılında Türkiye'nin biyokütle potansiyelinin belirlenmesi için yapılan çalışmada orman gülü, enerji çalışmaları için en uygun biyokütlelerden biri olarak seçilmiştir. Aynı zamanda melez kavak ve dişbudak ağaçları da yüksek ekonomik değerlerinin yanı sıra en hızlı büyüyen iki biyokütle türüdür. Bu sebeple bahsedilen bu biyokütleler bu çalışma kapsamında, Türkiye'deki bir çok enerji santralinde kullanılan Afşin-Elbistan (AE), Adıyaman-Gölbaşı (AG) ve Çorum-Dodurga (CD) linyitleri ile karıştırılmak üzere seçilmiştir.

Özellikle AE linyiti, 3.4 milyar tonluk rezervi ile Türkiye'nin en önemli yerli birincil enerji kaynağıdır. Bu linyitlerin yakılması; düşük sabit karbon, düşük kalorifik değer, yüksek kül miktarı ve yüksek kükürt miktarı sebebiyle giderilmesi gereken pek çok soruna yol açmaktadır. Sonuç olarak, düşük kaliteli linyit kömürleri ile yenilenebilir enerji kaynağı olan biyokütlelerin belli oranlarda karıştırılarak birlikte yakılması, her iki yakıtın da istenmeyen karakteristiklerinin giderilmesini sağlamaktadır. Kömür ve biyokütlenin yakıt özelliklerini iyileştirmek için; piroliz, koklaştırma, gazlaştırma ve sıvılaştırma gibi termokimyasal dönüşüm metotları uygulanmaktadır.

Biyokütlenin torefiye edilmesi, nem kaybı sebebiyle biyokütlede kütle kaybına yol açmakta ve buna bağlı olarak da kalorifik değerinde artış sağlamaktadır. Genel olarak, başlangıçtaki toplam enerji miktarının %90'ını içeren, %70'lik kısım torefiye edilen üründe kalmaktadır. Bu sayede biyokütlenin enerji yoğunluğu artmakta, bu da ürünün uzak mesafelere taşınmasını avantaja çevirmektedir.

Piroliz, oksijen yokluğunda, katı yakıtın termal bozunmasıyla karbonlu katılar, katran, metan, hidrojen, karbon monoksit ve karbon dioksit gibi kalıcı gazlar oluşturan termokimyasal dönüşüm prosesidir.

Bu çalışmanın amacı, orijinal ve piroliz edilmiş linyit numuneleri ile orijinal, torefiye ve piroliz edilmiş biyokütle numunelerinin birlikte yakılması ile yüksek kaliteli yakıt elde etmektir. Tasarım ve var olan dönüşüm sistemlerini optimize etmek amacıyla uygulanan termal prosesler sırasında kullanılan linyit ve biyokütlenin fiziksel ve kimyasal yapısının anlaşılması önem arz etmektedir. Bu nedenle, çalışmada kullanılan tüm ana yakıtlar ile karışımların termogravimetrik analiz cihazında yanma testleri yapılmıştır. Yanma testleri kuru hava atmosferi altında ortam sıcaklığından 900°C sıcaklığa kadar 40°C/dak ısıtma hızı ile çıkılarak yürütülmüştür.

Yanma testleri sonucunda elde edilen TGA, DTG, DTA ve DSC profilleri esas alınarak, orijinal, piroliz edilmiş kömür ve orijinal, torefiye, piroliz edilmiş biyokütle örneklerinden oluşan ana yakıtlar ile bunların karışımlarının yanma karakteristikleri belirlenmiştir.

Biyokütle numunelerinin 200°C'de torefiye edilmesi ve hem biyokütle hem de linyit numunelerinin sırasıyla 400°C ve 750°C'de piroliz edilmesi paslanmaz çelikten yapılmış olan yatay boru fırında gerçekleştirilmiştir. Azot atmosferi altında gerçekleşen bu işlemlerden elde edilen ürünler kütlece %10 biyokütle ve %90 kömür

içerecek şekilde karıştırılmıştır. Ana yakıtlara kısa analiz (nem %, uçucu madde %, sabit karbon % ve kül %), elementel analiz (C, H, N, S ve O), ısıl değer ölçümleri, ve SEM analizleri uygulanmıştır. Karışımların birlikte yanma davranışlarının gözlemlenmesi ve biyokütle ile kömür arasındaki sinerjik etkilerin belirlenebilmesi için hem ana hem de karışım numunelerinin termal analizi yapılmıştır. Ana yakıtlar ve karışımların içerdiği fonksiyonel grupların tespiti için ise FTIR analizi yapılmıştır.

İlaveten, ana ve karışım numunelerinin termal bozunmasını ve yanma süreçlerini daha iyi anlamak ve daha derin bilgiye sahip olmak için Borchardt & Daniels kinetik metoduna dayanan analizler gerçekleştirilmiştir. Sabit ısıtma altında reaksiyon mertebesi, reaksiyon ısısı ve aktivasyon enerjisi kinetik parametreleri hesaplanmış ve sonuçlar tartışılmıştır.

1. INTRODUCTION

Despite the technological and scientific developments in this era, approximately 1.2 billion people suffer from the lack of modern energy delivering services [1]. Since energy poverty is an international challenge that affects people's lives and welfare severely, the world has to struggle with this problem more strictly than ever [2]. In spite of the negative environmental credentials, supply and use of energy mostly comes from coal in many countries so that 40% of the global power generation is provided by utilization of coal [3].

As one of the energy dependent countries, Turkey generates energy by using indigenous fossil fuels and imported resources [4]. According to the data obtained in 2013, domestic energy production was only 26.5% (31.944 Million tons-of-equivalent, Mtoe) of total primary energy supply whereas; the country met 72.3% (86.978 Mtoe) of energy demand from imported fuels [5]. Since development, economic and social well-being levels of the countries are directly related to the energy production and consumption, Turkey has been focused on the usage of domestic lignite in order to diminish the foreign energy dependency and increase economic growth. Lignite is the biggest national energy resource in Turkey [6]. However, the share of domestic lignite in energy generation is 38% due to the low calorific value but high contents of volatile matter, moisture, ash and sulfur that are the typical features of Turkish lignites.

In spite of the presence of lignite reserves with low quality but large quantity, rising energy demand related to population growth and declining public investment owing to the economic instability compel the government to shift from the imported energy to the national energy by specifying new action plans and strategies. In this regard, Turkey's energy strategy aims to utilize available domestic lignite and hard coal to secure energy supply. However, coal-based energy generation leads to the hazardous waste discharges from power plants to the atmosphere that brings about serious drawbacks in terms of climate change, environmental and human health. Turkey is among the top 20 countries in the world in terms of greenhouse gas (GHG) emissions

such that the level of GHG emissions increased 110% in 2013 when compared to 1990. Emissions related to coal combustion comprise 33% of total GHG emissions that consist of primarily CO_2 [7]. Thus, it is essential for Turkey to control CO_2 emissions particularly created in power plants in order to prevent dramatic effects of global warming. In this context, co-combustion of coal with biomass renders possible utilization of Turkish lignites thanks to the carbon neutral nature of biomass that helps to decrease emissions such as SO_2, NO_X, CO and CO_2 per unit energy generated in power plant [8].

Since Turkey is rich in young lignite deposits of which calorific value is quite low for an efficient and sustainable energy production along with the huge amount of biomass potential, addition of biomass to lignite for co-combustion has been marked as a reasonable solution to decrease foreign energy dependency of the country by increasing national primary energy production in a relatively environmental friendly manner.

The aim of this thesis study is to enhance the quality of low rank Turkish lignite coals that have large reserves throughout the country by blending forestry biomass. In addition to unprocessed biomass and lignite blends, torrefied and pyrolysed biomass have also been mixed with original lignite and semicoke lignites in order to assess the contribution of pretreatment process applied to biomass and lignite samples. The other goal of this study is to diminish rapidly and highly accumulating biomass feedstock.

2. COAL

Van Krevelen, who was a prominent contributor to coal science, defined coal comprehensively as: “Coal is a rock, a sediment, a conglomerate, a biological fossil, a complex colloidal system, an enigma in solid-state physics, and an intriguing object for chemical and physical analyses.” [9]. A brief and clearer description of coal can also be made such that coal is a combustible, black or brownish-black sedimentary rocks consisting of both organic and inorganic material [10]. As a chemically and physically heterogeneous material, coal has various combinations of organic and mineral matter. Carbon, hydrogen, nitrogen, sulfur and oxygen constitute the key elements in the organic matter while about 60 elements in noticeable amounts present in the mineral matter and several minerals including clay minerals, pyrite, marcasite, calcite, silica, and smaller quantities of other minerals found in coal are compounds of those elements [11].

Coal is primarily an indigenous fuel because it is mostly consumed where it is produced that enables energy security for the countries. So that, 85% of coal is mined and used in 70 nations and the rest of them is traded in global coal market. Besides abundance and widespread distribution of coal, its stability in terms of both easy and versatile transport without the need for pipeline infrastructure, along with storage advantages and low cost also makes this fuel a reliable energy source and decrease fuel supply obstacles [12].

2.1 Major Ranks of Coal

There are mainly four ranks of coal, which is determined by the degree of transformation of the buried plant material to carbon rich substance [13]. The natural process of chemical and physical changes undergone by coal during the maturation period is called coalification [14]. The general sequence of the coalification from those with the least carbon to those with the most carbon content is lignite, sub-bituminous, bituminous and anthracite. High moisture, low concentration of carbon and relatedly low energy content are the typical features of lignite and sub-

bituminous which are the low rank coals. On the other hand, bituminous and anthracite are higher rank coals that contain lower amount of moisture, more carbon and yield more energy [13]. Moreover, the term 'hard coal' or black coal' is used for anthracite and bituminous coals since they are generally harder and black. In contrast, lower rank coals are softer and have brownish color [14]. Apart from these coal ranks, there is also peat which is a heterogeneous mixture of soft organic material derived from the decomposed plants and deposited mineral matter. Even though peat is not actually coal, it is transformed to coal under the effect of suitable temperature and pressure [15]. The stages and chemical reactions occurring in coalification process from peat to anthracite are shown in Table 2.1.

Table 2.1 : The phases of coalification process.

Stage	Process	Main chemical reaction
Decaying Vegetation	Peatification	Bacterial and fungal life cycles
Peat	Lignitification	Air oxidation followed by decarboxylation and dehydration
Lignite	Bituminization	Decarboxylation and hydrogen disproportioning
Bituminous coal	Preanthracitization	Condensation to small aromatic ring systems
Semi-anthracite	• Anthracitization	Condensation of small aromatic ring systems to larger ones; dehydrogenation
	• Graphitization	Complete carbonification

The origin of coal in terms of the vegetation type, depths of burial, length of time along with the temperature and pressure determines the quality of coal deposits. Over millions of years, organic maturity of coal increases from peat to anthracite under the right conditions [17].

2.2 Uses of Coal

Different ranks of coal have different uses worldwide including mainly power generation, iron and steel production, cement manufacturing and as a liquid fuel. Alumina refineries, paper manufacturers, and the chemical and pharmaceutical industries are the other important usages of coal. By-products of coal are ingredients of several chemical products. For instance, refined coal tar is used to manufacture chemicals such as naphthalene, phenol, and benzene and creosote oil. Furthermore, ammonia salts, nitric acid and agricultural fertilisers are produced by processing

ammonia gas that is recovered from coke ovens. Variety of products in daily life involve coal or by-products of coal in their compositions: soap, aspirins, solvents, dyes, plastics and fibers [18]. Specialist products such as activated carbon, carbon fibre and silicon metal are also manufactured by using coal as an ingredient.

Among the several usage purposes of coal, it is predominantly used as fuel for electricity generation. That is, coal was responsible for 62% of global electricity generation, whereas industrial coal consumption of the world was about 33%. The rest of the coal was used in the commercial and residential sectors in 2011. The share of OECD countries in 2015 is 82.7% of the global primary coal being used to generate electricity and commercial heat. On the other hand, non-OECD countries constitute 82.8% of the total global coal consumption. Thus, any statistical data regarding coal uses, which belongs to these two types of countries in the world, can be evaluated at global scale [3]. Figure 2.1 demonstrates the sector based coal consumption in OECD and non-OECD countries.

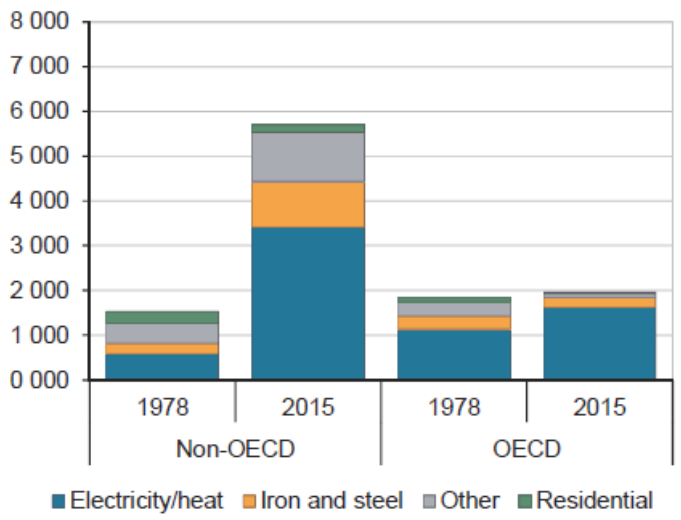

Figure 2.1 : Breakdown of primary coal broad activity in OECD and non-OECD countries (Mt) [3].

2.3 Global Coal Consumption and Production

Coal is the second most important fossil fuel and reliable energy resource in the world. 1.1 trillion tonnes of proven coal reserves were estimated worldwide and almost 70 countries have the recoverable reserves that indicates the presence of sufficient coal for around 150 years at the current production rate [17]. In comparison, proven oil and natural gas reserves lasts nearly 53 and 56 years,

respectively at current rates of production [12]. Despite the widespread distribution of coal, 76% of the world's recoverable reserves are sited in five regions: the United States (26%), Russia (18%), China (13%), non-OECD Europe and Eurasia outside of Russia (10%), and Australia/New Zealand (9%). In 2012, 6.4 billion tons of coal was produced in these regions or in other words, they were responsible for the 72% of total world coal production by tonnage. The share of Anthracite and bituminous coal in the world's estimated recoverable reserves on a tonnage basis was 45%, whereas subbituminous coal and lignite account for 32% and 23%, respectively [19]. World recoverable coal reserves in 2012 and projections with respect to that are indicated in Table 2.2 by rank.

Table 2.2 : Global recoverable coal reserves in the past and future [19].

	2012	2020	2025	2030		
Region/Country	Bituminous and anthracite	Sub-bituminous	Lignite	Total	2012 production	Reserves-to-production ratio (years
World Total	442.4	314.3	221.2	977.9	8.898	110
United States	117.5	106.3	32.9	256.7	1.016	253
Russia	54.1	107.4	11.5	173.1	0.392	442
China	68.6	37.1	20.5	126.2	4.256	30
Other non-OECD Europe and Eurasia	42.2	18.5	39.9	100.9	0.358	282
Australia and New Zealand	40.9	2.5	41.4	84.8	0.418	203
OECD Europe	5.7	0.9	61.9	66.8	0.630	106
India	61.8	0.0	5.0	61.6	0.666	92
Other non-OECD Asia	2.2	31.6	5.6	34.9	0.663	53
Africa	34.8	0.2	0.0	14.7	0.296	50
Other Central and South America	8.0	0.6	0.0	8.6	0.103	84
Brazil	0.0	7.3	0.0	7.3	0.007	995
Canada	3.8	1.0	2.5	5.0	0.073	69
Other	2.6	0.8	0.1	3.6	0.021	170

The largest coal producers distribute throughout the world. China, the US, India, Indonesia, Australia and South Africa are the top five producers. Most of the coal produced in a country is used domestically and only approximately 18% of hard coal production is traded between the countries [20]. Table 2.3 shows the world's top 10 countries with major coal production in recent years. World coal production

decreased in 2016 by 458 Mt, which doubles the one observed in 2015 and recorded as the largest decline in absolute terms since 1971 according to the IEA reports. China has remained the world's leading coal producer for many years even though noticeable decline has been observed by 13.5% since 2013. The amount of coal produced by China in 2016 was 3242.5 Mt, which is about 45% of the total world coal production that means even a slight decline in coal production of China affects world coal production considerably. Thus, setting quotas for mine operating days in China is one of the reasons for the global decline in coal production [3].

Table 2.3 : Major Coal Producing countries (in Million Tons) [3].

	2014	2015	2016
PR of China	3640.2	3563.2	3242.5
India	657.4	683.1	707.6
United States	918.2	813.7	671.8
Australia	488.8	512.4	503.3
Indonesia	488.3	453.5	460.5
Russian Federation	332.9	351.7	365.5
South Africa	260.5	258.6	256.9
Germany	186.5	184.7	175.6
Poland	137.1	135.8	130.9
Kazakhstan	114.0	107.3	97.9
Other	710.2	662.8	656.1
World	7934.1	7726.8	7268.6

World key statistics showed that approximately 77% of world coal production was steam coal, also known as thermal coal, is mostly used in power generation and other industries. The share of coking coal, which is mainly used in iron-steel production, was 13% and remaining was lignite in 2014 [20]. Table 2.4 shows the amount of coal produced in the last three years based on the type of the coal [3].

Table 2.4 : Coal production in the world (Mt) [3].

	2014	2015	2016
Steam coal	6010.1	5834.6	5407.0
Coking coal	1108.7	1081.1	1074.3
Lignite	815.4	811.1	783.3
Total coal	7934.1	7726.8	7268.6
Peat	15.2	10.1	NA
Oil Shale/sands	21.4	20.0	NA

According to the data in “World Energy Resources Coal 2016” published by World Energy Council, coal consumption of the world exceeds 7800 Mt [20]. In spite of the negative environmental credentials, supply and use of energy mostly comes from coal in many countries so that over 40% of the global power generation is provided by utilization of coal [1]. History and future projections of world energy consumption in terms of major fuel types is shown in Figure 2.2. According to the figure, the steepest increase in the first decade of the twenty-first century belongs to coal consumption, which can be explained by various reasons including lower price than other conventional fossil fuels, especially, natural gas and petroleum, reliable and a more stable energy source along with the technological developments succeeded in clean coal utilization and emission control [21].

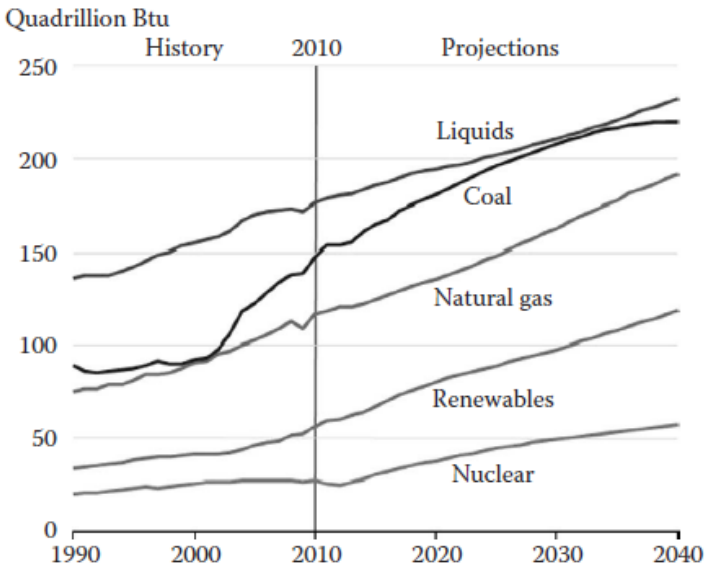

Figure 2.2 : World energy consumption by fuel type from 1990 to 2040 [21].

Owing to the overconsumption of coal in Asia, with large developing economies, the vitality of coal will continue in the future even though the European countries and North America aims to decrease coal consumption by shifting to alternative energy sources. In 2014, the first decline in China’s coal demand was seen by 2.9% to 3.9 billion tonnes since 1999. However, China has still been the world’s largest coal consumer with a share of 50%. Furthermore, a sharp decline took place in the US coal demand by more than 13% to 835 million tonnes in the same year. Competition between natural gas and shale gas in US lead to the decrease in natural gas prices and accordingly fall in coal demand. In addition, weaker power demand from coal, political issues and increasing environmental concerns also gave rise to a fall in US

coal demand [20]. European coal demand dropped by almost 6% that can be attributed to opposing attacks to coal fired power generation because of environmental regulations. Russian Federation which is one of the largest coal consumer also decreased coal demand by more than 4% mainly due to the economic turnaround after the substantial decline in oil prices. Worldwide coal consumption by regions and countries between 2008 and 2012 years are presented in Table 2.5 [21].

Table 2.5 : World coal consumption for the period from 2008 to 2012 [21].

	2008	2009	2010	2011	2012
North America	1200108	1069811	1124933	1071818	NA
United States	1120548	997478	1051307	1003066	890483
Central and South America	44791	39342	46971	49568	NA
Europe	1034173	959646	966325	1003697	NA
Eurasia	421200	395151	412682	428365	NA
Middle East	17159	15233	16316	16811	NA
Africa	230678	224394	222543	214972	NA
Asia and Oceania	4351152	4768246	4960749	5338369	NA
World	7299261	7471823	7750518	8123601	NA

2.4 Coal Production and Consumption in Turkey

Lignite is the biggest national energy resource in Turkey such that 12,152 Million metric tons (Mtonnes) of proven lignite and 523 Mtonnes of proven hard coal reserves were detected by 2012 while, oil and gas reserves were only 310.4 Mtoe and 7.1 Billion cubic meters, respectively [6]. Furthermore, discovery of new lignite reserves between years 2005 and 2015 led to 7.38 gigaton tons of increase in the country's reserves in addition to 8.3 gigaton of existing reserves [22]. Even though, almost 3.2% of the total world reserves of lignite and sub bituminous coal is found in Turkey, the share of domestic lignite in energy generation is 38% due to the low calorific value but high contents of volatile matter, moisture, ash and sulfur that are the typical features of Turkish lignites [7]. In 2016, the share of hard coal and lignite in the primary energy supply of Turkey was 17.67% and 9.02%, respectively [23]. Data gathered in 2015 regarding coal reserves including lignite and hard coal, primary energy production and consumption is indicated in Table 2.6.

Table 2.6 : Coal reserves and supply in Turkey [23].

Coal resources and reserves		
Total resources hard coal	Mt	1300
Total resources lignite	Mt	16000
Reserves hard coal	Mt	380
Reserves lignite	Mt	15600
Primary energy production		2015
Total primary energy production	Mtce	45.9
Hard coal (saleable output)	Mt/Mtce	1.5/1.2
Lignite (saleable output)	Mt/Mtce	41.8/14.0
Primary energy consumption		2015
Total primary energy consumption	Mtce	185.3
Hard coal consumption	Mtce	33.2
Lignite consumption	Mtce	16.9

Calorific value of lignite and subbituminous coal in Turkey varies between 1000-5000 kcal/kg and only around 5.1% of the total lignite and subbituminous coal reserves have a calorific value of more than 3000 kcal/kg. The heat content of hard coal reserves varies between 6200 and 7200 kcal/kg [24]. Since the calorific value of 79% of Turkish lignite coals is below 2500 kcal/kg, they are utilized mostly in thermal power plants. So that, 85% of the lignite production carried out in recent years was consumed in thermal power plants [25]. By the end of 2016, installed capacity of coal-based power plants was 17.316 MW that equals to 22.1% of the total installed capacity. 12.1% of installed capacity is provided by domestic coal whereas, the rest is supplied using imported coal [22]. The number of coal-fired power plants that are actively operated for electricity generation in Turkey is 38 [26]. Three new coal-fired power plants is under construction and more than 70 new stations has been planned to be implemented as part of the Turkey's energy policies towards increasing domestic energy production. Currently used coal-fired power plants in Turkey are sited in Çanakkale (Çan, Karabiga), Bursa (Orhaneli), Kocaeli(Gebze), Manisa (Soma), İzmir (Aliağa), Kütahya (Tunçbilek, Seyitömer), Zonguldak (Çatalağzı), Ankara (Nallıhan), Eskişehir (Mihalıççık), Muğla (Yatağan, Yeniköy, Gökova), Yalova (Taşköprü), Bolu (Göynük), Sivas (Kangal), Adana (Yumurtalık-Sugözü), Kahramanmaraş (Afşin-Elbistan), Hatay (İskenderun), and Şırnak (Silopi)

provinces. Other ongoing plants are in Adana (Tufanbeyli), Çanakkale (Karabiga), and Kütahya (Tunçbilek) provinces of Turkey [7].

Lignite resources of Turkey are distributed mostly in continental sedimentary basins of Tertiary age throughout the country and concentrated in the central and western part of Turkey. Small quantities of subbituminous coals also exist among these lignite basins [27]. The largest lignite reserves with nearly 46% share in the country's lignite reserves are located in the Afşin-Elbistan basin [22]. Konya-Karapınar, Thrace and Manisa-Soma basins are the other important lignite basins which have abundant quantity of reserves [28]. On the other hand, the most important bituminous coal reserves are found in Zonguldak and the neighboring regions on the Western Black Sea Region. Although the level of total anthracite reserves in the Zonguldak basin are 1.30 gigaton, the visible reserves are around 506 million tons [22]. Furthermore, small amounts of asphaltite and peat reserves also exist in Turkey. Figure 2.3 demonstrates the coal basins all over the country [29].

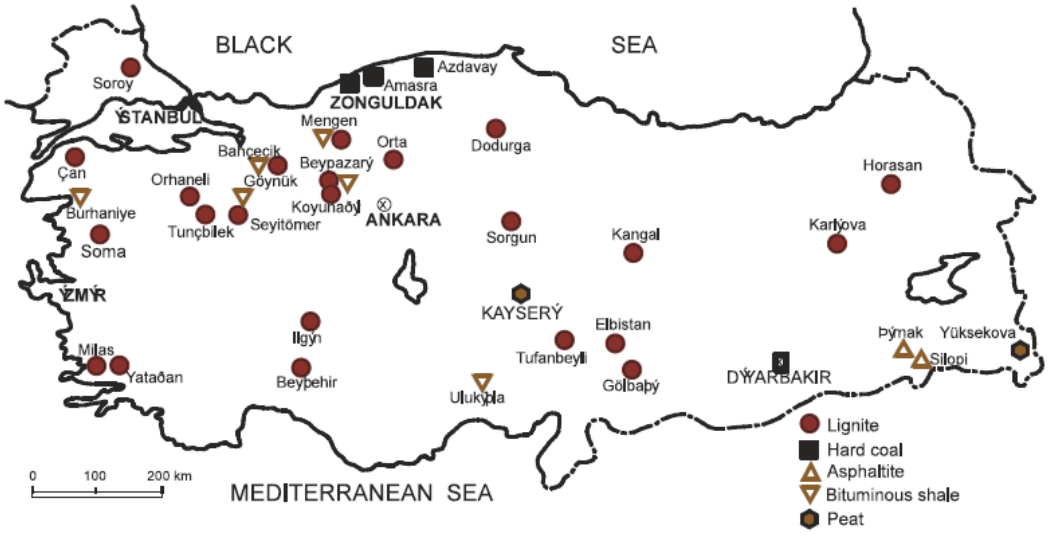

Figure 2.3 : Coal basins of Turkey with respect to the rank [29].

2.5 Coal Analysis

The value of a coal deposit mostly depends on the physical and chemical properties of coal rather than the quantity. Thus, comprehensive analytical methods were developed to detect and measure the metallurgical or thermal properties of coal in terms of determining the suitability for coking, power generation, or for iron and steel production. Besides assessing the utilization behavior of coal, analytical

methods are also applied to identify the true value of a coal reserve and environmental implications which arise during the coal processing [30].

Coal testing and analysis is performed by the methods that use national standards. International Organization for Standardization (ISO) standards, American Society for Testing and Materials (ASTM) Standards, British (BS) standards or Australian (AS) standards are the commonly used standards for characterization and classification of coal based on the generated results. Since coal is a heterogeneous commodity including different percentages and combinations of organic and mineral matter, no exact analysis results can be gathered from different parts of the coal. In spite of heterogeneity, the analysis of coal is usually carried out by representative samples taken from the coal by appropriate sample splitting and taking methods, which is regarded as the most important step in the whole process of coal characterization. No matter which international coal testing standard is applied, similar analysis results must be obtained at the end. Thermal and metallurgical properties along with the expected utilization behavior of coal can be assessed by comprehensive set of laboratory analysis. Distinctively, thermal test of coal is performed by determining the following:

- Total moisture,
- Proximate analysis,
- Ultimate analysis,
- Calorific value,
- Hardgrove grindability index (HGI),
- Abrasion index,
- Forms of sulfur,
- Chlorine,
- Ash fusibility temperatures,
- Ash analysis,
- Moisture holding capacity,
- Trace element analysis,
- Petrographic analysis.

Analysis results of major ranks of coal typically range between the specific values of essential analytical parameters that are shown in Table 2.7. In this table, hydrogen and oxygen values contain also the ones in sample moisture [7].

Table 2.7 : Representative composition and physical property ranges of principal ranks of coal [31].

	Anthracite	Bituminous	Subbituminous	Lignite
Moisture (%)	3-6	2-15	10-25	25-45
Volatile matter (%)	2-12	15-45	28-45	24-32
Fixed Carbon (%)	75-85	50-70	30-57	25-30
Ash (%)	4-15	4-15	3-10	3-15
Sulfur (%)	0.5-2.5	0.5-6	0.3-1.5	0.3-2.5
Hydrogen (%)	1.5-3.5	4.5-6	5.5-6.5	6-7.5
Carbon (%)	75-85	65-80	55-70	35-45
Nitrogen (%)	0.5-1	0.5-2.5	0.8-1.5	0.6-1.0
Oxygen	5.5-9	4.5-10	15-30	38-48
Btul/lb	12000-13500	12000-14500	7500-10000	6000-7500
Density (g/mL)	1.35-1.70	1.28-1.35	1.35-1.40	1.40-1.45

2.5.1 Proximate analysis

As it is understood from the term “proximate” that means “first” or “immediate”, this analysis constitutes the essence of the coal characterization and utilization. Proximate analysis is the determination of moisture, volatile matter, ash and fixed carbon content of analysis sample by approved methods [30]. Particle size of the coal sample is required to below 0.250 mm according to ASTM standard for the application of proximate analysis. Thus, analysis sample is crushed to a nominal-0.212 mm, 95% passing prior to the test. Analysis results are reported as a mean of duplicate determinations as a percentage to close 0.1%.

- Moisture: Surface, hydroscopic, decomposition and mineral moisture are the four possible forms of moisture present in coal. Water held on the surface of coal particles and macerals forms the surface moisture while, water held by capillary action within the micro breakages of coal resulted in hydroscopic moisture. On the other hand, water held within the coal’s decomposed organic matter causes decomposition moisture and water that forms part of the crystal structure of hydrous silicates, particularly clay minerals is the mineral moisture. Due to the existence of different types of moisture, total moisture content of coal is usually determined and calculated as the loss of mass between the untreated and analyzed sample. There are a number of procedures for the determination of moisture content. Heating coal with toluene and drying in a minimum-free-space oven at 150°C in nitrogen atmosphere until constant mass of the coal sample is obtained are the two

methods that can be used for low-rank coals. Drying in air at 100°C to 105°C is another method used for high-rank coals. Due to the possibility of oxidation, the last method cannot be performed for low rank coals. In addition to the total moisture, inherent moisture content can also be determined by the last method as long as the analysis is run in vacuum condition.

- Volatile matter: It is calculated from the percentage loss in mass of the analysis sample after the removal of moisture vapor during the heating of coal or coke under rigidly controlled conditions. Determination of volatile matter content of a sample is crucial for the assessment of coal rank. So that, as the rank of the coal increases, volatile matter content decreases. In thermal power plants, volatile matter is an important parameter that has a considerable influence on the ignitability and burnout characteristics of the coal. Lower volatile matter content lead to the higher fuel ratio, which is calculated by dividing fixed carbon to volatile matter, and the coal burns more slowly due to the hardened ignition. Thus, volatile matter content shows the ease of combustion of a coal. The fuel ratio is often required in boiler design.
- Ash content: The residue remained after the complete combustion of all organic compounds and oxidation of the mineral matter present in coal is called as ash content, which consists of mainly oxides and sulfates. Ash is the most essential parameter for the quality evaluation of coal and is critical for the expected coal's end use. According to the standard method for the determination of ash value, coal sample is heated in a crucible in air atmosphere to 500°C and kept at this temperature for over 30 min. Then the sample is further heated to 815^{o}C until constant mass is reached. The percentage of ash is calculated from the mass of residue remaining after incineration divided by mass of the untreated sample used in the test. Ash content of thermal coal affects power plant efficiency, collection of particulate emissions and ash disposal. Ash content and caloric value of thermal coal are proportional to each other inversely that means the higher the ash value, the lower the calorific value. Although ash is produced by the chemical changes occurring in the mineral matter, the amount of ash can be different from the quantity of mineral matter in coal due to the alteration of some mineral species during the ashing process such as CO_2 removal from

carbonates, SO_3 removal from the sulfides and H_2O removal from clay minerals and other minerals.

- Fixed carbon: The solid, combustible residue remained after removal of moisture, ash and volatile matters from coal, coke and bituminous materials is called fixed carbon and it is expressed as a percentage. As its definition indicates, fixed carbon is calculated by substracting the sum of moisture, volatile matter and ash values from 100%. Fixed carbon value in low volatile materials, such as coke and anthracite coal, is almost equal to the elemental carbon content of the sample [31].

2.5.2 Ultimate analysis

Determination of the organic-derived components of coal that are composed of mainly carbon (C), hydrogen (H), nitrogen (N), oxygen (O) and sulfur elements (S) is called ultimate analysis. The sum of these components comprises more than 99% of the organic constituents of coal, but results of the analysis is usually reported as they sum to 100% [30]. Automatic non-dispersive analyzer is used to determine elemental C, H and N content of the sample by converting those components into CO_2, H_2O, N_2 and NO_x through the combustion process. Then, the gaseous products are passed through infrared cells to measure C and H content as well as a thermal conductivity cell to determine N. Oxygen is often calculated by difference.

The carbon determination involves carbon found in both organic and inorganic structure of coal. Hydrogen determination also includes hydrogen that presents in the organic matter and moisture. Unless otherwise specified, assumption for nitrogen is made as it occurs in the organic matrix of coal. Similar to carbon, oxygen is found in the organic and inorganic parts of coal. It is found in phenol groups, carboxyl, methoxyl, and carbonyl that are associated with the organic portion of the coal, whereas the several forms of moisture, silicates, carbonates, oxides and sulfates are the inorganic portion of coal that contain oxygen [31]. On the other hand, sulfur present in coal as organic sulfur, inorganic sulfur, that is, iron sulfides, pyrite and marcasite (FeS); sulfate sulfur and elemental sulfur which occur in trace to minor amounts [32].

The results of the ultimate analysis is reported as the mean of duplicate determinations, reported to the close 0.1% for carbon and oxygen that is not analyzed but calculated, and nearest 0.01% for hydrogen and nitrogen [30].

2.5.3 Thermochemical analysis

Understanding the thermochemistry of coal is essential for the utilization of coal in numerous conversion processes such as combustion, carbonization, gasification and liquefaction. Activation energy, calorific value, ash fusibility, caking index and swelling index are among the thermal properties of coal. The most common analysis for the study of these thermal properties is thermogravimetric analysis (TGA).

The calorific value of a coal sample, which indicates the heat released by the combustion of a unit quantity of coal in a bomb calorimeter under a specified set of conditions, is an important parameter for evaluation of coal quality. There are two types of expression of calorific value: the gross calorific value of higher heating value and the net calorific value or lower calorific value. The difference between the higher and lower heating value is related with the liquid or vapor phase of the water that is produced as a result of the combustion process. That is, higher heating value is obtained when the combustion products are cooled down to the initial temperature and water in the vapor phase turns back to its liquid state. Conversely, the lower heating value is determined when all the water is in vapor state [33].

The relationship between the gross calorific value and the net calorific value is given by the equation (2.1).

$$Net\ calorific\ value\ (BTU/lb) = Gross\ calorific\ value - [(1030 \times \%\ total\ hydrogen \times 9)/100] \quad \textbf{(2.1)}$$

There are a great number of correlations developed by scientists to determine the calorific value of coal based on the elemental composition. Dulong, Boie, Grummel and Davis formulas can be presented as the most popular correlations to calculate the heating values of coals.

2.6 Coal Processing Technologies

Direct combustion of finely pulverized coal in large-scale utility furnaces is the most common manner of coal consumption worldwide. However, there are many other processes applied for the utilization of coal in the industrial sector for both producing

energy as electricity and steam, and manufacturing value added products like chemicals or gases. The major coal utilization processes are introduced in the next subsections [34].

2.6.1 Pyrolysis

Many thermal conversion processes of coal such as combustion, carbonization, gasification and liquefaction involve pyrolysis as a common sub-stage [35]. Pyrolysis is defined as the thermal decomposition of materials taking place in the absence of oxygen. Coke (or char), liquids and gases are the products of the pyrolysis of coal.

The basic understanding of the chemistry of coal pyrolysis along with the yields, characteristics and the rate of formation of the pyrolysis products during thermal treatment under different conditions is noteworthy for process design and optimization. The fundamental steps of pyrolysis process and optional routes with regarding reactants and products are demonstrated in Figure 2.4 [36].

Extensive research has been done on pyrolysis of coal resulting in the development of several processes that include fixed-bed, moving bed, fluidized-bed and rotary kiln technologies. These technologies are typically grouped as slow pyrolysis with heating rates usually less than K/s and fast pyrolysis with heating rates as high as 10^4 K/s [37].

Slow pyrolysis of coal has been practiced successfully to produce coke in fixed bed or moving bed reactors for metallurgical industry or Lurgi retort and Lurgi gasifiers. Due to the low tar yields of the coking technology which is about 3-5% and low productivity of the moving bed technologies because of long residence time of coal even in hours, fast pyrolysis technologies were developed.

Fluidized-bed, rotary kiln and other technologies in which coal is heated by solid heat carriers are the major fast pyrolysis technologies. However, these technologies has not been commercialized yet owing to some drawbacks that they have in common. Poor tar quality due to high solid and pitch contents along with repeated plugging of the volatile product lines are the common problems.

Even though considerable technical efforts have been exerted in the past to eradicate these problems such as increasing heating rate of coal and cooling rate of volatiles, integration of multiple high temperature dust removal devises, pretreatment of coals

and usage of catalysts, it is unfortunate that no significant improvement has been achieved. Thus, basic understanding of reactions undergoing in pyrolysis of coals in these reactors is essential [36].

In addition to the slow and fast pyrolysis processes, there is also flash pyrolysis that proceeds under rather mild reaction conditions, low temperature and low pressure, but rather at high heating rates of over 1000 K/s. Utilization of this pyrolysis type enables the recovery of liquid products in high yields. Schematic representation of the flash pyrolysis process is demonstrated in Figure 2.5 [38].

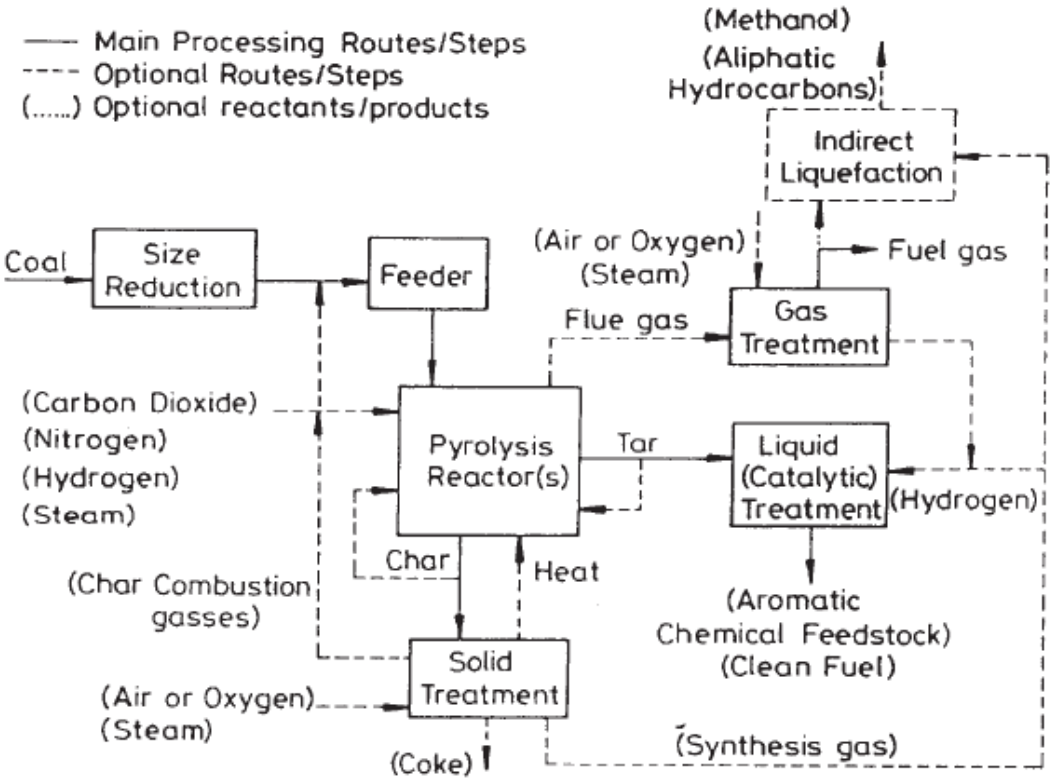

Figure 2.4 : The basic stages of coal pyrolysis process [36].

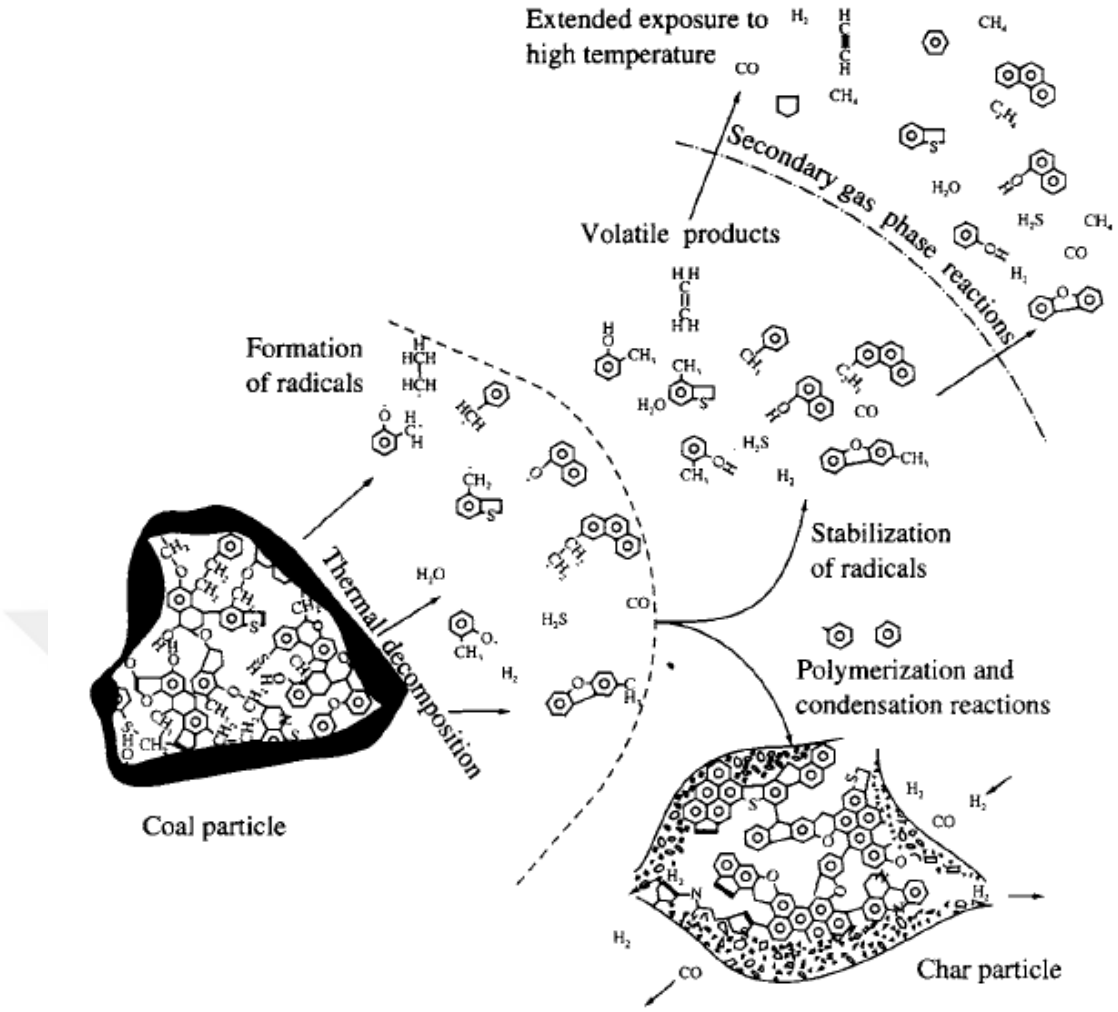

Figure 2.5 : Fundamental reactions and processes occurring during the flash pyrolysis of coal [38].

2.6.1.1 Basic mechanism of coal pyrolysis

The complicated pyrolysis process of coal consists of two main distinctive stages: the primary cleavage of weaker bonds between the aromatic units resulting in the production of volatile radical fragments and then secondary reactions of further cracking, hydrogenation or agglomeration of the primary products that lead to the formation of gas, condensable liquids, and coke or char [38]. The basic model of primary and secondary coal pyrolysis reactions are shown in Figure 2.6. The steps involved in pyrolysis of coal can also be introduced more elaborately:

- Cleavage of hydrogen bonds
- Vaporization and transport of non-covalently bonded molecules
- Low temperature crosslinking in coals that have 10% oxygen content
- Fragmentation of macro molecular network by breakage of bridges

- Stabilization of free radicals by hydrogen utilization
- Vaporization and gas phase transport of light fragments
- Mild temperature crosslinking to harden the macromolecular network
- Decomposition of functional groups to produce light species
- Condensation of the macromolecular network by hydrogen removal at high temperature [39].

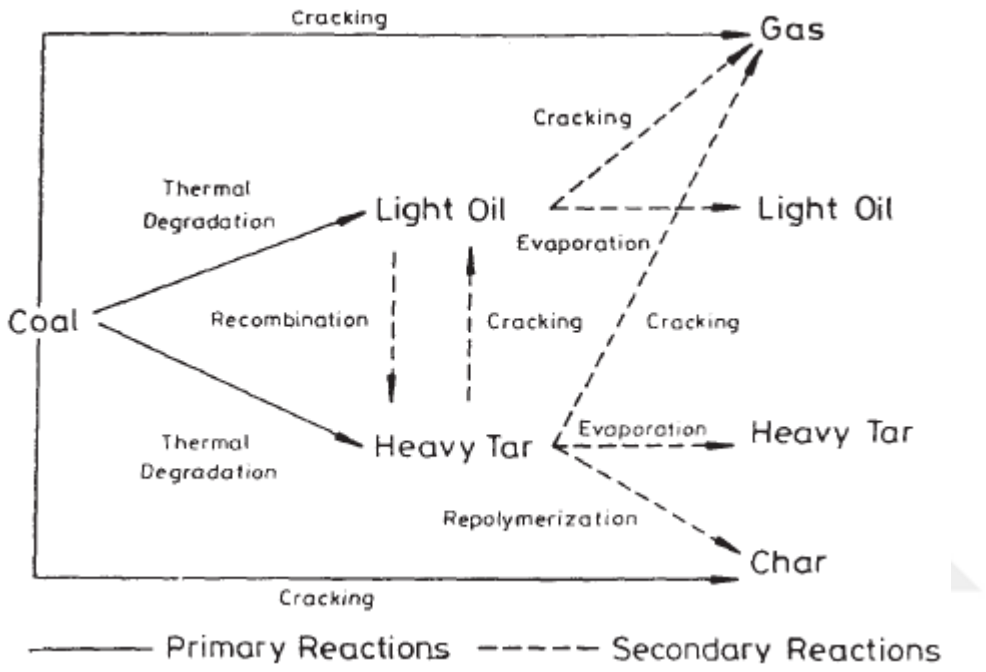

Figure 2.6 : Model of the primary and secondary reactions occurring during coal pyrolysis [39].

2.6.2 Combustion

Burning coal to derive its calorific value is the most straightforward utilization technology. Heat released during the reaction between carbon constituent of coal and oxygen in air is used to raise steam for power generation or process application [40]. Combustion of coal might occur in three ways based on the particle sizes: as large pieces in a fixed bed or on a grate, as smaller or crushed pieces in a fluidized bed, or as very fine particles in suspensions. Although coal can be burned by any of these three methods without considering the particle size in theory, engineering limitations specify ideal particle sizes for the three methods. Besides particle size, dominant reaction mechanism and other thermal behaviors are important parameters that determine the appropriate combustion technique. Table 2.8 introduces the main characteristics of the combustion techniques. [41]

Table 2.8 : Restrictions of combustion methods [41].

		Combustion Method	
Variables	Fixed Bed (Stoker)	Fluidized Bed	Suspension
Particle Size			
Approximate top size	<2 in.	<0.2 in.	180μm
Average size	0.25 in.	0.04 in.	45μm
System/bed temperature	<1500°F	1500-1800°F	>2200°F
Particle heating rate	1°/s	1000-10000°/s	1000-1000000°/s
Reaction time			
Volatiles	100s	10-50s	<0.1 s
Char	1000s	100-500s	<1 s
Reactive element description	Diffusion-controlled combustion	Diffusion-controlled combustion	Chemically controlled combustion

The combustion process involves many consecutive steps:

- Moisture is released from the coal particles when they are heated.
- Volatile organic matters are driven off that is called as devolatilization stage.
- Volatile matter constituents are combusted in the gas phase either before the combustion of the char particles or concurrently with them. As a general assumption, combustion of volatiles is a homogeneous reaction.
- Combustion of char particles that is a heterogeneous reaction occurs as the last step.

Mostly, burning reactions take place in order and the rate of overall process is determined by one of the reaction with the slowest rate. By a majority, the process of char combustion is slower than volatiles burning which is measured in milliseconds; therefore, it is the time determining step for complete combustion in a furnace.

2.6.2.1 Coal devolatilization

Coal quality in combustion chemistry is mostly determined by devolatilization behavior. Hence, the features such as particle residence time, near-burner heating rates that govern ignition, flame stability, and flammability limits of pulverized coal flames; and soot loadings that determine near-burner radiation fluxes are all depend on coal devolatilization. Heating value of volatiles driven off during this step can be up to the half of heating value of coal. The devolatilization step involves three

different physical processes: pyrolysis, volatile transport through the pores, and secondary reactions that can affect the formation of gas products and/or cause decomposition of volatile products on the wall of the pores. Temperature, heating rate, pressure, particle size, and coal type are the significant aspects that affect the pyrolysis behavior. Most part of the mass release during devolatilization occur at high temperatures. Moreover, the breakage of the bridges, which link the aromatic clusters, leads to detachment of finite size fragments from the macromolecule structure of coal with increasing temperature. The bridges consist of a variety of distinct types of functional groups and the weakest bonds are broken first. The fragments are called as metaplast or liquid coal components that either vaporize or removed from the coal particle or crosslinks back into the macromolecular structure. Vaporized metaplast is referred to as tar that is the primary source of soot.

In general, devolatilization behavior relies on the rank of coal. That is, lignites and subbituminous coals release large-amount of light gases and less tar to some extent. On the other hand, high rank coals release only small amounts of tar and lower amounts of light gas that consist mainly of methane, carbon dioxide, carbon monoxide, and water vapour . Olefins, nitrogen and sulfur compounds are the other constituents of light gas [34].

2.6.2.2 Char combustion

Chemisorption of oxygen (O_2) at active sites on char surfaces and generation of carbon monoxide (CO) initiate the char combustion. Then, CO is oxidized to carbon dioxide (CO_2) in a gaseous boundary layer around the porous char particle. Produced CO_2 is either transported to gas stream or reduced to CO by reacting with the carbon in the char endothermically. Figure 2.7 demonstrates the representative combustion process of a single char particle in terms of concentration and temperature profiles [42].

Despite the complexity of the coal combustion, the following reactions (2.2-2.7) typically summarize the process [34].

$$\text{Coal (raw)} \rightarrow \text{Char} + \text{Volatiles} + H_2O \quad \textbf{(2.2)}$$

$$\text{Volatiles} + O_2 \rightarrow CO + H_2O + SO_2 + NO \quad \textbf{(2.3)}$$

$$CO + \tfrac{1}{2}O_2 \rightarrow CO_2 \quad \textbf{(2.4)}$$

$$\text{Char} + \frac{1}{\phi} O_2 \rightarrow \left(2 - \frac{2}{\phi}\right) CO + \left(\frac{2}{\phi} - 1\right) CO_2 \quad \textbf{(2.5)}$$

$$\text{Char} + CO_2 \rightarrow CO + CO \quad \textbf{(2.6)}$$

$$\text{Char} + H_2O \rightarrow H_2 + CO \quad \textbf{(2.7)}$$

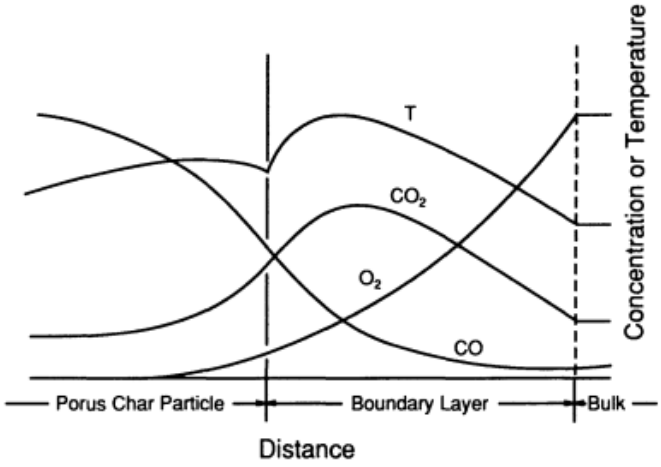

Figure 2.7 : Shematic representation of a char combustion in Cartesian coordinates [42].

2.6.2.3 Coal fired power generation

Pulverized coal-fired plant, which is shown in Figure 2.8 schematically, is the most common sort of coal-fired power station in operation currently. Approximately 90% of all coal-fired power stations operate based on this design. The coal-handling facility, boiler, steam turbine, generator and flue gas treatment system make up the backbone of such a power plant. Usually mined coal is directly delivered to a power plant where it is crushed and grinded to a suitable particle size that is required for injection into the furnace. Once coal particles are injected into the furnace that is a part of boiler, they burn in the presence of optimum amount of air both to reduce pollutant emissions and to fluidize the coal. By the help of arrays of tubes carrying water throughout the furnace, the radiant and convective heat produced by combustion is captured. The ash may be collected from the bottom of the furnace to be disposed or may leave the furnace with the flue gases [43].

Modern coal-fired power plants are targeted to be operated with higher efficiency that means lower emissions per unit of electricity produced. In order to maximize efficiency of a plant one can change some of the parameters related to energy conversion process during equipment design. Around 85% of chemical energy coal contains can be gathered in the form of hot steam produced in boiler while the rest is

lost and irreversible. Further conversion of steam to electricity follow the Carnot thermodynamic cycle. Efficiency of the cycle depends on the temperature and pressure drop between steam turbine inlet and outlet so that the achieving the highest steam temperature and pressure is the crucial goal of the state-of-the-art power plant technology.

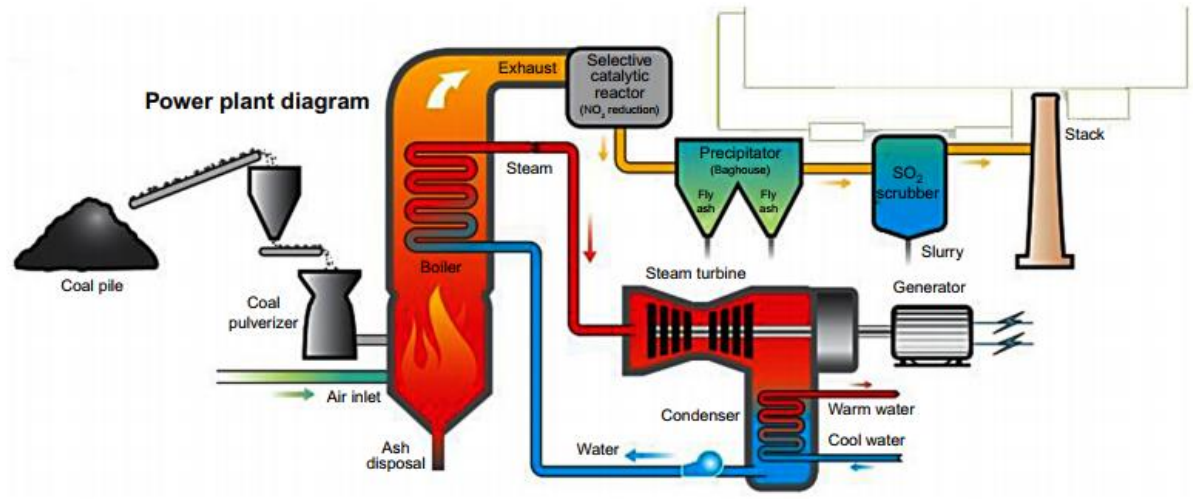

Figure 2.8 : A basic schematic of a pulverized coal-fired power plant [43].

2.6.3 Carbonization

Conversion of organic constituents of coal into a carbonaceous residue in the absence of air is called carbonization that is one the most popular and oldest uses of coal as well as combustion. Solid, liquid and gaseous substances are produced as a result of carbonization of coal. There are different terms used to name the solid carbonaceous residue those are coke, char and carbon.

$$C_{organic} \xrightarrow{yields} C_{coke/char/carbon} + liquids + gases \qquad \textbf{(2.8)}$$

Coke, which is produced by heating coal in ovens at temperatures around 1000°C, is essentially used in the iron and steel industry and as a domestic smokeless fuel. Even though only the coals in the bituminous rank range are utilized for the production of metallurgical coke, some of the bituminous coals are not suitable for this application.

Thermal decomposition of coal is intensely dependent on the rank of coal. As the rank increases, the production level of light gases decreases, but tar formation rises. Due to the complex events that take place during coal pyrolysis, many investigators have studied for the determination of each sequential step involved in the process. Moisture removal from coal at temperatures around 100°C is the initial stage. Then,

formation of light gases that consists primarily of carbon monoxide (CO), carbon dioxide (CO_2) and hydrocarbons with low-boiling point begins in the temperature range of 200°C-500°C. At low heating rates, production of tar begins at around 330°C and enhances to temperatures above 530°C. The highest formation of tar, hydrocarbons and combustible gases generally occurs over the temperature range of 450°C -500°C. Visible changes to the coal are almost completed at about 550°C and a semi coke residue is produced. Then, semi coke shrinks and becomes harder to be converted into coke by the release of CH_4, H_2, and traces of CO and CO_2 from its structure at temperatures greater than 550°C.

Understanding the general characteristics of the physiochemical changes undergone by coal is essential for determining the extent to which coal is carbonized in terms of the utilization purposes of the liquid and gaseous by-products. Accordingly, coal carbonization processes are usually divided into three categories as low temperature, medium temperature and high temperature that are introduced in Table 2.9 [44].

Table 2.9 : Categories of carbonization processes [44].

Carbonization Process	Final Temperature		Products	Processes
	°C	°F		
Low temperature	500-700	930-1290	Reactive coke and high tar yield	Rexco (700°C) made in cylindrical vertical retorts. Coalite (650°C) made in vertical tubes
Medium temperature	700-900	1290-1650	Reactive coke with high gas yield, or domestic briquettes	Town gas and gas coke (obsolete). Phurnacite, low-volatile steam coal, pitch-boud briquettes carbonized at 800°C-
High temperature	900-1050	1650-1920	Hard, unreactive coal for metallurgical use	Foundry coke (900°C). Blast furnace coke (950°C-1050°C)

2.6.4 Gasification

Gasification is the thermochemical conversion of the carbon-based solid or liquid into the combustible gas products in the presence of gasification agents. Even though majority of the gas products are combustible chemical species, generation of gaseous fuel is not the only aim of gasification because these gases can also be handled for

generation of other valuable chemical and petrochemical feedstock. In commercial gasification, a fraction of stochiometric ratio of oxygen is introduced to the coal as a gasification agent. During direct gasification, oxidizing agent (air) is used to partially oxidize the feed stream. If oxidizing agent is not being used, then the process is called indirect gasification, where the energy is outsourced. The most common indirect gasification agent is steam as it is easily available and increases hydrogen content of the produced gas. Indirect gasification is called pyrolysis when the gasification agent is an inert gas such as nitrogen [45].

Conversion of coal to gaseous products consisting of CO_2, H_2O, N_2, CO, H_2, CH_4, trace hydrocarbons, fuel traces, ash and tar occurs via a series of reactions in a reactor vessel where the temperature, pressure and flow pattern (moving bed, fluidized, or entrained bed) are controlled. Rank of coal and its composition, the gasifying agent, thermodynamics and chemistry of the gasification reactions that are controlled by the process operating parameters affect the proportions of products in the resultant gas mixture.

Coal gasification technology is primarily utilized to generate electricity in integrated gasification combined cycle (IGCC) plants, to manufacture syngas for use as pipeline gas supplies and chemical feedstock, to produce hydrogen for fuel cell applications which is becoming even more important use of gasification. Due to the presence of sulfur, alkali metal compounds and trace elements in the composition of coal, special gasification technology is chosen to produce a different quality of syngas depending on the certain target chemicals that are manufactured with downstream processes [46].

2.6.5 Liquefaction

Liquid fuel production from solid coal is one of the main coal conversion process applied mostly because of its inconvenient handling as a consumer fuel. In order for the easy utilization of coal, researches have been carrying out to convert it into pipeline-quality gaseous fuel or clean liquid fuel [47]. Increasing oil prices draw interest on coal liquefaction owing to the widespread distribution and high amount of coal in the world. The recent emphases of this technology are to facilitate operating conditions, minimize the hydrogen need and make the liquid product more

environmentally tolerable. Coal-derived liquid fuels are produced primarily by coal pyrolysis, direct liquefaction and indirect liquefaction methods.

Condensable tar, oil, water vapor and noncondensable gases are formed as a result of coal pyrolysis. C-C bonds available in coal macromolecular structure are cleaved through a process called destructive distillation that plays a vital role in molecular weight reduction in coal hydrocarbons. In addition to the foremost cleavage of C-C bonds, partial decomposition of C-S and C-H bonds takes place yielding lower molecular weight products such as liquid hydrocarbons.

Generally, the condensed pyrolysis products are further hydrogenated to get rid of sulfur and nitrogen species as well as to enhance the quality of liquid fuel because of the undesired effects of these components. Rank and particle size of coal, reactor type, process mechanics, partial pressure of hydrogen, reactor pressure and temperature, coal residence time are the predominant factors that affect the liquefaction efficiency. The proportion of liquid hydrocarbons obtained by coal pyrolysis is higher at shorter residence time since further thermal cracking cannot be achieved due to the lack of sufficient time for the conversion of produced oil to gaseous hydrocarbons. Moreover, the fluidity of coal hydrocarbons is improved by addition of hydrogen (H) that increases the ratio of H/C and supports the production of a liquid fuel. Since H content of coal decreases by removal of volatile hydrocarbons, conversion of coal to coal char is in the direction of the H/C ratio decreasing, while the production of coal liquid from coal occurs in the opposite direction.

Direct and indirect liquefaction differ from each other by only the requirement of gasification step which is applied prior to the production of liquid fuel. The term, hydoliquefaction is used to define direct liquefaction of coal in order to make a distinction between it and other liquefaction processes [48]. Direct conversion of coal to liquids by the reaction with hydrogen under controlled temperature and pressure conditions occur in hydroliquefaction process. Direct liquefaction may be classified into a single-stage and a two-stage process. Two-stage process involves two consecutive hydrogenation steps. Firsty, the coal is hydrogenated in liquid-phase stage and liquid products are formed. Then, second hydrogenation is carried out in vapor-phase stage in which the catalytic conversion of liquid products to clean and light distillate fuels takes place. On the other hand, indirect liquefaction of coal

requires the production of syngas by gasification process and then liquid hydrocarbons and other oxygenates are produced from syngas by catalytic reactions [47]. There are two principal areas of indirect liquefaction of coal: conversion of syngas to light hydrocarbon fuels by Fischer-Tropsch synthesis and to oxygenates such as methanol, higher alcohols, dimethyl ether and ethers [48].

3. BIOMASS

Biomass is a renewable resource and derived from the plant materials and animal wastes. Solar energy is absorbed by biological species to turn atmospheric CO_2 into carbohydrates and O_2 by a process called photosynthesis. Then, the chemical energy stored in plants is transferred to animals and humans that consume plants as food [49]. In case of burning biomass, chemical energy in biomass is released as heat.

Although biomass has been defined differently by many scientists and researchers, a universally accepted definition was made by the United Nations Framework Convention on Climate Change (UNFCCC) as:

"Non-fossilized and biodegradable organic material originating from plants, animals and micro-organisms. This shall also include products, by-products, residues and waste from agriculture, forestry and related industries as well as the non-fossilized and biodegradable organic fractions of industrial and municipal wastes" [50].

Unlike fossil fuels, only atmospheric CO_2 that is absorbed by plants recently during photosynthesis is released when biomass burns and it is recycled into the plants achieving net zero emission of CO_2. The unique feature of 'carbon neutral' nature of biomass makes it the most attractive renewable fuel for energy generation worldwide [51]. Due to the almost depleted fossil fuel sources, biomass based power generation is of growing importance to get rid of environmental concerns and the anxieties related to the security of energy supply.

3.1 Biomass Sources

The general classification of biomass materials as fuel resources can be divided into five groups according to their biological diversity, similarity and origin as shown in Table 3.1 [49].

Biomass sources are utilized to produce three types of primary fuels that are as follows:

- Liquid fuels (ethanol, biodiesel, methanol, vegetable oil, and pyrolysis oil).
- Gaseous fuels (biogas (CH_4, CO_2), producer gas (CO, H_2, CH_4, CO_2, H_2), syngas (CO, H_2), substitute natural gas (CH_4).
- Solid fuels (charcoal, torrefied biomass, biocoke, biochar) [49].

Table 3.1 : General classification of biomass materials [49].

Biomass groups	Examples
Agricultural	food grain, bagasse (crushed sugarcane), corn stalks, straw, seed hulls, nutshells, and manure from cattle, poultry, and hogs.
Forestry	trees, wood waste, wood or bark, sawdust (SW), timber slash, and mill scrap.
Municipal	sewage sludge, refuse-derived fuel (RDF), food waste, waste paper, and yard clippings.
Energy Crops	poplars, willows, switchgrass, alfalfa, prairie bluestem, corn, and soybean, canola, and other plant oils.
Biological	animal waste, aquatic species, and biological waste.

A considerable portion of biomass energy is produced from wood and wood wastes with 64%. Municipal solid waste, agricultural waste and landfill gases follow it by 24%, 5% and 5% shares, respectively [52,53]. Even though all types of biomass sources can either be used for energy generation by combustion or to derive fuel from it through conversion processes, better quality of fuels are produced by some species in a cost effective manner. Thus, several types of biomass have been grown specific to energy production. Studies on energy crops that encompasses woody crops and grasses/herbaceous plants, starch and sugar crops and oilseeds have been carried out in this context. The main desired characteristics of the ideal energy crops are listed as follows:

- High yield (maximum production of dry matter per hectare),
- Low energy input to produce,
- Low cost,
- Composition with the least contaminants,
- Low nutrient necessities.
- Drought resistance (especially countries with limited water sources)
- Pest resistance [54]

3.2 Composition and Properties of Biomass

Biomass is a complex mixture of organic and inorganic materials. Carbohydrates, lipids, proteins and extractives are examples to organic constituents, while minerals such as sodium, phosphorus, calcium and iron are examples to inorganic matters. The relative amount of the major organic components in biomass is especially important in the development of biomass conversion processes [51].

Cellulose, hemicellulose, and lignin are the main polymers in the structure of biomass and their combination is called 'lignocellulose'. Cellulose constitutes a large portion of lignocellulosic materials followed by hemicellulose and lignin [55]. Typical levels and brief description of these components are given in Table 3.2.

Table 3.2: The proportion of major polymeric compounds in biomass and their description [55]

Component	Percent dry weight (%)	Description
Cellulose	40-60	A high molecular weight (10^6 or more) and linear chain of glucose molecules. Stable chain provides high strength to the skeletal structure of most terrestrial biomass. High insoluble and dominant component of wood.
Hemicellulose	20-40	A group of carbohydrates with short and highly branched chains of five-carbon. Unlike cellulose, it has a random, amorphous structure with little strength. Lower molecular weight than cellulose. Relatively easy to be hydrolyzed into basic sugars
Lignin	10-25	A three dimensional amorphous biopolymer consisting of highly branched polyphenolic constituents that provide structural integrity to plants. No exact structure and more difficult to be dehydrated than cellulose and hemicellulose.

Choosing a suitable biomass source that is utilized in a selected energy conversion process is essential to obtain maximum yield. Thus, understanding the particular material characteristics and deciding on the right type of biomass prior to be handled as an energy source become important. The principal biomass properties of interest that need to be taken into account during energy generation processes are as follows:

- Both intrinsic and extrinsic moisture content,
- Calorific value,
- Proportions of fixed carbon and volatiles,
- Ash/residue content,

- Alkali metal content,
- The ratio of cellulose to lignin

All of these properties excluding the last one are vital in dry biomass conversion processes whereas, the prime concerns of wet biomass conversion processes are the first and last properties. In addition to the main intrinsic biomass properties, which are listed above, growth rate of plant species, ease of management and harvesting are the other factors affecting the selection of biomass materials as an energy source [55].

Atomic ratios of O:C and H:C significantly affect the calorific value of solid fuels. Compared to fossil fuels, biomass has lower heating value due to its higher H:C and O:C ratios. Since the heating value of solid fuels is directly related to carbon content, the fuels with older geologic age like anthracite have the lower atomic ratios while, younger fuels such as peat and biomass have higher atomic ratios [56]. Comparison of various solid fuels from carbon-rich anthracite to carbon-deficient woody biomass based on the atomic ratios on a dry ash-free basis is known as Van Krevelen diagram, which is shown in Figure 3.1.

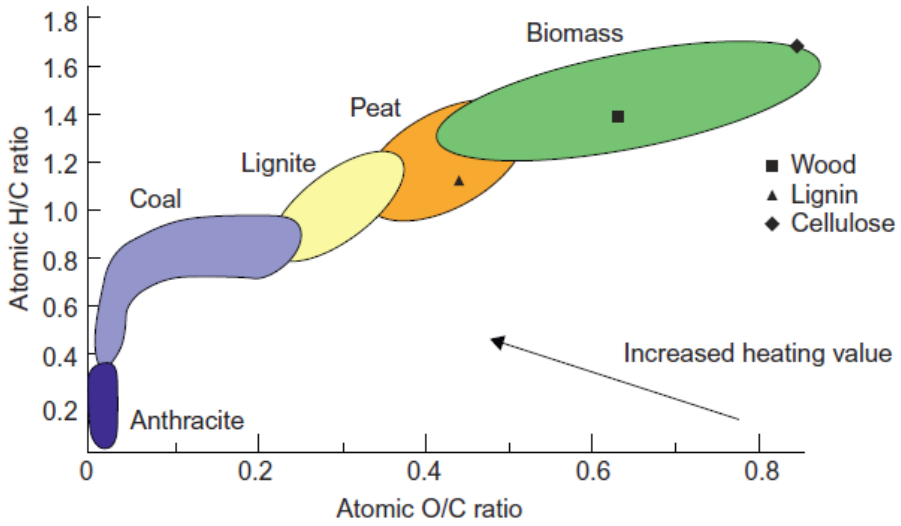

Figure 3.1 : Van Krevelen diagram for the classification of solid fuels by H/C and O/C ratio[57].

H:C ratio of biomass ranges between the values of 1.4-1.6 while, O:C ratio ranges from 0.55 to 0.75 according to Van Krevelen diagram. These atomic ratios of biomass can be changed by thermal treatment processes such as pyrolysis and torrefaction. As a result, the proportion of carbon increases and composition of biomass approaches to coal [58].

In general, the ultimate analyses of biomass species reveal that 30-40 wt% oxygen in dry matter basis present in the composition. Carbon, which is the other principal element in biomass, ranges between 30 wt% and 60wt% on dry basis depending on ash content. Furthermore, hydrogen constitute 5-6 wt% of biomass composition on dry basis. Low quantity of nitrogen, sulfur and chlorine also exist in biomass so that they comprise approximately 1% of dry basis of matter [59]. A typical proximate analysis of woody biomass shows the following results: volatile matter (80.0%, 74.7%), fixed carbon (19.4%, 24.0%) and ash (0.65%, 1.3%), respectively [60, 61].

The major elements in the inorganic matter of biomass are Na, K, Mg, P, Ca, Si and Cl [62]. Due to the pollutant emissions arising from the thermochemical conversion processes, significant attention must be given to prevent those emissions. The reaction between the alkali metals and silica in ash composition lead to the production of sticky, mobile liquid phase that result in fouling and slagging in the furnace and boiler plants. Moreover, alkali sulfates are formed on heat transfer surfaces of the furnace when alkali metals reacts with sulfur. Among the all alkali metals in biomass, potassium is the key source of alkali. Therefore, in order not to face with possible operational obstacles, ash composition should be analyzed prior to the utilization of biomass in conversion processes [63].

Du et al. studied the effect of fuel properties on biomass combustion and they showed that following components in biomass has gradually decreasing melting temperature that means ashes with high Al_2O_3 content do not cause agglomeration of ash owing to melting at relatively higher temperature [64]:

$$Al_2O_3 > MgO > CaO > P_2O_5 > Na_2O > K_2O.$$

3.3 Advantages and Disadvantages of Biomass as an Energy Source

Due to the decreasing fossil fuel resources and increasing concerns about global warming, biofuel production has gained considerable importance in recent years. However, use of biomass as an energy source has some advantages and disadvantages that need to be taken into account. The major advantages of biomass over coal or other fossil fuels, which are mostly presented by relating to environmental, technological, economic and social issues, are listed below considering composition and properties of each type of solid fuel [65,66].

- Renewable energy source for natural biomass
- Zero net emissions of CO_2 and climate change benefits
- Switching to low carbon economy, that is from hydrocarbon to carbohydrate and hydrogen resources
- Use of non-edible biomass, namely food supply is not affected
- Conservation of fossil fuels
- Low amount of ash, C, FC, N, S, Si and most trace elements in the composition
- High proportions of volatile matter, Ca, H, Mg and P, structural organic components, extractives, water-soluble nutrient elements
- Biodegradable resource with great reactivity and low initial ignition and combustion temperatures during conversion
- Huge and cheap resource for production of biofuels, sorbents, fertilizers, liming and neutralizing alkaline agents, building materials, synthesis of some minerals and recovery of certain elements and compounds
- Reduction of biomass residues and wastes
- Decrease of hazardous emissions (CH_4, CO_2, NO_X, SO_X, toxic trace elements)
- Capture and storage of toxic components by ash
- Use of oceans, seas, low-quality soils and non-agricultural, degraded and contaminated lands
- Restoration of degraded and contaminated lands
- Diversification of fuel supply and energy security
- Rural revitalization with creation of new jobs and income

The major disadvantages of biomass and fuels obtained from it by conversion processes are summarized and listed in below [67,68]:

- Lack of a full life cycle assessment of renewable energy resources of biofuels
- Rivalry with eatable biomass, fiber and biomaterial productions
- Natural ecosystem loss (water, soil, land use changes, deforestation, biodiversity, land degradation, fertilizers, pesticides, contaminants)
- Uncertainty of sustainable availability of biomass resources for production of biofuels and chemicals
- Lack of global monitoring and control of biofuels production with certification of origin and source

- Lack of common terminology, methodologies, standards and classification and certification systems
- Inadequate data and variability of composition, properties and quality for evaluation and validation
- High contents of moisture, water-soluble fraction, Cl, K, Na, O and some trace elements (Ag, Br, Cd, Co, Cr, Cu, Hg, Mn, Ni, Pb, Se, Tl, Zn, others)
- Low energy density (bulk density and calorific value)
- Low pH and ash-fusion temperatures
- Low bulk density and fine size of ash with increased dust inhalation risk
- Technical problems faced during processes (agglomeration, deposit formation, slagging, fouling, corrosion, erosion)
- Odor, emission and leaching during disposal and processing due to hazardous components
- Need for extra water, fertilizers and pesticides
- High costs of growing, harvesting, collection, transportation, storage and pre-treatment
- Regional and seasonal availability and local energy supply
- Limited practical experience in biofuel production and indistinct use of waste products
- Lack of developed biomass markets
- High investment cost

3.4 Biomass Energy Potential in the World

Among the all-renewable energy sources that are solar, wind, hydroelectric, biomass and geothermal power, biomass is the largest and versatile energy source [69]. Its dominance is expected to continue in the future as well since bioenergy contributes to climate change mitigations, provide energy security and generate new jobs. In 2013, the share of renewables in the final energy consumption of the world was 18% in which the contribution of bioenergy was 14% while hydroelectric and other types of renewable energy sources accounted for 4% in total as shown in Figure 3.2. The amount of sustainable biomass supply is estimated to increase up to three times in the near future. Furthermore, biomass is the only renewable energy source that can substitute fossil fuels in many different industrial sectors thanks to production of solid, liquid and gas fuels [70].

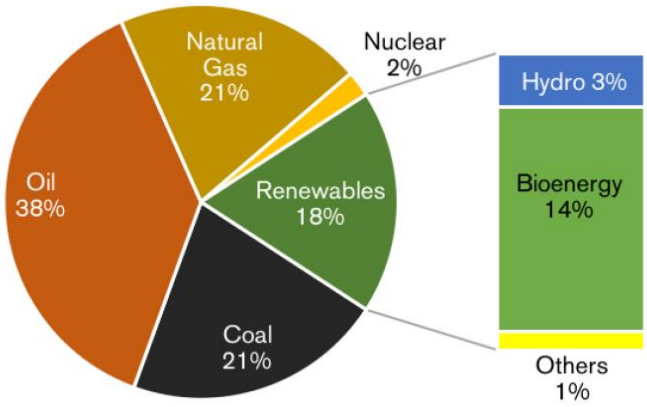

Figure 3.2 : Breakdown of global final energy consumption in 2013 [70].

The rate of global biomass production is estimated 146 billion metric tons per year involving mostly wild plant growth [71]. USA and Brazil, which are responsible for approximately 80% of world's biomass production, act as the leader countries in production and consumption of liquid biofuels for transport. 63 billion litres increase in the production of all biofuels was observed in the Americas between the years 2000 and 2012. It is considered that aviation sector will be crucial for use of biofuels in the future. On the other hand, biomass is mostly used for electricity generation in Europe and North America, particularly produced from forestry products and residues. So that, both continents account for more than 70% of all consumption of biomass for electricity. In recent years, biomass energy has been becoming a great interest of developing countries in Asia and Africa that suffer from the lack of electricity access even in this era.

Since time immemorial, biomass has been used for heating purpose, predominantly in rural and developing countries. Approximately 90% of all the bioenergy consumption is because of traditional use that referred to firewood and other small-scale use of bioenergy, which is still a relatively large energy source for heating and cooking. On the other hand, use of well-developed technology such as modern wood boiler or modern pellet boiler are named as modern use of biomass. Figure 3.3 demonstrates the share of biomass in final energy consumption worldwide according to the traditional and modern uses [70].

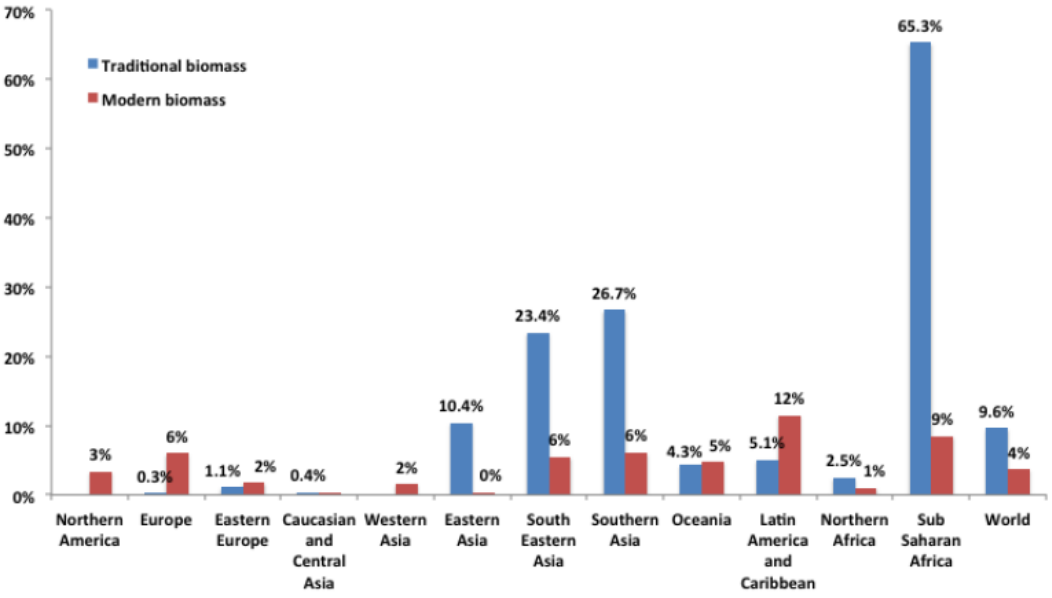

Figure 3.3 : Proportions of traditional and modern biomass consumption in final energy consumption worldwide [70].

Currently, biomass accounts for only 5% of primary energy consumption in industrialized countries contrary to developing countries where this percentage rises to 35% due to the dependence on biomass as an energy source [72]. Furthermore, woody biomass presents nearly 90% of the global primary energy annually produced from all types of biomass sources.

3.5 Biomass Energy Potential in Turkey

Thanks to the geographic location, Turkey is rich by most of the renewable energy sources. Due to the dependence on foreign energy, particularly oil, gas and high rank coal, utilization of biomass such as wood, hazelnut shell, agricultural waste residues, waste paper and wheat straw, tea waste and olive husk for energy production has become prominent in the country's energy strategy [73]. Turkey's biomass potential is approximately 8,6 million tonnes of equivalent petrol (MTEP) and the amount of biogas that can be produced from the available biomass sources is estimated in the range of 1,5-2 MTEP [74]. As an agricultural country, greatest amount of biomass energy is generated from agricultural wastes in Turkey. Besides, forestry and animal wastes are also important biomass energy sources [75]. Current data for the quantities of several biomass in Turkey along with their energy equivalent values, the number of companies with biodiesel and bioethanol processing license and the

number of electricity generating biomass-based power plants is shown in Table 3.3 [74].

Table 3.3 : Current status of biomass energy in Turkey [74].

Biomass sources	**Energy value (TEP/year)**
Animal wastes	1 323 714.67
Agricultural wastes	15 941 321.26
Forestry wastes	855 805
Municipal solid organic wastes	2 186 228.09
Total	**20 307 069.02**
The number of companies that have biodiesel processing license	24
The number of companies that have bioethanol processing license	3
The number of biomass based power plants	42

Wood is the most significant biomass energy source in Turkey since it accounts for almost 20% of the total biomass production. Moreover, conversion of wood to useful energy is relatively easy when compared to other biomass types [76]. It is estimated that electricity production in biomass based power plants where wood is used primarily, will rise to about 50 GW in 2030 while it was 10 GW in 2009. Related to this capacity increase, 6.4 billion USD in personal and corporate income along with the 250,000 job opportunities is expected as the economic welfares [77].

Table 3.4 : Current and planned energy production by biomass in Turkey [79].

Years	Modern Biomass (ktoe)	Classic biomass (ktoe)	Total (ktoe)
2008	1640	5976	7616
2010	1710	5754	7464
2012	2121	5364	7485
2014	2543	5082	7625
2016	2854	4856	7710
2018	3284	4568	7852
2020	3598	4234	7832
2022	3860	3976	7836
2024	4086	3785	7871
2026	4472	3556	8028
2028	4732	3322	8054
2030	4940	3300	8240
Total	**39840**	**53773**	**93613**

At present, conventional biomass has an important role in energy production in Turkey. So that, wood which, is the major classic biomass resource, is mainly used for directly heating and cooking in rural regions [75]. Contrary to conventional biomass, modern biomass is obtained in sustainable way from renewable resources [78]. The conventional and planned modern biomass energy production in Turkey is given in Table 3.4 [79].

3.6 Thermochemical Conversion of Biomass

Conversion of biomass into solid, liquid and gaseous products via thermochemical methods is performed to improve biomass characteristics and produce biofuel. The primary thermochemical methods for conversion of biomass are combustion, carbonization, torrefaction, pyrolysis, gasification and liquefaction, which were described elaborately in Section 2.6 except torrefaction. Thus, only torrefaction will be described comprehensively in this section. In addition, although pyrolysis was explained for coal in Section 2.6.1, a brief description of biomass pyrolysis will also be introduced here. Comparison of thermochemical conversion methods for biomass along with the typical range of their reaction temperatures are given in Table 3.5 [80].

Table 3.5 : Comparison of main thermochemical conversion technologies [80].

Process	Temperature (°C)	Pressure (MPa)	Catalyst	Drying
Liquefaction	250-330	5-20	Essential	Not required
Pyrolysis	300-600	0.1-0.5	Not required	Necessary
Combustion	700-1400	≥0.1	Not required	Not essential, but may help
Gasification	500-1300	≥0.1	Not essential	Necessary
Torrefaction	200-300	0.1	Not required	Necessary

3.6.1 Pyrolysis

The basis of the thermochemical conversion processes is biomass pyrolysis that yield products including charcoal (carbonaceous solid), tars and permanent gases such as methane, hydrogen, carbon monoxide and carbon dioxide by thermal decomposition of biomass in the absence of oxygen [81]. Pyrolysis can be carried out at different final temperatures and heating rates with respect to the desired product. Table 3.6 depicts the several modes of biomass pyrolysis and proportions of liquid, solid and

gas products obtained in each case. As it can be seen from the table, lower temperatures and longer vapor residence times favor the production of charcoal, whereas, high temperatures and longer residence times lead to the formation of gas products mostly. Moderate temperatures and short vapor residence time result in the production of liquids [36].

Table 3.6 : Different conditions of biomass pyrolysis [36].

Mode	Conditions	Liquid (%)	Char (%)	Gas (%)
Fast	Moderate temperature, around 500°C, Short hot vapour residence time, ~1 s	75	12	13
Intermediate	Moderate temperature, around 500°C, Moderate hot vapour residence time, ~10-20 s	50	20	30
Slow (Carbonization)	Low temperature, around 400°C, very long residence time	30	35	35
Gasification	High temperature, around 800°C, long residence time, ~1 s	5	10	85

Since liquids are easy to store and transport at a lower cost than solid biomass, fast pyrolysis for liquid production has been a hot topic in recent years. Fast pyrolysis takes place in a time of a few seconds or less that requires special care during the process in order to obtain high yields of liquid.

Ensuring that the reaction between the biomass particles occurs at the optimum process temperature and minimizing their exposure to lower temperatures to prevent formation of charcoal are the critical concerns of fast pyrolysis. Hence, finely ground biomass particles are used in most cases to achieve constant reaction temperature throughout the whole feed [82].

3.6.2 Torrefaction

Torrefaction is a thermochemical process that is carried out under inert or limited oxygen atmosphere and operated slowly within a specified low temperature range to upgrade lingo-cellulosic biomass to a higher quality and more attractive biofuel. Torrefaction is applied to prepare biomass for further use such as gasification and co-firing instead of direct use in its raw form. The main fields in which torrefied biomass is used are as follows:

- Co-combustion of biomass and coal blends in large coal-based power plant boilers
- Use as fuel in distributed or residential heating system
- Use as a suitable fuel for gasification
- Potential feedstock for chemical industries
- Substitute for coke in blast furnace for decline in carbon footprint [49].

Torrefaction process is operated at low temperature range of 200-300°C. Although some researchers has increased the typical minimum temperature to some extent, none surpasses the maximum temperature of 300°C since extensive devolatilization and carbonization of polymers, which are unwanted for torrefaction, occur.

Fibrous structure and tenacity of biomass is destructed as a result of the thermal treatment so that biomass becomes easily grindable. The removal of oxygen with a final solid product is the main principle of torrefaction process [84]. In other words, O/C ratio is lower in torrefied biomass compared to the raw biomass.

Change in the elemental composition of raw biomass after torrefaction process is illustrated by Van Krevelen diagram that is shown in Figure 3.4. As it is seen from the figure, torrefied biomass approaches to coal due to the property changes in the direction of carbon [85].

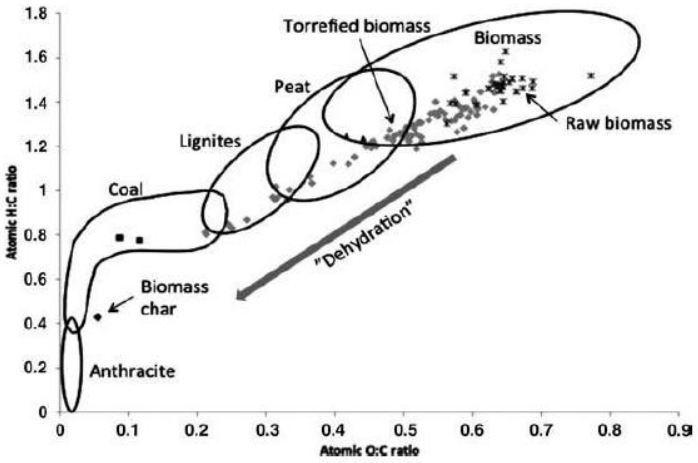

Figure 3.4 : Van Krevelen diagram that demonstrates the changes in atomic ratio of torrefied biomass [58].

As a thermal pretreatment process, torrefaction is accomplished by contact with a heating medium or heat carrier. Basic illustration of torrefaction process is

demonstrated in Figure 3.5 that shows the changes in mass and energy content of woody biomass during conversion into torrefied form.

Torrefaction of biomass causes a mass loss due to devolatilization, but increases the calorific value. Typically, 70% of the mass is retained in solid products that contain 90% of the initial energy content [86]. Thus, energy density of biomass increases by torrefaction in comparison with original biomass that facilitates transportation to large distances [87].

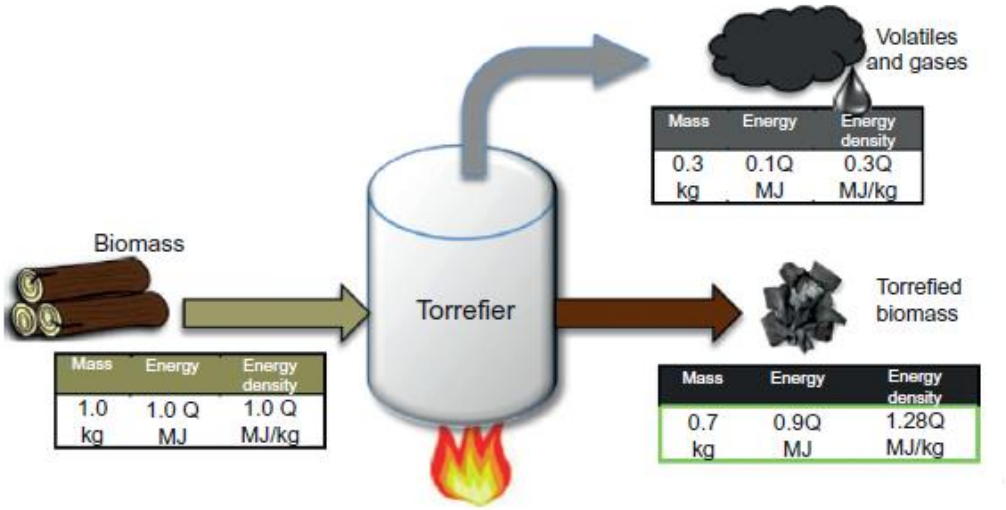

Figure 3.5 : Mass and energy balance during torrefaction of biomass [49].

The overall torrefaction process may be divided into five regimes:

- Regime A (50-120°C): Physical moisture in biomass structure is released such that chemical composition remains unchanged. Biomass shrinks during this step; however, it may recover its structure if rewetted [88].
- Regime B (120-150°C): Lignin is exposed to softening and as a result, it acts as a binder.
- Regime C (150-200°C): This stage called reactive drying because of the destructions in fibrous structure and tenacity of biomass. Breakage of hydrogen and carbon bonds along with the depolymerization of hemicelluloses is initiated in this stage. At the end of this regime, biomass cannot regain its structure upon wetting.
- Regime D (200-250°C): This regime initiates the torrefaction which continues and ended in the next stage. Limited devolatilization and carbonization of

solid product obtained in regime C take place in this stage. Most inter and intramolecular hydrogen, C-C and C-O bonds are cracked resulting in the formation of condensable liquids and non-condensable gases.

- Regime E (250-300°C): During this period, most of the mass loss of the biomass due to the decomposition of hemicellulose into volatiles and solid products occurs. On the other hand, lignin and cellulose go through only a limited amount of devolatilization and carbonization. Biomass structure is entirely destroyed in this regime and turned into brittle and nonfibrous form [49].

Devolatilization and carbonization of the three major biomass polymers occur in different temperature range. That is between 225-300°C for hemicellulose, 305-375 °C for cellulose and 250-500°C for lignin. Since upper temperature limit for torrefaction process is 300°C, degradation of hemicellulose content of the biomass is the principal attractions of torrefaction technology.

Liquid, solid and gas products are obtained at the end of the torrefaction process. Figure 3.6 shows the content of torrefaction products based on the different phases.

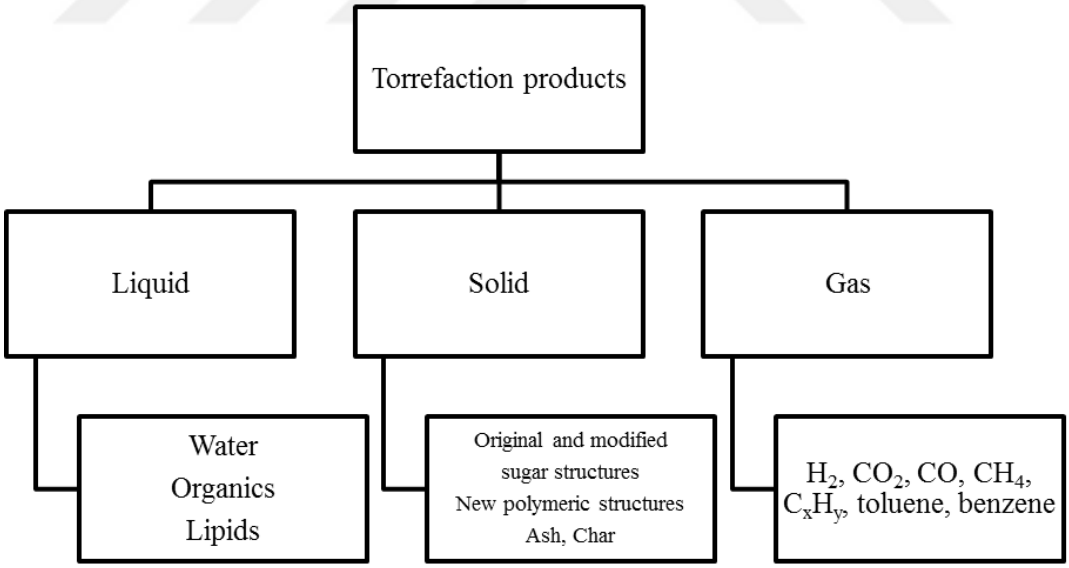

Figure 3.6 : Products obtained by torrefaction of biomass [49].

In order to maximize the solid yield of the process, it is operated at slow heating rate that is one the main important characteristics of torrefaction. Normally, heating rate of torrefaction is less than 50°C/min. Higher heating rate causes the formation of more amount of liquid products, which is aimed in pyrolysis [49].

Advantages of torrefaction in terms of improved product characteristics and system benefits along with the challenges and some issues against that require further researches to attain commercial success are listed in Table 3.7.

Table 3.7 : Advantages and challenges of torrefaction process [58].

Advantages	Challenges and important development areas
Improved product characteristics	
• Enhanced bulk energy densities along with densification	• Investment costs
• Increased heating value	• Operating costs
• Better heating value	• Yield (Energy loss)
• Decrease in oxygen content	• Secure densified product yield and quality
• Dry and hydrophobic nature	• Not yet commercially available
• Lack of biological presence	• Storage issues
• Reduced chlorine content	- Leakage to recipient
• Increased friability, reducing grinding costs and particle size, increase of particle surface area	- Smell and dust
• Better quality and homogeneity	• Neither processes nor product yet fully industrially proven
• Cleaner burning fuel with less acid rains	
System benefits	
• Refined fuel facilitating efficient gasification	
• Allowing co-firing ratios	
• Increased feed ability (after grinding) facilitating use of existing and new dry and wet feeding systems	
• Torrefaction plant full year heat sink for CHP integration	

Although torrefaction process can be confused with carbonization, mild pyrolysis, roasting and wood cooking, the aim and process conditions of these methods are different. Table 3.8 shows major differences between torrefaction, pyrolysis and carbonization.

Table 3.8 : Sequential thermal degradation processes of biomass when it is heated in inert environment [49].

Temperature Range of Heating (°C)	Process that Occurs	Heating Rate	Process	Solid Product
20-110	The wood is preheated and it approaches 100°C, moisture starts evaporating	Low/fast	Drying	Bone dry wood
110-200	Further preheating removes traces of moisture and slight decomposition starts	Low/fast	Postdrying preheating	Preheated dry wood
200-270	Wood decomposes realizing various volatile	Low	Torrefaction	Mildly torrefied wood
270-300	Exothermic decomposition starts releasing condensable and noncondensable vapors	Low	Torrefaction	Severely torrefied wood
300-400	Wood structure continues to break down. Tar release starts to predominate	Low	Low temperature carbonization	Low fixed carbon charcoal
		High	Pyrolysis	Liquid
400-500	Residueal tar from charcoal is released	Low	Carbonization	High fixed carbon charcoal
		High	Pyrolysis	Liquid
>500	Carbonization is complete		High temperature carbonization	Tar-free charcoal
			Pyrolysis	Liquid, higher gas release

4. CO-COMBUSTION OF LIGNITE AND BIOMASS BLENDS

Utilization of coal and biomass within the same process, so called co-combustion or co-firing is a promising technology which needs further study to achieve definitive results and applications. Studies on co-combustion were conducted with the pursuit of pollutant reduction, use of rapidly accumulating non-utilized biomass feedstock instead of diminishing fossil fuels and achieving better combustion process conditions.

Biomass is a sustainably renewable resource having net zero carbon dioxide emission and very low sulphur content [89]. Co-combustion of coal and biomass in conventional coal-fired power plants is one of the best short term solutions for reducing CO_2 emission using renewable fuels. Plus, biomass co-combustion has higher energy conversion efficiency than other biomass combustion methods for power generation. Studies show that 60 Mt of CO_2 could be reduced annually in case of sole 1% of electricity generation could be provided by using biomass [90]. Utilizing the mixture of biomass and coal reduce the fossil fuel dependence. Using biomass contributes to achieve optimum combustion conditions and it has also economic advantages in retrofitting to existing plants [91].

Various techno-economic aspects should be considered before co-combusting biomass and coal, including:

- Accessibility of biomass fuel and logistics,
- Biomass characteristics, delivery and storage,
- Pre-treatment of biomass to be in compliance with combustion and boiler conditions,
- Alteration in combustion behavior,
- Effects of slagging, fouling and corrosion in combustion chamber due to high inorganic components of biomass,
- By-product utilization [92].

In order to understand co-combustion behaviors of biomass and coal, many studies were conducted on characterization of biomass and coal blends. Technical advantages and difficulties, discussion of past experiences, current applications and co-combustion methods were also presented in various publications.

Xiao et al. studied the combustion behavior of coal, straw, sewage sludge and their blends in a thermogravimetric analyzer. In order to see the effect of oxygen concentration on combustion, oxygen/nitrogen mixtures with five varying ratio was used. It was concluded that temperature volatile matters were released, weight loss and final temperature of weight stabilization decreased as the oxygen concentration increased. It was also obtained that maximum weight loss increases with increasing heating rate [93].

Kastanaki and Vamvuka worked with four biomass chars, lignite and a hard coal char and their blends. Using the specific reaction rate as a function of conversion, reactivities of ssamples were calculated. It was found that biomass chars are more reactive compared to hard coal and lignite. Ratio of each component in the mixture and rank of coals vaguely affected the combustion behavior. Lignite-biomass chars were found to be more susceptible to reactivity change than coal-wood chars, which was an imperative outcome [94].

Demirbas studied co-combustion of several biomass fuels with coal, comparing their physical, chemical, combustion and ash properties. He also argued technology choices for co-combustion and co-combustion, gasification and pyrolysis mechanism [95].

Tillman summarized his past experiences at several US based co-combustion power plants providing boiler efficiency emission and co-combustion process data for many plants with brief descriptions of technologies [96].

Sami et al. did a literature review on co-combustion of coal with biomass. Fundamental concepts and technologies for co-combustion was argued. Various experimental and numerical results of studies regarding co-combustion was provided along with problems related to co-combustion [66].

Savolainen presented his experiences at Naantali Power plant utilizing sawdust with coal co-combustion. Effects of sawdust on boiler performance, flame stability and emissions were discussed [97].

Baxter studied technical boiler problems due to co-combustion mainly include fuel supply, treatment, storage, ash deposition, fuel conversion, emission, corrosion. Possible methods to deal with corrosion, fly ash handling and impacts on selective catalytic reduction are presented [98].

Al-Mansour and Zuwala summarized worldwide co-combustion applications, along with contemporary technologies, crucial points to evaluate biomass co-combustion methods. Indirect co-combustion was found to be the most preferable method after evaluations conducted on co-combustion technologies in Europe [99].

Amand et al. showed that potassium is a crucial element in most biomass that gives rise to deposition and fouling on the equipment surfaces. However, sulphur content of the coal that biomass is mixed may interact with potassium to inhibit these harmful effects [100].

4.1 Advantages and Disadvantages

Similar to many other fuel utilization techniques co-combustion of biomass and coal has various advantages and disadvantages. The most crucial advantages are depicted in below [66,101]:

- In case of one of the sources of fuel is not available, power production could be sustained by suitable alterations of the co-combustion rate, which is very desirable for large power plants
- Improving local economy by also utilizing unproductive lands
- Preservation of fossil fuel reserves
- Reduce in pollutants
- Less need for landfills in case of using waste materials as biomass, which also reduce methane emissions damaging the environment
- Considerably lower investment cost due to retrofitting to existing power plants
- Lower CO_2 emission due to net zero carbon dioxide release nature of biomass
- Higher volatile matter content of biomass give rise to better burn out and lower unburnt carbon content in the ash.

Apart from its many promising advantages, co-combustion has also several disadvantages to be considered. Some of these disadvantages are given in the following [66,101]:

- Reduce in power generation due to lower heating value of biomass and waste in general
- Seasonal dependence on biomass sources
- Cost of pre-treatment of biomass
- Storage and logistic problems due to intrinsic biomass properties such as biodegradation and low density
- Additional gas scrubbing costs due to some biomass having high chlorine content
- Additional particulate removing cost due to excessive particulate generating nature of biomass

4.2 Commercial Applications of Co-Combustion in the World

It is possible to categorize co-combustion methods used in coal-fired power plants in three models, which are given below [102]:

- Direct co-combustion: Direct co-combustion is the most cost-efficient, simple and thus, conventional choice in the industry. Biomass and coal are burned in same combustion chamber and also in same mills and burners if the biomass fuel characteristics comply.
- Indirect co-combustion: In this method, biomass is gasified and the produced gas is combusted in the main chamber along with the other fuel. The need for gas to be cleaned or cooled could lead to complexity and higher operational costs. This method could be preferred due to its fuel variability.
- Parallel co-combustion: A completely different biomass boiler can be used for steam generation. The steam is then utilized in the power plant along with the main steam. Pulp and paper industries prefer this method as they have dedicated biomass boilers for the bark and waste wood.

Co-combustion is now a common application in the United Kingdom. The most plants in UK burn biomass with a varying 5-10% biomass-coal ratio. The United States plants also started utilizing biomass mostly using a 10% ratio. Boiler

efficiency in these circumstances can decrease by up to 2%. Biomass used in these plants is generally wood wastes and wood pellets [103]. As it can be seen from Figure 4.1, Europe and North America are places having the most biomass utilizing co-combustion power plants in the world [99].

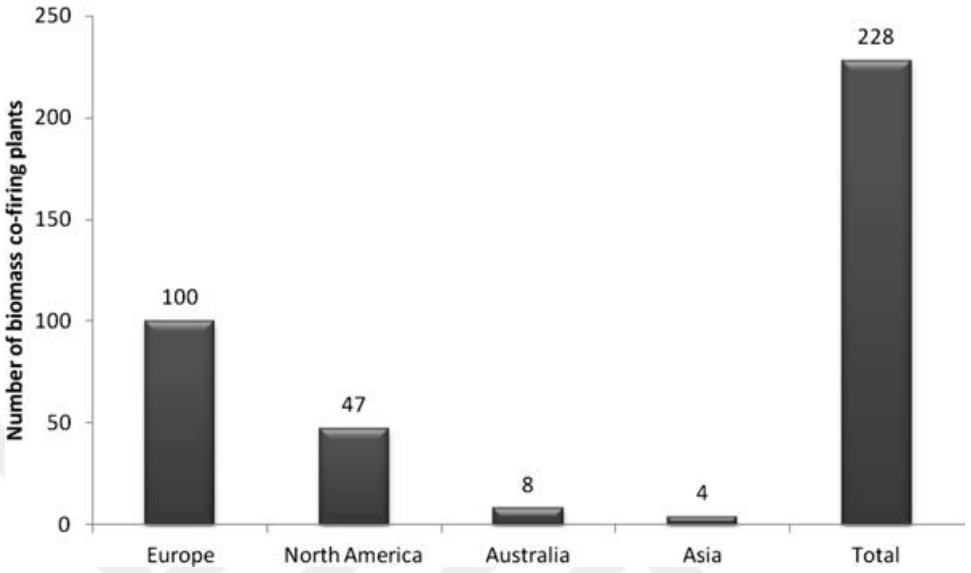

Figure 4.1 : Worldwide distribution of biomass co-firing power plants [99].

The two most preferred biomass utilizing co-combustion power plant types are pulverized and circulated fluidized bed power plants. Table 4.1 and Table 4.2 show locations of the largest power plants with their feedstock type and capacity [104].

Table 4.1 : Pulverized coal plants co-utilizing coal and biomass/wastes [104].

Owner/Location	Feedstock/Capacity
Epon/Nijmegen, Holland	Coal and waste wood/602 MW
Lakeland Electric/Florida, United States	Coal and RDF/350e and RDF/350 MW
VEAG/Magdeburg, Germany	Coal and wood/350 MW
Vasthamnsvert Uppsala Energi/Uppsala, Sweden	Coal, peat, and wood/320 MW
Elsam/Amager, Denmark	Coal, straw, and miscanthus/250 MW
Vasthamnsvert CHP/Halsingbourgi, Sweden	Coal and wood/180 MW
TVA/Tennessee, United States	Coal and waste wood/150 MW
Midkraft/Esbjerg, Denmark	Coal and Straw/150 MW
GPU GENCO/Illinois, United States	States Coal and waste wood/130 MW
Bayernwerke Ag/Bavaria, Germany	Coal and straw/108 MW
Georgia Power/Hammond, United States	Coal and waste wood/100 MW
Ames municipal/Iowa, United States	Coal and RDF/75 MW
Saarbergwerke, AG/Saarberg, Germany	Coal and sewage sludge/75 MW
SEPCO/Savannah, United States	Coal and waste wood/54 MW
Stockholm Energy/Hasselbyvaerket, Sweden	Coal, wood, and olive waste/54 MW
Iowa light and power/Iowa, United States	Coal and agri waste/45 MW

Table 4.2 : Circulating Fluidized Beds Co-utilizing Coal and Biomass/Wastes [104].

Owner/Location	Feedstock/Capacity
Rumford, Cogen Co./Rumford, United States	Coal, oil, wood/260 MWth, 76 MWe
Kainuun Voima Oy/Kajaani, Finland	Coal, peat, wood sludge/240 MWth, 85 MWe
Black River Partners/Fort Drum, United States	Coal, anthracite, wood/168 MWth
Rauma mill/Rauma, Finland	Coal, peat, sludge, bark/160 MWth
UDG Niagara, Goodyear/Niagara Falls, United States	Coal, tires/149 MWth
P.H. Glatfelter Co./Spring Grove, United States	Coal, anthracite, wood, oil/132th
Norrkopings Kraft/Norrkoping, Sweden	Coal, wood/125 MWth
Southeast paper/Dublin, GA, United States	Coal, sludge/125 MWth, 65 MWe
IVO/Kokkola, Finland	Coal, peat, RDF, wood/98th
Lenzing, AG/Lenzing, Austria	Coal, lignite, wood, sludge/94th
Karlstad Energiverken/Karlstad, Sweden	Coal, wood, waste/90 MWth
Etela-Savon Energia/Mikkeli, Finland	Coal, lignite, wood waste, oil, gas/84 MWth
Brista, Kraft AB/Sweden	Coal, wood, various wastes/80 MWth, 40 MWe
Nykoping Energiverk/Nykoping, Sweden	Coal, wood, peat/80 MWth
Metsa-Sellu Oy/Aanekoski, Finland	Coal, wood waste, peat, oil/76 MWth
Midkraft Power Co./Grenaa, Denmark	Coal, straw/60 MWth, 17 MWe
Papyrus Kopparfors AB/Fors, Sweden	Coal, peat, wood/56 MWth
Patria Papier & Zellstoff/Frantschach, Austria	Coal, lignite, oil, wood/55th
Hunosa power station/La Pereda, Spain	Coal, coal wastes, wood wastes/50 MWe
Caledonian paper plc./Scotland, United Kingdom	Coal, wood, oil/43 MWth
Solvay Osterreich/Ebensee, Austria	Coal, lignite, gas, oil, wood/38th
Sande Paper Mill A/S, Norway	Coal, wood, RDF/26 MWth
Ostersunds Fjarrvarme/Ostersund, Sweden	Coal, wood, peat/25 MWth
Lieksa, Finland/Lieksa, Finland	Coal, peat, bark, sawdust/22 MWth, 8 MWe
Kuhmon Lampo Oy/Kuhmo, Finland	Coal, peat, wood waste/18 MWth
Avesta Energiverk/Avesta, Sweden	Coal, peat, wood/15 MWth
Ba Yu paper/Peikang, Taiwan	Coal, sludge/NA
Slough Estates/Slough, United Kingdom	Coal, wastepaper/NA

5. DSC KINETICS METHODS

Differential Scanning Calorimetry (DSC) is a technique to measure incoming or outgoing heat flow of a sample under a controlled thermal profile. Both qualitative and quantitative properties of sample can be obtained using DSC such as glass transition, crystallization, curing, melting and decomposition. DSC not only measures the transition temperature or heat, but also the rate (kinetics) of reaction.

There are three common methods for DSC kinetic studies which are Borchardt and Daniels, ASTM E698 thermal stability and isothermal kinetics. All methods are used for only particular transitions in which they are accurate so that selecting the appropriate method is very important [105].

5.1 Borchardt and Daniels Kinetics Approach

Borchardt and Daniels (B/D) approach allow the calculation of activation energy (E_a), pre-exponential factor (Z), heat of reaction (ΔH), reaction order (n), and rate constant (k) from a sole DSC scan [106]. This approach based on the idea of the reaction follows nth order kinetics, comply with general rate equation and Arrhenius principle.

$$\frac{d\alpha}{dt} = k(T) * [1 - \alpha]^n \quad \textbf{(5.1)}$$

Where $\frac{da}{dt}$ = reaction rate (s^{-1})

α = fractional conversion

k(T) = specific rate constant at temperature T

n= reaction order

$$k(T) = Z.e^{-Ea/RT} \quad \textbf{(5.2)}$$

Where E_a = activation energy (J/mol)

Z = pre-exponential factor (s^-1)

R = universal gas constant = 8.314 (J/molK)

Substituting equation (5.2) into equation (5.1) and rearranging gives:

$$\frac{d\alpha}{dt} = Z.e^{-Ea/RT}(1-\alpha)^n \quad \textbf{(5.3)}$$

$$Ln\left(\frac{d\alpha}{dt}\right) = Ln(Z) - \frac{Ea}{RT} + n\ln(1-\alpha) \quad \textbf{(5.4)}$$

Multiple linear regression can be used to solve Equation (5.4) where $d\alpha/dt$ and α are determined from DSC exotherm as given in Figure 5.1. Activation energy (E_a) and pre-exponential factor (Z) are obtained from the slope and intercept of plot of $\ln[k(T)]$ versus $1/T$ as given in Figure 5.2.

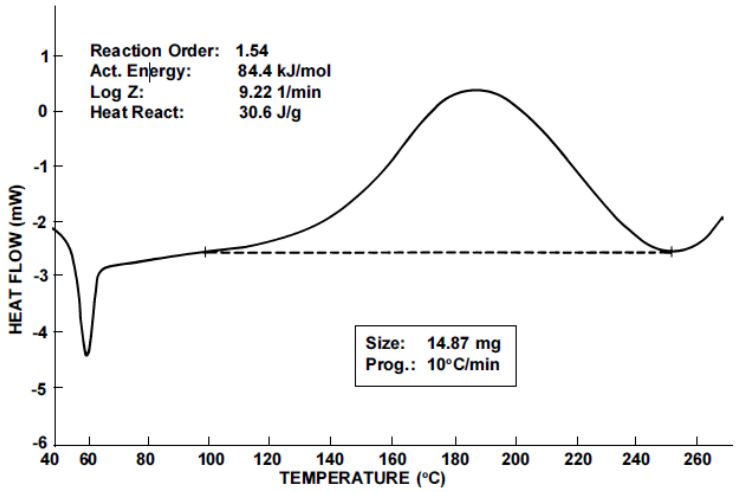

Figure 5.1 : An example of DSC exotherm for kinetic analysis.

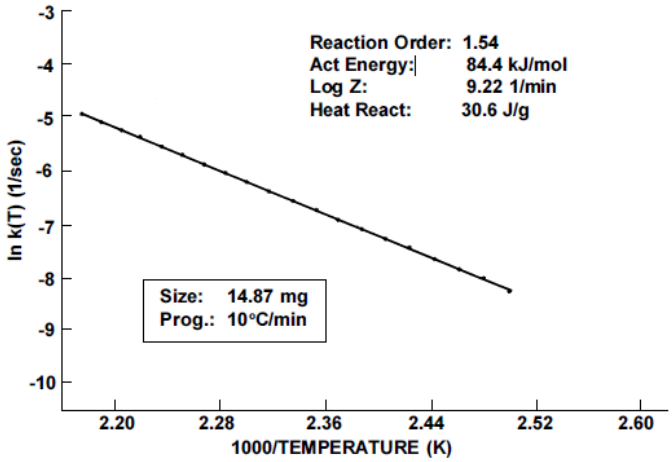

Figure 5.2 : Calculation of kinetic parameters.

B/D kinetic approach provides two predictive curves which are isothermal plots and isoconversion plots as shown in Figure 5.3 and Figure 5.4, respectively. Degree of conversion and time conditions are gathered from isothermal plots while

isoconversion plots gives time and temperature condition for a particular conversion rate. Both plots are very helpful for obtaining preferred final product.

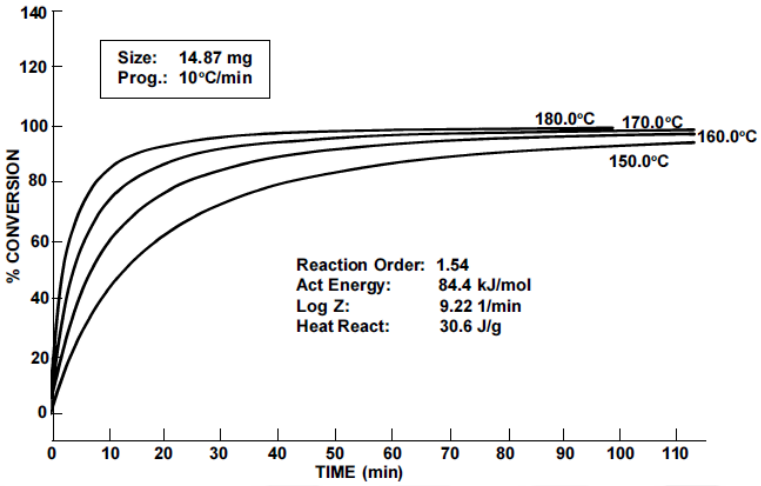

Figure 5.3 : An example of isothermal plot.

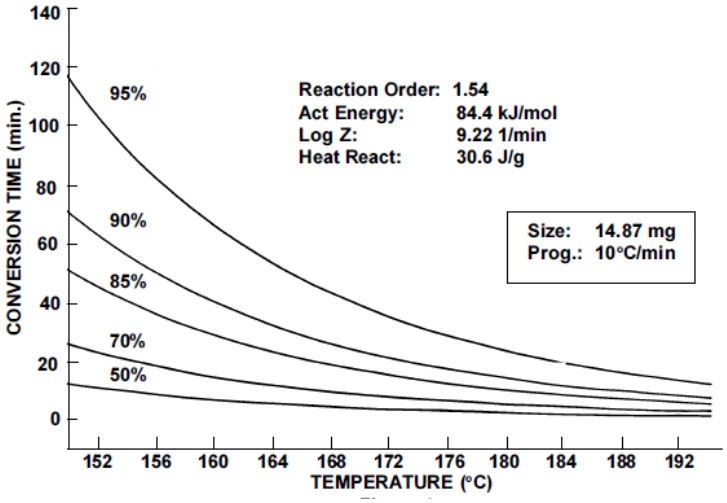

Figure 5.4 : An example of isoconversion plot.

5.2 ASTM E698 Thermal Stability approach

ASTM E698 kinetics method is based on the works of Ozawa on variable program rate method which requires three or more experiment at various heating rates, mostly between 1 and 1C/min. This method based on the principle of Arrhenius behavior and first order reaction kinetics giving the equation:

$$\frac{d\alpha}{dt} = Z.e^{-Ea/RT} * (1-\alpha) \qquad \textbf{(5.5)}$$

Where $\frac{da}{dt}$ = reaction rate (sec^{-1})

α = fractional conversion

E_a = activation energy (J/mol)

Z = pre-exponential factor (sec^{-1})

R = universal gas constant = 8.314 (J/molK)

Since $\beta = \frac{dT}{dt}$, where β is heating rate, equation 5 can be rearranged to:

$$\beta.\frac{d\alpha}{dT} = Z.e^{-Ea/RT} * (1-a) \qquad \textbf{(5.6)}$$

ASTM E698 kinetics method assumes that extent of the reation at the peak exotherm, α_p, is constant and not related to heating rate [107].

Activation energy (E_a), pre-exponential factor (Z), rate constant (k), and half-life ($t_{1/2}$) can be calculated from the information obtained from the plot of natural logarithm of the program rate versus the peak temperature. It is also possible to plot isothermal, isoconversion and half-life data using calculated kinetic parameters E_a, Z and k.

5.3 Isothermal kinetics approach

Both B/D and ASTM E698 approaches are dynamic and not applicable to quantitative studies on autocatalyzed systems, although they are fast and easy to use. Autocatalyzed systems have intermediate species which has a catalytic effect on the reaction rate. Isothermal kinetics can be applied the reaction with nth order and autocatalyzed exothermic systems. Commonly, this approach is not chosen to model endothermic reactions or crystallization kinetics [105].

$$\frac{da}{dt} = k\,\alpha^m\,(1-\alpha)^n \qquad \textbf{(5.7)}$$

$$k = Z\,e^{-Ea/RT} \qquad \textbf{(5.8)}$$

Where $\frac{da}{dt}$ = reaction rate (sec^{-1})

k = rate constant (sec^{-1})

α = fractional conversion

m,n = reaction orders

Follow algorithm given in Figure 5.5 can be followed in order to reach the best option of kinetics model for DSC [105].

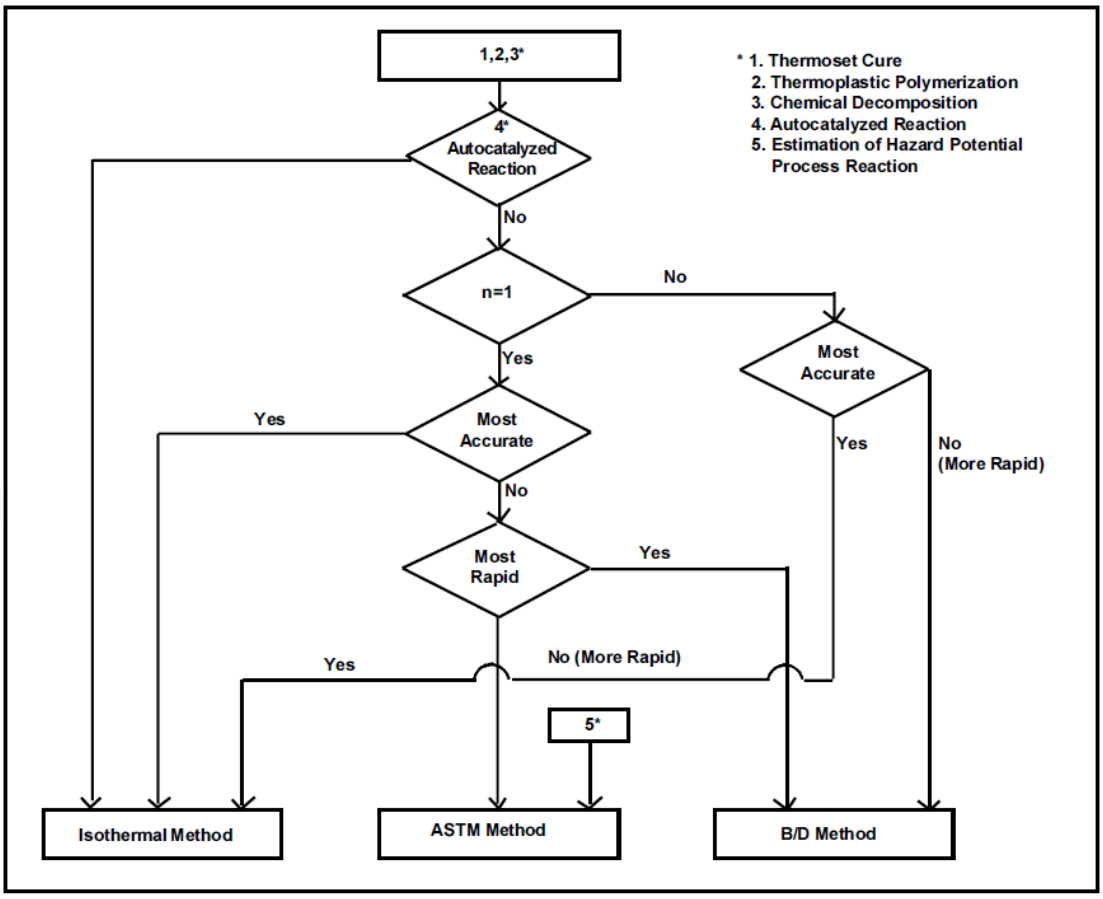

Figure 5.5 : Algorithm for calculation of kinetic parameters.

6. EXPERIMENTAL STUDIES

Experimental studies were summarized in flowchart, displayed in Figure 6.1.

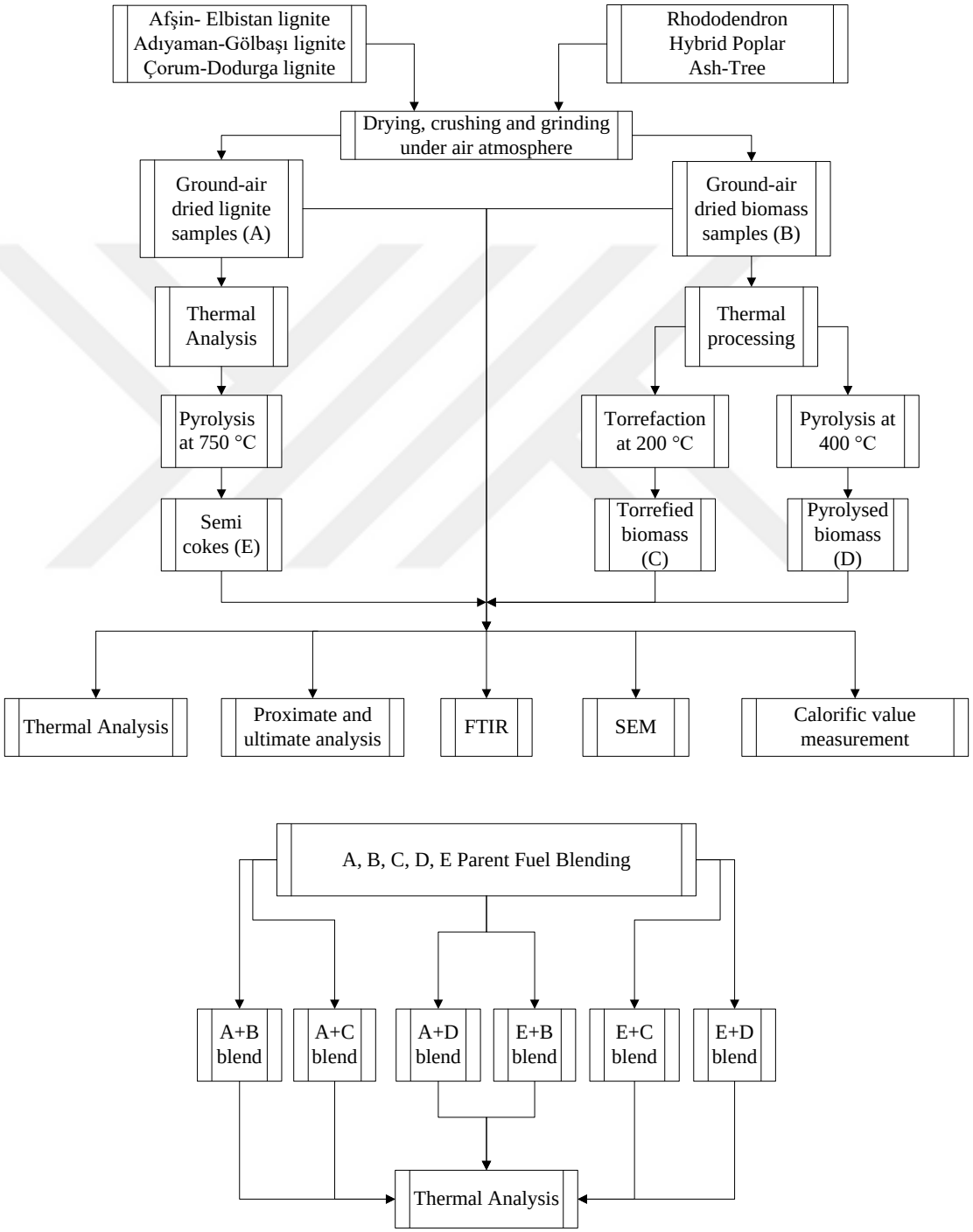

Figure 6.1 : Flowchart of experimental studies.

6.1 Materials

Afşin-Elbistan (AE), Adıyaman-Gölbaşı (AG), Çorum-Dodurga (CD) lignites and rhododendron (RD), hybrid poplar (HP), ash-tree (AT) biomass were used in this study.

6.1.1 Lignites

Afşin-Elbistan lignite deposit, which is located in the southeast of Turkey in Kahramanmaraş Province within Afşin and Elbistan regions as shown in Figure 6.2 is the most important domestic primary energy resource in Turkey with a reserve of 3.4 billion metric tonnes [108]. Despite the low quality of lignite deposit which is characterized by the average calorific value of 1070 cal/kg, ash content of 17% and moisture content of 55%, Afşin-Elbistan (A and B) power plant that was constructed in the close proximity to the Afşin-Elbistan mine serves as the biggest lignite-fired power plant in Turkey [109].

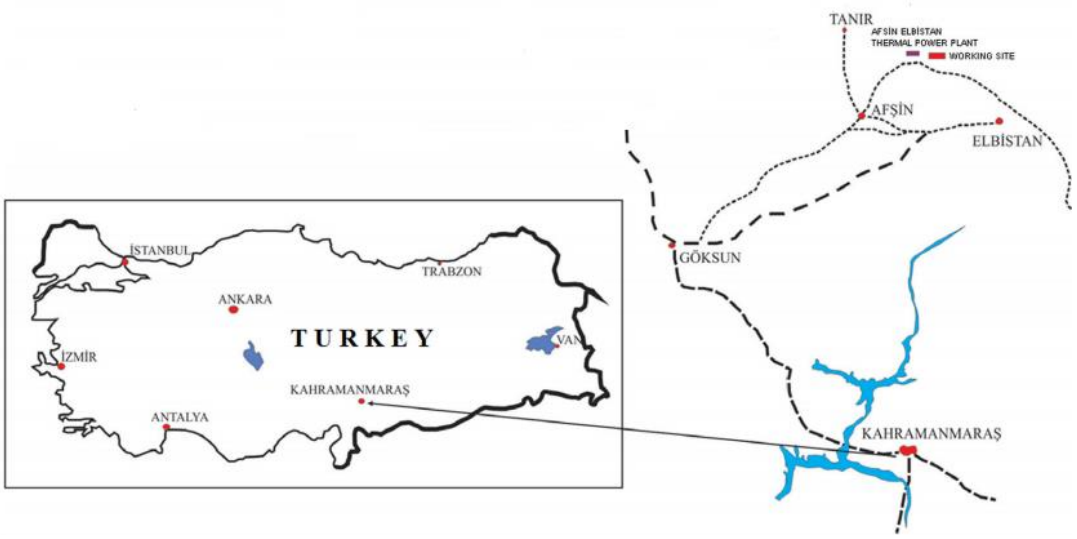

Figure 6.2 : Afşin-Elbistan lignite deposit and the nearby thermal power plant [109].

Adıyaman-Gölbaşı lignite basin is located in the southeastern part of Turkey and has 53 million tonnes (Mtonnes) of proven reserves [110]. It consists of 49.07% moisture, 14.54% ash, 22.74% volatile matter, 13.65% fixed carbon and 1.45% total sulfur in original base. Lower heating value of this lignite is 1736 kcal/kg [111]. Figure 6.3 shows the site location of Adıyaman-Gölbaşı lignite basin.

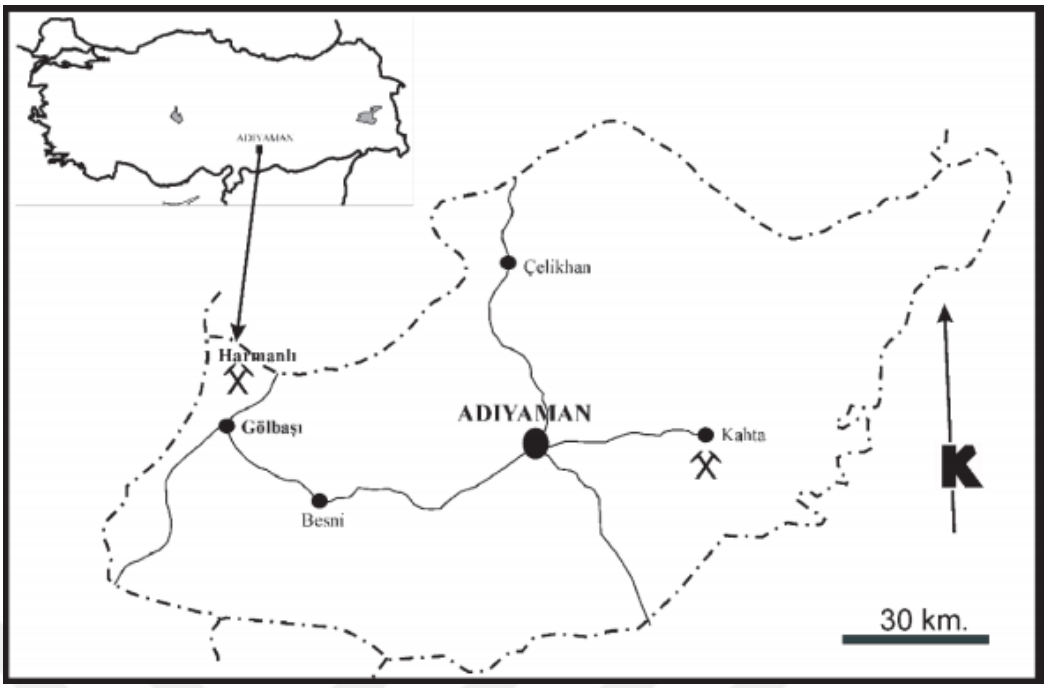

Figure 6.3 : Location map of Adıyaman-Gölbaşı lignite basin [112].

Çorum-Dodurga lignite deposits are located in the Black Sea Region of Turkey [113]. Total proven and probable lignite reserves in this deposit were detected as 38 473 000 tonnes. Lower heating value of Dodurga lignites ranges from 2500 to 3151 kcal/kg. In addition to the lignite reserves, bituminous shale with very low calorific value is also found in this district [114]. Annual lignite production in Çorum-Dodurga mine is 300 000 tonnes which is run by private sector since 2002 [115].

6.1.2 Biomass Feedstock

Hybrid poplar is a fast growing tree and can be harvested throughout the year [116]. In comparison with similar biomass species, growing rate of hybrid poplar trees is six to ten times faster and their lifespan is more than forty years [117]. Thanks to the desired features of hybrid poplar in terms sustainable biomass energy generation, bio-fuel production is one of the important beneficial uses of hybrid poplar. There are about 130000 ha of poplar plantations in Turkey, of which 70000 ha are hybrid poplars and 60.000 ha consist of various clones of black poplar. Due to the superior properties of hybrid poplar, researches have been carried out to develop new technologies for poplar plantation, conserve country's poplar genetic resources and improve soil properties [118].

Twenty seven percent of Turkey's land area is covered by forestlands that are mostly located in the Black Sea Region. Rhododendron, which is used as a biomass material in this study, is the primary biomass species with about 40 metric ton ha^{-1} in the understory of the forests of this region that damages the other species by restricting tree growth, preventing regeneration of target tree species and decreasing the diversity of species. Thus, use of Rhododendron as biomass resource for bio-fuel production helps to control their invasion as well as increase renewable energy generation [119].

Ash-tree, which is the another biomass feed stock used in this study, spread through the Thrace, East and West Black Sea Region, Marmara and Aegean Region of Turkey. The area it covers is 9443.5 ha. Maximum length of ash tree changes between 10 and 30 m based on the species. Ash tree is one of the fastest growing native biomass after poplar and alder; therefore, it is considered as valuable biomass resource to be utilized in energy generation in Turkey besides in forest products industry [120].

6.2 Sample Preparation

Lignites were crushed with a hammer and left to dry in air atmosphere for 24 hours to obtain air-dried samples. Drying of biomass materials were performed in two steps of which the first in laboratory medium and the second in oven at 105^{o}C. Then, both lignite and biomass samples were grounded and sieved to a particle size of <250 μm using Retsch AS 200 sieves which is shown in Figure 6.4.

Figure 6.4 : Retsch AS 200 sieves.

6.3 Torrefaction and Pyrolysis Experiments in a Horizontal Tube Furnace

Torrefaction of biomass samples and pyrolysis of both biomass and lignite samples were carried out in the horizontal tube furnace which is shown in Figure 6.5. Horizontal tube furnace is made of stainless steel and the size of combustion unit (tube) is 15 cm x 72 cm. Moreover, the inner diameter of ceramic combustion unit is 5 cm. Pyrolysis experiments were conducted at 750^{o}C for lignites and 400^{o}C for biomass samples with a heating rate of 10^{o}C/min under a nitrogen atmosphere with a flow rate of 100 mL/min. In order for the further decline in the volatile matter content, the samples were kept at these final temperatures for 30 minutes. Torrefaction of biomass samples were conducted similar to the pyrolysis experiments with the only difference of final temperature that was determined as 200^{o}C. Prior to the heating process in each case, approximately 8 g of sample was weighed and spread uniformly in a sample holder made of quartz. Then, the sample holder was placed in the middle of the combustion unit of which both ends were sealed by a cover subsequently and PTFE band was wrapped around it to avoid gas leakage. Nitrogen gas was allowed to pass through the combustion tube at adjusted flow rate and the sample in the furnace was kept at room temperature for 20 minutes to reach equilibrium with the nitrogen atmosphere. Then, parameters related to heating conditions were set and heating process was started. At the end of the thermal treatment, the sample was left to cool down in its own atmosphere in the furnace to minimize the possible experimental errors.

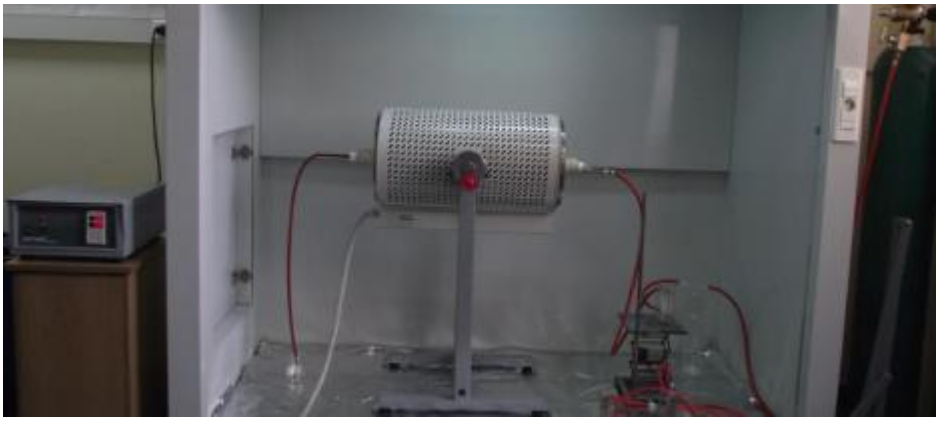

Figure 6.5 : Horizontal tube furnace.

6.4 Preparation of Lignite and Biomass Blends

The number of blends, which were prepared by lignite and biomass samples, was 54 such that six sets of lignite-biomass blends were formed as each single set contains nine blends. In all cases, the blending ratio of biomass was 10 wt% and the lignite was the dominant component in the fuel blends. Since there are three different lignites and biomass separately, blend of original lignites with original biomass samples yielded 9 blends that is one of the sets. In the same manner, second set was formed by the blend of semi cokes (three types) with original biomass (three types). Original lignites and semi cokes were also blended with torrefied and pyrolyzed biomass samples that produce the rest of the four sets.

6.5 Analyses for Parent Fuels and Blends

Parent fuels refer to the original lignites, semi cokes, original biomass, torrefied and pyrolyzed biomass samples in order to discriminate them from the blend fuels. Proximate and ultimate analyses, calorific value measurements, SEM analysis was applied to parent fuels only excluding thermal analyses which was conducted for both parent and blend fuels in order to assess the co-combustion behavior of the blends and determine synergistic effects between biomass and lignites.

6.5.1 Proximate and ultimate analyses

Proximate analyses were carried out using TA Instruments SDT Q600 model thermal analyzer with a cylindrical alumina crucible as shown in Figure 6.6. Approximately 10 mg of each sample was weighed in a sample holder which is made of platinum and proximate analysis was started. Although the procedures of proximate analysis for biomass and coal follow the same pathways during the heating steps, they differ in the cooling step. Firstly, each type of biomass and lignite was heated from ambient temperature to 105^{o}C with a heating rate of 10^{o}C/min under nitrogen flow of 100 mL/min. Then, the sample was kept at this temperature for 10 min in order for the moisture removal. After that, temperature of the sample was increased to 900^{o}C under the same heating conditions. Following this stage, the sample was kept at this temperature for 7 min to be sure that devolatilization process is complete. Then, the temperature of biomass was decreased to 600^{o}C whereas; temperature of lignite was reduced to 755^{o}C. In spite of the different temperature falls, both biomass and lignite

were cooled at a rate of 20^{o}C/min under nitrogen flow of 100 mL/min. At 755^{o}C for lignites and 600^{o}C for biomass samples, nitrogen flow was ceased and dry air was fed to the system until the weight of the sample become unchanged. The remaining weight indicated the ash yield.

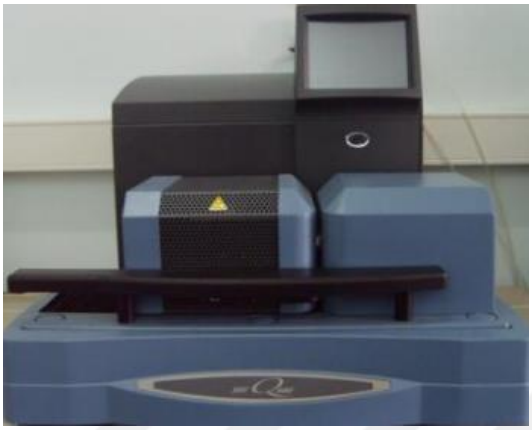

Figure 6.6 : TA Instruments SDT Q600 model thermal analyzer.

Ultimate analyses of parent fuels were performed using the Elemental Analyzer Leco TruSpec CHN, and S modules that is shown in Figure 6.7. Before conducting the experiments, the device was calibrated with coal and biomass calibrants separately. After calibration, weighed samples were placed into the device for analyses. The C, H, N and S constituents of the samples were obtained. The percentage of elemental oxygen present in the sample was calculated by subtracting the sum of C, H, N, S and ash contents on dry bases from 100. Tests were repeated twice to minimize experimental errors.

Figure 6.7 : Leco TruSpec® CHN model elemental analyzer with S module.

6.5.2 Thermal analyses (TGA, DTG, DTA, DSC)

Thermal analyses were performed for both parent and blend fuels using TA Instruments SDT Q600 model thermal analyzer that is shown in Figure 6.6. In this study, each sample was weighed around 10 mg and heated up to 900^{o}C with a heating rate of 40ºC/min under dry air atmosphere at flow rate of 100 mL/min. TGA (Thermogravimetric Analysis), DTG (Differential Thermogravimetric), DTA (Differential Thermal Analysis) and DSC (Differential Scanning Calorimetry) curves were obtained as a result of thermal analyses.

Pyrolysis temperature of each lignite was determined from the DTG curves that were obtained by thermal analysis experiments under nitrogen atmosphere. Lignites were heated from ambient temperature to 900^{o}C with a heating rate of 10^{o}C/min in the introduced thermal analyzer. After determining the pyrolysis temperature, semi cokes were produced in the horizontal tube furnace, which is explained in Section 6.3.

6.5.3 Calorific value measurement

Higher heating value of the ground original lignites, origional biomass, pyrolysed lignites (semi cokes), torrefied and pyrolysed biomass samples were determined by using IKA C2000 Basic Calorimeter, which has stainless steel calorimeter bomb and is shown in Figure 6.8. Calorific value of the prepared blends were calculated according to the blending ratio.

Figure 6.8 : IKA C2000 Basic Bomb Calorimeter.

6.5.4 Scanning electron microscopy (SEM) analyses

Scanning electron microscopy is a sort of electron microscope that produces images of a sample with high resolution by scanning it with a focused beam of electrons.

Thus, valuable information about the morphology of the analyzed sample is gathered by SEM analysis. In this study, the structural differences between original lignite and biomass samples along with thermally treated samples (pyrolysed, torrefied) were investigated by using Jeol JSM-5410 instrument with magnification of 750X.

6.5.5 Fourier transform infrared (FTIR) spectroscopy analyses

Fourier Transform Infrared Spectroscopy is an analytical technique used for identification of organic materials. Chemical bond structure of sample molecule is understood from the infrared absorption spectrum which is created as a result of FTIR analysis. The absorption or transmittance versus wavelength was plotted via the data provided by Perkin Elmer FTIR Analyzer so that the compounds which constitute the parent fuels and their blends with original, torrefied and pyrolysed biomass sample were determined.

7. RESULTS AND DISCUSSION

7.1 Results of Proximate Analyses and Calorific Value Measurement

Proximate analysis results of parent fuels, which are referred to original lignite, pyrolysed lignite samples and original, torrefied, pyrolysed biomass, derived from the TGA profiles and higher heating values determined from the bomb calorimeter experiments are given in Table 7.1.

Table 7.1 : Proximate analyses and calorific value determination results of original lignite, pyrolysed lignite samples and original, torrefied, pyrolysed biomass samples.

Sample	Moisture (%)	Volatile matter (%)	Fixed carbon (%)	Ash (%)	HHV (cal/g)
AE	45.0	27.0	9.5	32.3	2600
AE750	4.3	26.5	15.0	54.1	2160
AG	30.7	30.9	17.0	21.3	2635
AG750	2.9	15.7	32.9	40.1	3526
CD	7.5	32.0	32.5	28.0	4286
CD750	2.9	9.9	43.1	31.7	4182
RD	5.2	79.0	13.7	2.1	4318
RD200	5.7	80.3	12.9	1.0	4449
RD400	7.4	32.0	58.3	2.2	6583
HP	9.3	79.0	10.9	0.8	4176
HP200	7.2	80.7	11.2	1.0	4201
HP400	7.9	30.1	55.8	6.2	5729
AT	7.6	80.3	11.1	1.1	4143
AT200	2.6	84.0	13.5	0.0	4370
AT400	7.9	30.9	61.0	0.1	6396

Results in Table 7.1 indicate that lignite samples differ from the biomass species in terms of volatile matter and ash content, while moisture and fixed carbon content of both fuel types are comparable with each other to some extent regardless of the applied thermal pretreatments. Namely, biomass species yield much more volatile matter, while the ash yield of lignite samples is disproportionally higher than those for the biomasses.

According to Table 7.1, a significant decrease was observed in the higher heating value of AE when it was pyrolysed at 750°C and pyrolytic char of CD was resulted in

lower calorific value than original CD, slightly. On the other hand, pyrolytic treatment of AG lignite exhibits expected results regarding to higher heating value that was increased when original AG lignite sample was pyrolysed under nitrogen atmosphere at 750°C. In contrast to lignite samples, higher heating values of biomass species increased gradually as the temperature of thermal pretreatment increased from room temperature to 400°C through torrefaction and pyrolysis processes. In the light of these results, it is likely to say that the effect of pyrolysis on the calorific value of biomass materials is dominant compared to torrefaction since main increase in the higher heating value was observed when temperature rises from 200°C to 400°C.

AE lignite has the lowest calorific value among the lignite samples as well as the biomass species that can be explained by the highest moisture content of this lignite which is quite noticeable in Table 7.1 as 45%. Moreover, calorific value of CD is higher than other lignite samples by far due to its nearly two fold of fixed carbon content. On the other hand, RD is the leading species in all biomass samples in terms of the highest calorific value, while AT is the lowest one in spite of the close value to HP.

Proximate analysis results of lignite samples revealed that pyrolytic chars have higher ash content than original lignites, whereas ash content of biomass species do not follow the similar trend. That is to say, ash content of RD decreased to half of the value when torrefaction was applied and increased to slightly above its previous value in the pyrolysis stage. Although torrefaction and pyrolysis processes lead to the similar change in the ash content of AT, the effect of latter is negligible due to the minor increase observed after 200°C to 400°C. On the other hand, the behavior of HP is different in terms of ash content which increased from 0.83% to 1% and then to 6.2% through torrefaction and pyrolysis processes, respectively. Thus, it is clearly comprehended that pyrolysis is the governing thermal treatment for HP for the increased ash content.

Volatile matter content of all species presented in Table 7.1 decreased when pyrolysis applied. Nevertheless, torrefaction caused a slight increase in the volatile matter content of each biomass species. The degree of devolatilization depends on the temperature. Thus, extensive devolatilization occurs in pyrolysis process due to

its higher temperature range, while torrefaction lead to only degredation of homocellulose content of biomass and limited release of volatiles.

When moisture contents of the original coal and biomass samples used in the experimental studies are examined, it is seen that RD and AE lignite samples have the lowest and highest moisture contents, respectively. Pyrolysis of lignite samples at 750^{o}C lead to the decrease in moisture content. So that, 90.4% fall in moisture content of AE750, which was produced by pyrolysis of AE lignite at 750^{o}C, was observed. The biggest decline in the moisture content of the lignite samples as a result of pyrolytic treatment was detected in AG sample as 90.5% which is very close to AE lignite, while the lowest drop was seen in CD sample as 61.3%.

As it is seen in Table 7.1, torrefied biomass samples do not differentiate from their original forms significantly in terms of moisture content. Increase in the moisture content of RD samples which are torrefied at 200^{o}C and pyrolysed at 400^{o}C is due to the absorbed moisture of air by the porous structure that was formed as a result of torrefaction and pyrolysis. Thermally treated samples were cooled down to ambient temperature from the torrefaction or pyrolysis temperature under nitrogen atmosphere in the horizontal tube furnace. During the cooling stage, treated samples could absorb the moisture in the air because of their porous structure. SEM images of original, torrefied and pyrolysed biomass samples also support this explanation by demonstrating high porous structure of the treated samples clearly. On the other hand, decrease in moisture content of torrefied and pyrolysed HP samples can be explained by the low porous structure that is seen in the SEM images. Results for AT sample regarding to the change in the moisture content also indicate that it has lower porosity than the other biomass samples after torrefaction and it becomes more porous structurally as the temperature increases to 400^{o}C that can be comprehended from the SEM images.

Table 7.1 shows that biomass samples have higher volatile matter contents conspicuously in comparison with lignite samples. Volatile matter contents of pyrolysed lignite samples decrease in the range of 2% and 69% of which the first belongs to AE lignite and the second belongs to CD lignite. Volatile matter content of RD200, which was obtained by torrefaction of RD at 200^{o}C, increased to a degree since porous structure of torrefied biomass absorbed the gases present in the medium. Further heating to 400^{o}C at nitrogen atmosphere lead to decrease in volatile matter

content of RD contrary to the torrefaction process. Thus, nearly 60% fall in volatile matter content was observed in RD when it was pyrolysed at 400^{o}C. The same is also valid for AT sample. It is understood from the SEM images that structure of original biomass samples has become highly porous due to torrefaction at 200^{o}C. Moreover, SEM images obtained for original, torrefied and pyrolysed biomass samples also revealed that porosity of biomass samples increased depending on the temperature rise from 200°C to 400°C and owing to the removal of some of the volatile matter. As a result of pyrolysis of the biomass samples at 400°C, it was determined that volatile matter content of all samples were almost same around 30%.

When fixed carbon results are examined, it was seen that CD, which has the highest calorific value among the lignite samples, has also highest fixed carbon content. Pyrolysis of AE sample at 750°C resulted in ~58% increase in the fixed carbon content. In addition, fixed carbon content of AG and CD lignites at the end of the pyrolysis process at 750°C increased by 93% and 33%, respectively. Highest increase in the fixed carbon was determined in AG sample which can be explained by the release of high moisture content of the sample during the pyrolysis stage. Furthermore, AG is the lignite sample with the lowest higher heating value among the all lignite samples used in this study.

Concerning the change in the calorific value of the biomass samples, it was observed that there was no significant increase in the calorific values of the torrefied biomass samples and relatedly fixed carbon contents. However, noticeable increase in the fixed carbon contents and higher heating values of the biomass samples were identified such that fixed carbon contents of RD, HP and AT samples increased to about five times when compared to original samples. Increase in the fixed carbon content of the biomass samples during the pyrolysis stage is also supported by the increase in higher heating values. Highest increase in the both fixed carbon content and calorific value was observed in AT sample. In the light of these results, it can be inferred that pyrolysis of biomass samples at 400°C is more convenient than torrefying at 200°C in order to obtain quality fuel from biomass samples.

Due to the pyrolysis of lignite samples at 750°C, increase in the ash values was observed in the range of 13% and 88%. Accordingly, it was determined that calorific values of the lignite samples decreased excluding AG sample of which calorific value increased from 2635 cal/g to 3526 cal/g. When ash results of biomass samples

are analyzed, torrefaction lead to the decrease in the ash content, but pyrolysis reversed this effect and ash content of pyrolysed biomass samples increased.

Table 7.1 reveals that RD400 sample that was obtained by pyrolysis of original RD sample at 400°C along with the AG750 pyrolysed lignite sample at 750°C are determined as the biomass and lignite samples of which highest increase in the calorific value was monitored. According to the results of proximate analyses and calorific value measurements, higher heating value of the blend prepared by mixing 90 wt% AG750 and 10 wt% RD400 samples was calculated as 3832 cal/g. As a crucial outcome of Table 7.1, co-combustion of pyrolysed AG lignite, which has the lowest calorific value among the lignite samples used in this experiment, with pyrolysed RD biomass sample enables to obtain a fuel having 45% more high calorific value compared to original AG lignite. Finding such result for the low grade AG lignite is another important consequence of this experiment.

Proximate analysis results and higher heating value of fuel blends that are prepared by adding 10 wt% of original, torrefied and pyrolysed biomass samples separately to lignites are presented in Table 7.2-Table 7.4. Accordingly, higher heating value of the blends is higher than of original lignites in general without considering a few exceptions. The effect of treated biomass samples to the improved characteristics of the blends is also clearly understood from the results such that original lignite and pyrolysed biomass blends have the highest calorific value than the blends formed by torrefied and original biomass samples. Although a significant difference in higher heating values of the each type of blend was detected, ash content of the blends remained almost unchanged in all cases. However, thanks to the noticeably lower ash content of biomass species, blends given in Table 7.2-7.5 yielded slightly lower ash content in comparison with the original fuel regardless of the treated and untreated biomass samples present in the blend. On the other hand, pyrolysed biomass in the blends lead to the increased fixed carbon and decreased volatile matter content contrary to the torrefied and original biomass samples that can be seen in Table 7.4. Noticeable change in the moisture content of the blends was not observed. Thus, torrefied and pyrolysed biomass samples do not affect the moisture content of the blends, considerably.

Table 7.2 : Proximate analyses and calorific value determination results of original lignite and biomass blends.

Blends	Moisture (%)	Volatile matter (%)	Fixed carbon (%)	Ash (%)	HHV (cal/g)
AE+RD	41.0	32.2	9.9	29.3	2772
AE+HP	41.4	32.2	9.6	29.2	2758
AE+AT	41.3	32.3	9.6	29.2	2754
AG+RD	28.2	35.7	16.7	19.4	2803
AG+HP	28.6	35.7	16.4	19.3	2789
AG+AT	28.4	35.9	16.4	19.3	2786
CD+RD	7.3	36.7	30.6	25.4	4289
CD+HP	7.7	36.7	30.3	25.3	4275
CD+AT	7.5	36.9	30.3	25.3	4272

Comparing the higher heating values of the original lignite and 10 wt% of biomass added lignite and biomass blends, it has been observed that addition of biomass to lignite did not affect the calorific values of the original lignite samples significantly due to the negligible increase in the calorific values as it is seen in Table 7.2. Likewise, higher heating values of the blends that were prepared by adding 10 wt% of torrefied biomass samples to original lignite samples also measured as little higher than original lignites along with the blends of original lignite and original biomass samples. Addition of RD sample to lignites resulted in the highest increase in the calorific value of the blends.

Table 7.3 : Proximate analysis and calorific value determination results of original lignite and torrefied biomass blends.

Blends	Moisture (%)	Volatile matter (%)	Fixed carbon (%)	Ash (%)	HHV (cal/g)
AE+RD200	41.1	32.3	9.8	29.2	2785
AE+HP200	41.2	32.4	9.6	29.2	2760
AE+AT200	40.8	32.7	9.9	29.1	2777
AG+RD200	28.2	35.9	16.6	19.3	2816
AG+HP200	28.4	35.9	16.4	19.3	2792
AG+AT200	27.9	36.2	16.7	19.2	2809
CD+RD200	7.3	36.9	30.5	25.3	4302
CD+HP200	7.5	36.9	30.3	25.3	4278
CD+AT200	7.0	37.2	30.6	25.2	4294

Results of higher heating value measurements of the blends prepared by adding 10 wt% of pyrolysed biomass samples at 400°C to original lignite samples indicate that RD400 is the biomass sample providing highest increase in the calorific value as it is

seen in Table 7.4. When all the results presented in Table 7.2-Table 7.4 are taken into account, it was determined that highest increase in the calorific value was achieved by the blend of original AG lignite and pyrolysed RD sample.

Table 7.4 : Proximate analysis and calorific value determination results of original lignite and pyrolysed biomass blends.

Blends	Moisture (%)	Volatile matter (%)	Fixed carbon (%)	Ash (%)	HHV (cal/g)
AE+RD400	41.2	27.5	14.3	29.3	2998
AE+HP400	41.3	27.3	14.1	29.7	2913
AE+AT400	41.3	27.4	14.6	29.1	2980
AG+RD400	28.4	31.0	21.2	19.4	3030
AG+HP400	28.4	30.8	20.9	19.8	2944
AG+AT400	28.5	30.9	21.4	19.2	3011
CD+RD400	7.5	32.0	35.1	25.4	4516
CD+HP400	7.5	31.8	34.8	25.8	4430
CD+AT400	7.6	31.9	35.3	25.2	4497

Proximate analysis results and higher heating value of fuel blends that are prepared by adding 10 wt% of original, torrefied and pyrolysed biomass samples separately to pyrolytic chars are presented in Table 7.5-Table 7.7.

Table 7.5 : Proximate analysis and calorific value determination results of pyrolysed chars and original biomass blends.

Blends	Moisture (%)	Volatile matter (%)	Fixed carbon (%)	Ash (%)	HHV (cal/g)
AE750+RD	4.4	31.8	14.9	48.9	2376
AE750+HP	4.8	31.8	14.6	48.8	2362
AE750+AT	4.6	31.9	14.6	48.8	2358
AG750+RD	3.2	22.0	31.0	36.3	3605
AG750+HP	3.6	22.0	30.7	36.1	3591
AG750+AT	3.4	22.2	30.7	36.2	3588
CD750+RD	3.1	16.8	40.1	28.8	4196
CD750+HP	3.5	16.8	39.9	28.6	4181
CD750+AT	3.4	16.9	39.9	28.7	4178

The results showed that fixed carbon content of the blends are the highest when compared to other cases. Moreover, an increase in the ash content was observed in all blends. Use of pyrolytic chars in the blends did not affect the calorific value of the fuel, noteworthy. Among all fuels including parent and blends, highest calorific value was obtained as 4515.7 cal/g that belongs to CD and RD400 blend. Thus, it can be said there is no meaningful difference between the original lignite and pyrolysed

char in the blend. Even, higher heating value of AE lignite decreased substantially and a slight decline was observed in case of CD lignite.

As it was observed in the blends that were prepared by original lignite and torrefied biomass samples, no significant variation was detected in the calorific value of the blends of pyrolysed CD lignite and torrefied biomass samples. On the other hand, approximately 2% increase in the blends of pyrolysed AG sample and 10% increase in the blends of pyrolysed AE sample in terms of calorific values were determined as it is understood from Table 7.6. Hence, even though torrefied biomass samples were added to each pyrolysed lignite sample in the same ratio of 10 wt%, the direct effect of biomass addition to lignite was only observed in the blends of pyrolysed AE sample proportionally as 10% increase in the calorific value. The reason of observing no meaningful change in the calorific value of the blends prepared by pyrolysed CD and around 2% increase in pyrolysed AG blends can be explained by the synergic effects created by the biomass species with the corresponding lignites.

Table 7.6 : Proximate analysis and calorific value determination results of pyrolysed chars and torrefied biomass blends.

Blends	Moisture (%)	Volatile matter (%)	Fixed carbon (%)	Ash (%)	HHV (cal/g)
AE750+RD200	4.5	31.9	14.8	48.8	2389
AE750+HP200	4.6	31.9	14.7	48.8	2364
AE750+AT200	4.1	32.3	14.9	48.7	2381
AG750+RD200	3.2	22.2	30.9	36.2	3618
AG750+HP200	3.4	22.2	30.7	36.2	3594
AG750+AT200	2.9	22.5	31.0	36.1	3610
CD750+RD200	3.2	16.9	40.1	28.7	4209
CD750+HP200	3.3	17.0	39.9	28.6	4184
CD750+AT200	2.9	17.3	40.1	28.5	4201

According to Table 7.4 and Table 7.7, blend of pyrolysed RD biomass sample with original AG lignite or pyrolysed AG lignite at 750°C has 30% difference in terms of calorific value. Since 45% increase in calorific value was determined in case of mixing 10 wt% of RD400 and 90 wt% of AG750 which was mentioned above, usage of pyrolysed lignites at 750°C is preferred to prepare lignite-biomass blends for obtaining high quality fuel rather than original lignite. As an important biomass source in Turkey, RD is distributed throughout a field of 40 metric ton ha^{-1}. Thus, in order for the disposal of RD due to reclamation of forests and production of high quality fuel by blending with low rank lignite coals which is abundant domestic

fossil fuel resource of Turkey, utilization of RD is essential for our country. Results of this study showed that RD, especially in pyrolysed form, can be blended with low rank coal to achieve the stated objectives.

Table 7.7 : Proximate analysis and calorific value determination results of pyrolysed chars and pyrolysed biomass blends.

Blends	Moisture (%)	Volatile matter (%)	Fixed carbon (%)	Ash (%)	HHV (cal/g)
AE750+RD400	4.6	27.1	19.4	48.9	2602
AE750+HP400	4.7	26.9	19.1	49.3	2517
AE750+AT400	4.7	27.0	19.6	48.7	2584
AG750+RD400	3.4	17.3	35.4	36.3	3832
AG750+HP400	3.4	17.1	35.2	36.7	3746
AG750+AT400	3.4	17.2	35.7	36.1	3813
CD750+RD400	3.4	12.1	44.6	28.8	4422
CD750+HP400	3.4	11.9	44.4	29.2	4337
CD750+AT400	3.4	12.0	44.9	28.6	4403

When calorific values of the blends that were prepared by addition of pyrolysed biomass samples at 400°C to the pyrolysed lignite samples at 750°C are examined, nearly 20%, 8% and 5% increase in the calorific values of AE, AG and CD samples were determined, respectively. In the light of the results given in Table 7.6 and Table 7.7, it is clear that calorific value of AE sample increased two times when 10 wt% of pyrolysed biomass samples at 400°C were added to pyrolysed AE sample at 750°C compared to the addition of torrefied biomass sample at 200°C. Increase in calorific values of AG and CD lignite samples when their semi cokes produced at 750°C were mixed with pyrolysed biomass samples was observed less than the ratio of biomass addition. This behavior can be explained by synergic effects of biomass samples in the blends. Instead of torrefying biomass samples at 200°C, raising the temperature to two times at which pyrolysis occurs resulted in 10% increase in calorific value of pyrolysed AE lignite at 750°C when it was blended with torrefied or pyrolysed biomass samples. Thus, it can be concluded that temperature of bio char and the ratio of increase in higher heating value of pyrolysed AE lignite are directly proportional to each other. Contrary to AG and CD lignites, calorific value of AE lignite was affected in the same way from the torrefied and pyrolysed biomass samples that were added by 10 wt%.

7.2 Results of Ultimate (Elemental) Analyses

Ultimate analyses results of parent fuels and blends prepared by adding 10 wt% of original, torrefied and pyrolysed biomass samples to both original lignite and pyrolysed chars, separately are introduced in Table 7.8 – Table 7.10.

Table 7.8 : Ultimate analyses results of original lignite, pyrolysed chars and original, torrefied, pyrolysed biomass samples.

Sample	C (%)	H (%	N (%)	S (%)	O (%)
AE	38.90	3.16	1.49	0.76	21.62
AE750	39.50	0.53	1.57	0.04	1.81
AG	42.80	4.06	1.44	0.61	20.32
AG750	54.30	0.60	1.80	0.70	1.31
CD	50.90	3.84	2.71	2.94	9.37
CD750	60.60	0.68	2.58	2.50	0.97
RD	48.50	6.48	0.00	0.34	42.44
RD200	49.64	6.56	0.00	0.34	42.36
RD400	73.26	3.80	0.40	0.33	19.83
HP	47.18	6.67	0.00	0.37	44.88
HP200	47.94	6.56	0.00	0.37	44.06
HP400	70.60	3.72	0.11	0.33	18.51
AT	46.64	6.63	0.00	0.35	45.20
AT200	49.29	6.46	0.00	0.34	43.90
AT400	70.15	3.77	0.60	0.31	25.03

When ultimate analyses results of the parent samples were examined in Table 7.8, original lignite samples among which CD has the highest calorific value and AE has the lowest one, follow same trend in terms of elemental carbon contents (CD>AG>AE). Even though higher heating value of AE sample decreased by 17% when it was pyrolysed at 750°C, contrary to expectations only 0.6% minor increase was observed in elemental carbon content of AE sample in case of pyrolysis. The reason of this contradiction can be explained by the decrease in the total hydrogen and sulfur content of AE sample during pyrolysis process. Thus, a slight increase in the elemental carbon content and considerable decrease in the hydrogen content of AE sample as a result of pyrolysis prevented to observe anticipated rise in the higher heating value. Despite the fact that pyrolysis of AG lead to 21.2% increase in the elemental carbon content of original AG, 85.2% fall in the hydrogen content was observed. In terms of higher heating value, 33.8% increase was observed in

pyrolysed AG char compared to original form. This outcome shows that increase in the elemental carbon content is dominant on the higher heating value.

Similar to AE lignite sample, higher heating value of CD decreased when it was exposed to pyrolytic treatment at 750°C in spite of the expected rise. As it is seen in Table 7.8, 16% increase and 82.3% decrease in the elemental and hydrogen content of CD, respectively was observed. In general, pyrolysis of lignite samples caused a huge decrease in the hydrogen contents which ranges between 80-85% roughly. However, the leading effect on the higher heating value was determined as the increase in the elemental carbon content. Correspondingly, AG was recorded as the lignite which has the highest increase in the elemental carbon content with 6% more rise among the three lignite samples.

According to Table 7.8, biomass species do not differ from each other significantly in terms of elemental carbon, hydrogen, nitrogen, sulfur and oxygen contents contrary to lignite samples that show much more differences between each other. Elemental carbon contents of biomass species were determined as RD>HP>AT which is consistent with higher heating values. Torrefaction of biomass samples at 200°C was resulted in minor increase in the elemental carbon content of each species that changes between 1.61-5.68%. The biggest rise was detected in torrefied AT specie whereas; HP was recorded as the least affected biomass sample from torrefaction process that was deduced from its 1.61% increase in the elemental carbon content. On the other hand, pyrolysis of biomass samples at 400°C lead to significant increase in the elemental carbon content which is approximately 50%. This result indicates that biomass species were affected from pyrolytic treatment much more than lignite samples. When the change in the hydrogen contents of biomass samples were analyzed, unsurprisingly torrefaction did not cause a considerable alteration, while pyrolysis gave rise to substantial drop ranging between 41% and 43% that was also seen in higher heating value results.

Due to the different chemical compositions of biomass and lignite samples, nitrogen content of biomass species were determined as zero and sulfur contents are almost half of the lignite samples. Concerning oxygen contents, Table 7.8 reveals that biomass species are rich by oxygen that is nearly two fold of lignite samples. Since most of the oxygenates were released during the pyrolysis process, oxygen contents of biomass species decreased greatly as it was expected. With the 59% decrease in

oxygen content, HP was determined as the biomass species showing the highest amount of volatile matter release that was also supported by proximate analyses results.

Ultimate analyses results of the blends given in Table 7.9 indicate that addition of original and torrefied biomass to AE lignite sample lead to only 2.2% and 2.6% increases in the elemental carbon contents, respectively. On the other hand, nearly 8.4% rise was observed in the blends of AE and pyrolysed biomass species.

Table 7.9 : Ultimate analyses results of original lignite and original, torrefied, pyrolysed biomass blends.

Sample	C (%)	H (%	N (%)	S (%)	O (%)
AE+RD	39.86	3.49	1.34	0.72	23.71
AE+HP	39.73	3.51	1.34	0.72	23.95
AE+AT	39.67	3.51	1.34	0.72	23.98
AG+RD	43.37	4.30	1.30	0.59	22.53
AG+HP	43.24	4.32	1.30	0.59	22.77
AG+AT	43.18	4.32	1.30	0.59	22.81
CD+RD	50.66	4.10	2.44	2.68	12.67
CD+HP	50.53	4.12	2.44	2.69	12.92
CD+AT	50.47	4.12	2.44	2.68	12.95
AE+RD200	39.97	3.50	1.34	0.72	23.70
AE+HP200	39.80	3.50	1.34	0.72	23.87
AE+AT200	39.94	3.49	1.34	0.72	23.85
AG+RD200	43.48	4.31	1.30	0.59	22.52
AG+HP200	43.31	4.31	1.30	0.59	22.69
AG+AT200	43.45	4.30	1.30	0.59	22.68
CD+RD200	50.77	4.11	2.44	2.68	12.67
CD+HP200	50.60	4.11	2.44	2.69	12.84
CD+AT200	50.74	4.10	2.44	2.68	12.82
AE+RD400	42.34	3.22	1.38	0.72	21.45
AE+HP400	42.07	3.22	1.35	0.72	21.31
AE+AT400	42.03	3.22	1.40	0.72	21.96
AG+RD400	45.85	4.03	1.34	0.58	20.27
AG+HP400	45.58	4.03	1.31	0.58	20.14
AG+AT400	45.54	4.03	1.36	0.58	20.79
CD+RD400	53.14	3.84	2.48	2.68	10.41
CD+HP400	52.87	3.83	2.45	2.68	10.28
CD+AT400	52.83	3.83	2.50	2.68	10.93

Gradual increase in the elemental carbon content of AG lignite was observed as 1.2%, 1.4% and 6.7% when original, torrefied and pyrolysed biomass samples were added individually. Unlike AE and AG lignites, elemental carbon content of CD

decreased by 0.7% upon addition of original biomass. Similar behavior was also seen in case of blending CD with torrefied biomass samples. However, adding pyrolysed biomass species to original CD lignite increased the elemental carbon content of CD by almost 4%.

As it is seen in Table 7.9, addition of each type of biomass species to lignite samples decreased nitrogen and sulfur content to some extent. Moreover, blends prepared by original or torrefied biomass samples have the same amount of nitrogen in their chemical compositions. On the other hand, adding pyrolysed biomass species to lignites gave rise to a minor increase in nitrogen contents. Regarding sulfur content, thermal pretreatments applied to biomass species did not affect sulfur contents of the lignite samples since adding torrefied, pyrolysed and original biomass samples to lignites were resulted in the same amount of sulfur contents. The biggest change in the oxygen content of the lignite samples was observed in the blends of CD. Adding original and torrefied biomass to CD increased oxygen content of CD by 37.1% and 36.6%, respectively. However, a lower increase with 12.5% in the oxygen content of CD was detected when it was blended with pyrolysed biomass species. Oxygen content of AE and AG lignite samples were affected from the addition of original and torrefied biomass samples in a similar way. The percentage of increases recorded for both samples in each case was between 10.3 and 11.6. Different from CD, pyrolysed RD and HP biomass species in the blends of AE and AG lead to the negligible decrease in oxygen contents whereas, small increase was observed in case of using pyrolysed AT biomass sample. Significant variation was not noticed in the hydrogen contents of the lignite samples that can be explained by the dominance of lignites in the blends.

According to Table 7.10, it was clearly seen that the blend of AG lignite and RD biomass specie that were pyrolysed at 750°C and 400°C under nitrogen atmosphere, respectively showed improved fuel characteristics due to the fact that maximum increase in the elemental carbon content was observed in this fuel blend. Similar to the blends prepared by using original lignite samples, almost same amount of increase was observed in elemental carbon contents of the lignite samples when original and torrefied biomass samples were added to pyrolysed lignites. Much more increase in the elemental carbon contents of the lignites was seen when their pyrolysed chars and pyrolysed biomass species were blended. Meanwhile, decrease

in the hydrogen, nitrogen, sulfur and oxygen contents was observed owing to the effect of pyrolytic treatment applied to lignite samples. It is quite noticeable in Table 7.10 that the percentage of hydrogen and nitrogen content of the blends remained unchanged when original biomass and torrefied biomass species were added. However, pyrolysed biomass addition to pyrolysed lignite samples excluding the HP biomass sample was resulted in a slight increase in hydrogen and nitrogen contents. When sulfur contents of the blends in the mentioned table was analyzed, it was detected that neither torrefaction nor pyrolysis of biomass have an effect on the sulfur content of the blends.

Table 7.10 : Ultimate analyses results of pyrolysed chars and original, torrefied, pyrolysed biomass blends.

Sample	C (%)	H (%	N (%)	S (%)	O (%)
AE750+RD	40.4	1.1	1.4	0.1	5.9
AE750+HP	40.3	1.1	1.4	0.1	6.1
AE750+AT	40.2	1.1	1.4	0.1	6.2
AG750+RD	53.7	1.2	1.6	0.7	5.4
AG750+HP	53.6	1.2	1.6	0.7	5.7
AG750+AT	53.5	1.2	1.6	0.7	5.7
CD750+RD	59.4	1.3	2.3	2.3	5.1
CD750+HP	59.3	1.3	2.3	2.3	5.4
CD750+AT	59.2	1.3	2.3	2.3	5.4
AE750+RD200	40.5	1.1	1.4	0.1	5.9
AE750+HP200	40.3	1.1	1.4	0.1	6.0
AE750+AT200	40.5	1.1	1.4	0.1	6.0
AG750+RD200	53.8	1.2	1.6	0.7	5.4
AG750+HP200	53.7	1.2	1.6	0.7	5.6
AG750+AT200	53.8	1.2	1.6	0.7	5.6
CD750+RD200	59.5	1.3	2.3	2.3	5.1
CD750+HP200	59.3	1.3	2.3	2.3	5.3
CD750+AT200	59.5	1.3	2.3	2.3	5.3
AE750+RD400	42.9	0.9	1.5	0.1	3.6
AE750+HP400	42.6	0.8	1.4	0.1	3.5
AE750+AT400	42.6	0.9	1.5	0.1	4.1
AG750+RD400	56.2	0.9	1.7	0.7	3.2
AG750+HP400	55.9	0.9	1.6	0.7	3.0
AG750+AT400	55.9	0.9	1.7	0.7	3.7
CD750+RD400	61.9	1.0	2.4	2.3	2.9
CD750+HP400	61.6	1.0	2.3	2.3	2.7
CD750+AT400	61.6	1.0	2.4	2.3	3.4

In general, although blends containing pyrolysed CD lignite have the best fuel characteristics when proximate and ultimate analyses along with the calorific value measurement results are taken into account as a whole, pyrolysed AG lignite and its blends with pyrolysed biomass samples demonstrated the greatest improvement in terms of fuel properties.

7.3 Thermal Analysis Results

Burning profiles (TGA, DTG, DTA and DSC curves) of the parent samples and the blends where biomass samples was added 10 wt% to lignite were derived from the thermal analysis and introduced in Appendix.

TGA and DTG curves show the weight losses and the rates of weight losses, respectively. Even though weight loss characteristics of a sample during combustion process are derived from TGA and DTG profiles, a clear information about endothermic or exothermic behavior of the sample can be obtained from DSC and DTA curves. DTA plot shows the temperature difference between the sample and heating medium while DSC is used to measure heat flow into the sample from medium or vice versa. Endothermic and exothermic behavior of the burning sample can be comprehended from both plots by looking at the fact that the curves are in the positive or negative parts of the ordinate axis. The positive peaks above the ordinate axis represent the exothermic phenomena whereas the negative ones below the axis indicate the endothermic events. It can be seen that the endothermic phenomena takes place from the moisture removal at temperatures around 100°C and some other weight losses due to the volatile matter release at temperatures below 300°C, while exothermic process is attributed to the burning mechanism of the samples. Moreover, calorific value of the samples are related to the bigness of the peaks or the area under them.

Some important parameters relevant in combustion process such as ignition temperature, burning time, maximum rate of weight loss (R_{max}) due to the burning of combustibles, temperature value at the maximum rate of mass loss (T_{Rmax}), end temperature of combustion (T_{final}) and the temperature at 50% of weight loss occurs are given in Table 7.11 – Table 7.13. Ignition temperature of the samples were determined from the point on DTA curves where the reaction transits from the endothermic to exothermic state. The point where the weight loss ceases in DTG or

TGA profiles was used to detect burning time for each parent and blend sample. Moreover, maximum rate of mass loss and corresponding temperature were obtained from DTG curves.

TGA curves presented in Appendix indicate that there is significant difference in the weight loss characteristics of lignites and the biomass materials. That is, biomass samples showed so rapid weight losses in temperature interval of 300-350°C that they lost the most part of the weight in a period of very short time. On the other hand, the lignite samples did not show such a high reactivity in the mentioned temperature range. Accordingly, the burning process for biomasses completed earlier than lignite. Besides, although the lignite/biomass blends showed thermal reactivity which is between the reactivities of lignite and biomasses, it is mainly under the effect of lignite that is the dominant constituent in the blends. Meanwhile, DTG profiles revealed that there exist so fundamental differences in the weight loss rates that the maximum rate of weight loss (R_{max}) for lignites was only 13.7 %/min belonging to CD sample, while corresponding value for HP was 75.7 %/min and the other biomass samples also had disproportionally higher R_{max} values compared to lignite samples.

Once the profiles of lignite samples obtained via thermal analyses in the Appendix are examined, it can be said that weight loss of AG lignite is so rapid in comparison with AE and CD particularly until 100^{o}C when mostly moisture release occurs. On the other hand a sharp decrease in weight was observed for CD lignite in temperature range of 350-550^{o}C. Although TGA curves of AE and CD show similar trends until 450^{o}C, they follow different pathways from that point to the end of combustion process. The reason of this segregation is the simultaneous combustion of volatile and char, in case of CD consecutive ignition of volatiles and char combustion that were inferred from the two peaks in case of AE.

The biggest peak in DTG curves of lignites was observed for AG that proves the sharp decrease in weight loss during the moisture release. The maximum rate of weight loss (R_{max}) due to the burning of combustibles and the relevant temperature of CD is 13.7 %/min and 463.4°C, respectively. Since R_{max} is related to the reactivity of the sample proportionally, it can be said that CD is the most reactive lignite sample among the others [121]. On the other hand, previous studies revealed that the temperature value at the maximum rate of mass loss (T_{Rmax}) is inversely proportional

to the reactivity and combustibility of the sample [2]. Combustion properties of the samples presented in Table 7.11 support this point of view. Moreover, char combustion of AE begins at around 600^{o}C. High burning temperature indicates the difficulty of a material to burn that causes the requirement of longer residence time in combustion chambers for complete thermal conversion [122]. Hence, utilization of AE lignite necessitates special care in comparison with CD and AG.

Table 7.11 : Burning characteristics of original lignite, pyrolysed chars and original, torrefied and pyrolysed biomass.

Sample	Ignition temperature (^{o}C)	Burning time (min)	T_{R-max} (^{o}C)	R_{max} (%/min)	$T_{\%50}$	T_{final}
AE	282.4	20.1	774.2	8.8	649.0	792
AE750	300.0	14.4	406.0	13.3	549.4	727
AG	298.0	12.4	397.0	12	387.4	731
AG750	305.4	14.8	493.0	12.6	561.0	725
CD	200.3	14.2	463.4	13.7	490.5	620
CD750	346.0	15.7	466.9	15.7	583.0	610
RD	326.0	11.3	334.4	72.7	333.4	452
RD200	290.5	10.2	326.8	96.8	329.6	434
RD-400	251.0	13.3	306	24.9	417.6	518
HP	272.0	11.1	350.9	75.7	343.0	446
HP200	297.3	9.7	330.5	91	330.9	422
HP400	253.6	12.9	310.4	32.9	408.0	672.4
AT	268.0	11.1	333.4	64.3	330.7	444
AT200	296.2	10.1	321.7	98	323.2	414
AT400	253.3	16.2	390.8	26.3	432.6	692.5

When burning characteristics of the parent samples were examined in Table 7.11, ignition temperatures of AE and AG lignite samples increased slightly due to their pyrolysis at 750°C in contrast to CD lignite sample which showed significant rise as 73%. Regarding to biomass samples, ignition temperature of RD sample decreased by torrefaction process which was carried out at 200°C. Contrarily, ignition temperatures of HP and AT samples were observed to increase as a result of torrefaction. 23% decrease in the ignition temperature of RD sample was detected after its pyrolysis at 400°C, whereas 6.8% and 5.5% were the corresponding values for HP and AT samples, respectively. It was observed that while the burning time of torrefied biomass samples at 200°C decreased, burning time of pyrolysed samples at 400°C increased. The highest increase in burning time was observed in AT sample with a 46% increase.

T_{Rmax} values of coal samples were observed to be 47.5% less in AE, 24% more in AG and an insignificant change in AT sample. It was seen that torrefaction of biomass samples resulted in decrease in T_{Rmax} values. It was observed that there was a decrease in T_{Rmax} values of RD and HP samples pyrolysed at 400 °C. On the contrary, T_{Rmax} value of AT sample, which was also pyrolysed at 400 °C increased by 14.7%.

When R_{max} values are evaluated, it was found that pyrolysis has an contributing effect on coal samples with AE lignite having the best results with a significant 33.8% raise. R_{max} values also increased with torrefaction of samples at 200 °C. The most increase was observed in AT sample with a 34.4% increase. R_{max} values of semi cokes gathered via pyrolization of biomass samples at 400 °C decreased. The most dramatic decline was on RD sample with a 66% decrease. Once the consequences are assessed it was determined that R_{max} values increases as the coal samples were pyrolysed. On the contrary, the samples produced via pyrolysis of biomass had 30% less numbers.

$T_{\%50}$ temperatures of coal samples were studied to conclude that, the samples made from pyrolysis of original lignite samples are in need of higher temperatures to burnt out by 50%. Although $T_{\%50}$ temperature of AE pyrolysed lignite sample decreased, the same value of AG and CD samples increased. There was no significant change in comparison of $T_{\%50}$ values of original and torrefied biomass. It was observed that biomass pyrolysed at 400 °C has a positive effect on $T_{\%50}$ values. The highest increase was belong to AT sample with a 30% increase.

It was found to be that T_{final}, the temperature where the burning process comes to an end, decreased due to pyrolysis. Biomass samples have very similar T_{final} values and they all decreased due to torrefaction. However, pyrolysis lead to a significant rise in $T_{final,}$ while the highest increase belonging to AT sample with 56% increase. The highest final temperature was achieved during pyrolysis of AT400 sample.

When the burning times were examined, no remarkable change was observed. It was concluded that pyrolysis of AG and CD samples has no significant benefit on T_{Rmax} values. However, T_{Rmax} value of AE sample decreased by 47.5%.

According to Table 7.12, there was not any noticeable difference on AE sample by the addition original biomass which is also valid for AG sample. For the CD sample,

however, it was observed that there is approximately 75 °C increase in its ignition point. Addition of torrefied biomass to AG sample was resulted in no important difference on its ignition point. Addition of pyrolysed biomass to AE and AG sample show no prominent difference on ignition points. On the other side, blending of pyrolysed biomass to CD lignite resulted in 75 °C increase on ignition point.

Table 7.12 : Burning characteristics of original lignite and original, torrefied and pyrolysed biomass blends.

Sample	Ignition temperature (^oC)	Burning time (min)	T_{R-max} (^oC)	R_{max} (%/min)	$T_{\%50}$	T_{final}
AE+RD	284.5	19.4	338	14.6	472.0	779
AE+HP	286.0	19.4	336	15	475.0	784
AE+AT	287.2	19.4	338	14.5	474.0	785
AG+RD	297.0	15.4	406.7	14.5	408.4	646
AG+HP	296.4	15.3	419.4	14.0	409.0	629
AG+AT	296.3	15.2	415.2	14.1	398.4	623
CD+RD	273.5	13.9	479	13.5	484.3	611
CD+HP	279.0	13.8	417.3	13.2	463.4	589
CD+AT	275.6	14.0	482	13.4	483.7	617
AE+RD200	283.4	19.5	319	32.3	462.3	784
AE+HP200	293.7	19.4	347.2	12.3	481.6	773
AE+AT200	283.2	19.5	341	12.1	482.7	776
AG+RD200	299.0	15.3	410.0	14.4	411.5	620
AG+HP200	294.6	12.3	405.7	14.9	402.3	606
AG+AT200	296.7	15.2	385.5	18.2	393.8	625
CD+RD200	275.0	14.0	446	13.1	479.2	613
CD+HP200	276.0	13.9	420.5	14.5	475.2	586
CD+AT200	278.7	14.2	491.4	13.2	493.0	573
AE+RD400	284.1	19.5	471.3	9.2	495.4	777
AE+HP400	281.3	19.6	322	15	485.0	784
AE+AT400	286.7	19.5	480.9	9.6	496.9	775
AG+RD400	291.8	15.2	387.7	15.5	421.5	612
AG+HP400	286.7	14.7	381.3	17.0	422.0	616
AG+AT400	285.3	14.1	370.0	18.6	419.7	613
CD+RD400	272.9	14.1	464	13.8	486.4	614
CD+HP400	272.3	14.0	466	14.4	492.7	612
CD+AT400	273.9	14.7	481	14.1	497.6	610

Once the results are assessed it is determined that addition of biomass to CD sample is beneficial while other lignite samples were not affected. When CD lignite sample is compared with other lignites, one can see that CD lignite has more calorific value and a quality product. Addition of biomass to low quality lignite has no effect on

ignition point, while addition to high quality lignites are relatively more beneficial. Concerning the burning times, no coal or biomass sample showed a noticeable difference in this regard.

Table 7.13 indicate that addition of original biomass samples to pyrolysed AE lignite sample did not cause any significant change in the ignition temperature similar to CD750 sample. However, blending with original biomass samples increased the ignition temperature of AG by 20°C after it was pyrolysed at 750°C. Moreover, no obvious alteration was observed in the ignition temperatures of pyrolysed AE sample when torrefied biomass samples were added onto it. Likewise, pyrolysed CD lignite was not affected from torrefied biomass samples significantly. Nevertheless, ignition temperature of pyrolysed AG sample increased by 20°C once torrefied biomass samples were added. On the other hand, 20°C increase in the ignition temperature of pyrolysed AE lignite sample was observed when pyrolysed biomass samples were mixed with it. In this context, AG750 revealed the same result with AE750, but it was observed that no significant change took place in pyrolysed CD lignite sample upon addition of pyrolysed biomass samples.

When the results tabulated in Table 7.13 were analyzed, it was observed that even though 75°C increase in the ignition temperature of CD lignite sample occurred by adding 10 wt% of pyrolysed biomass samples onto it, no change was observed in case of blending pyrolysed CD lignite with pyrolysed biomass samples. As a result, it was determined that the effect of the volatile matter content of lignite coal on the ignition temperature is high.

Co-combustion of pyrolysed lignite samples and original, torrefied, pyrolysed biomass samples did not cause a significant variation in burning time when the results in Table 7.11 and Table 7.13 were compared.

Maximum rate of weight loss of AE sample increased by 56% when it was pyrolysed at 750°C and blended with original RD sample, whereas HP and AT did not affect meaningfully. On the other hand, no change was observed in AG750 sample by adding original biomass samples to prepare blends for co-combustion. Moreover, increases between 9% and 15% in the R_{max} values of CD lignite sample were observed when RD, HP and AT samples were added to CD750 sample. Addition of torrefied biomass samples to AE750 and CD750 samples resulted in 18% and

approximately 12% increase in the R_{max} values of original AE and CD samples, respectively. However, no significant change was observed in AG sample in terms of R_{max} value when torrefied biomass samples were added to AG750. It was determined that addition of original, torrefied or pyrolysed biomass sample onto pyrolysed CD sample affected R_{max} value of the original CD sample in the same manner. Furthermore, R_{max} value of AE sample increased slightly that can be negligible when AE750 was mixed with pyrolysed biomass samples. The same is also valid for AG sample. As a result, addition of original, torrefied and pyrolysed biomass samples to pyrolysed lignite sample lead to the nearly same effect on only CD750 sample.

Concerning the change in the $T_{\%50}$ values by adding original biomass samples to pyrolysed lignite samples, 42% increase in AE750, 5.3% decrease in AG750 and negligible increase by 1.7% in CD750 samples were observed. On the other hand, $T_{\%50}$ values of AE750, AG750 and CD750 pyrolysed lignite samples changed in the order of 43% increase, 5.6% decrease and 1.7% increase as a result of blending with 10 wt% of torrefied biomass samples. Same trend was seen in CD750 by adding original biomass or torrefied biomass. Moreover, 45.5% and 3% increase in $T_{\%50}$ values was observed in AE750 and CD750 pyrolysed lignite samples, respectively when pyrolysed biomass samples were added onto them. Negligible decrease by 1.82% was detected in AG750 sample in terms of $T_{\%50}$ value. When the results were examined, the same change in $T_{\%50}$ values of pyrolysed AE sample was seen with the addition of original or torrefied biomass samples. Thus, it is likely to say that $T_{\%50}$ value of AE750 sample was affected by addition of original, torrefied and pyrolysed biomass samples more than the other lignite samples.

End temperature of combustion of AE750, AG750 and CD750 pyrolysed lignite samples changed in different ways such that 9% increase, 6.6% decrease and only 3.3% increase were observed, respectively by adding original biomass samples. On the other hand, addition of torrefied biomass samples to pyrolysed lignites resulted in 9% increase in AE750 sample and negligible increase by 2.5% in CD750 sample in terms of final temperature. Correspondingly, no significant change was observed in AG750 sample. Similar outcomes for each pyrolysed lignite samples were obtained when pyrolysed biomass samples were added. In general, change in the final temperature of pyrolysed lignite samples with the addition of original, torrefied and pyrolysed biomass samples to them remained same. Thus, it has been determined

that there was no considerable difference of adding original, torrefied and pyrolysed biomass samples to pyrolysed lignite samples.

Table 7.13 : Burning characteristics of pyrolysed chars and original, torrefied, pyrolysed biomass blends.

Sample	Ignition temperature (^oC)	Burning time (min)	T_{R-max} (^oC)	R_{max} (%/min)	$T_{\%50}$	T_{final}
AE750+RD	314.0	19.7	347.4	13.7	784	789
AE750+HP	312.1	19.7	392	9.6	780	786
AE750+AT	309.0	19.9	775.1	8.6	777	793
AG750+RD	325.7	14.2	484.0	12.5	537	687
AG750+HP	329.0	17.9	474.5	13.0	525	662
AG750+AT	326.6	13.6	410.9	13.0	528	687
CD750+RD	340.0	16.0	555.0	14.9	594	630
CD750+HP	337.2	16.0	545.4	15.7	598	631
CD750+AT	335.3	15.8	558.1	14.9	592	628
AE750+RD200	313.4	19.9	352.7	10.4	789	800
AE750+HP200	311.2	20.0	780.4	10.4	793	796
AE750+AT200	309.0	20.0	783.6	10.3	793	797
AG750+RD200	335.4	13.9	480.8	12.4	536	717
AG750+HP200	322.3	13.7	484.0	13.1	528	719
AG750+AT200	321.8	14.0	503	13.0	542	721
CD750+RD200	349.3	15.8	535	14.3	576	621
CD750+HP200	341.0	15.7	550.7	15.4	591	625
CD750+AT200	336.9	15.7	543.3	15.2	589	627
AE750+RD400	322.3	20.0	451.2	9.8	798	798
AE750+HP400	318.8	20.0	453.3	10.2	797	801
AE750+AT400	324.3	20.0	453.3	9.4	799	826
AG750+RD400	319.3	14.2	496.7	13.1	551	713
AG750+HP400	322.2	13.9	490.3	13.3	543	718
AG750+AT400	324.8	13.5	512.6	14.2	546	720
CD750+RD400	357.0	16.0	539.0	14.0	602	638
CD750+HP400	340.2	15.8	525.3	15.1	582	627
CD750+AT400	339.6	15.9	559.2	15.4	595	626

7.4 Kinetic Study

DSC profiles of the parent and blend fuels were used to determine the kinetic parameters including heat of reaction, activation energy, pre-exponential factor and the order of reaction based on Arrhenius Equation. Kinetic study was carried out by applying the Borchardt & Daniels (B&D) kinetic analysis method on a single linear heating rate scan.

Results of the kinetic analysis for parent fuel were summarized in Table 7.14. As it is seen from the table, reaction orders of CD and AG are close to each other and far from the value obtained for AE. On the other hand, the heat of reaction value of CD is almost twice of AE and AG which have close values. Moreover, activation energy is inversely proportional to reactivity thus, the order of reactivity of the samples from high to low is CD, AG and AE, respectively. It was observed that reaction orders of the lignite samples changed differently after they were pyrolysed at 750°C such that nearly three and two fold of the reaction orders were determined for AG750 and CD750 samples respectively, while only 9% increase was seen in AE750 lignite. Activation energy of lignite samples increased by more than two times due to the pyrolytic treatments at 750°C. The largest increase was detected in CD sample which has the lowest activation energy and highest heat of reaction. These kinetics results are compatible with the outcomes of proximate analysis and calorific value measurements.

Table 7.14 : Burning characteristics of pyrolysed chars and original, torrefied, pyrolysed biomass blends.

Sample	Reaction order	Activation energy (kJ/mol)	Heat of reaction (J/g)
AE	2.98	78.0	7392.0
AE750	3.25	162.2	9617.0
AG	1.10	65.5	7773.7
AG750	2.67	147.0	9394.4
CD	1.07	40.7	13996.0
CD750	3.26	173.9	10655.8
RD	3.13	148.3	7221.4
RD200	2.27	115.5	5577
RD400	3.44	81.4	16281.2
HP	1.54	92.9	7264.5
HP200	2.03	124.3	5961.3
HP400	3.06	87.3	16239.1
AT	2.08	96.3	8195.5
AT200	2.98	171.1	4741.9
AT400	2.90	71.5	16496.3

Among the biomass samples, RD has the highest reaction order and activation energy, but least heat of reaction. Torrefaction of biomass samples at 200°C resulted in the 27% decrease in RD, 32% increase in HP, 43% increase in AT sample in terms of reaction order. Pyrolysis of biomass samples at 400°C lead to increase in reaction orders so that corresponding rises in each sample was determined as 10%, 98% and

39% for RD, HP and AT samples in an order. Activation energy of the pyrolysed biomass samples were recorded as less than both torrefied and original forms. AT400 has the lowest activation energy and highest heat of reaction in comparison with the other pyrolysed biomass samples. Since activation energy of a sample indicates the ability of molecules to overcome the barrier for the achievement of burning reactions, lower values are related to the higher reactivity of the investigated sample and easiness of the reaction. Thus, it is likely to say that CD is the most reactive lignite and pyrolysed AT sample is the most reactive biomass sample. Kinetic parameters of the lignite and biomass blends were introduced in Table 7.15 and Table 7.16.

Table 7.15 : Kinetic parameters of original lignite and original, torrefied and pyrolysed biomass blends.

Sample	Reaction order	Activation energy (kJ/mol)	Heat of reaction (J/g)
AE+RD	3.14	83.4	7898.6
AE+HP	3.22	86.2	7695.7
AE+AT	3.34	87.0	7686.2
AG+RD	0.77	81.8	7124.3
AG+HP	0.49	74.4	6918.3
AG+AT	0.60	80.3	6655.2
CD+RD	0.58	43.5	12109.4
CD+HP	1.37	51.3	9672.0
CD+AT	0.76	44.5	11668.7
AE+RD200	4.06	106.3	7731.5
AE+HP200	3.02	89.5	7337.5
AE+AT200	3.51	94.6	7261.9
AG+RD200	0.37	65.0	7678.4
AG+HP200	0.36	64.4	7527.1
AG+AT200	0.93	75.9	7615.6
CD+RD200	0.81	43.3	12018.9
CD+HP200	1.04	49.8	10761.5
CD+AT200	0.90	51.0	12886.3
AE+RD400	3.34	83.6	8228.0
AE+HP400	3.78	87.5	8323.9
AE+AT400	3.06	79.3	8289.2
AG+RD400	1.28	70.0	6980.7
AG+HP400	1.60	73.0	9949.1
AG+AT400	1.94	75.9	10352.3
CD+RD400	0.88	44.2	13471.6
CD+HP400	0.67	41.2	13383.8
CD+AT400	0.69	43.2	13233.3

Reaction order and heat of reaction was increased in the blends of AE and biomass samples compared to the higher heat of reaction value of AE when it was utilized alone Activation energy of the blends is between the values of AE lignite and biomass samples but even closer to lignite since it is the dominant constituent by 90 wt% in the blend. Contrary to AE, addition of original biomass samples to AG and CD lignites caused a decline in the heat of reaction values. Even though blends containing torrefied biomass and original lignite samples did not show a significant variation, addition of pyrolysed biomass samples to original lignites resulted in increase in the heat of reaction values, relatively.

Table 7.16 : Kinetic parameters of pyrolysed char and original, torrefied and pyrolysed biomass blends.

Sample	Reaction order	Activation energy (kJ/mol)	Heat of reaction (J/g)
AE750+RD	6.00	191.0	6245.1
AE750+HP	0.83	74.1	7001.9
AE750+AT	1.30	85.5	7801.1
AG750+RD	2.30	134.9	9520.0
AG750+HP	1.87	121.4	8770.6
AG750+AT	2.47	134.0	9881.2
CD750+RD	2.65	160.6	11388.5
CD750+HP	1.37	52.7	9551.8
CD750+AT	0.76	43.8	11825.0
AE750+RD200	4.36	140.2	6571.0
AE750+HP200	1.04	115.6	5717.9
AE750+AT200	1.01	80.8	7452.7
AG750+RD200	1.62	108.6	8089.0
AG750+HP200	2.01	126.8	9746.6
AG750+AT200	1.46	100.1	10406.2
CD750+RD200	3.19	180.7	9116.5
CD750+HP200	1.04	47.5	10668.3
CD750+AT200	1.00	55.6	12295.2
AE750+RD400	2.38	137.6	7868.1
AE750+HP400	3.33	177.9	7397.5
AE750+AT400	3.08	158.3	7786.6
AG750+RD400	2.08	113.2	11095.1
AG750+HP400	2.21	118.4	11295.9
AG750+AT400	1.70	99.1	12191.3
CD750+RD400	2.93	153.5	10366.3
CD750+HP400	0.53	42.0	11377.6
CD750+AT400	2.32	135.0	12766.2

According to Table 7.16, the effect of adding original or torrefied biomass samples to pyrolysed lignite samples was almost same. However, blends prepared by pyrolysed biomass and pyrolysed lignite samples had higher heat of reaction, comparatively. The lowest activation energy was determined as 41.2 kJ/kmol for the blend of original CD lignite and pyrolysed HP biomass samples.

7.5 FTIR Results

The FTIR spectra of original AE lignite and its blends with original, torrefied and pyrolysed biomass samples are shown in Figure 7.1-Figure 7.3. It is clearly understood from these figures that the absorption levels at certain wavenumbers are highly characteristics and they confirm the existence of special functional groups in such complex structures. Functional groups can be simply categorized into aliphatic, aromatic and oxygen functional groups.

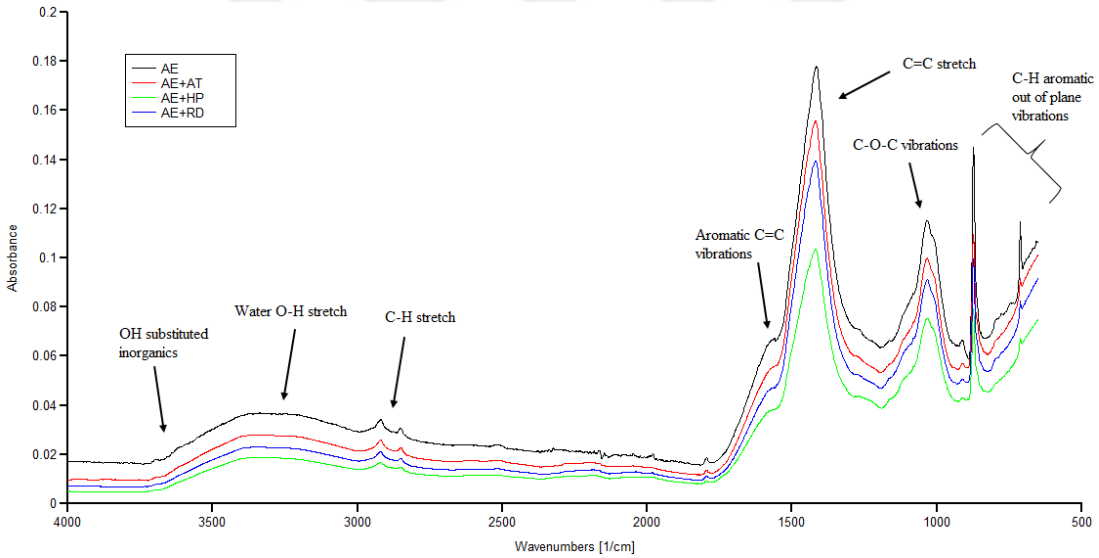

Figure 7.1 : FTIR spectra of original AE lignite and blends of original AE lignite with original biomass samples.

The band at 3700 cm^{-1} appeared in the FTIR spectra of AE lignite and its blends due to the association of a variety of hydroxyls in clay minerals, mainly kaolinite minerals present in the composition of lignite, through hydrogen bonds. The broad band between 3662 cm^{-1} and 3000 cm^{-1} was attributed to –OH groups that depicts the existence of phenols, alcohols and carboxylic acids. The absorption peaks at 2921 cm^{-1} and 2846 cm^{-1} shows the presence of asymmetric and symmetric stretching of –CH groups, respectively. Aromatic C=C stretches was observed at 1600 cm^{-1}. Moreover, the strongest band was seen at 1420 cm^{-1} that belongs to C=C bonds.

Other strong bands pointing out the C-O-C vibrations, which were resulted by ethers and alcohols, was detected at around 1026 cm^{-1}. C-H aromatic out of plane vibrations appeared at 877 cm^{-1} and 712 cm^{-1} demonstrates the presence of minerals.

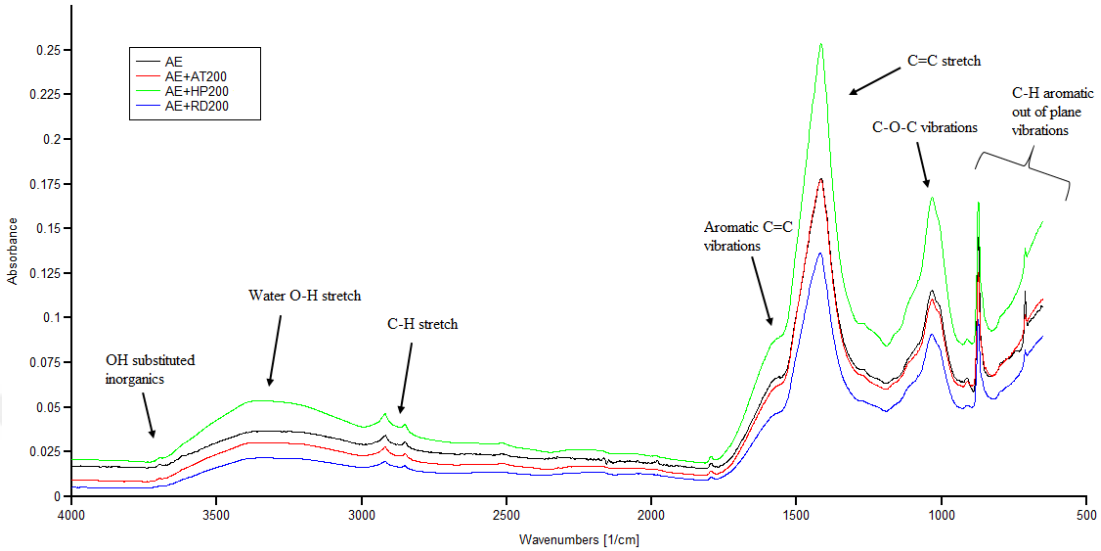

Figure 7.2 : FTIR spectra of original AE lignite and blends of original AE lignite with torrefied biomass samples at 200°C.

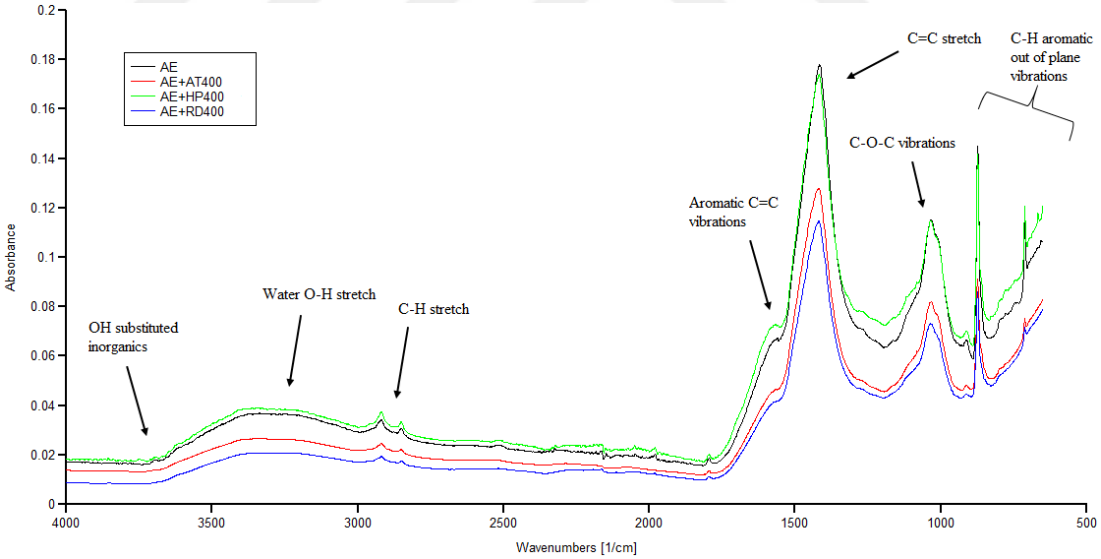

Figure 7.3 : FTIR spectra of original AE lignite and blends of original AE lignite with pyrolysed biomass samples at 400°C.

As it was seen in these figures, addition of original, torrefied and pyrolysed biomass samples to original AE lignite did not cause any change in the FTIR spectra that might be due to the dominance of lignite samples in the blends. Even though the observed functional groups are same in each case, the absorbance levels of the blends prepared by torrefied and pyrolysed biomass samples altered a bit such that intensity

of the absorbance peaks increased in the blends of original AE lignite and torrefied biomass samples. The biggest increase was observed in the blend of AE and torrefied HP sample; however, a slight decrease was detected in the blend of AE and pyrolysed HP sample.

FTIR spectra of pyrolysed AE lignite and its blends with different forms of biomass species are demonstrated in Figure 7.4-7.6. The band at 3646 cm^{-1} which was attributed to O-H stretching, was seen only in the blends of pyrolysed AE lignite. That can be interpreted as O-H stretching bonds comes from the biomass samples. Furthermore, pyrolysis of AE lignite at 750°C lead to the removal of water O-H and C-H stretching bonds along with the aromatic C=C vibrations by thermal decomposition.

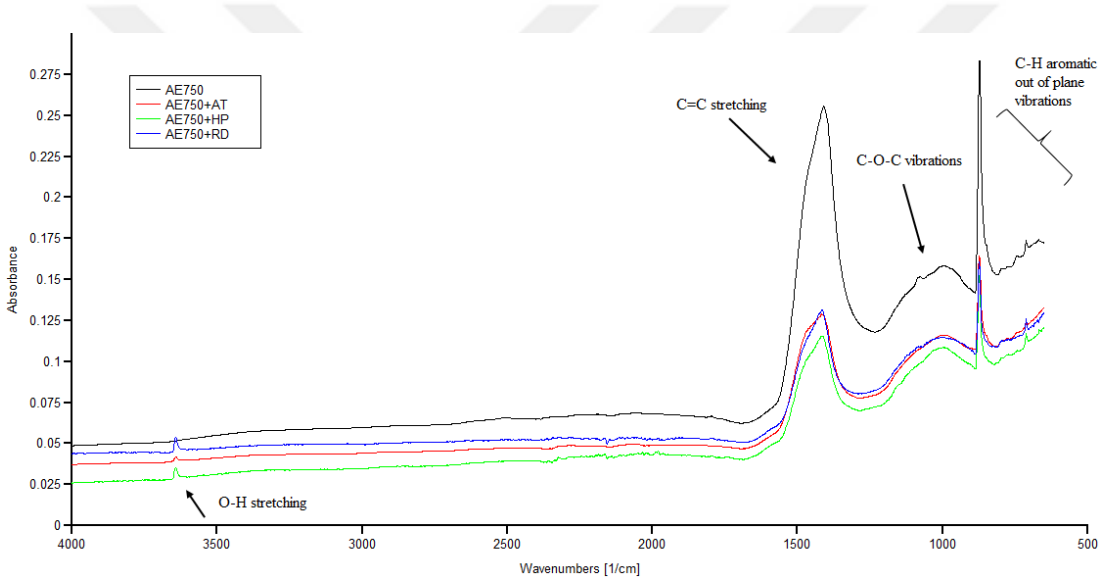

Figure 7.4 : FTIR spectra of pyrolysed AE lignite at 750°C and blends of pyrolysed AE lignite with original biomass samples.

Although functional groups observed in each FTIR spectra of pyrolysed AE lignite and its blends are same, absorption intensity of the blends altered considerably depending on the type of the biomass. That is, presence of pyrolysed AT and HP biomass species in the blends gave rise to increase in the intensity; whereas, pyrolysed RD sample lead to the major decrease in the intensity of the blends.

When Figure 7.4 and Figure 7.5 were compared with each other, it was concluded that some amplification took place in the intensities of C=C stretching bands at 1410 cm^{-1} due to the torrefaction of biomass samples excluding the blend that involve torrefied RD specie. In spite of the higher band intensity of the blend prepared by pyrolysed AE lignite and torrefied RD biomass sample throughout the FTIR spectra,

the blend of pyrolysed AE lignite and torrefied AT specie surpasses it only at the C=C stretching band.

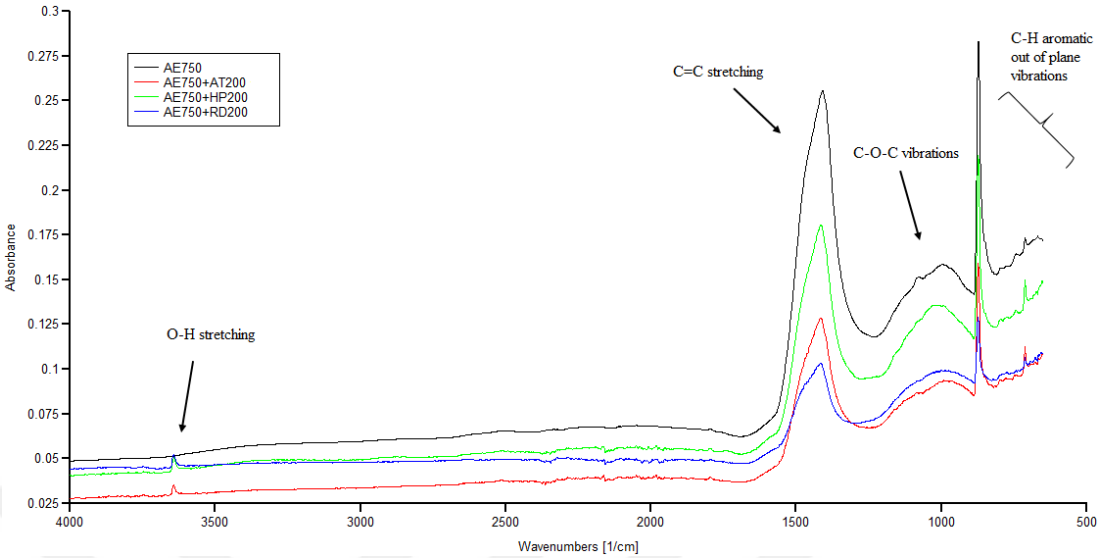

Figure 7.5 : FTIR spectra of pyrolysed AE lignite at 750°C and blends of pyrolysed AE lignite with torrefied biomass samples at 200°C.

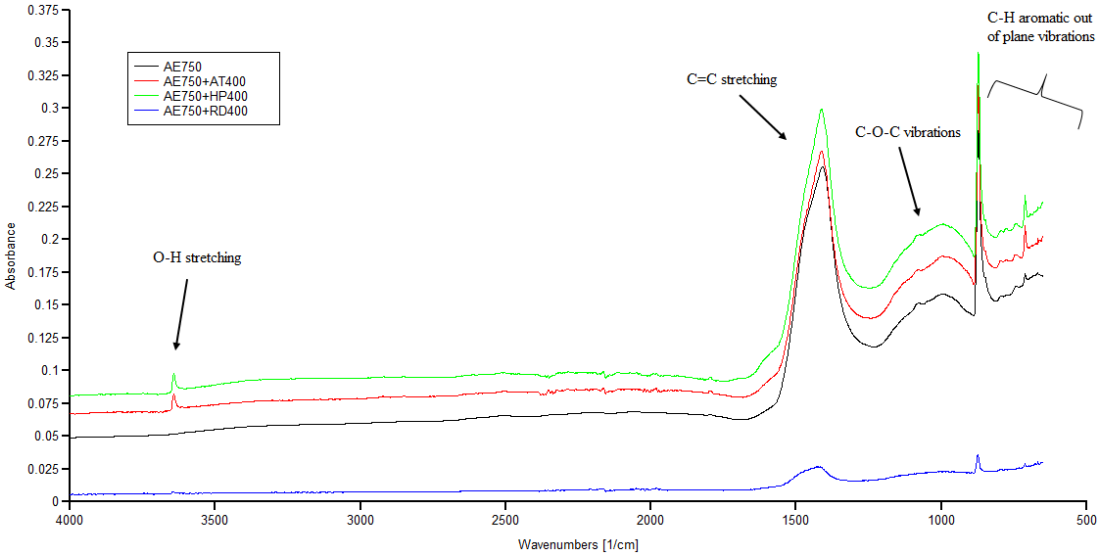

Figure 7.6 : FTIR spectra of pyrolysed AE lignite at 750°C and blends of pyrolysed AE lignite with pyrolysed biomass samples at 400°C.

The FTIR spectra of original AG lignite and its blends with original, torrefied and pyrolysed biomass samples are given in Figure 7.7-Figure 7.9. The broad vibration band between 3726 cm^{-1} and 2985 cm^{-1} was attributed to the presence of –OH bonds, which was caused by phenols, alcohols, carboxylic acid and especially moisture. The bands at 2917 cm^{-1} and 2846 cm^{-1} were ascribed to asymmetric and symmetric C-H stretches, respectively. Furthermore, AG lignite and its blends exhibited bands at around 1575 cm^{-1} due to vibration of aromatic C=C bonds. The bands at 1383 cm^{-1}

and 1255 cm^{-1} were assigned to aliphatic chain (CH_3) deformation vibration, while the band at 1010 cm^{-1} pointed out the presence of C-O vibrations which were resulted from the ethers and alcohols. The band at 905 cm^{-1} were assigned to C-H bending vibrations in aromatic structures. The strength of these bands were not affected from the torrefaction and pyrolysis of biomass samples since similar trend was observed in each case except in the blend which was formed by adding pyrolysed HP to original AG lignite sample. The FTIR spectra of the mentioned blend resembles to the spectra of original AG lignite somewhat.

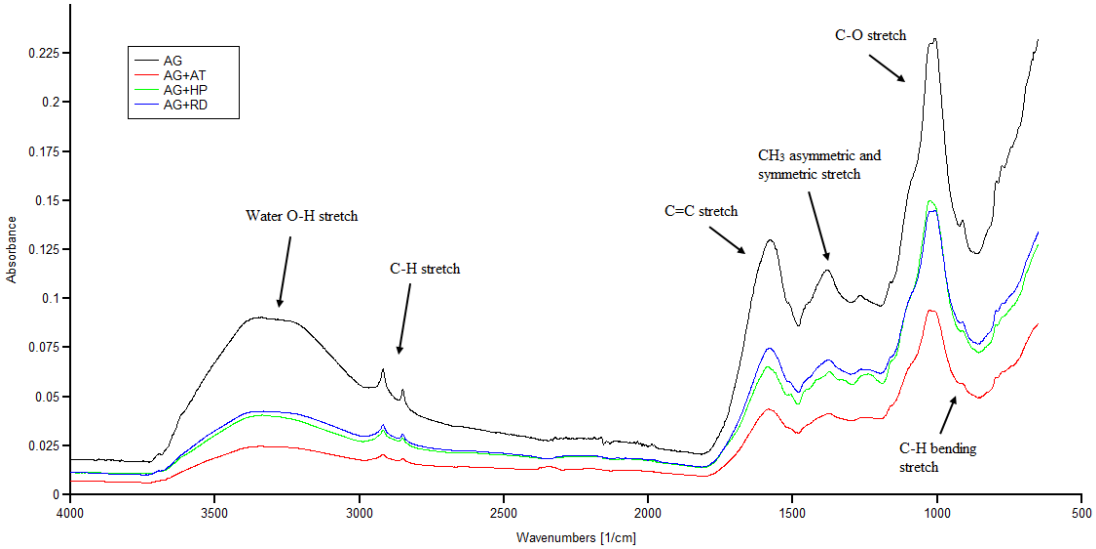

Figure 7.7 : FTIR spectra of original AG lignite and blends of original AG lignite with original biomass samples.

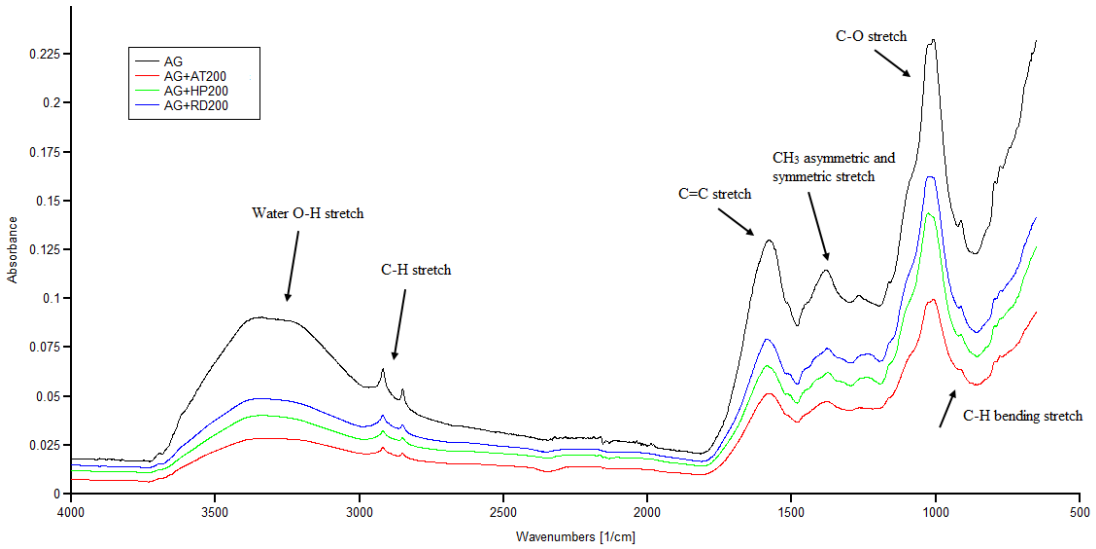

Figure 7.8 : FTIR spectra of original AG lignite and blends of original AG lignite with torrefied biomass samples at 200°C.

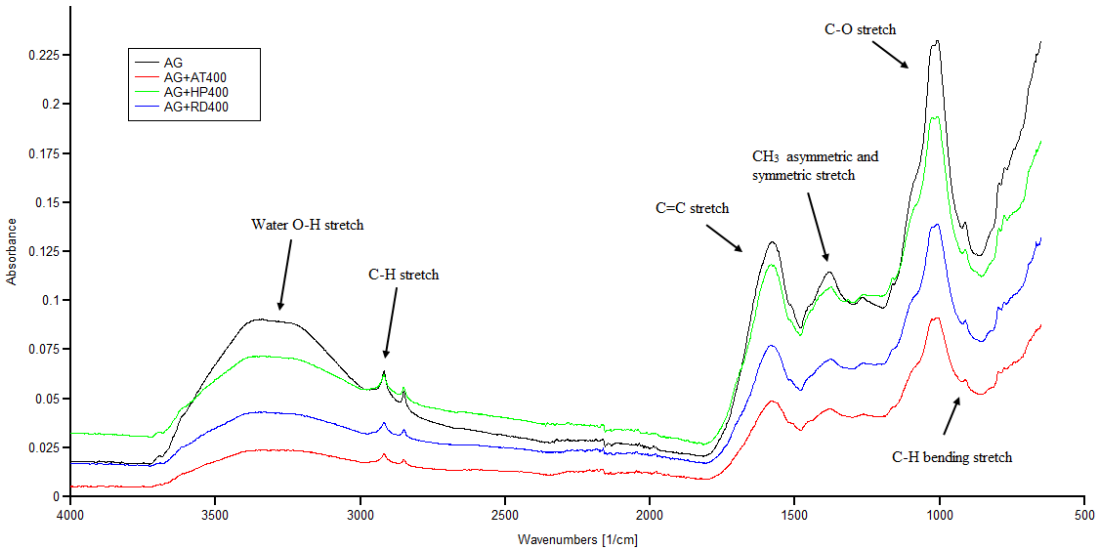

Figure 7.9 : FTIR spectra of original AG lignite and blends of original AG lignite with pyrolysed biomass samples at 400°C.

FTIR spectra of pyrolysed AG lignite and its blends with original, torrefied and pyrolysed biomass samples are shown in Figure 7.10-7.12. The common functional groups in each FTIR spectra are C=C stretching, C-O-C vibrations and C-H aromatic out of plane stretch observed at 1420 cm^{-1}, 978 cm^{-1} and in the range of 900-641 cm^{-1}, respectively.

When these three figures were analyzed, it was easily noticed that the blend of pyrolysed AG and original RD resulted in different FTIR spectra compared to other blends and parent pyrolysed AG lignite sample. Such that, aromatic C-H stretching at 3028 cm-1, C-H bending at 2958 cm^{-1} and 2910 cm^{-1}, C-O-C vibrations or P-OC stretching in polyphosphate esters at 1117 cm^{-1} and 1053 cm^{-1} were detected only in this blend. However, those functional groups did not appear in the blends of pyrolysed AG lignite and torrefied or pyrolysed RD biomass sample.

As it is seen in the FTIR spectra of both original AG and pyrolysed AG lignite along with their blends with biomass samples, water O-H stretch, C-H stretch, CH_3 symmetric and asymmetric stretch and C-H bending stretch disappeared when AG lignite sample was pyrolysed at 750°C. Moreover, absorbance intensity of the functional groups present in the AG lignite and its corresponding blends decreased as a result of pyrolytic treatment.

Although absorption levels of the blends that include original HP and AT as biomass samples were close to parent pyrolysed AG lignite, torrefaction of HP lead to a minor

decrease in the band intensity while, a huge decline in the band intensity of the blend of pyrolysed AG lignite and torrefied AT biomass sample was observed. On the other hand, FTIR spectra of pyrolysed AG and torrefied RD blend overlapped with the spectra of the blend that involve torrefied HP sample. Pyrolysis of HP further decreased the absorption levels of the regarding blend and pyrolysis of AT lead to a small increase compared to the torrefaction. However, blend of pyrolysed AG lignite and pyrolysed RD biomass sample did not reveal any significant variation in terms of band intensity.

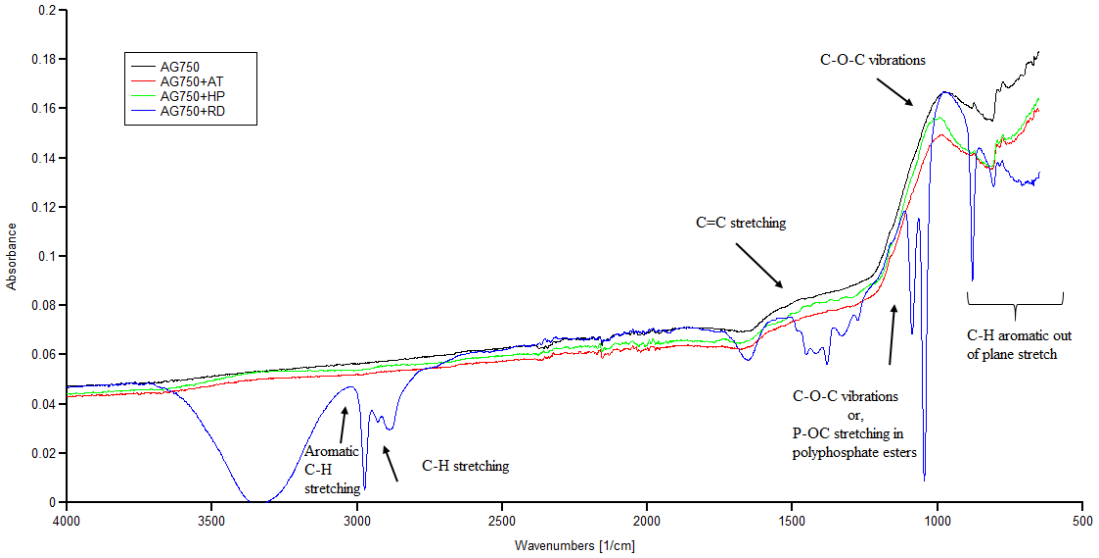

Figure 7.10 : FTIR spectra of pyrolysed AG lignite at 750°C and blends of pyrolysed AG lignite with original biomass samples.

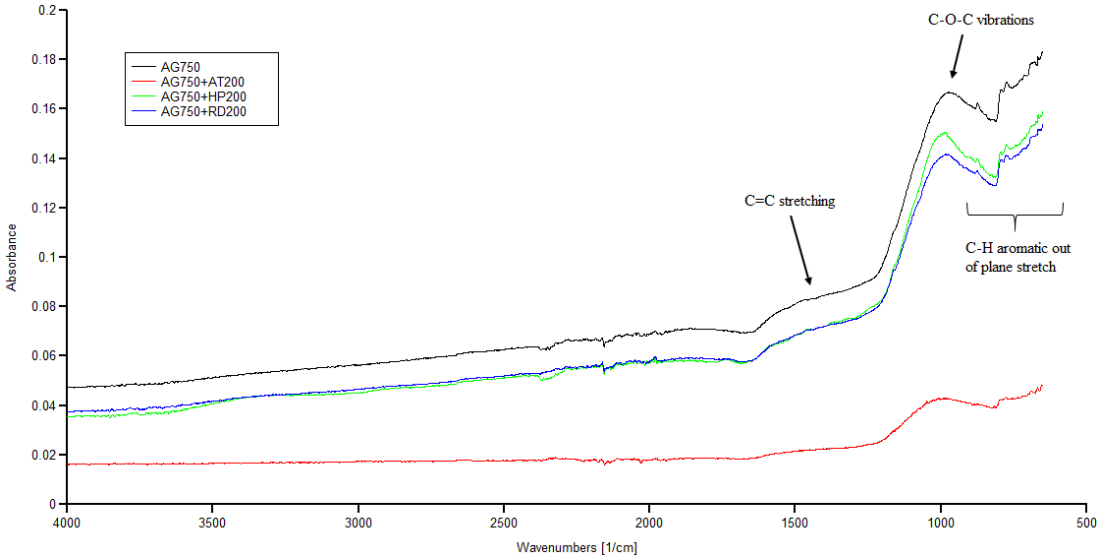

Figure 7.11 : FTIR spectra of pyrolysed AG lignite at 750°C and blends of pyrolysed AG lignite with torrefied biomass samples at 200°C.

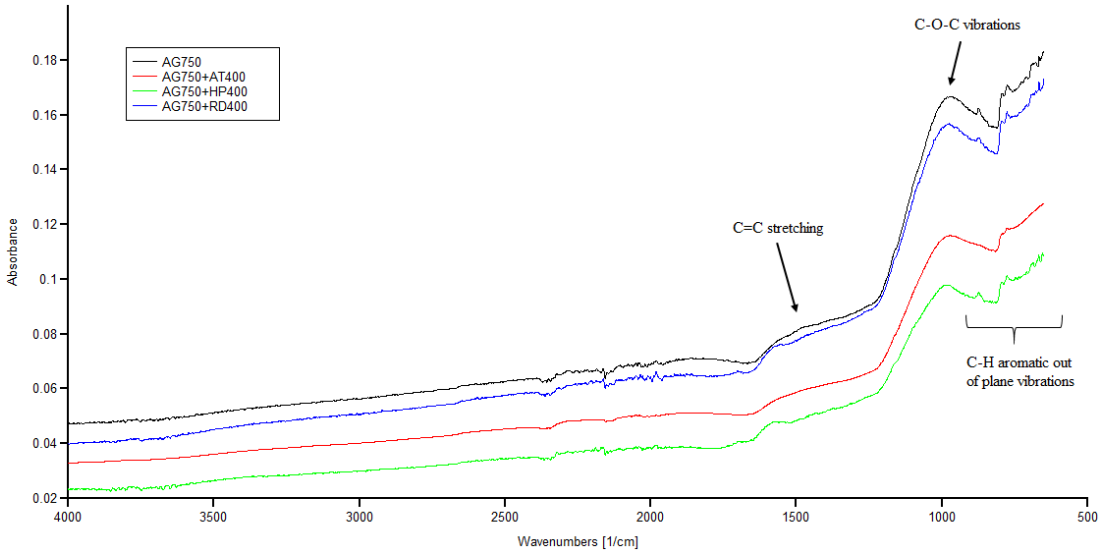

Figure 7.12 : FTIR spectra of pyrolysed AG lignite at 750°C and blends of pyrolysed AG lignite with pyrolysed biomass samples at 400°C.

The FTIR spectra of original CD lignite and its blends with original, torrefied and pyrolysed biomass samples are demonstrated in Figure 7.13-Figure 7.15. When FTIR spectra of the lignite samples were compared with each other, similarity between the FTIR spectra of CD and AG was straightforwardly remarked. The only difference of CD in terms of the present functional groups was OH substituted inorganics and C=O stretch that were pointed out in Figure 7.13.

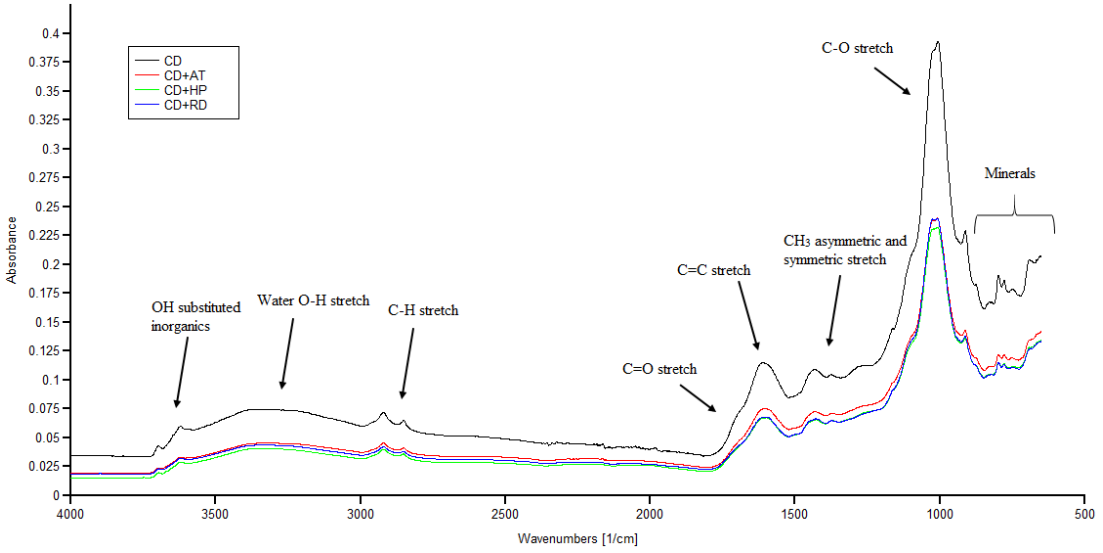

Figure 7.13: FTIR spectra of original CD lignite and blends of original CD lignite with original biomass samples.

Although lignite samples have common functional groups in general, variation in their absorption levels at certain wavenumbers was observed. Such that, in spite of

detecting same functional groups in original AE and CD lignite samples, higher absorption level in CD lignite was seen in the FTIR spectra.

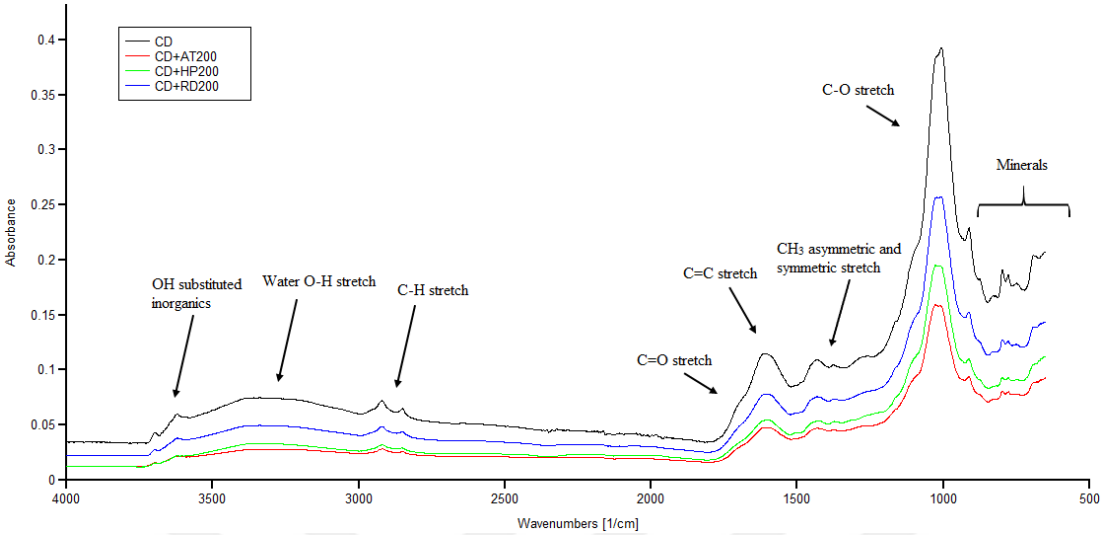

Figure 7.14 : FTIR spectra of original CD lignite and blends of original CD lignite with torrefied biomass samples.

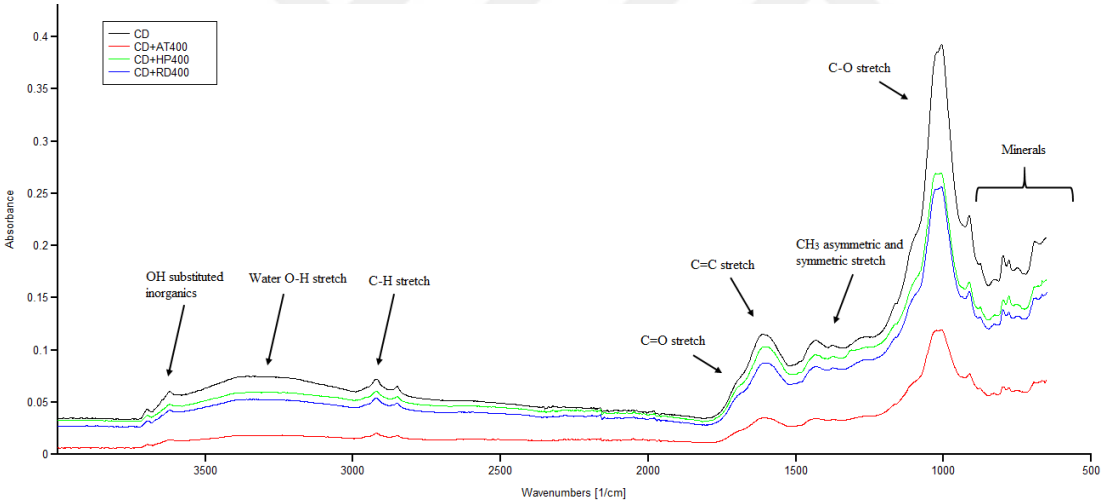

Figure 7.15 : FTIR spectra of original CD lignite and blends of original CD lignite with pyrolysed biomass samples.

According to Figure 7.13 and 7.14, it was understood that torrefaction of HP and AT lead to decrease in the band intensity of the functional groups whereas, no significant change was observed in RD biomass sample. On the other hand, further decline in the absorption level of the functional groups was observed in the blend of original CD and pyrolysed AT that can be explained by the decomposition of the functional groups due to the effect of pyrolytic treatment. In contrast to the torrefaction, pyrolysis of HP caused an increase in the band intensity of the functional groups. Since FTIR spectra of the blend that involve pyrolysed RD was very close to the

other cases, it was concluded that addition of original, torrefied and pyrolysed RD biomass to original CD lignite was resulted in the same outcome.

FTIR spectra of pyrolysed CD lignite and its blends with original, torrefied and pyrolysed biomass samples are shown in Figure 7.16-7.18.

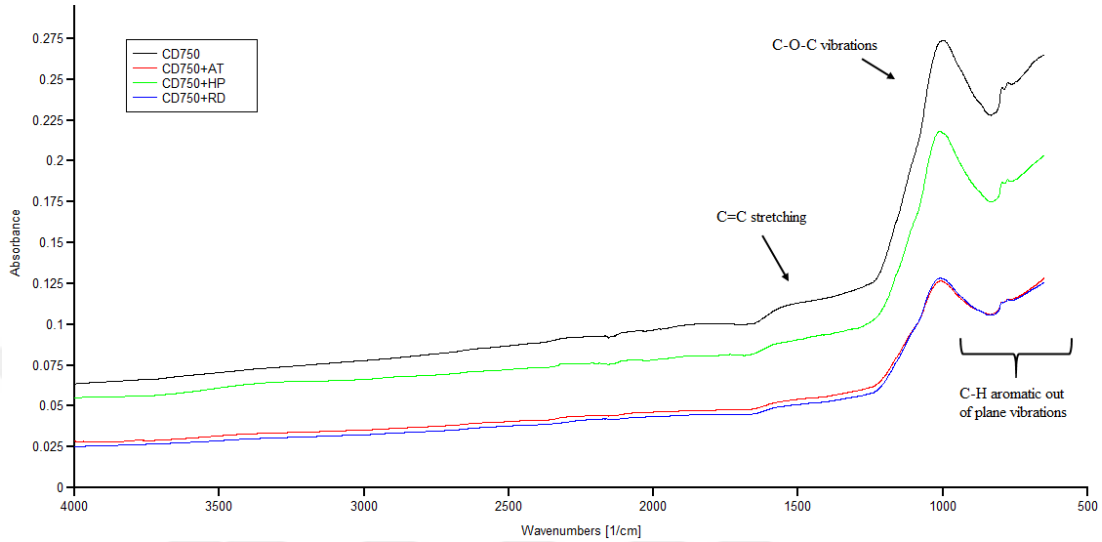

Figure 7.16 : FTIR spectra of pyrolysed CD lignite and blends of pyrolysed CD lignite with original biomass samples.

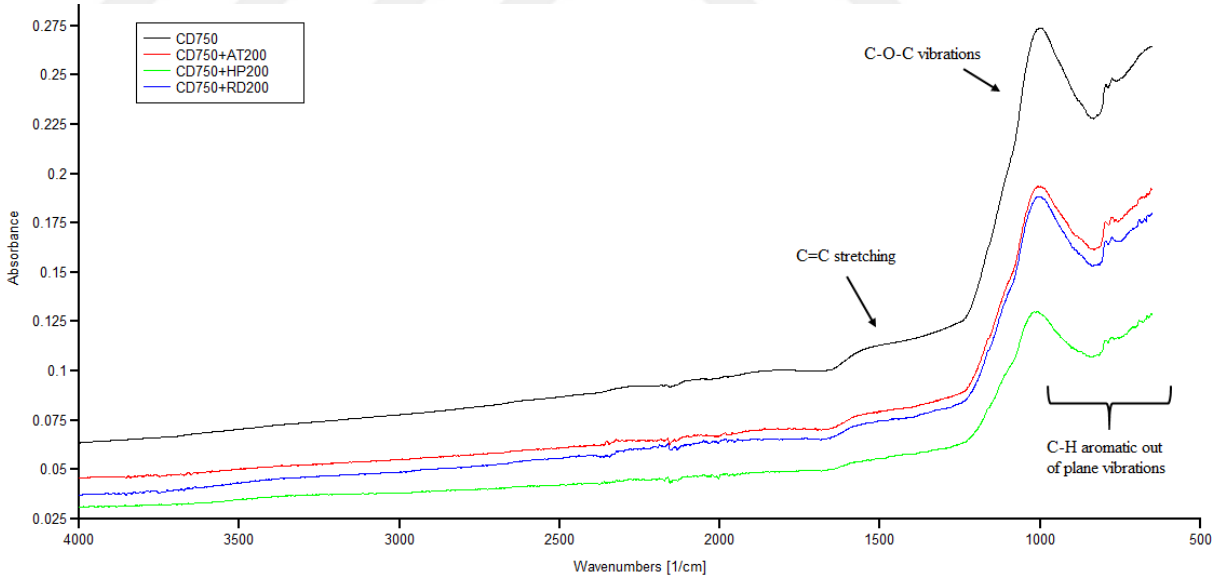

Figure 7.17 : FTIR spectra of pyrolysed CD lignite and blends of pyrolysed CD lignite with torrefied biomass samples.

Evaluation of the FTIR spectra of pyrolysed CD lignite and its corresponding blends with biomass samples revealed that FTIR results are almost identical and independent of the applied thermal pretreatment to biomass species. The bands at 1500 cm^{-1} and 1000 cm^{-1} were attributed to C=C stretching and C-O-C vibrations,

respectively. C-H aromatic out of plan vibrations were observed in the broad range of 931 cm^{-1} and 695 cm^{-1}. In comparison with the original CD lignite and its blends, removal of OH substituted inorganics, O-H stretch that comes from moisture content, C-H stretch and C=O stretch was observed due to the increased carbon content and decreased oxygen and hydrogen content as a consequence of carbonization process. In addition to that, absorption level of the pyrolysed CD lignite and the regarding blends decreased to some extent.

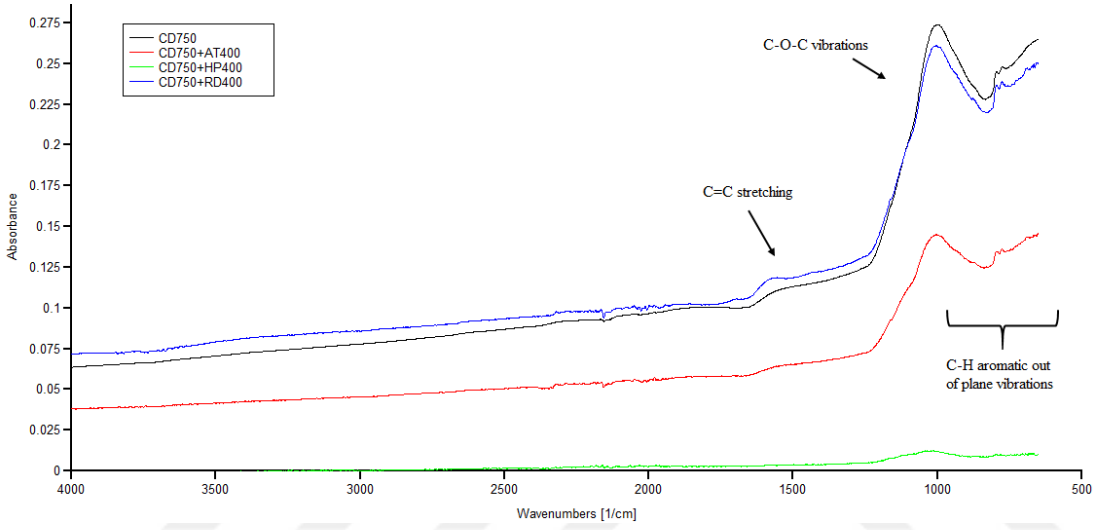

Figure 7.18 : FTIR spectra of pyrolysed CD lignite and blends of pyrolysed CD lignite with pyrolysed biomass samples.

Even though addition of original AT and RD biomass samples to pyrolysed CD lignite decreased the band intensity of the lignite and their FTIR spectra were observed very close to each other as it is seen in Figure 7.17, torrefaction and pyrolysis of those biomasses lead to the gradual increase in the absorption levels. Contrarily, presence of torrefied and pyrolysed HP in the blends decreased the absorption level of the pyrolysed CD lignite gradually such that almost no functional groups observed in case of adding pyrolysed HP to pyrolysed CD lignite.

7.6 SEM Results

SEM images of the original AE, AG and CD lignite samples along with their pyrolysed chars at 750°C under nitrogen atmosphere are shown in Figure 7.19. In general, application of pyrolytic treatment on each lignite sample was resulted in more porous structure due to the removal of moisture and volatile matter content.

Moreover, brighter images were obtained that can be the reason of rising ash contents of the pyrolysed chars.

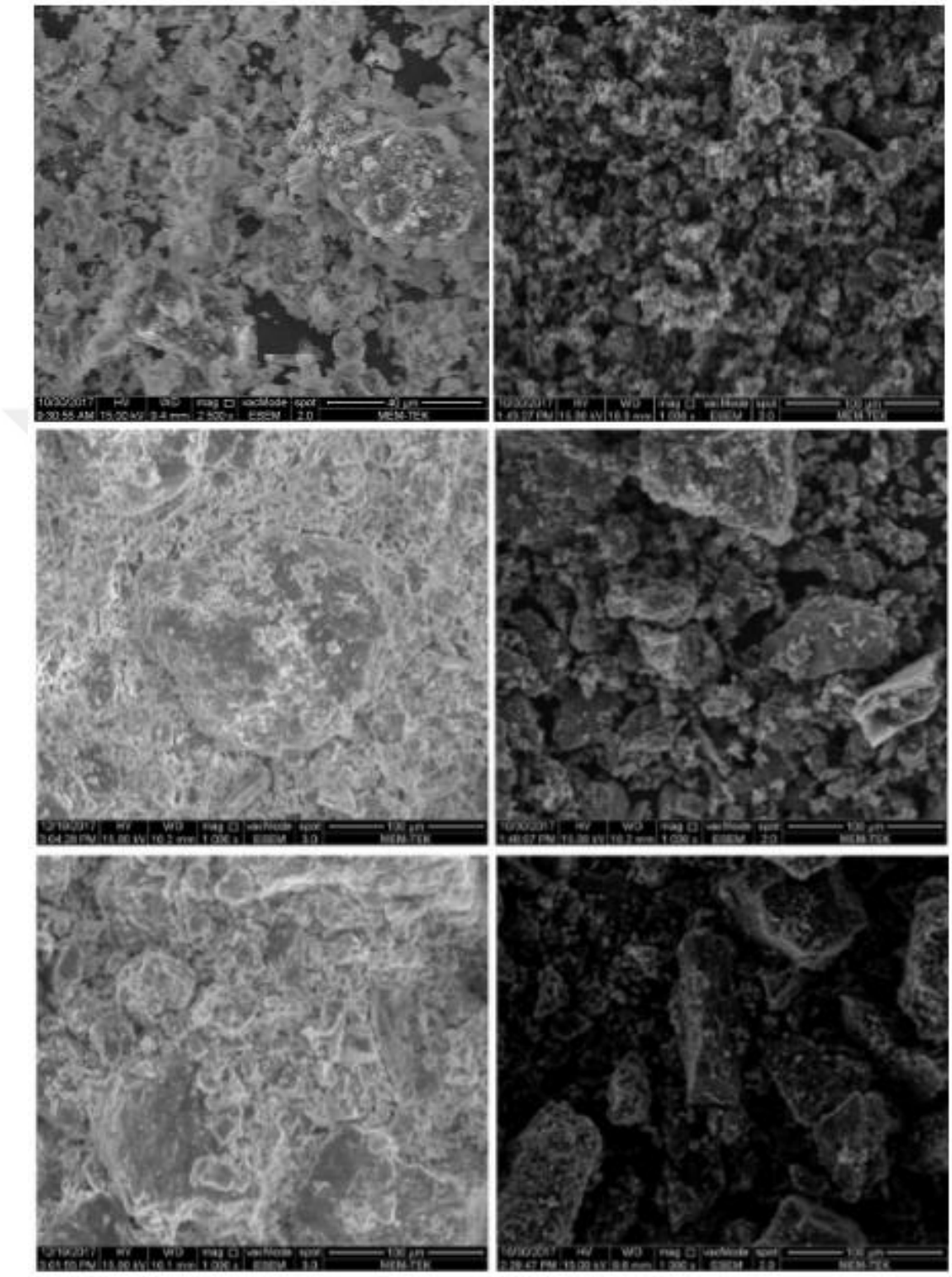

Figure 7.19 : SEM images of the original lignite (left) and their pyrolysed chars at 750°C (right) a) AE lignite, b) AG lignite, c) CD lignite (from top to the bottom).

Analysis of the SEM images demonstrated in Figure 7.19 revealed that original AE lignite has less compact structure than AG and CD while, the most compact structure

was observed in original AG lignite. When lignite samples were pyrolysed at 750°C, a more fragmented structure was seen in AE lignite compared to others.

Figure 7.20 shows the SEM images of the original, torrefied and pyrolysed biomass samples at 200°C and 400°C, respectively. Torrefaction and pyrolysis processes lead to some changes in the biomass structures in several ways such that the bright points resulting from the presence of inorganics became more evident due to the rising ash contents in the thermally treated samples. Besides, the removal of volatile matter during these thermal processes was resulted in the formation of more fragile and fractal biomass structure.

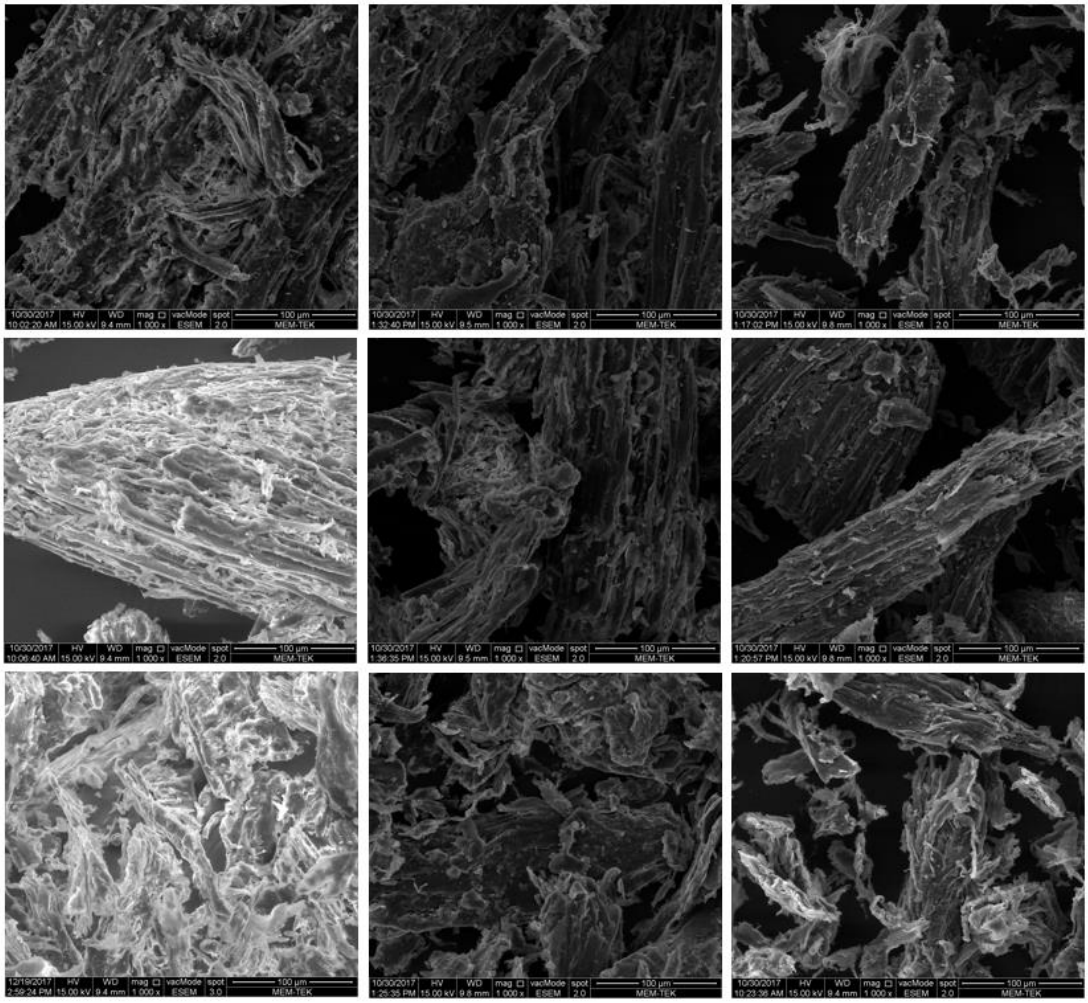

Figure 7.20 : SEM images of the original biomass (left), torrefied biomass at 200°C (center) and pyrolysed biomass at 400°C (right) a) AT biomass sample, b) RD biomass sample, c) HP biomass sample (from top to the bottom).

As it is clearly seen in Figure 7.20, the structure of original biomass samples has become highly porous due to the torrefaction process carried out at 200°C. Depending on the temperature rise from 200°C to 400°C, porosity of biomass species

further increased. However, decline in the porosity of AT biomass sample was observed as a result of torrefaction and when it was exposed to pyrolytic treatment, more porous structure was seen.

8. CONCLUSION AND RECOMMENDATION

- Pyrolysis of biomass samples at 400°C is more convenient than torrefying at 200°C in order to obtain quality fuel from biomass samples.
- Co-combustion of original AG lignite, which has the lowest calorific value among the lignite samples used in this study, with pyrolysed RD biomass sample enables to obtain a fuel having 45% more high calorific value compared to original AG lignite.
- Addition of 10 wt% of original biomass to lignite did not affect the calorific values of the original lignite samples significantly due to the negligible increase in the calorific values. Likewise, higher heating values of the blends that were prepared by adding 10 wt% of torrefied biomass samples to original lignite samples also measured as little higher than original lignites along with the blends prepared by original lignite and biomass samples. Addition of RD sample to lignites resulted in the highest increase in the calorific value of the blends.
- Blend of pyrolysed RD biomass sample with original AG lignite or pyrolysed AG lignite at 750°C has 30% difference in terms of calorific value. Since 45% increase in calorific value was determined in case of mixing 10 wt% of RD400 and 90 wt% of AG750 which was mentioned above, usage of pyrolysed lignites at 750°C is preferred to prepare lignite-biomass blends for obtaining high quality fuel rather than original lignite.
- Instead of torrefying biomass samples at 200°C, raising the temperature to two times at which pyrolysis occurs resulted in 10% increase in calorific value of pyrolysed AE lignite at 750°C when it was blended with torrefied or pyrolysed biomass samples. Thus, temperature of bio char and the ratio of increase in higher heating value of pyrolysed AE lignite are directly proportional to each other.
- Contrary to AG and CD lignites, calorific value of AE lignite was affected in the same way from the torrefied and pyrolysed biomass samples that were added by 10 wt%.

- Pyrolysis of lignite samples caused a huge decrease in the hydrogen contents which ranges between 80-85% roughly. However, the leading effect on the higher heating value was determined as the increase in the elemental carbon content. On the other hand, pyrolysis of biomass samples at 400°C lead to significant increase in the elemental carbon content which is approximately 50%. This result indicates that biomass species were affected from pyrolytic treatment much more than lignite samples.
- Burning characteristics of parent fuels revealed that the highest final temperature was achieved during pyrolysis of AT400 sample.
- Addition of biomass to CD sample is beneficial while other lignite samples were not affected. When CD lignite sample is compared with other lignites, one can see that CD lignite has more calorific value and a quality product. Addition of biomass to low quality lignite has no effect on ignition point, while addition to high quality lignites are relatively more beneficial.
- Despite the fact 75°C increase in the ignition temperature of CD lignite sample occurred by adding 10 wt% of pyrolysed biomass samples onto it, no change was observed in case of blending pyrolysed CD lignite with pyrolysed biomass samples. As a result, it was determined that the effect of the volatile matter content of lignite coal on the ignition temperature is high.
- Addition of original, torrefied or pyrolysed biomass sample onto pyrolysed CD sample affected R_{max} value of the original CD sample in the same manner.
- Same change in $T_{\%50}$ values of pyrolysed AE sample was seen with the addition of original or torrefied biomass samples. Moreover, $T_{\%50}$ value of AE750 sample was affected by addition of original, torrefied and pyrolysed biomass samples more than the other lignites.
- In terms of end temperature of combustion no considerable difference was detected between the addition of original, torrefied and pyrolysed biomass samples to pyrolysed lignites.
- CD is the most reactive lignite and pyrolysed AT sample is the most reactive biomass sample. The lowest activation energy was determined as 41.2 kJ/kmol for the blend of original CD lignite and pyrolysed HP biomass samples.
- FTIR spectra of the parent fuels revealed that although lignite samples have common functional groups in general, variation in their absorption levels at

certain wavenumbers was observed. Such that, in spite of detecting same functional groups in original AE and CD lignite samples, higher absorption level in CD lignite was seen in the FTIR spectra.

- SEM images demonstrated that application of pyrolytic treatment on each lignite sample was resulted in more porous structure due to the removal of moisture and volatile matter content. Similarly, the structure of original biomass samples has become highly porous due to the torrefaction process carried out at 200°C and depending on the temperature rise from 200°C to 400°C, porosity of biomass species further increased.

- This study showed that the lignite and the biomass species investigated in this work are highly different fuels with respect to the fuel properties as well the burning characteristics. For this reason, these fuel characteristics must be taken into consideration and required measures should be taken when biomass is added to lignite in a co-firing application. Otherwise, segregation of individual ingredients in the blends are inevitable that may create problems in the combustion systems.
- In order to move this work one step further, the type of the gaseous and liquid products that were produced during pyrolysis process can be determined for the beneficial use of combustible gases. Convenient processes can also be chosen to extract the utilization potential of the liquid and gaseous products generated from lignite and biomass materials by characterization.
- It is always possible to utilize different biomass and coal blends or blend ratios instead of the ones used in this study to find co-combustion couple and conditions.
- In addition to work done in this study, ash melting temperature of the blends can also be determined to prevent contamination in combustion systems.
- To augment this study, the suitable blends can be pelleted, briquetted and characterized after the search of gasification and liquefaction processes of the blends.

REFERENCES

[1] **World Energy Council.** (2013). *World Energy Resources: 2013 survey*. London: World Energy Council.

[2] **Haykırı-Açma, H.** (2003). Combustion characteristics of different biomass materials. *Energy Conversion & Management.*, ***44***, 155-162.

[3] **International Energy Agency**. *Coal Information 2017*. Paris: International Energy Agency.

[4] **Balat, M.** (2008). Energy consumption and economic growth in Turkey during the past two decades. *Energy Policy.*, ***36***, 118–127.

[5] **Berk, I. And Ediger, V. Ş.** (2016). Forecasting the coal production: Hubbert curve application on Turkey's lignite fields. *Resources Policy.*, ***50***, 193-203.

[6] **World Energy Council Turkish National Committee.** (2015). *Energy Statistics.* Ankara: World Energy World Energy Council Turkish National Committee.

[7] **Şahin, Ü. (Ed.), Aşıcı, A. A., Acar, S., Gedikkaya-Bal, P., Karababa, A. O. and Kurnaz, L.** (2016). Turkey's coal policies related to climate change, economy and health. *Istanbul Policy Center*. Sabancı University, Turkey.

[8] **Chao, C.Y.H., Kwong, P. C. W., Wang, J. H. Cheung, C.W. and Kendall, G.** (2008). Co-firing coal with rice husk and bamboo and the impact on particulate matters and associated polycyclic aromatic hydrocarbon emissions. *Bioresource Technology.*, ***99***, 83-93.

[9] **Krevelen, D.W.** (1993). *Coal--Typology, Physics, Chemistry, Constitution*. Amsterdam: Elsevier Science.

[10] **Miller, B.G.** (2004). *Coal Energy Systems*. Cambridge: Academic Press.

[11] **Riley, J.** (2014). *Routine Coal and Coke Analysis - Collection, Interpretation, and Use of Analytical Data*. West Conshohocken, PA: ASTM International.

[12] **National Coal Council.** (2015). *Coal = Reliable Energy.* Washington: National Coal Council, Inc.

[13] **United States Geological Survey.** (n.d.). *What are the types of coal?* Retrieved November 11, 2017, from https://www.usgs.gov/faqs/what-are-types-coal?Qt-news_science_products=7#qt-news_science_products.

[14] **Flores, R. M.** (2013). *Coal and Coalbed Gas: Fueling the Future*. China: Elsevier Science.

[15] **Larry, T.** (2013). *Coal Geology. West Sussex, UK: Wiley-Blackwell.*

[16] **Reddy, P. J.** (2013). *Clean Coal Technologies for Power Generation.* Leiden, The Netherlands: CRC Press/Balkama.

[17] **World Coal Institute.** (2005). *The Coal Resource: A Comprehensive Overview of Coal.* London: World Coal Institute.

[18] **World Coal Institute.** (n.d.). Uses of coal. Retrieved November 11, 2017, from https://www.worldcoal.org/coal/uses-coal.

[19] **U.S. Energy Information Administration.** (2016). *International Energy Outlook 2016*. Washington: U.S. Energy Information Administration.

[20] **World Energy Council.** (2016). World Energy Resources: Coal 2016. London: World Energy Council.

[21] **Lee, S. and Wheelden, B. (2007).** Global and US energy overview. *Handbook of Alternative Fuel Technologies* Boca Raton, FL: CRC Press.

[22] **Republic of Turkey Ministry of Energy and Natural Resources.** (n.d.). *Coal.* Retrieved November 11, 2017, from http://www.enerji.gov.tr/en-US/Pages/Coal.

[23] **Turkey Hard Coal Authority,** (2017). 2016 Industrial report for hard coal. Retrieved November 11, 2017, from http://www.taskomuru.gov.tr/file/duyuru/TTKGM_Sektor_Raporu_2016.PDF_Sektor.

[24] **Eurocoal.** (n.d.). *Turkey.* Retrieved November 12, 2017 from https://euracoal.eu/info/country-profiles/turkey/.

[25] **General Directorate of Mineral Research and Exploration.** (n.d.). *Coal exploration investigations.* Retrieved November 12, 2017, from http://www.mta.gov.tr/v3.0/arastirmalar/komur-arama-arastirmalari.

[26] **Coal and lignite fired power plants.** (n.d.). Retrieved November 12, 2017, from http://www.enerjiatlasi.com/komur/.

[27] **Toprak, S.** (2009). Petrographic properties of major coal seams in Turkey and their formation, *International Journal of Coal Geology, **78***, 263-275.

[28] **Ediger, V.Ş., Berk, I. and Kösebalaban, A.** (2014). Lignite resources of Turkey: Geology, reserves, and exploration history, *International Journal of Coal Geology, **132***, 13-22.

[29] **Capik, M., Kolaylı, H. and Yılmaz, A. O.** (2013). A comparative study on the energy demand of Turkey: Coal or natural gas. *Energy Exploration & Exploitation, **31,*** 119-138.

[30] **Miller, K.** (2013). Coal analysis. In D. Osborne. (Ed.), *The Coal Handbook: Towards Cleaner Production, Vol 1*. Cambridge: Woodhead Publishing.

[31] **Saikia, B. K., Saikia, A., and Baruah, B. P.** (2015). Nature and chemistry of coal and its products. *Coal Production and Processing Technology*. Boca Raton, FL: CRC Press.

[32] **Liu, G., Peng, Z., Yang, P., Wang, G.** (2001). Sulfur in coal and its environmental impact from Yanzhou mining district, China, *Chinese Journal of Geochemistry, **20,*** 273-281.

[33] **Kreith, F.** (2000). *The CRC Handbook of Thermal Engineering*. Heidelberg: Springer.

[34] **Toporov, D.** (2014). *Combustion of Pulverised Coal in a Mixture of Oxygen and Recycled Flue Gas.* London: Elsevier.

[35] **Donahue, W.S. and Brandt, J. C.** (2009). *Pyrolysis.Types, Processes, and Industrial Sources and Products.* New York: Nova Science Publishers.

[36] **Bridgwater, T.** (2006). Biomass for energy. *Journal of the Science of Food and Agriculture*, ***86,*** 1755-1768.

[37] **Liu, Z., Guo, X., Shi, L., He, W., Wu, J., Liu, Q. and Liu, J. (**2015). Reaction of volatiles – A crucial step in pyrolysis of coals. *Fuel*, ***154***, 361-369.

[38] **Kabe, T., Ishihara, A., Qian, E. W., Sutrisna, I. P., Kabe, Y.** (2004). *Coal and Coal Related Compounds: Structures, Reactivity And Catalytic Reactions.* Tokyo: Elsevier.

[39] **Zhang, J.** (2010). Advances in coal combustion research. In Grace, C. T. (Ed.), *Coal Combustion Research*, 1-37. New York: Nova Science Publishers.

[40] **Mazumder, B.** (2012). *Coal Science and Engineering*. India: Woodhead Publishing.

[41] **Miller, B. G.** (2011). Clean Coal Engineering Technology. Burlington, MA: Butterworth-Heinemann.

[42] **Smith, K.L., Smoot, L.D., Fletcher, Th.H., Pugmire, R.J.** (1994). *The Structure and Reaction Processes of Coal.* New York: Plenum Press.

[43] **Breeze, Paul.** (2015). *Coal-fired Generation*. London : Academic Press.

[44] **Speight, J. G.** (2012). The Chemistry and Technology of Coal Boca Raton, FL: CRC Press.

[45] **Belgiorno, V., De Feo, G., Della Rocca, C., and Napoli, R. M. A**. (2003). Energy from gasification of solid wastes, *Waste Manangement*, ***23***, 1-15.

[46] **Sunggyu, L.** (2007). Gasification of Coal. In Sunggyu L., Speight, J.G. and Loyalka, S.K. (eds.). *Handbook of Alternative Fuel Technologies*. Boca Raton, FL: CRC Press.

[47] **Weller, S. W.** (1995). Aspects of catalyzed coal liquefaction. In I. Hargittai and T. Vidoczy (eds.). *Combustion Efficiency and Air Quality*. New York: Plenum Press.

[48] **Sunggyu, L.** (2007). Clean liquid fuels from coal. In L. Sunggyu , J. G. Speight and S. K. Loyalka (eds.). *Handbook of Alternative Fuel Technologies*. Boca Raton, FL: CRC Press.

[49] **Basu, P.** (2013). *Biomass, Gasification, Pyrolysis and Torrefaction: Practical Design and Theory*. London: Academic Press.

[50] **The United Nations Framework Convention on Climate Change (UNFCCC).** (2005). Grid-connected electricity generation using biomass from newly developed dedicated plantations, approved baseline and monitoring Methodology AM0042. Retrieved November 12, 2017, from http://cdm.unfccc.int/EB/027/eb27_repan03.pdf.

[51] **Abbasi, T. and Abbasi, S.A.** (2010). Biomass energy and the environmental impacts associated with its production and utilization. *Renewable and Sustainable Energy Reviews,* ***14,*** 919–937.

[52] **Demirbas, A.** (2007). Combustion systems for biomass fuel. *Energy Sources*, ***29***, 303-312.

[53] **Demirbas, A.** (2007). Modernization of biomass energy conversion facilities. *Energy Sources*, ***2,*** 227-235.

[54] **McKendry, P.** (2002). Energy production from biomass (part 1): Overview of biomass, *Bioresource Technology*, ***83***, 37–46.

[55] **Zhang, L., Xu, C. and Champagne, P.** (2010). Overview of recent advances in thermo-chemical conversion of biomass. *Energy Conversion and Management*, ***51***, 969-982.

[56] **McKendry, P.** (2002). Energy production from biomass (part 2): Conversion technologies, *Bioresource Technology*, ***83***, 47–54.

[57] **Jones, J.M., Nawaz, M., Darvell, L.I., Ross, A.B., Pourkashanian, M., and Williams, A.** (2006). Towards biomass classification for energy applications. In A. V. Bridgwater and D. G. B. Boocock (Eds.), *Science in Thermal and Chemical Biomass Conversion*. United Kingdom: CPL Press.

[58] **Nordin, A., Pommer, L., Nordwaeger, M. And Olofsson, I.** (2013). Biomass Conversion Through Torrefaction. In E. Dahlquist (Ed.), *Technologies for converting biomass to useful energy combustion, gasification, pyrolysis, torrefaction and fermentation*. London: CRC Press.

[59] **Jenkins, B.M., Baxter, L.L., Miles Jr., T.R. and Miles, T.R.** (1998). Combustion properties of biomass, *Fuel Processing Technology*, ***54***, 17–46.

[60] **Demirbas A.** (2000). Biomass resources for energy and chemical industry. *Energy Education Science and Technology*, ***5***, 21–45.

[61] **Demirbas A.** (2001). Biomass resource facilities and biomass conversion processing for fuels and chemicals. *Energy Conversion and Management*, 42, 1357–1378.

[62] **White, J. E., Catallo, W. J. and Legendre, B.L.** (2011). Biomass pyrolysis kinetics: a comparative critical review with relevant agricultural residue case studies. Journal of Analytical and Applied Pyrolysis, ***91***, 1-33.

[63] **Ryu, C., Yang, Y.B., Khor, A., Yates, N.E., Sharifi, V.N. and Swithenbank, J. (**2006). Effect of fuel properties on biomass combustion: Part I. Experiments—fuel type, equivalence ratio and particle size. *Fuel, **85***, 1039-1046.

[64] **Du, S., Yang, H., Qian, K., Wang, X. and Chen, H.** (2014). Fusion and transformation properties of the inorganic components in biomass ash. *Fuel*, ***117***, 1281-1287.

[65] **Vassilev, S. V., Vassileva, C. G., and Vassilev, V. S.** (2015). Advantages and disadvantages of composition and properties of biomass in comparison with coal: An overview. *Fuel, **158,*** 330-350.

[66] **Sami, M., Annamalai, K., and Wooldridge, M.** (2001). Co-firing of coal and biomass fuel blends. *Progress in Energy and Combustion Science, **27,*** 171-214.

[67] **Vassilev, S. Baxter, D., and Vassileva, C.** (2014). An overview of the behavior of biomass during combustion: Part II. Ash fusion and ash formation mechanisms of biomass types. *Fuel*, ***117,*** 152–83.

[68] **Van Loo, S. and Koppejan, J.** (2008). *The Hand Book of Biomass Combustion and Co-firing.* London: Earthscan.

[69] **B. Metz, O.R. Davidson, P.R. Bosch, R. Dave, L.A. Meyer (eds.).** (2007). Climate change 2007: Mitigation of climate change. *Intergovernmental Panel on Climate Change.* Cambridge, UK: Cambridge University.

[70] **World Energy Council.** (2016). *World Energy Resources: Bioenergy 2016*. London: World Energy Council.

[71] **World Energy Council.** (2010). *2010 Survey of Energy Resources*. London: World Energy Council.

[72] **O. Edenhofer, R. Pichs-Madruga, Y. Sokona (eds.).** (2011). Special report on renewable energy sources and climate change mitigation. *Intergovernmental Panel on Climate Change.* Abu Dhabi, United Arab Emirates.

[73] **Kaygusuz, K. and Keles, S.** (2012). Sustainable bioenergy policies in Turkey. *Journal of Engineering Research and Applied Science, **1,*** 34-43.

[74] **Republic of Turkey Ministry of Energy and Natural Resources.** (n.d.). *Bio-Fuels.* Retrieved November 13, 2017, from http://www.enerji.gov.tr/en-US/Pages/Bio-Fuels.

[75] **Acaroglu, M. and Aydoğan, H.** (2012). Biofuels energy sources and future of biofuels energy in Turkey. *Biomass and Bioenergy, **36**,* 69-76.

[76] **Toklu, E.** (2017). Biomass energy potential and utilization in Turkey. *Renewable Energy, **107**,* 235-244.

[77] **Toklu, E. and Kaygusuz, K.** (2012). Present situation and future prospect of energy utilization in Turkey. *Journal of Engineering Research and Applied Science, **1***, 73-86.

[78] **Erdem, Z. B.** (2010). The contribution of renewable resources in meeting Turkey's energy-related challenges, *Renewable and Sustainable Energy Reviews, **14**,* 2710-2722.

[79] **World Energy Council Turkish National Committee.** (2008). *Turkey Energy Report in 2008.* Ankara: World Energy World Energy Council Turkish National Committee.

[80] **Demirbas, A.,** (2009). Biorefineries: Current activities and future developments. Energy Conversion Management, ***50***, 2782-2801.

[81] **Bhaskar, T., and Pandey, A.** (2015). Advances in thermochemical conversion of biomass-Introduction. In A. Pandey, T. Bhaskar, M. Stöcker, R. Sukumaran (eds.). *Recent Advances in Thermochemical Conversion of Biomass*. Amsterdam: Elsevier.

[82] **Czernik, S. and Bridgwater, A.** (2004). Overview of applications of biomass fast pyrolysis oil, *Energy & Fuels, **18***, 590-598.

[83] **Pütün, A.E., Önal, E., Uzun, B.B. and Özbay, N.** (2007). Comparison between the "slow" and "fast" pyrolysis of tobacco residue, *Industrial Crops and Products, **26**,* 307-314.

[84] **Prins, M. J., Ptanski, K. J., and Janssen, F. J. J. G.** (2006). More efficient biomass gasification via torrefaction, *Energy, **31***, 3458-3470.

[85] **Prins, M. J.** (2005). *Thermodynamic analysis of biomass gasification and torrefaction*. (Phd Thesis). Technische Universiteit Eindhoven;The Netherlands.

[86] **Bergman, P. C. A, Boersma, A. R., Zwart, R. W. R., Kiel, J, H, A.** (2005). Torrefaction for biomass co-firing in existing coal-fired power stations: Biocoal. (Report ECN-C-05-013). Petten, The Netherlands: ECN.

[87] **van der Stelt, M. J. C., Gerhauser, H., Kiel, J. H. A., and Ptanski, K. J.** (2011). Biomass upgrading by torrefaction for the production of biofuels: A review. *Biomass and Bioenergy, **35**, 3748-3762.*

[88] **Tumuluru, J. S., Hess, J. R., Boardman, R. D., and Westover, T.** (2011). Formulation, pretreatment, and densification options to ımprove biomass specifications for co-firing high percentages with coal. *Industrial Biotechnology*, ***8***, 113-132.

[89] **Idris, S. S., Rahman, N. A., and Ismail, K.** (2012. Combustion characteristics of Malaysian oil palm biomass, sub-bituminous coal and their respective blends via thermogravimetic analysis (TGA). *Bioresource Technology*, ***123***, 581-591.

[90] **M. F. G. Cremers (ed.).** (2009). Technical status of biomass co-firing. *IEA Bioenergy Task 32, Deliverable 4.* (Report 50831165-Consulting 09-1654). Retrieved November 13, 2017, from http://citeseerx.ist.psu.edu /viewdoc/download?doi=10.1.1.462.4766 &rep= rep1&type=pdf.

[91] **Gil, M. V., Casal, D., Pevida, C., Pis, J. J., and Rubiera, F.** (2010). Thermal behavior and kinetics of coal/biomass blends during co-combustion. *Bioresource Technology*, ***101***, 5601 – 5608.

[92] **Zheng, L., CanmetENERGY, Canada and YAN, J.** (2013). Thermal coal utilization. In D. Osborne. (Ed.), *The Coal Handbook: Towards Cleaner Production, Vol 2*. Cambridge: Woodhead Publishing.

[93] **Xiao, H., Ma, X. and Lai, Z.** (2009). Isoconversional kinetic analysis of co-combustion of sewage sludge with straw and coal. *Applied Energy, **86***, 1741–1745.

[94] **Kastanaki, E. and Vamvuka, D.** (2006). A comparative reactivity and kinetic study on the combustion of coal–biomass char blends, *Fuel*, ***85***, 1186–1193.

[95] **Demirbas, A.** (2003). Sustainable cofiring of biomass with coal. *Energy Conversion and Management. **44***, 1465–1479.

[96] **Tillman, D.A.** (2000). Biomass cofiring: the technology, the experience, the combustion consequences. *Biomass Bioenergy, **19***, 365–384.

[97] **Savolainen, K.** (2003). Co-firing of biomass in coal-fired utility boilers. *Applied Energy*, ***74***, 369–381.

[98] **Baxter, L.** (2005). Biomass-coal co-combustion: opportunity for affordable renewable energy. *Fuel, **84***, 1295–1302.

[99] **Al-Mansour, F. and Zuwala, J.** (2010). An evaluation of biomass co-firing in Europe. *Biomass Bioenergy, **34***, 620–629.

[100] **Amand, L.E., Leckner, B., Eskilsson, D., Tullin, C.** (2006). Deposits on heat transfer tubes during co-combustion of biofuels and sewage sludge. *Fuel*, ***85***, 1313–1322.

[101] **Nussbaumer, T.** (2003). Combustion and co-combustion of biomass: Fundamentals, technologies, and primary measures for emission reductions. *Energy Fuels*, ***17***, 1510–1521.

[102] **Dong, C. and Hu, X.** (2013). Co-combustion coal and bioenergy and biomass gasification: Chinese experiences. In E. Dahlquist (Ed.), *Technologies for converting biomass to useful energy combustion, gasification, pyrolysis, torrefaction and fermentation*. London: CRC Press.

[103] **Breeze, P.** (2014). Biomass-based power generation. *Power Generation Technologies*. Biomass-based Power Generation. Oxford, UK: Newnes.

[104] **Shah, Y. T.** (2015). Heat and power by co-combustion. *Energy and Fuel Systems Integration.* Boca Raton, FL: CRC Press.

[105] **TA Instruments** (n.d.). *A review of DSC kinetics methods*. (Report TA073). Retrieved November 13, 2017, from www.tainstruments.com/pdf/literature /TA073.pdf.

[106] **Borchardt, H.J. and Daniels, F.J.** (1957). The Application of Differential Thermal Analysis to the Study of Reaction Kinetics. *Journal of The American Chemical Society*, ***79***, 41-46.

[107] **Peyser, P. and Bascom, W.D.** (1974). Kinetics of an Anhydride-epoxy polymerization as determined by differential scanning calorimetry. *Analytical Calorimetry*, ***3***, 537-554.

[108] **Ural, S.** (2005). Comparison of fly ash properties from Afsin-Elbistan coal basin Turkey. *Journal of Hazardous Materials*, ***119***, 85–92.

[109] **Kubesova, M., Orucoglu, E., Haciyakupoglu, S., Erenturk, S., Krausova, I. and Kucera, J.** (2015). Elemental characterization of lignite from Afsin-Elbistan in Turkey by k_0-NAA. *Journal of Radioanalytical and Nuclear Chemistry*, ***306***, 1055-1062.

[110] **Temel, H. A. And Ayhan, F. D.** (2005). Washability properties of Adıyaman-Gölbaşı lignite, Diyarbakır-Hazro lignite and Şırnak asphaltite in GAP region. *Proceedings for Symposium of Evaluation of East and South East Anatolian mineral Deposits.* Diyarbakır, Turkey. Retrieved November 15, 2017, from http://www.maden.org.tr/resimler/ekler/b01078e96f65f2a_ek.pdf.

[111] **General Directorate of Mineral Rmadenesearch and Explorations.** (2002). *Chemical and Technological Properties of Turkey Tertiary Coals.* Ankara: Türkiye Publishing.

[112] **Kavak, O., Toprak, S.** (2011). Organic geochemical properties of Adiyaman Golbasi (South East of Turkey) coals. *Journal of Geology Engineering*, ***35***, 43-78.

[113] **Paul, M., Seferinoğlu, M., Ayçık, G. A. Sandstrom, A., Smith, M. L. And Paul, J.** (2006). Acid leaching of ash and coal: Time dependence and trace element occurrences. *International Journal of Mineral Processing*, ***79***, 27-41.

[114] **General Directorate of Mineral Research and Explorations.** (n.d.). *Mine and Energy Resources of Çorum Province.* Retrieved November 15, 2017, from http://www.mta.gov.tr/v3.0/sayfalar/bilgi-merkezi/maden_potansiyel _2010/Corum_Madenler.pdf.

[115] **Celikler Conglamerate.** (n.d.). Alpagut Dodurga Lignite Incorporation. Retrived November 15, 2017, from http://celiklerholding.net/yatirimlarimiz _20/alpagut-dodurga-linyit-isletmesi.

[116] **Grooms, L.** (2009). A poplar solution, *Farm Industry News,* **42,** 34-34.

[117] **Özyurtkan, M. H., Özçimen, D. and Meriçboyu A. E.** (2008). Investigation of the carbonization behavior of hybrid poplar. *Fuel Processing Technology, **89**,* 858-863.

[118] **Tufekciglu, A., Altun, L., Kalay, H. Z., and Yılmaz, M.** (2005). Effect of some soil properties on the growth of hybrid poplar in the terme-gölardı region of Turkey, *Turkish Journal of Agriculture and forestry,* **29,** 221-226.

[119] **Akgül, M. And Çamlibel, O.** (2008). Manufacture of medium density fiberboard (MDF) panels from rhododendron (R. ponticum L.) biomass. *Building and Environment, **43***, 438-443.

[120] **Republic of Turkey General Directorate of Forestry.** (2013). *Forest Atlas*. Retrived November 15, 2017, from https://www.ogm.gov.tr/ekutuphane /Yayinlar/Orman%20Atlasi.pdf.

[121] **Zheng, J. A. and Kozinski, J. A.** (2000). Thermal events occurring during the combustion of biomass residue. *Fuel, **79,*** 181–192.

[122] **Miranda, T., Esteban, A., Rojas, S., Montero, I. and Ruiz, A.** (2008). Combustion analysis of different olive residues. *International Journal of Molecular Sciences, **9,*** 512–525.

A. APPENDIX

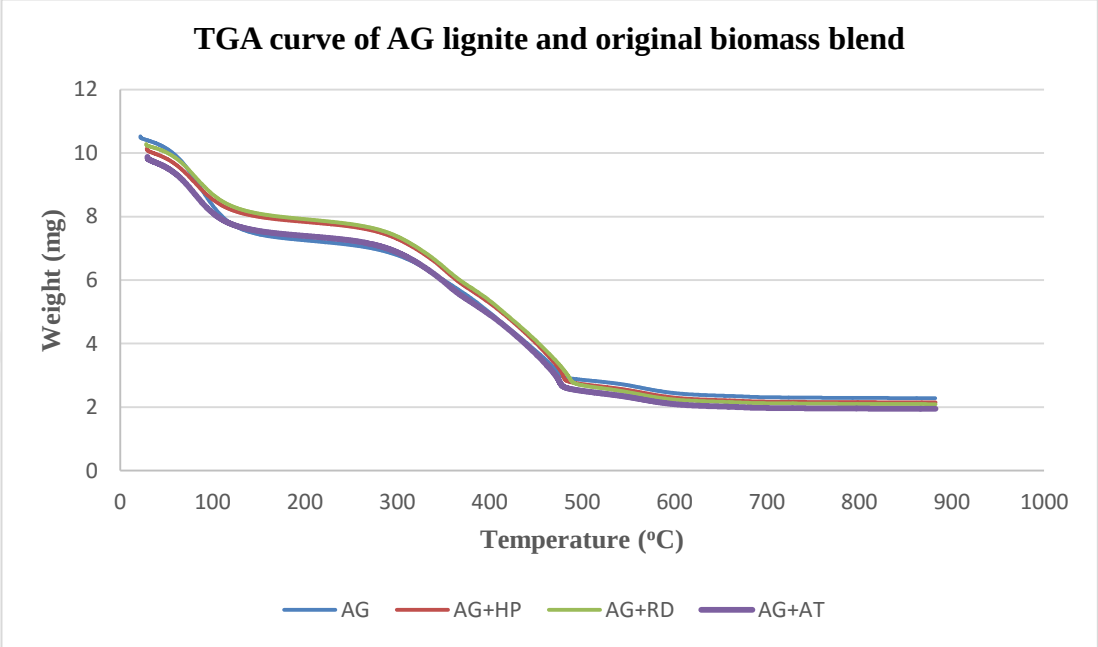

Figure A.1 : TGA curve of AG lignite and original biomass blend.

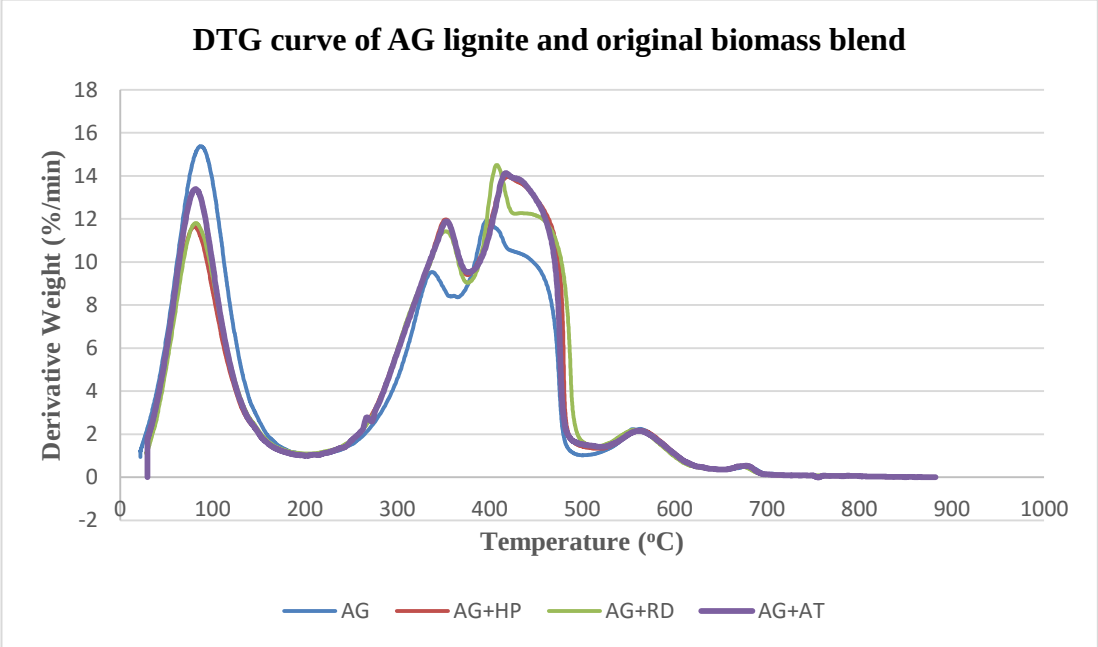

Figure A.2 : DTG curve of AG lignite and original biomass blend.

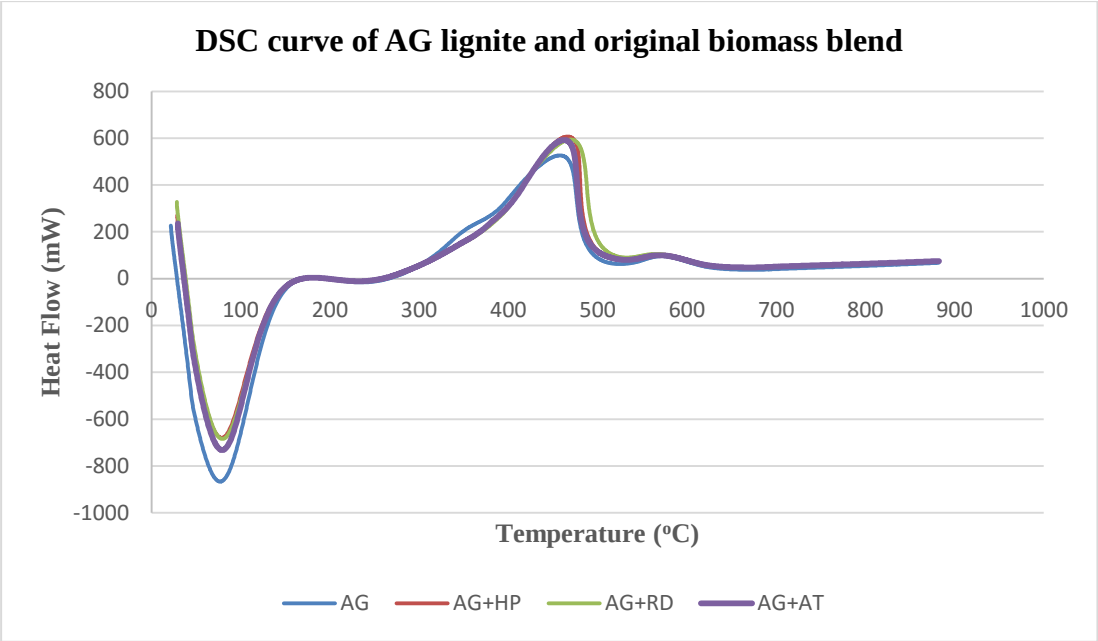

Figure A.3 : DSC curve of AG lignite and original biomass blend.

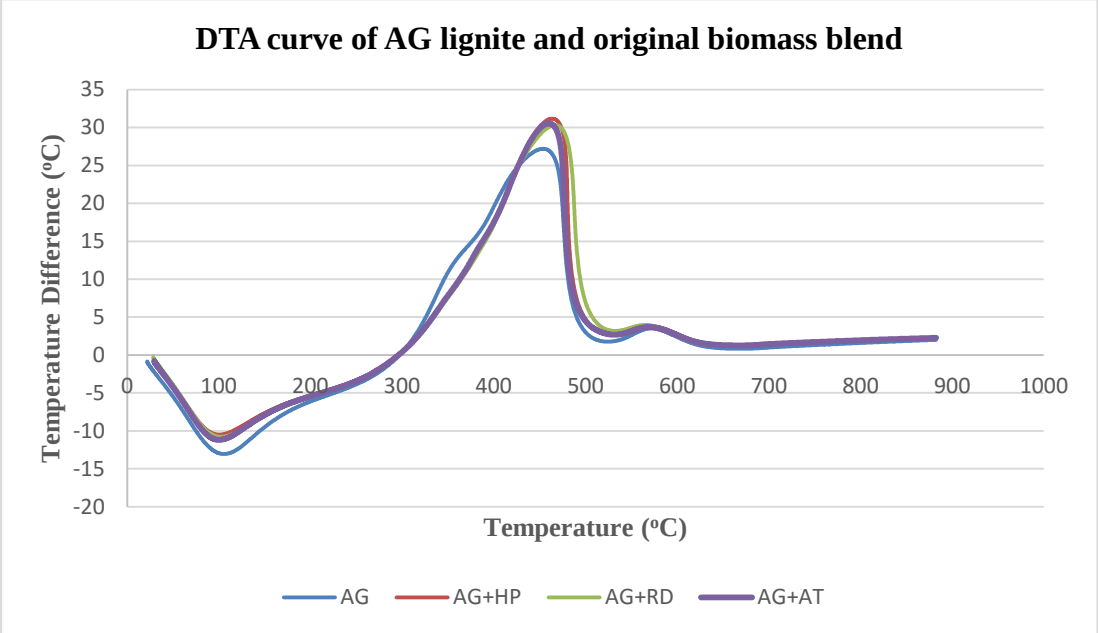

Figure A.4 : DTA curve of AG lignite and original biomass blend.

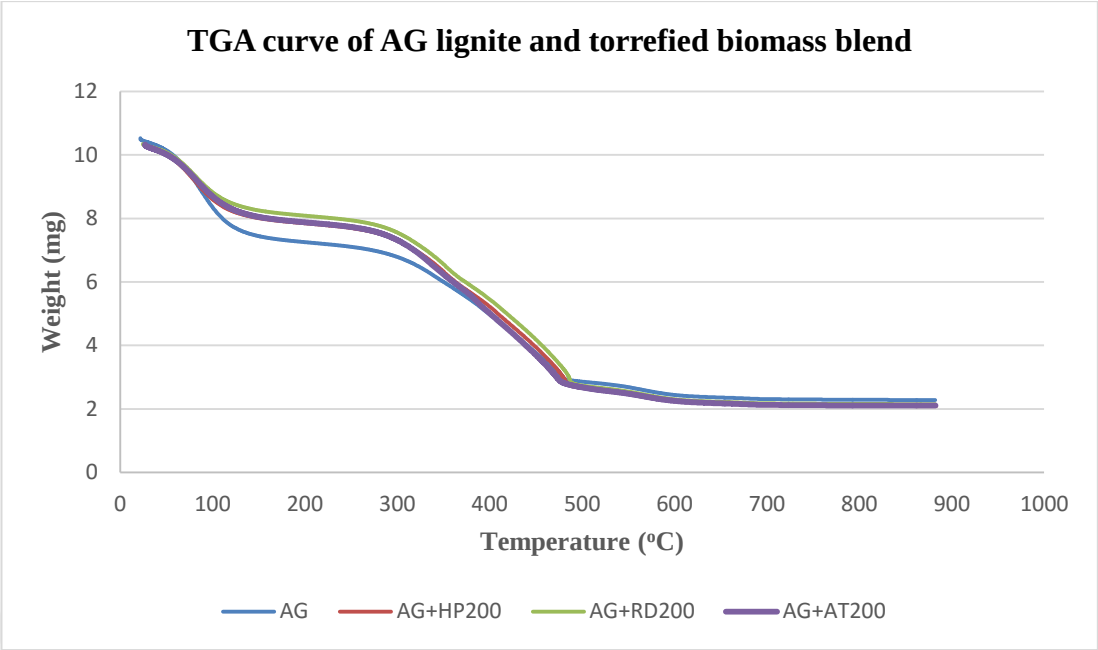

Figure A.5 : TGA curve of AG lignite and torrefied biomass blend.

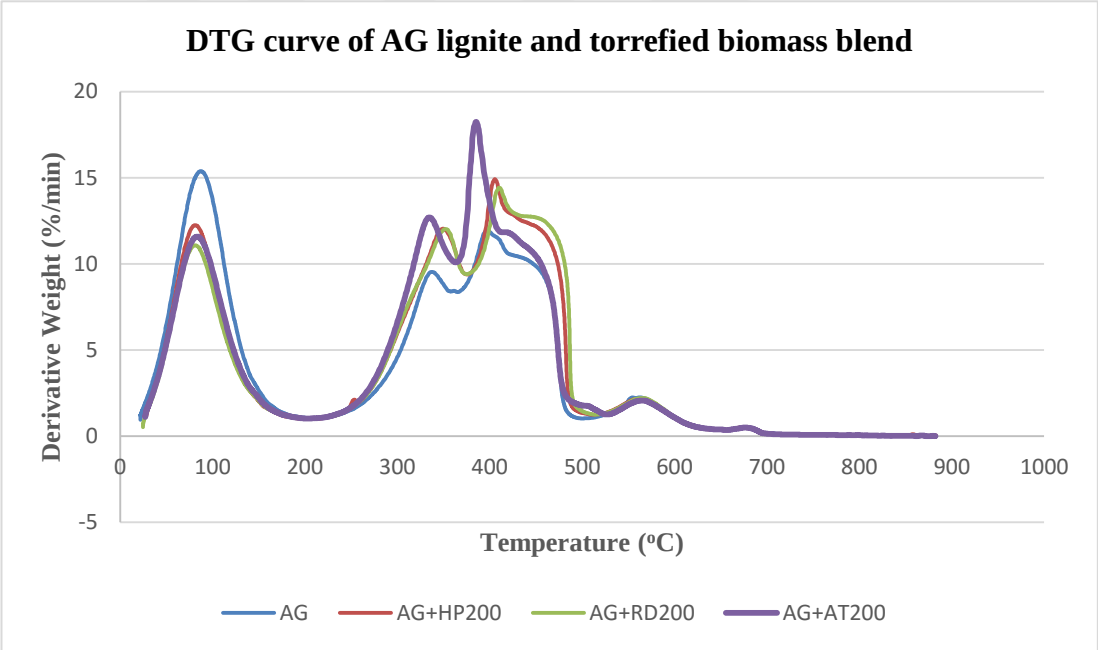

Figure A.6 : DTG curve of AG lignite and torrefied biomass blend.

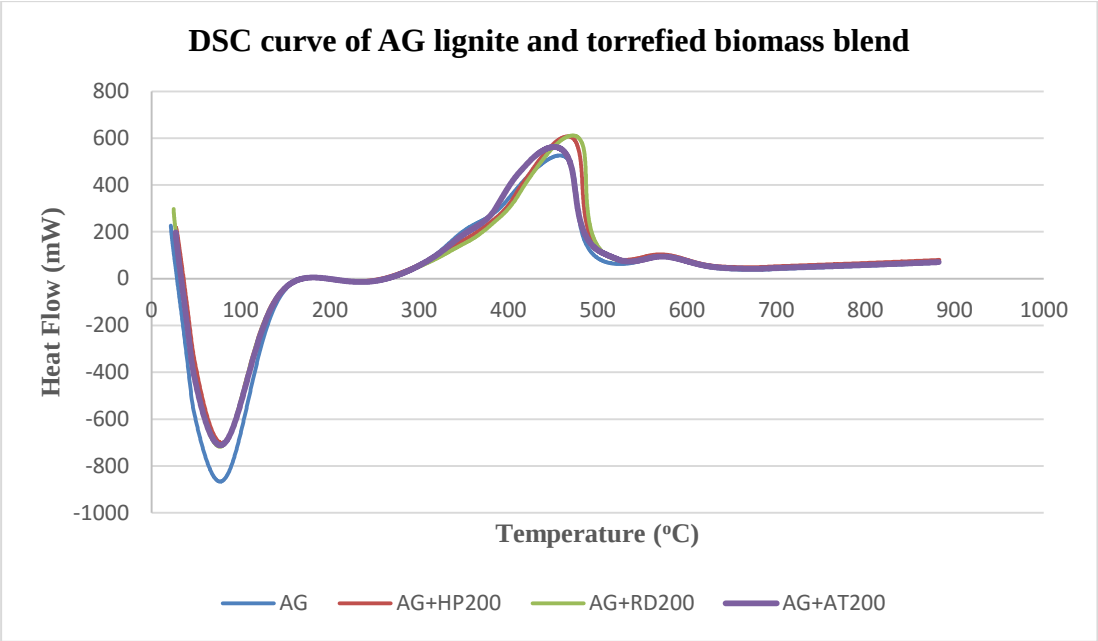

Figure A.7 : DSC curve of AG lignite and torrefied biomass blend.

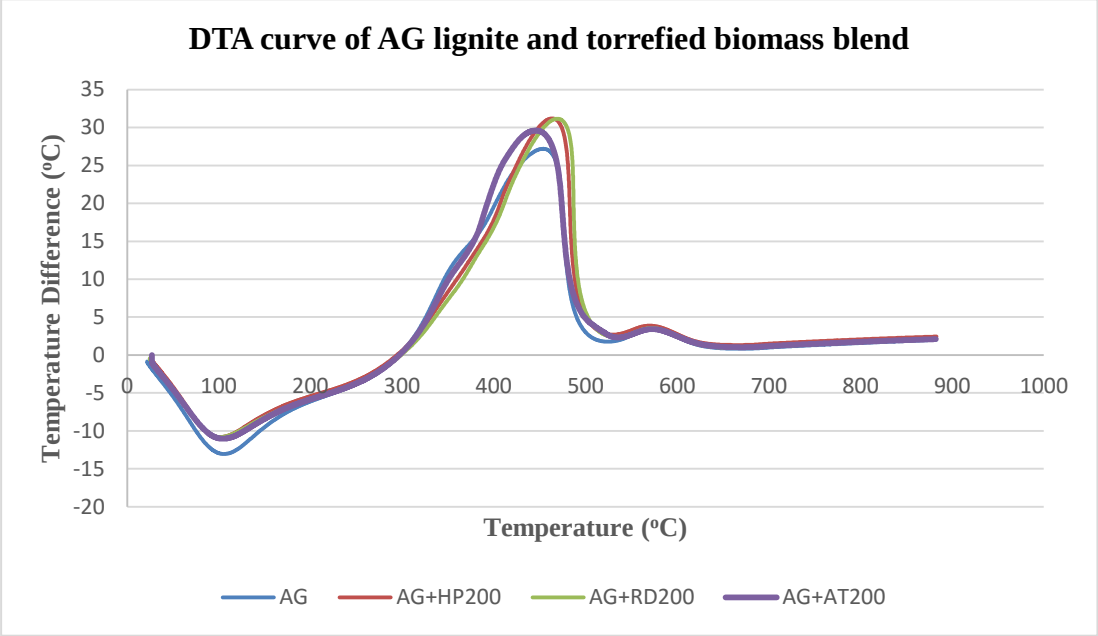

Figure A.8 : DTA curve of AG lignite and torrefied biomass blend.

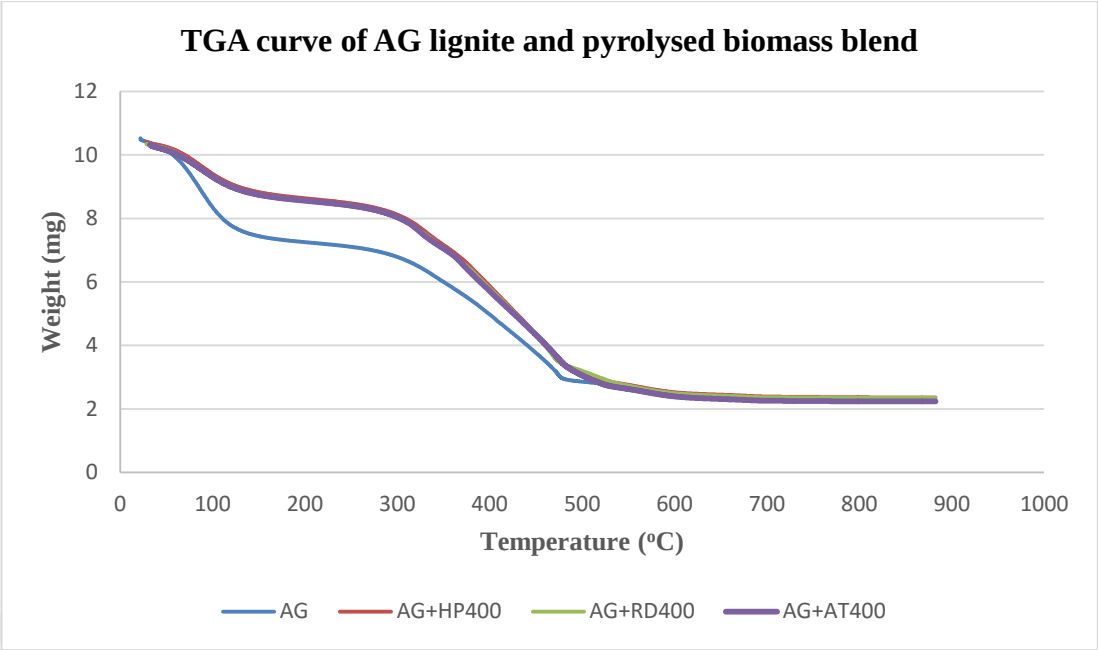

Figure A.9 : TGA curve of AG lignite and pyrolysed biomass blend.

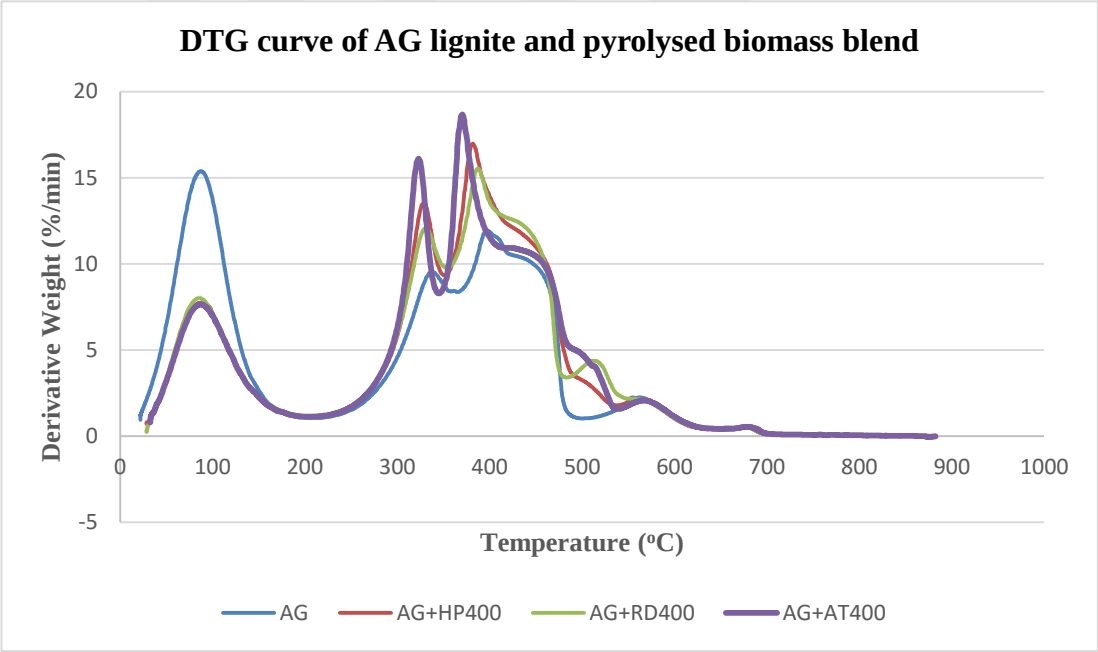

Figure A.10 : DTG curve of AG lignite and pyrolysed biomass blend.

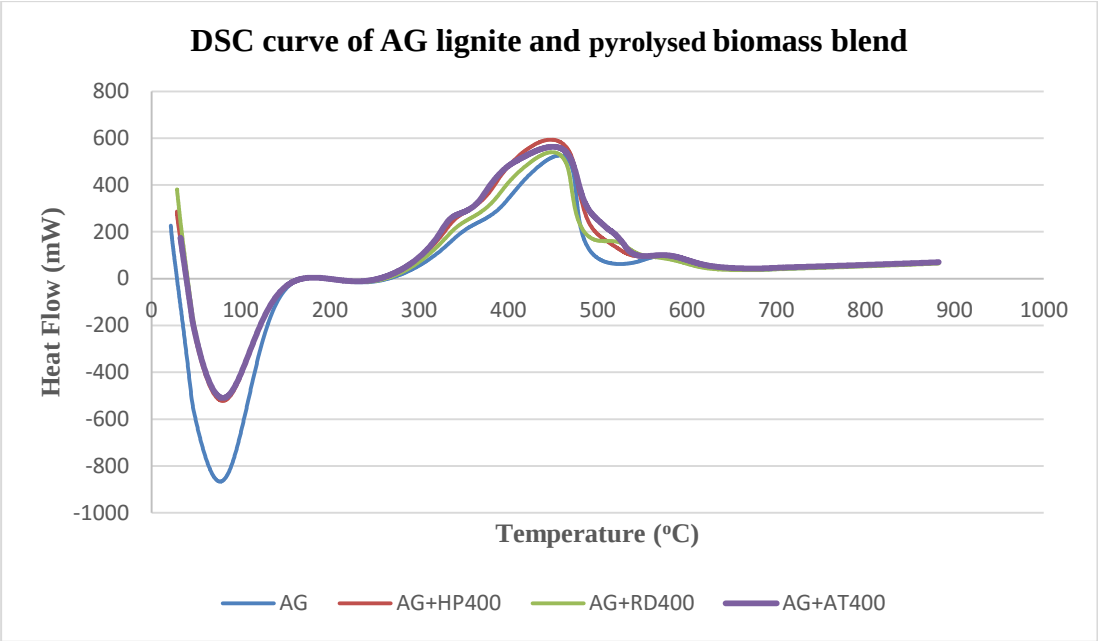

Figure A.11 : DSC curve of AG lignite and pyrolysed biomass blend.

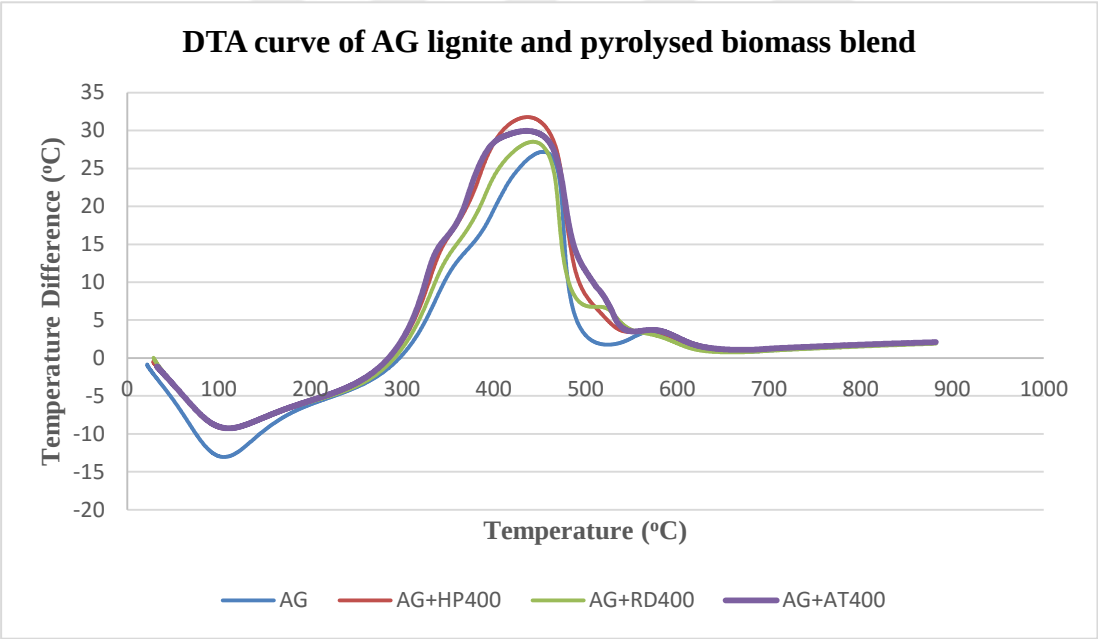

Figure A.12 : DTA curve of AG lignite and pyrolysed biomass blend.

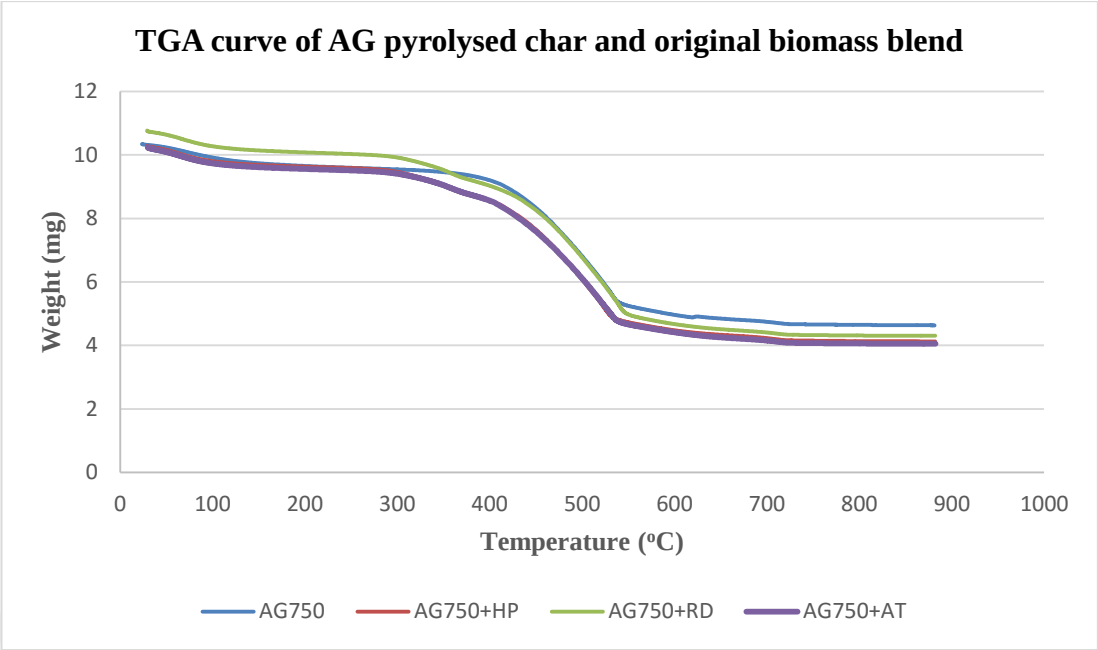

Figure A.13 : TGA curve of AG pyrolysed char and original biomass blend.

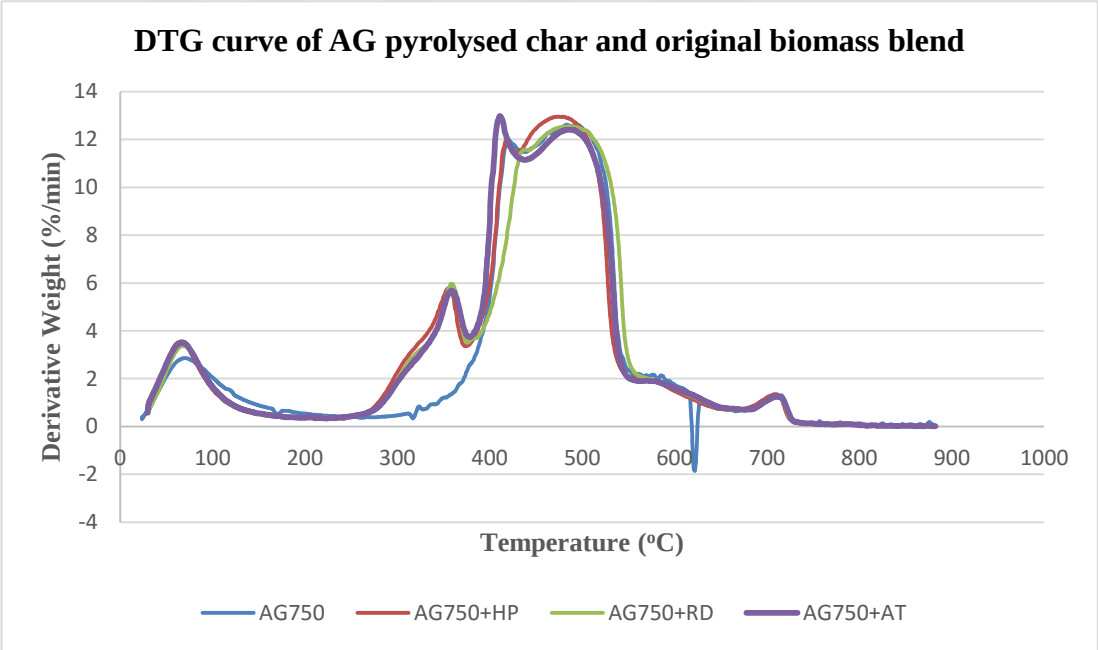

Figure A.14 : DTG curve of AG pyrolysed char and original biomass blend.

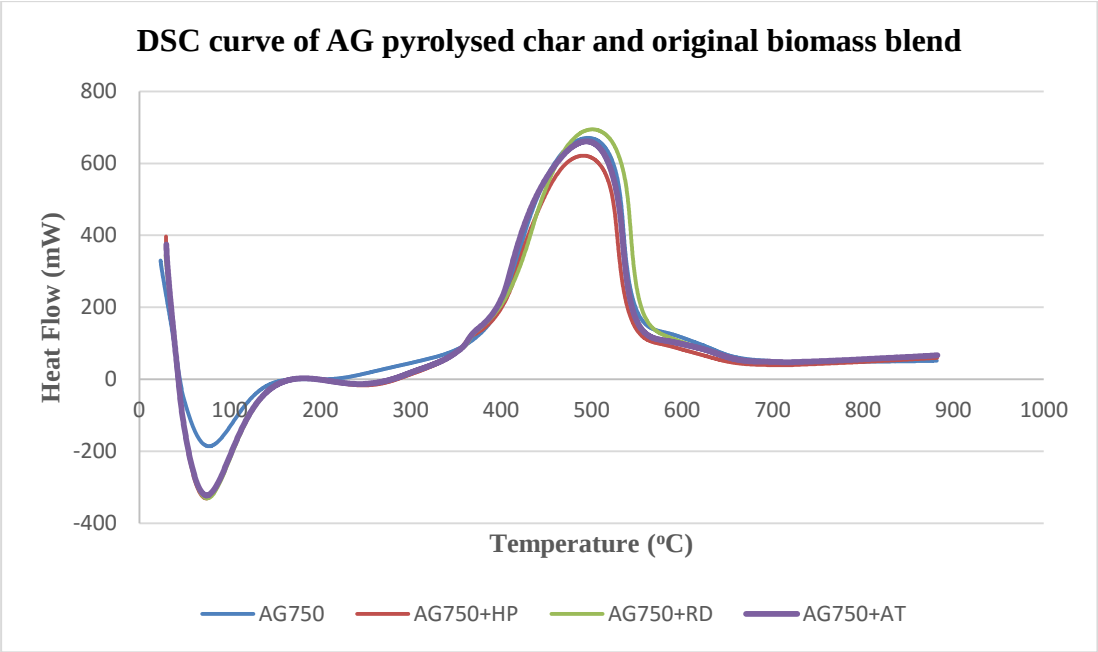

Figure A.15 : DSC curve of AG pyrolysed char and original biomass blend.

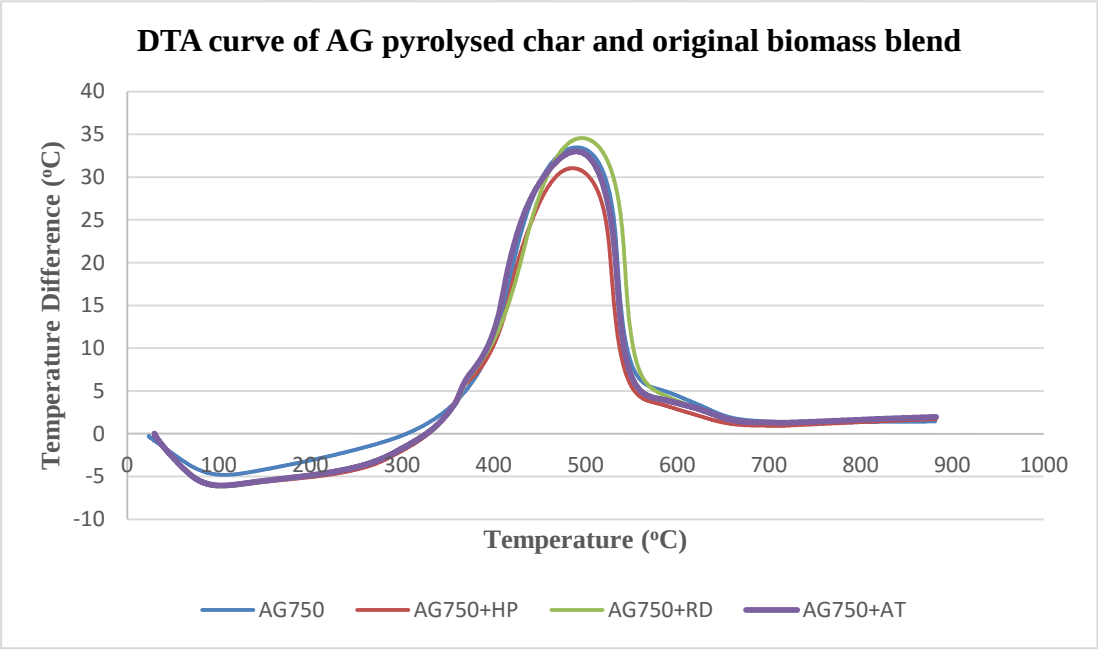

Figure A.16 : DTA curve of AG pyrolysed char and original biomass blend.

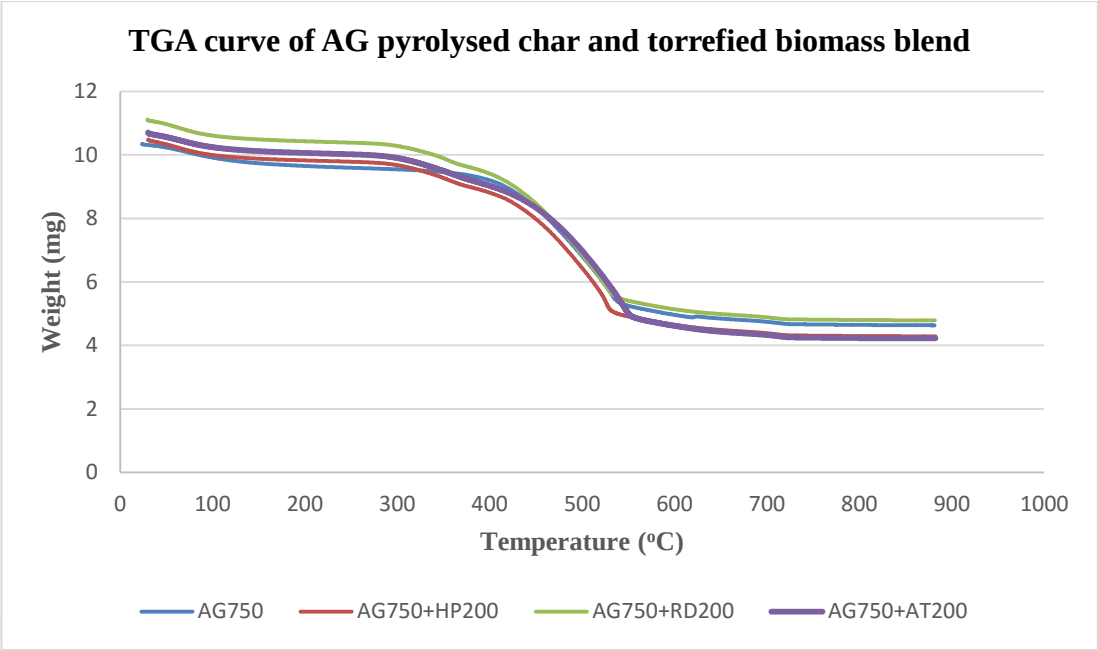

Figure A.17 : TGA curve of AG pyrolysed char and torrefied biomass blend.

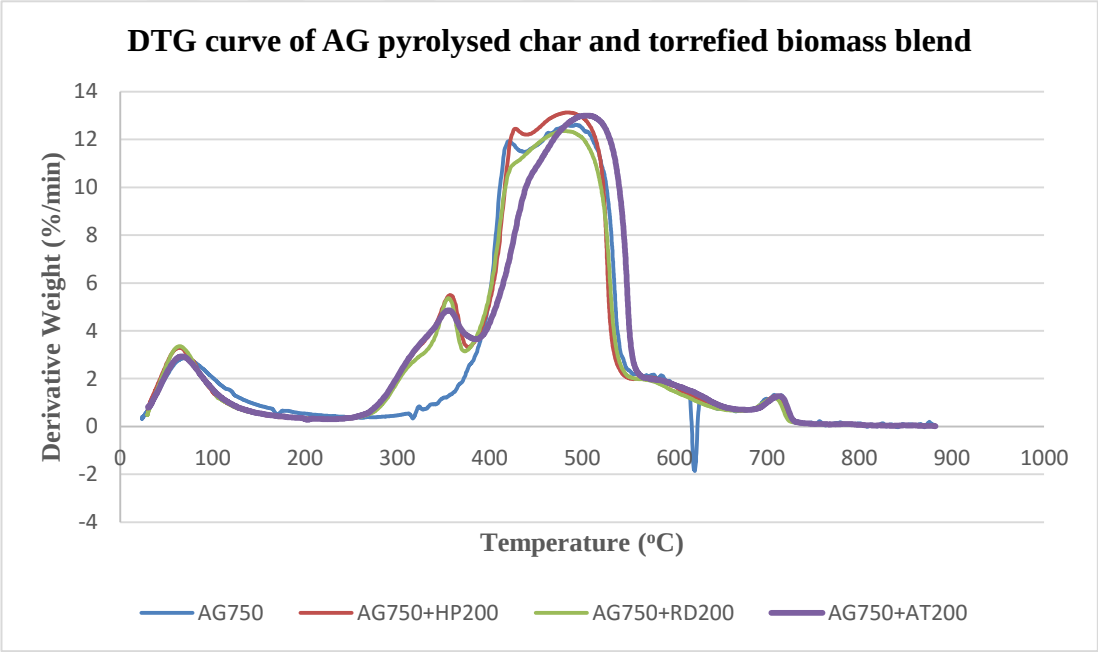

Figure A.18 : DTG curve of AG pyrolysed char and torrefied biomass blend.

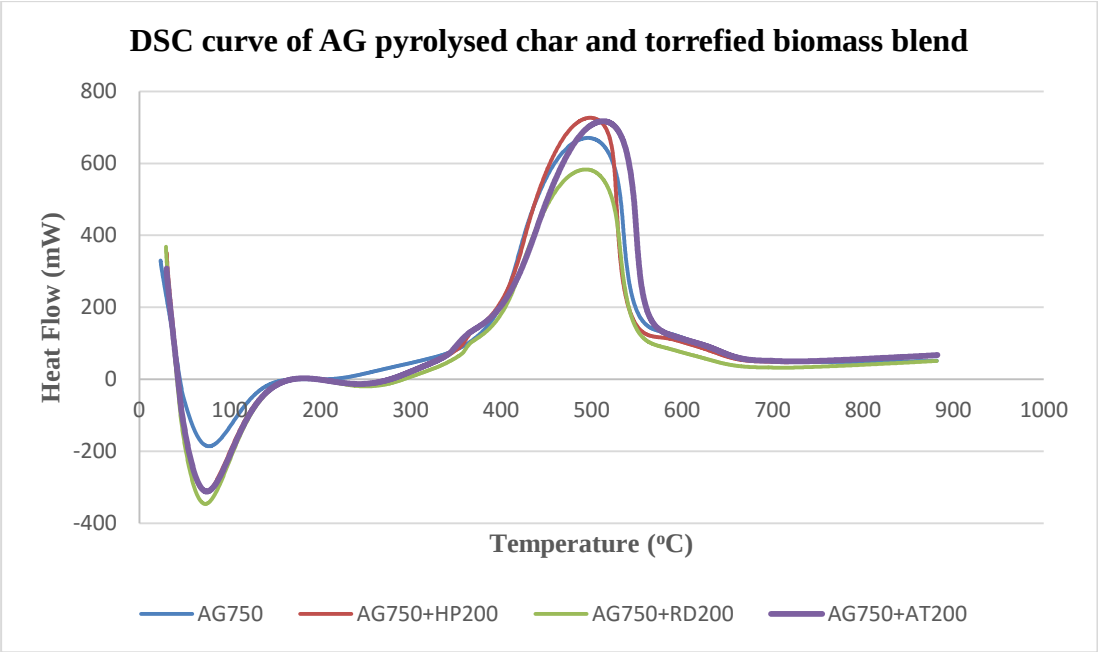

Figure A.19 : DSC curve of AG pyrolysed char and torrefied biomass blend.

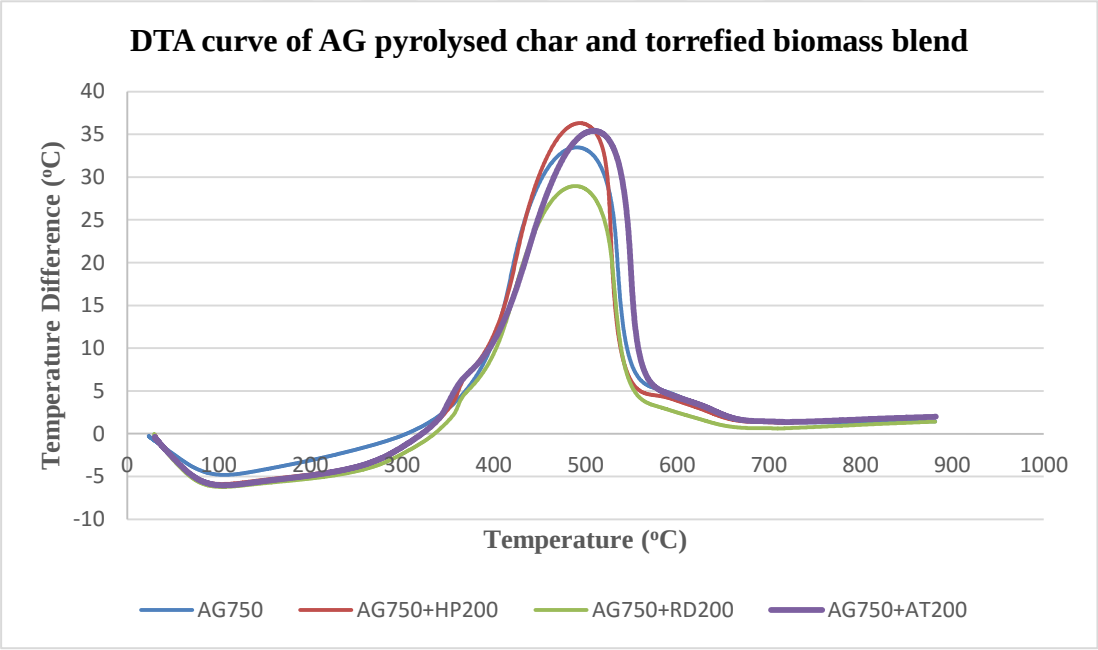

Figure A.20 : DTA curve of AG pyrolysed char and torrefied biomass blend.

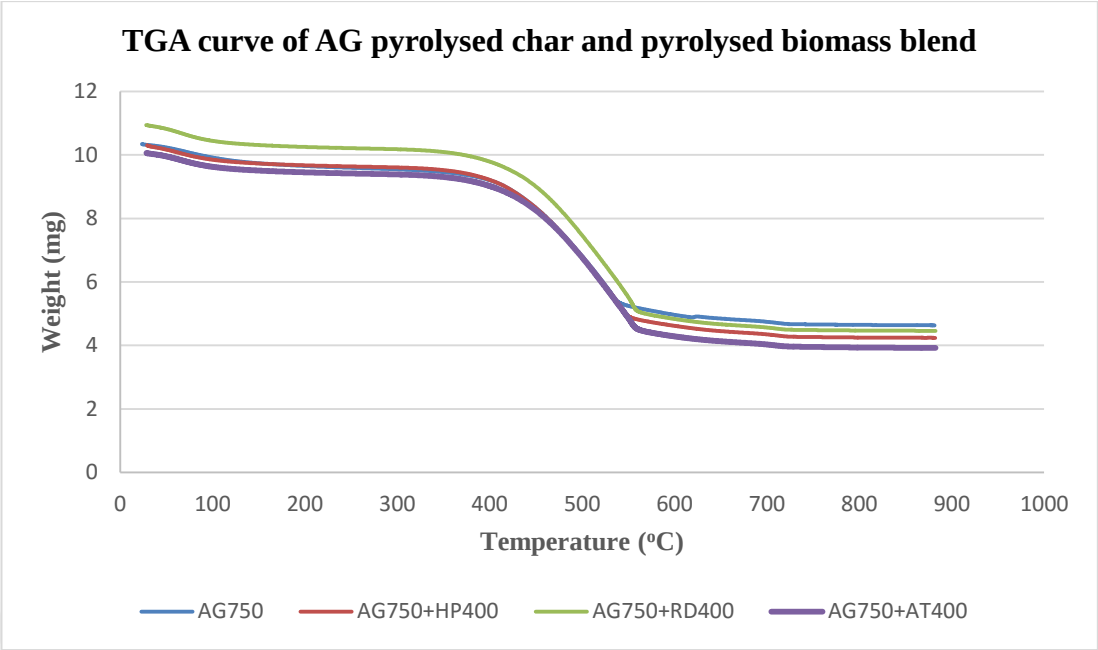

Figure A.21 : TGA curve of AG pyrolysed char and pyrolysed biomass blend.

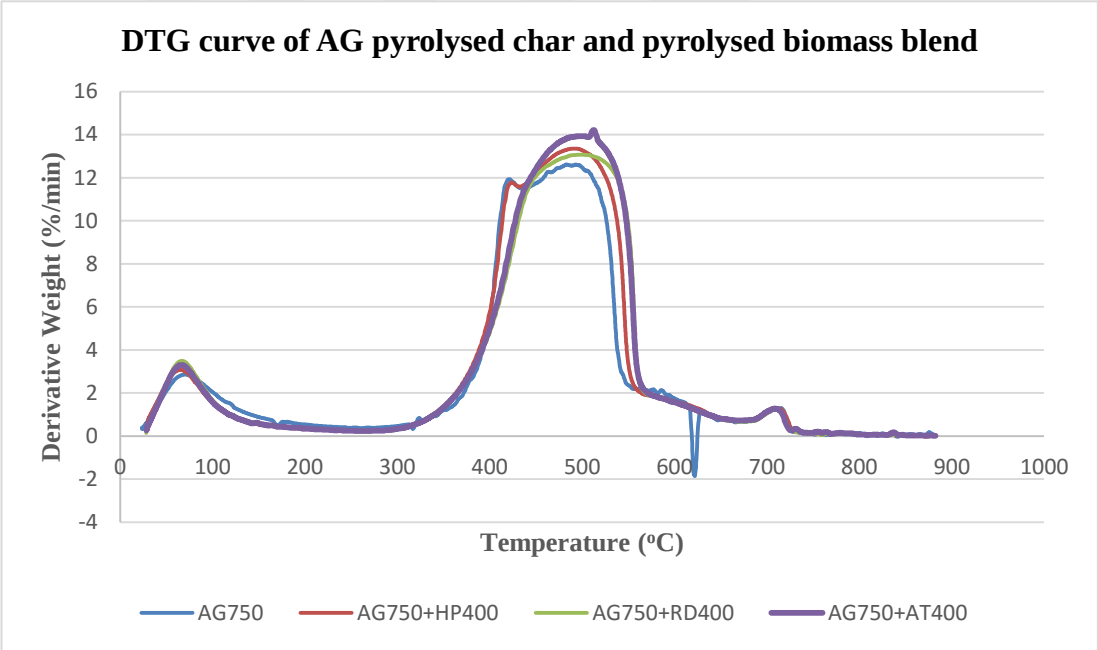

Figure A.22 : DTG curve of AG pyrolysed char and pyrolysed biomass blend.

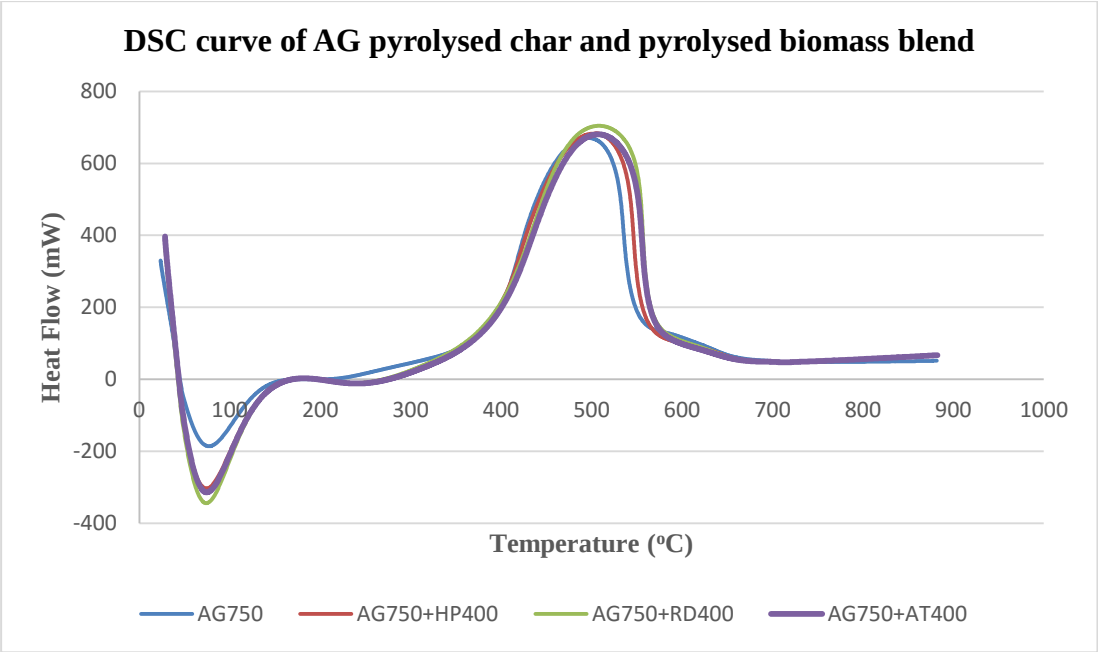

Figure A.23 : DSC curve of AG pyrolysed char and pyrolysed biomass blend.

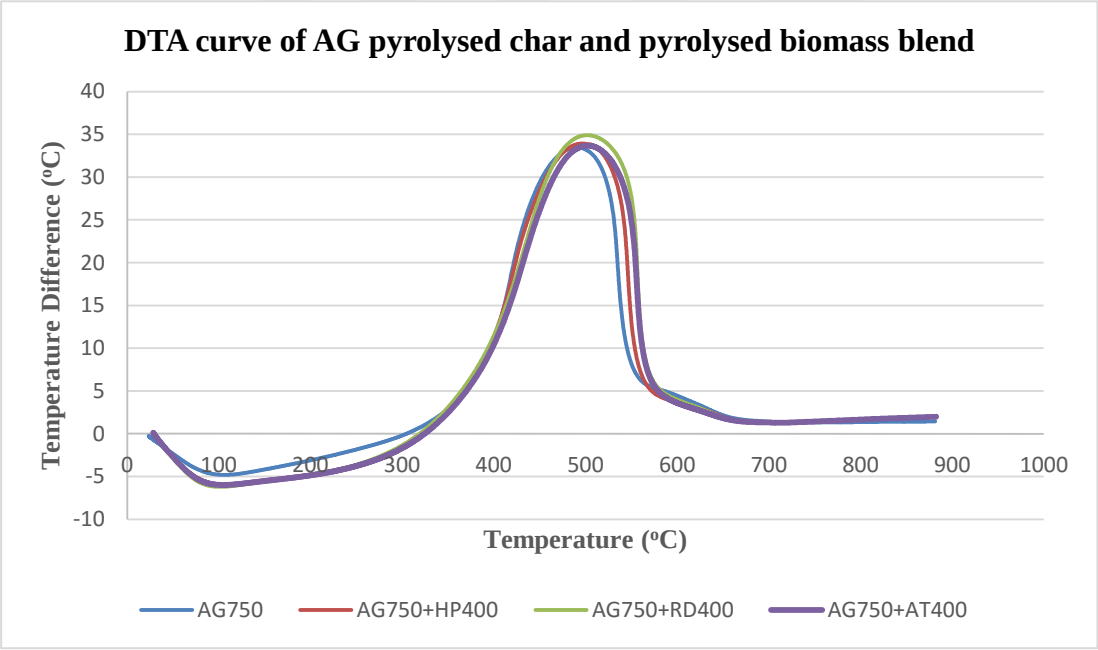

Figure A.24 : DTA curve of AG pyrolysed char and pyrolysed biomass blend.

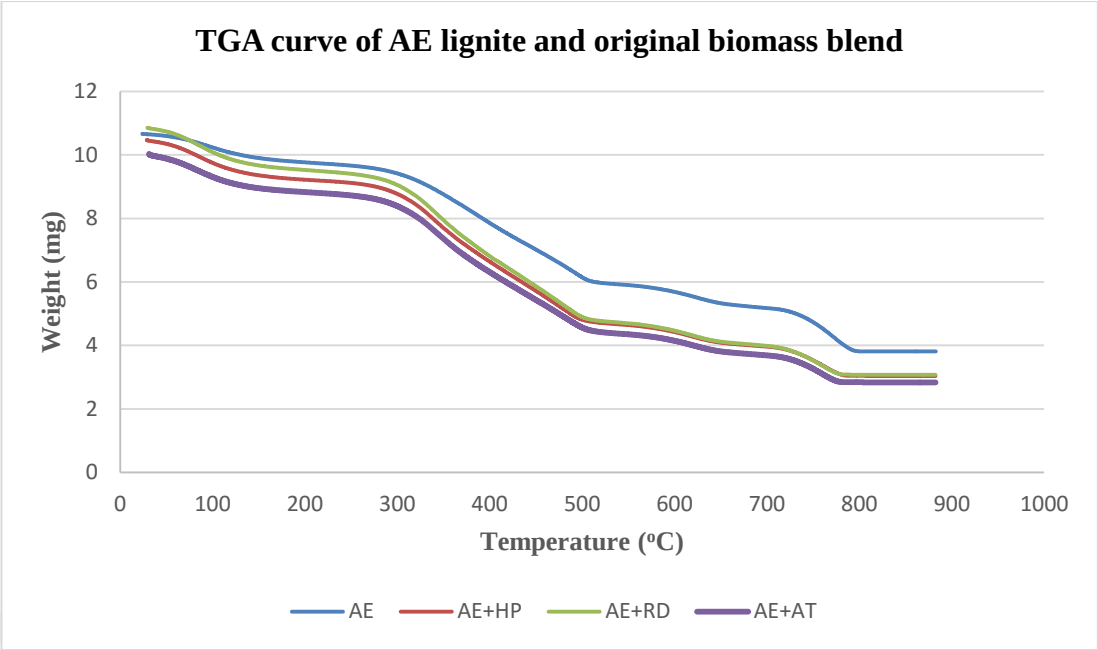

Figure A.25 : TGA curve of AE lignite and original biomass blend.

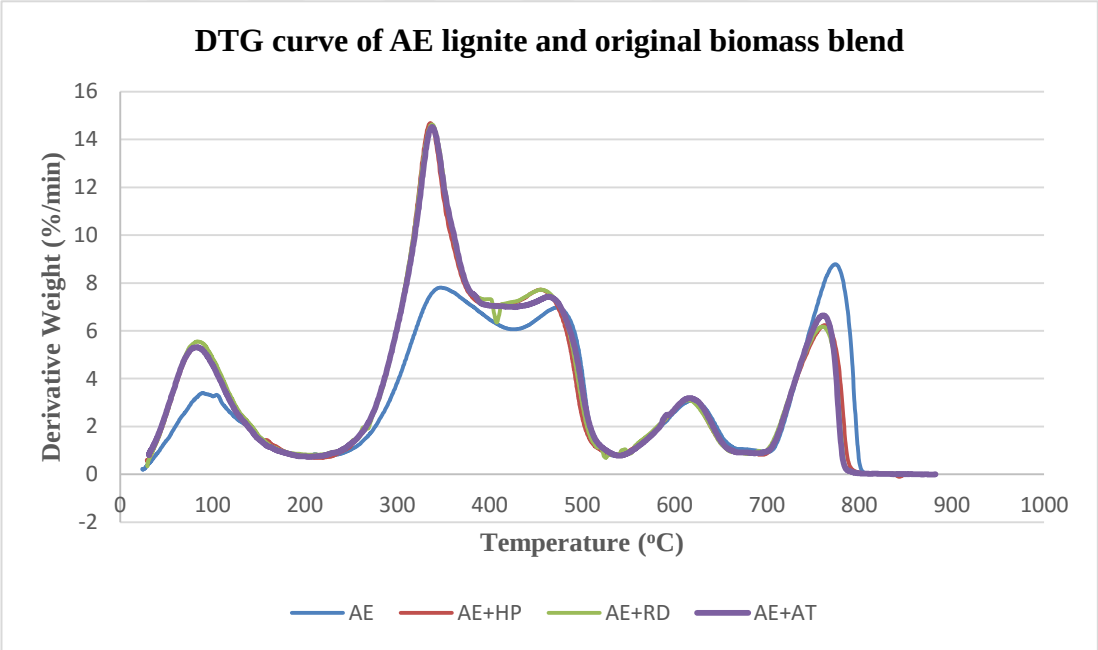

Figure A.26 : DTG curve of AE lignite and original biomass blend.

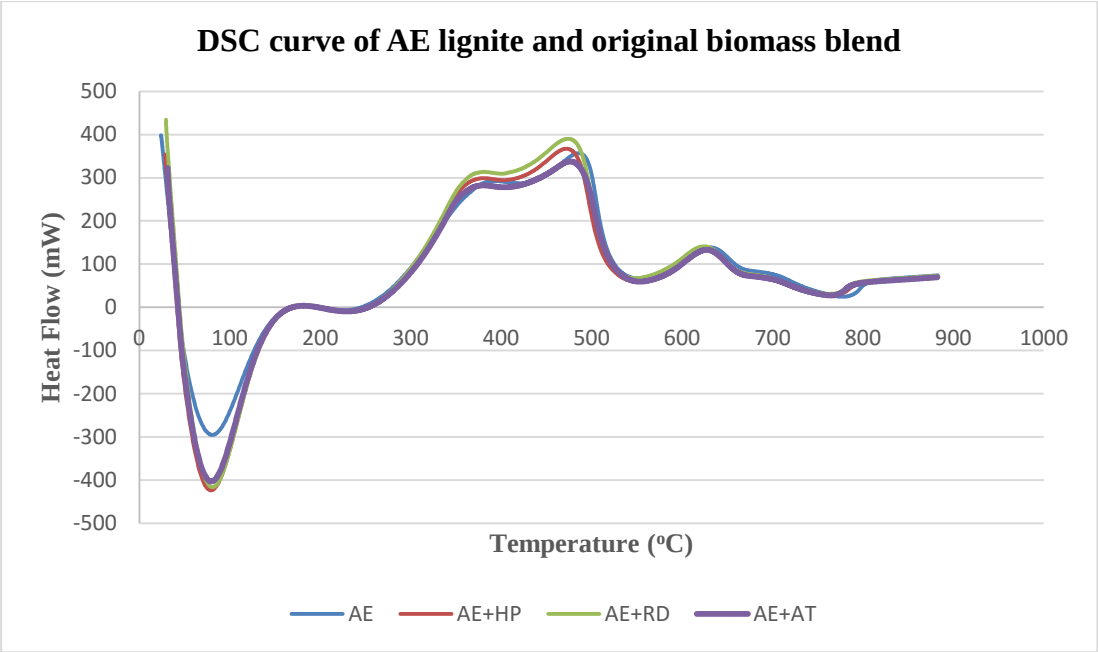

Figure A.27 : DSC curve of AE lignite and original biomass blend.

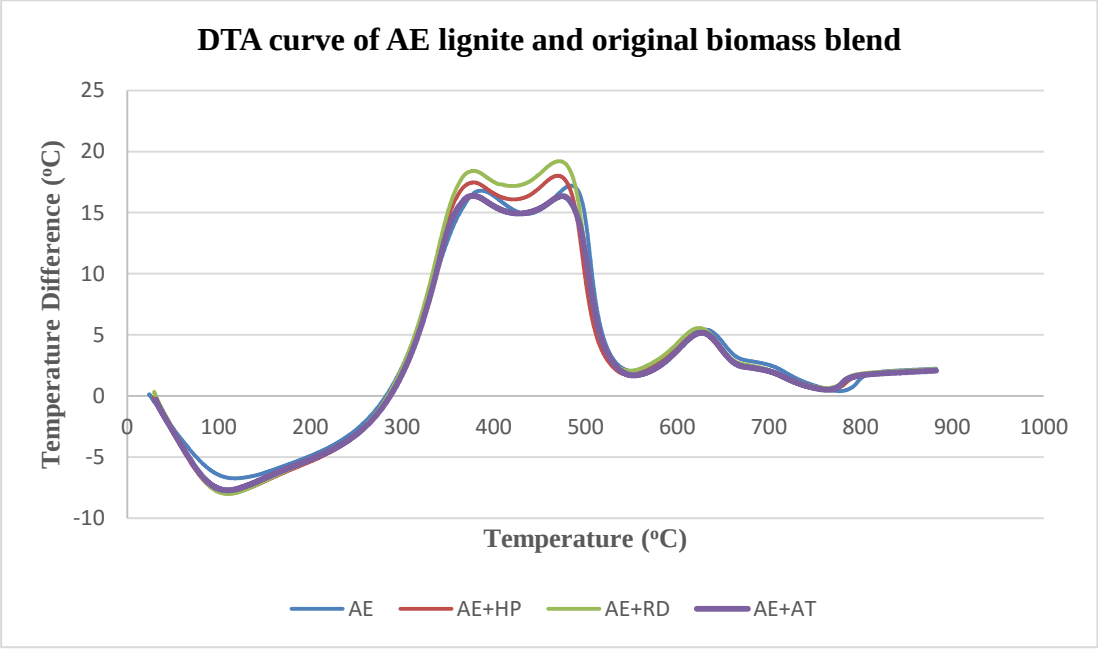

Figure A.28 : DTA curve of AE lignite and original biomass blend.

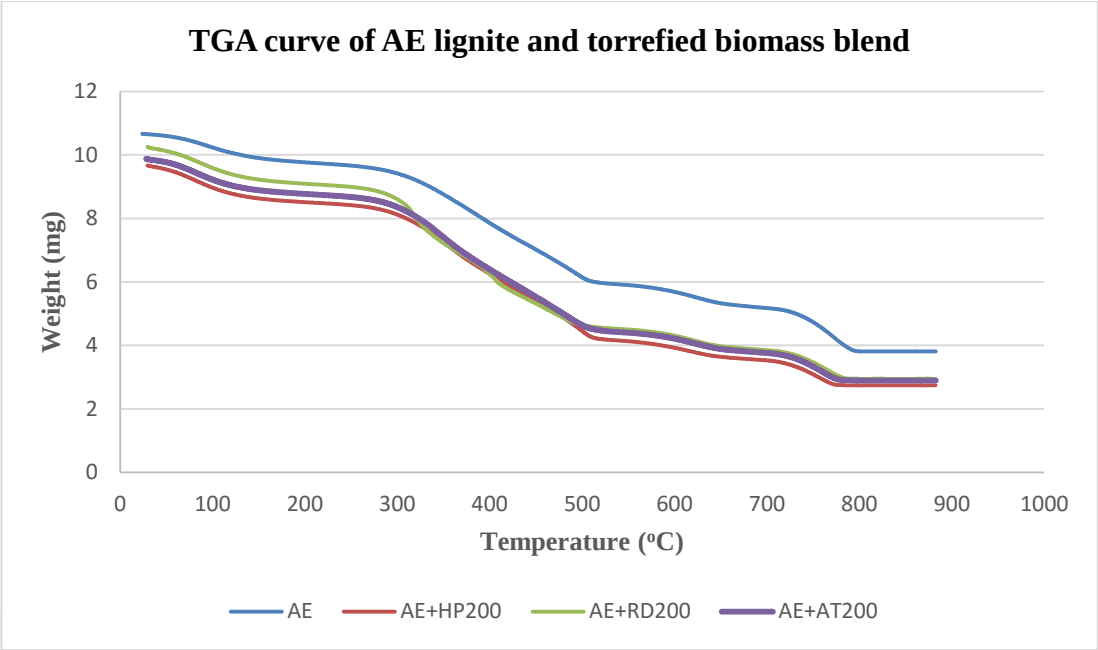

Figure A.29 : TGA curve of AE lignite and torrefied biomass blend.

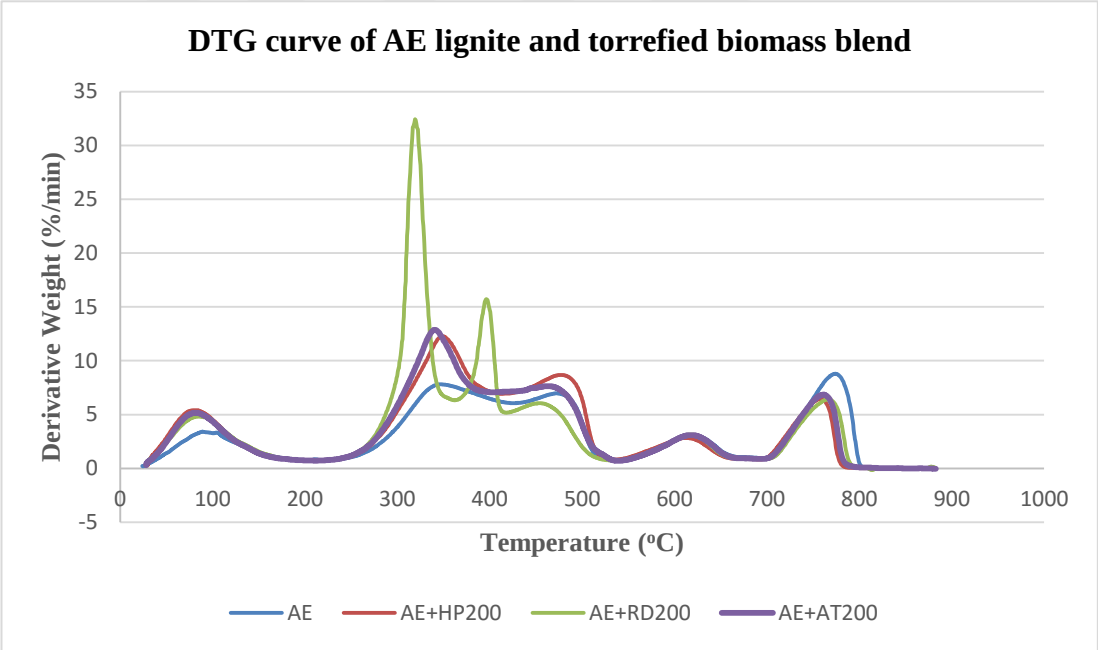

Figure A.30 : DTG curve of AE lignite and torrefied biomass blend.

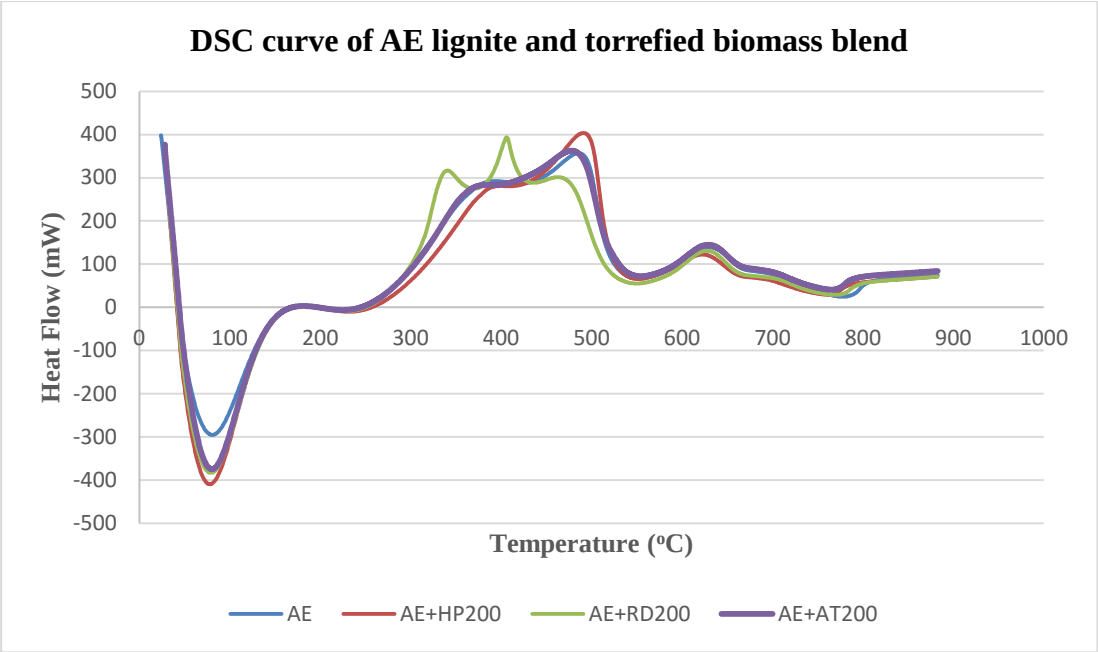

Figure A.31 : DSC curve of AE lignite and torrefied biomass blend.

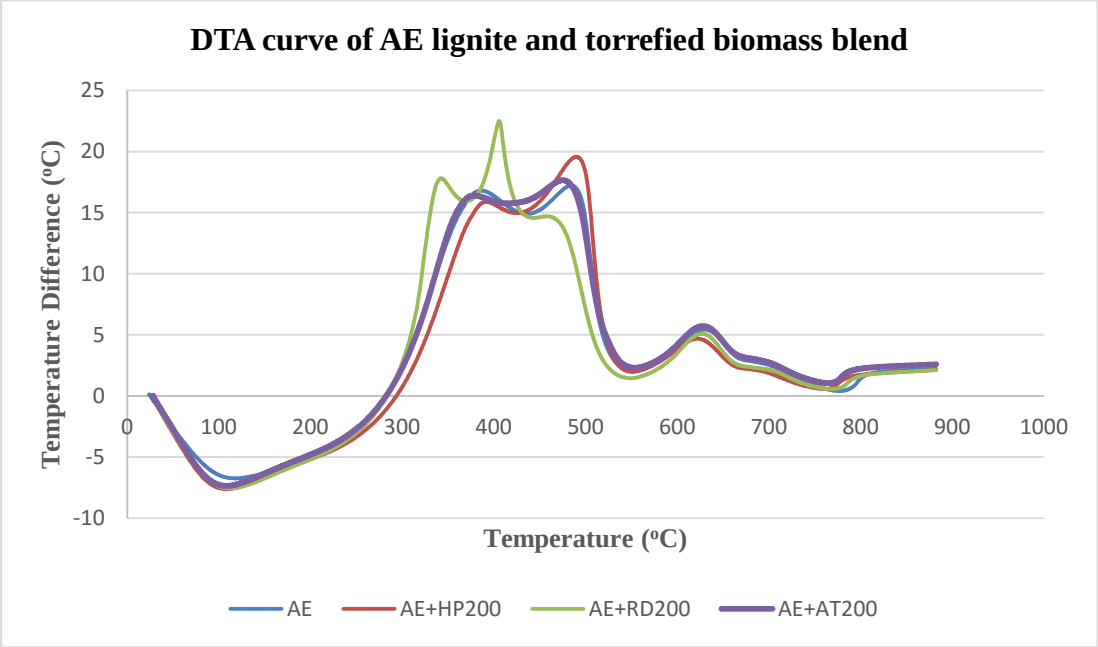

Figure A.32 : DTA curve of AE lignite and torrefied biomass blend.

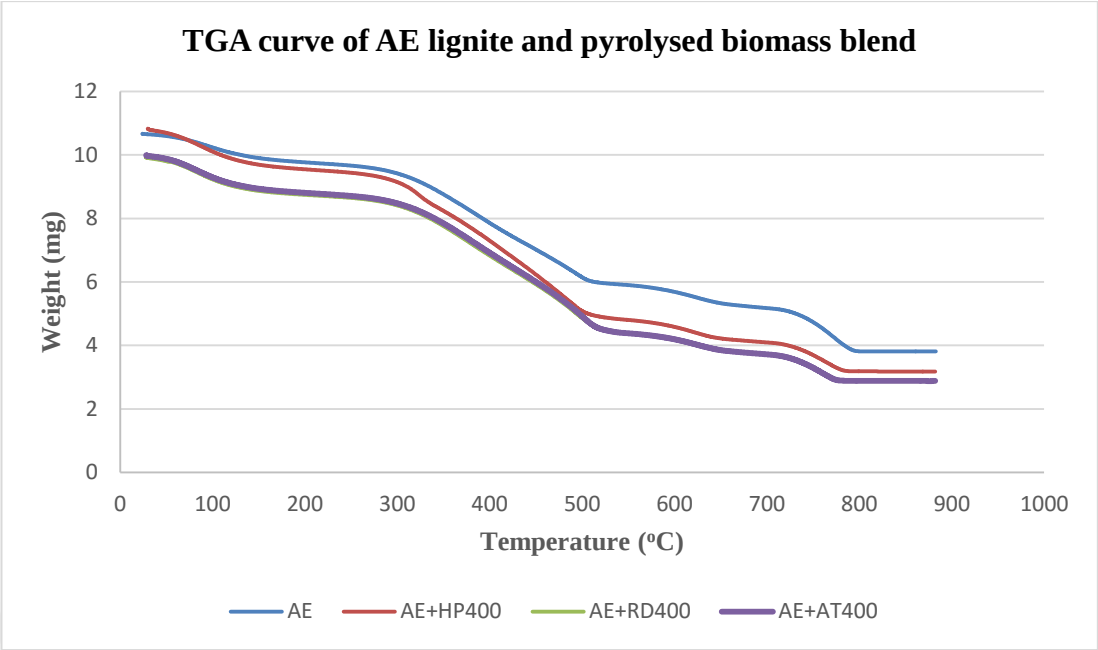

Figure A.33 : TGA curve of AE lignite and pyrolysed biomass blend.

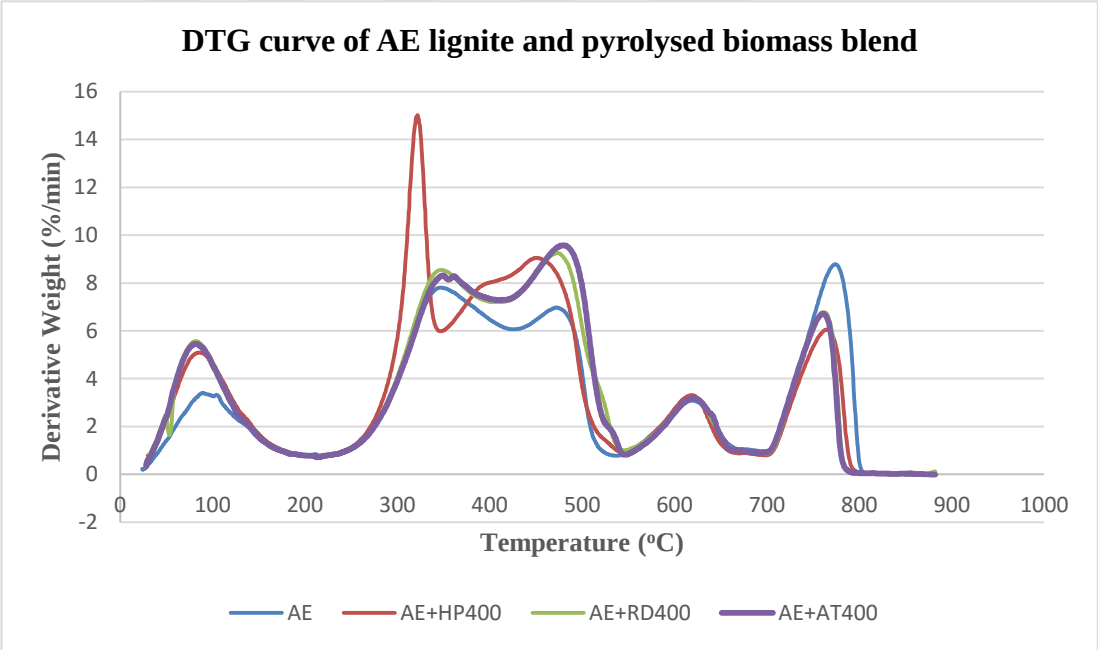

Figure A.34 : DTG curve of AE lignite and pyrolysed biomass blend.

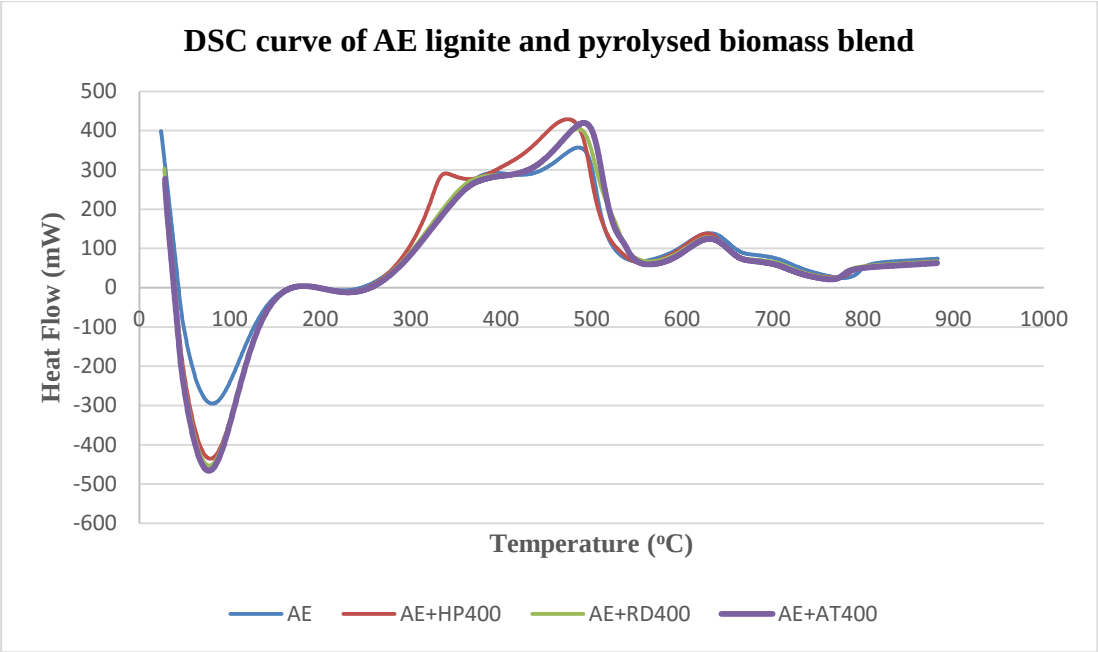

Figure A.35 : DSC curve of AE lignite and pyrolysed biomass blend.

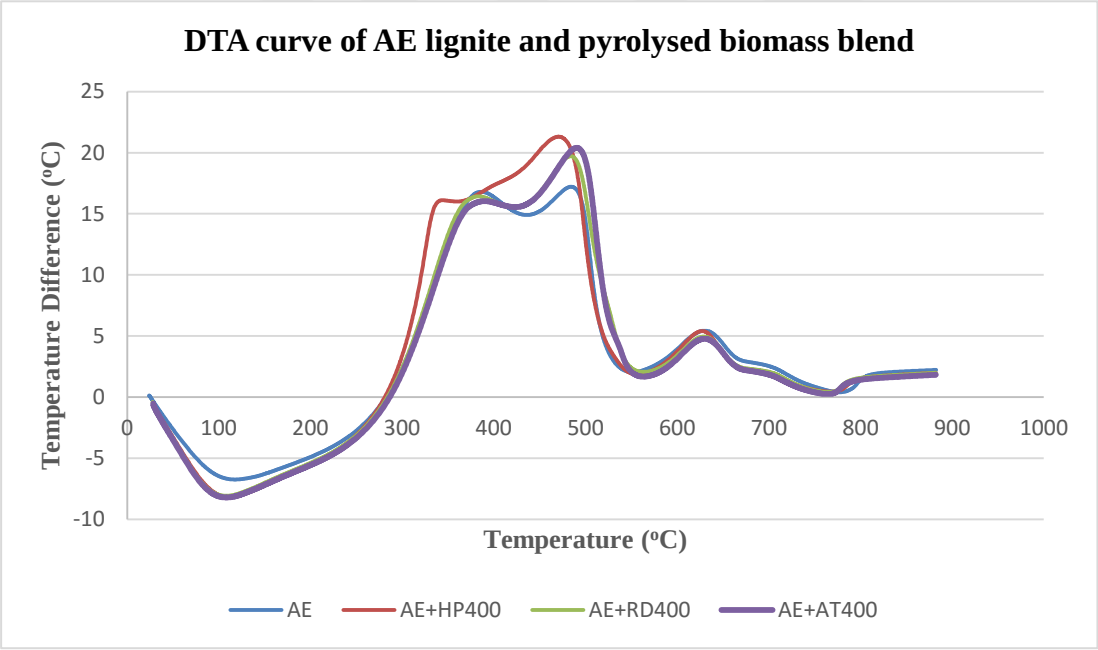

Figure A.36 : DTA curve of AE lignite and pyrolysed biomass blend.

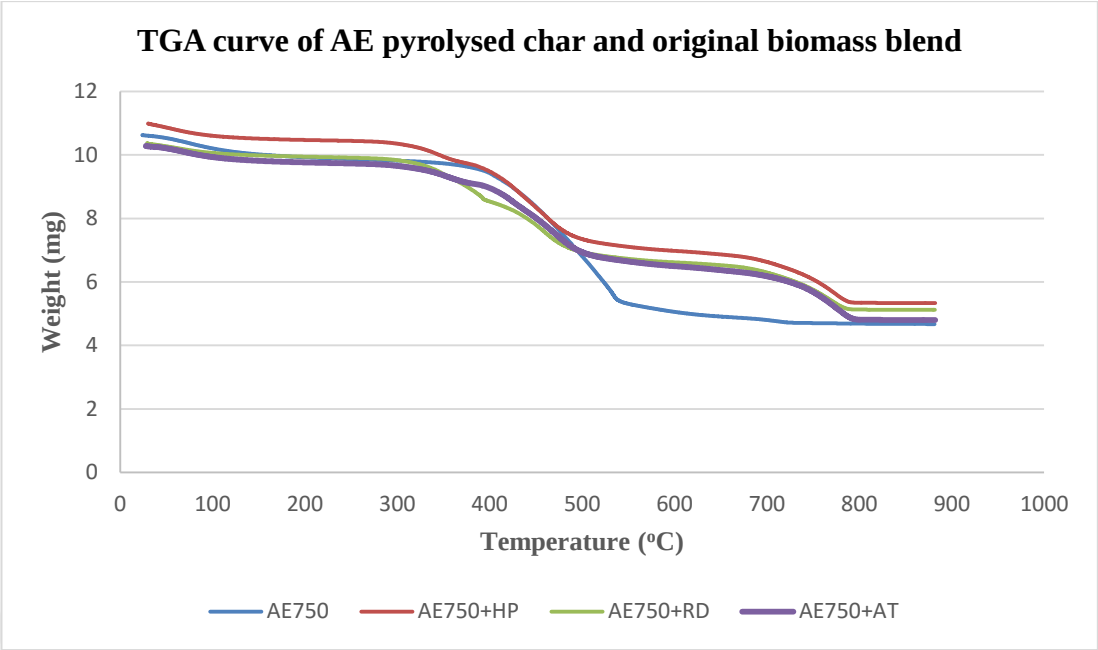

Figure A.37 : TGA curve of AE pyrolysed char and original biomass blend.

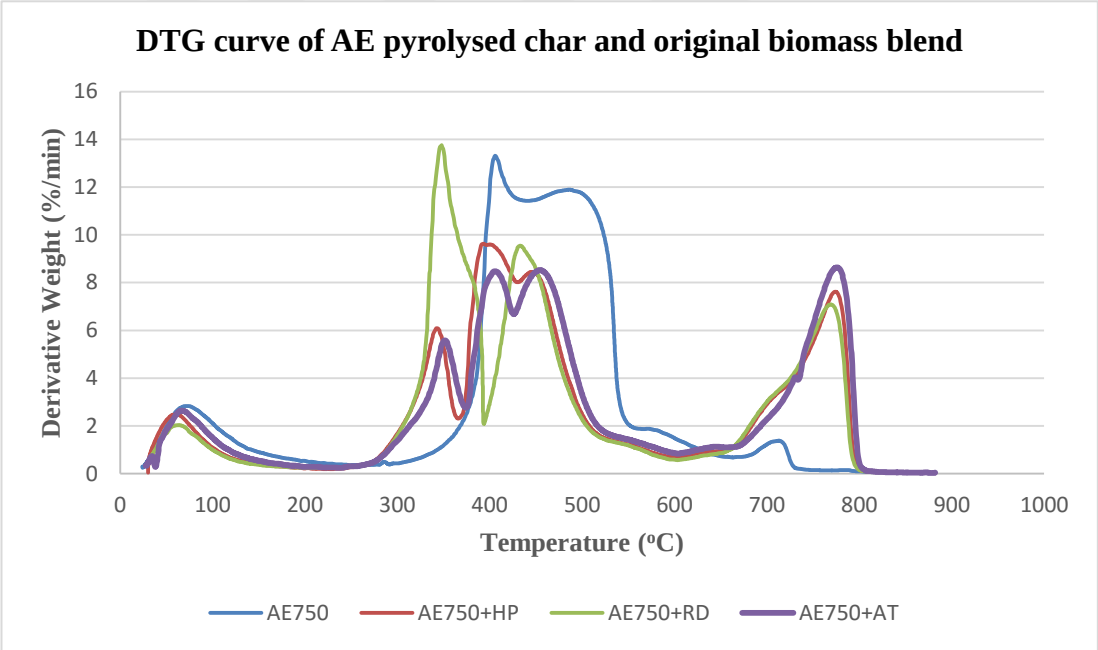

Figure A.38 : DTG curve of AE pyrolysed char and original biomass blend.

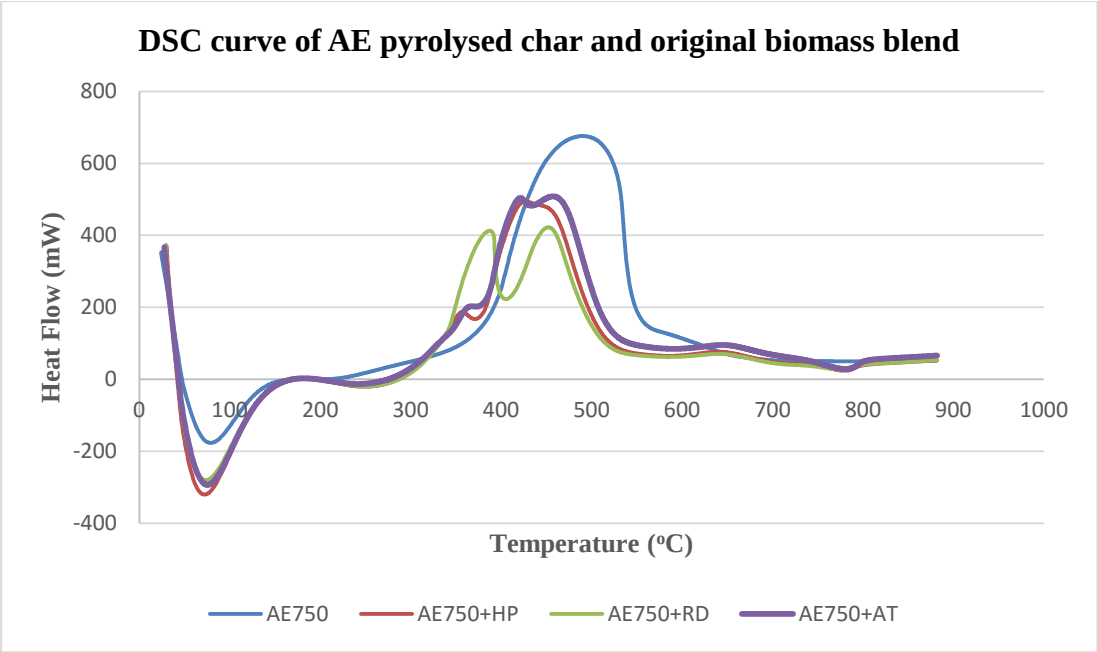

Figure A.39 : DSC curve of AE pyrolysed char and original biomass blend.

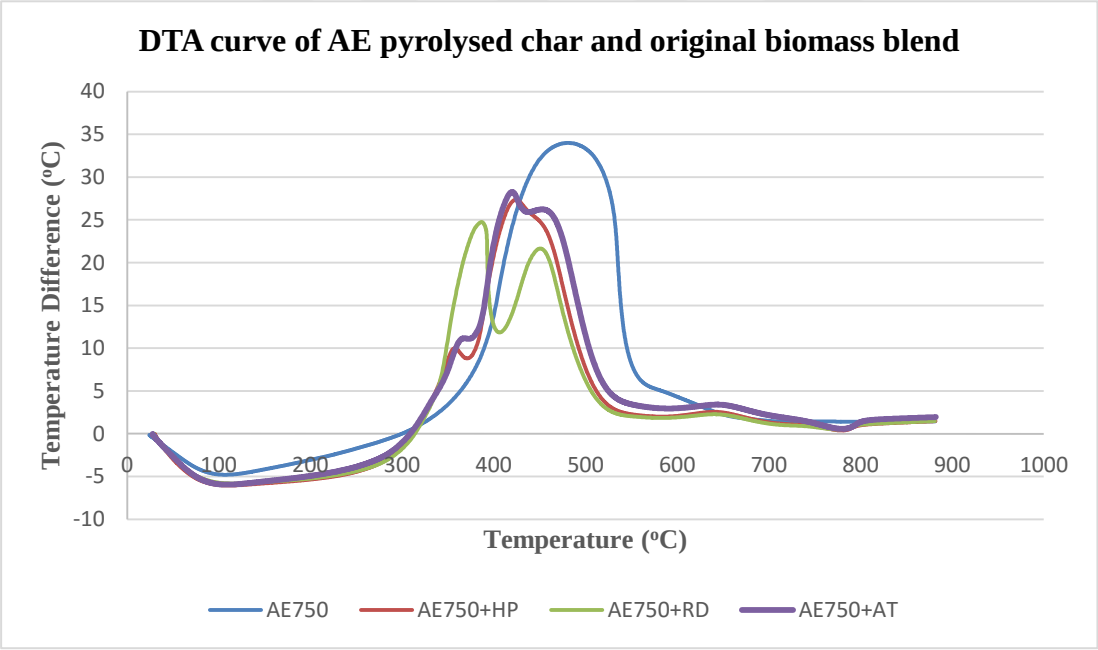

Figure A.40 : DTA curve of AE pyrolysed char and original biomass blend.

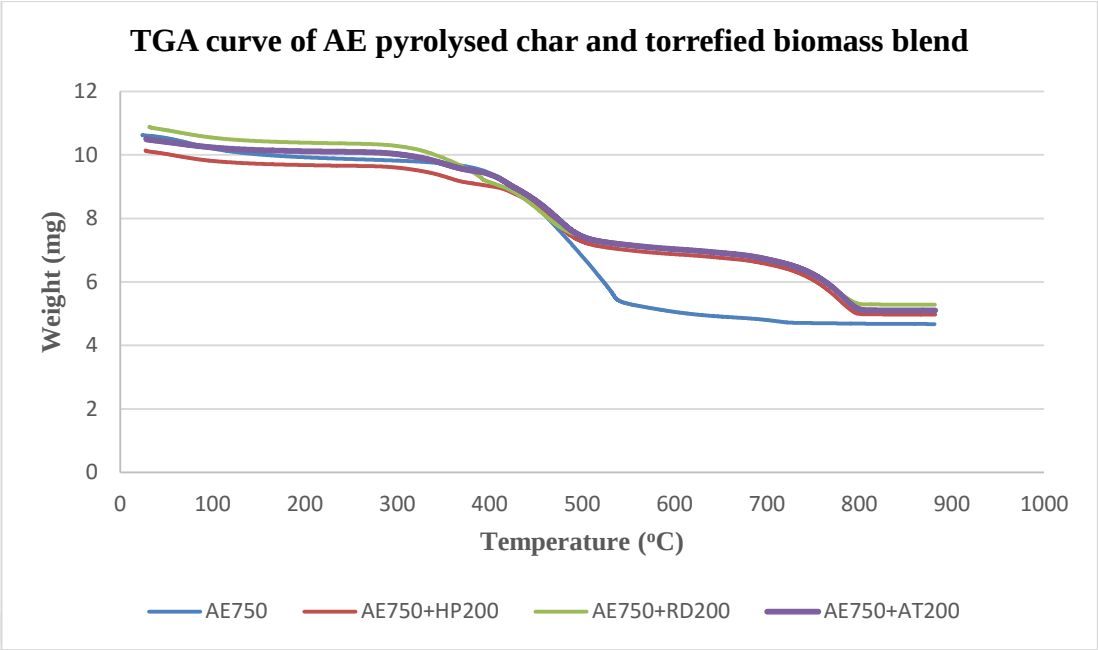

Figure A.41 : TGA curve of AE pyrolysed char and torrefied biomass blend.

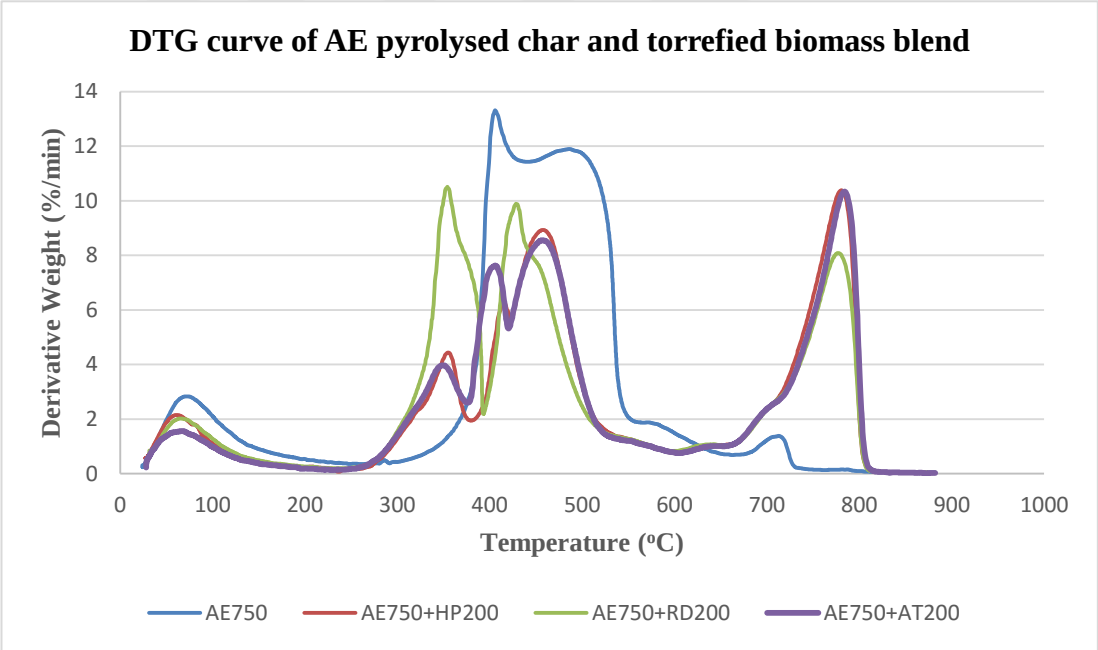

Figure A.42 : DTG curve of AE pyrolysed char and torrefied biomass blend.

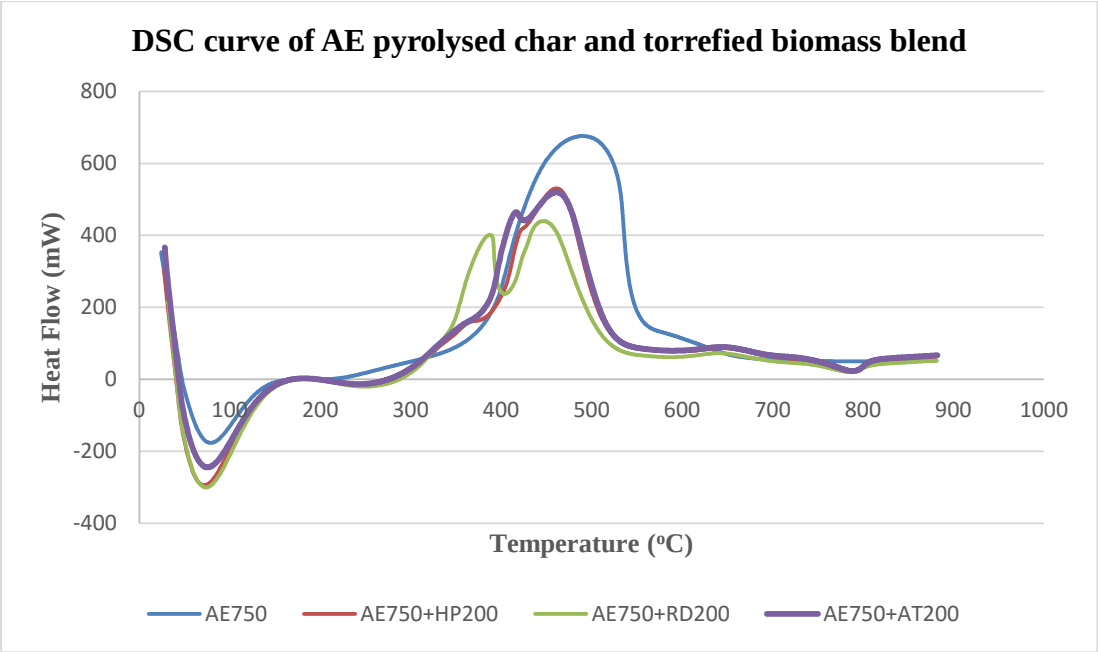

Figure A.43 : DSC curve of AE pyrolysed char and torrefied biomass blend.

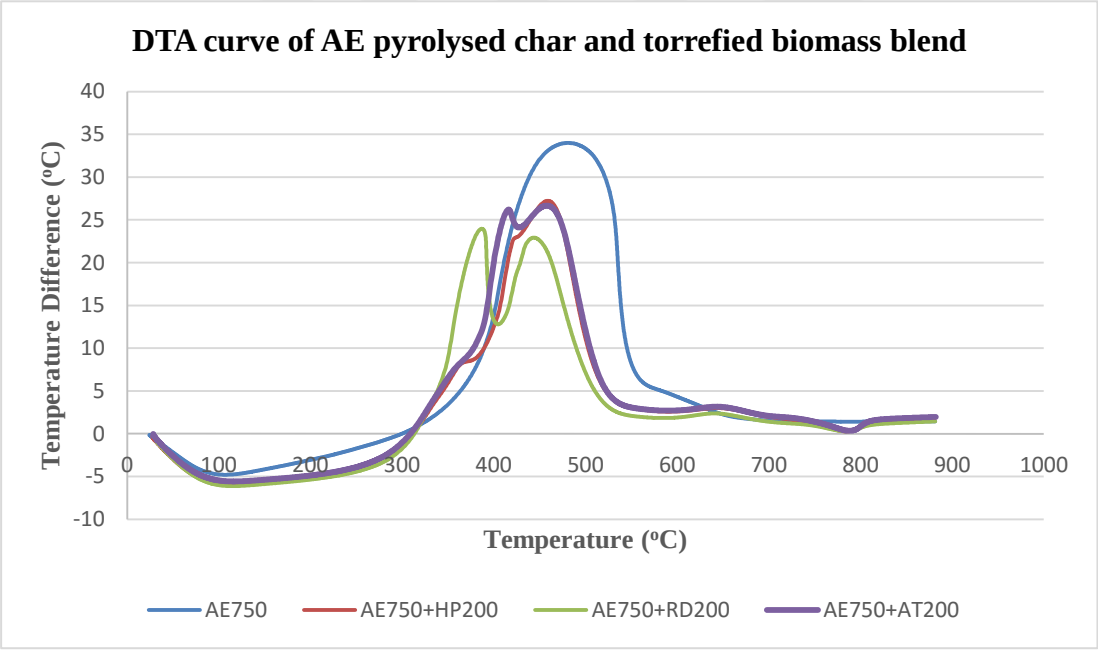

Figure A.44 : DTA curve of AE pyrolysed char and torrefied biomass blend.

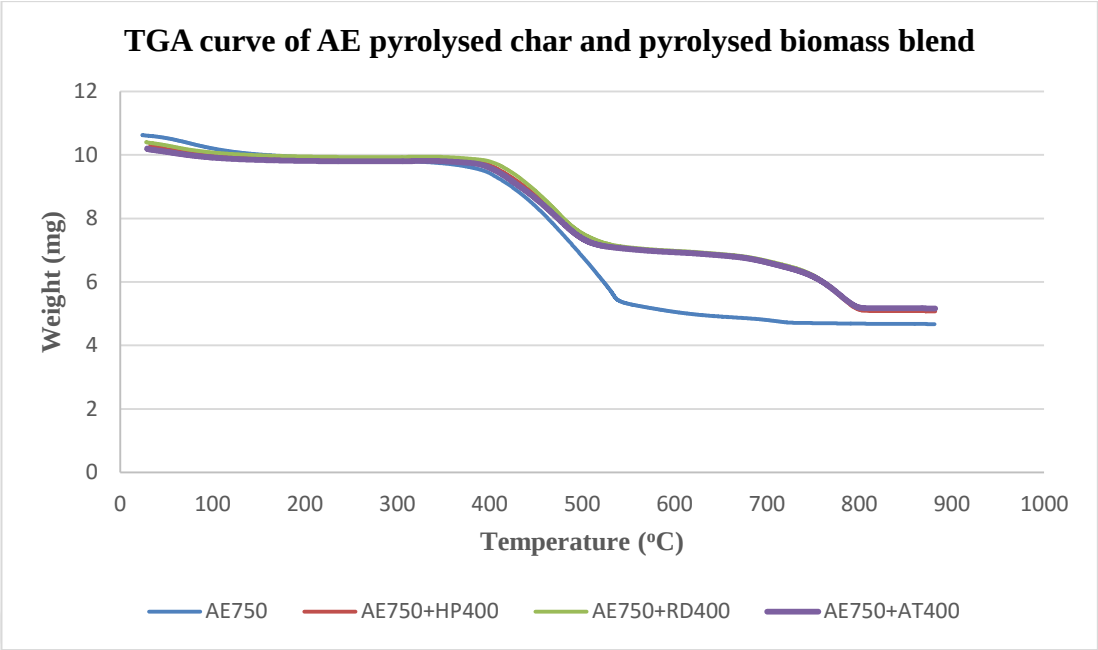

Figure A.45 : TGA curve of AE pyrolysed char and pyrolysed biomass blend.

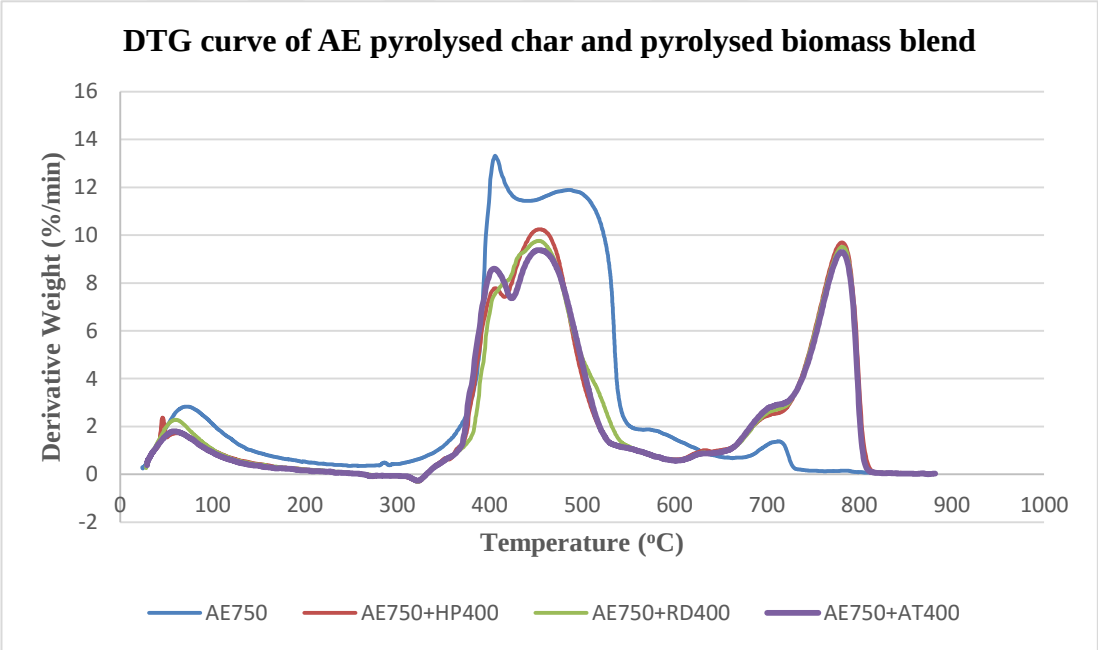

Figure A.46 : DTG curve of AE pyrolysed char and pyrolysed biomass blend.

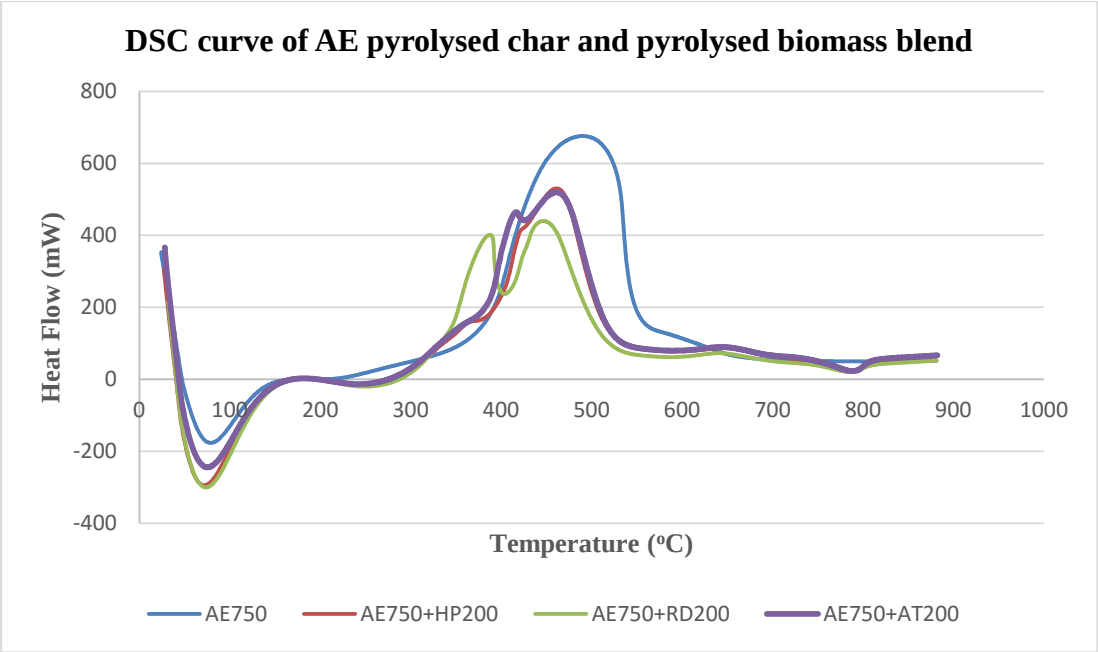

Figure A.47 : DSC curve of AE pyrolysed char and pyrolysed biomass blend.

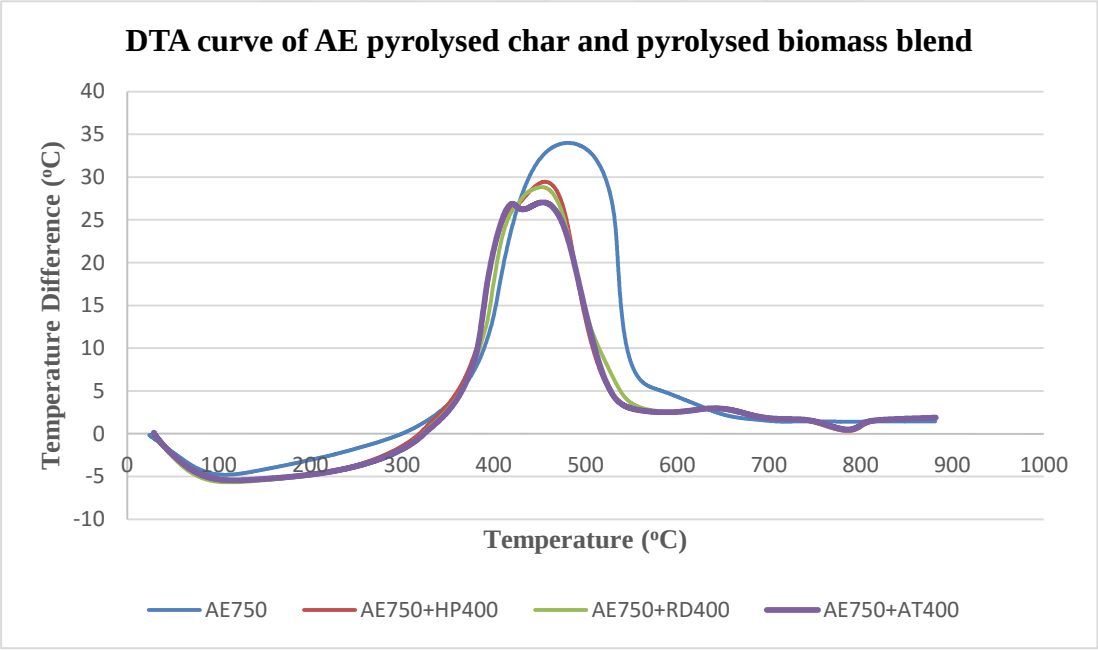

Figure A.48 : DTA curve of AE pyrolysed char and pyrolysed biomass blend.

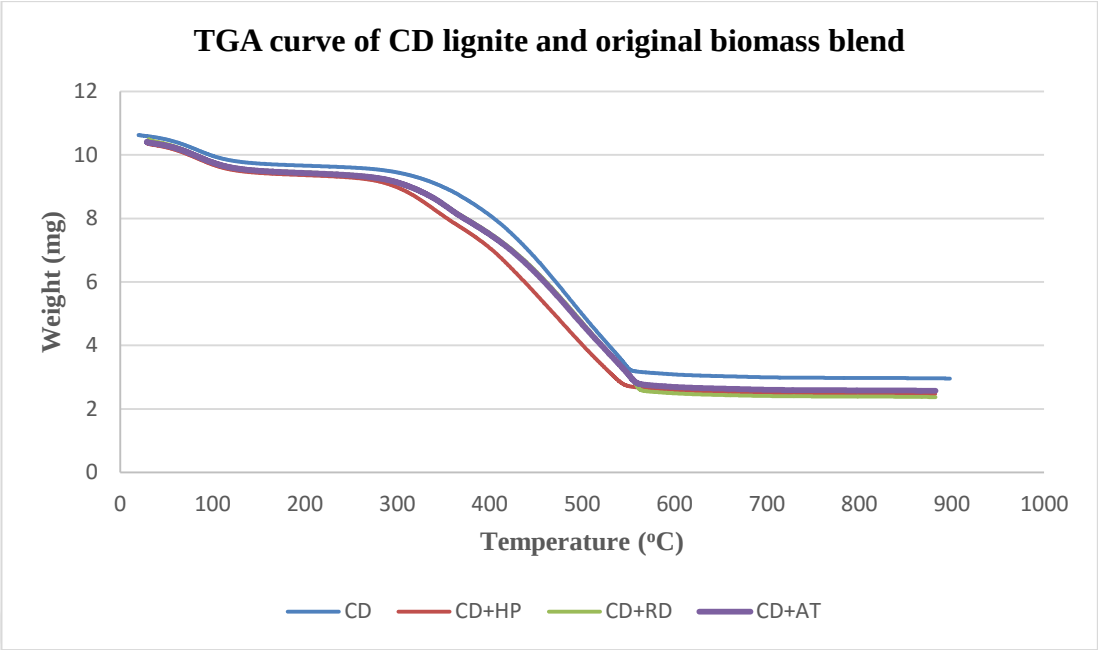

Figure A.49 : TGA curve of CD lignite and original biomass blend.

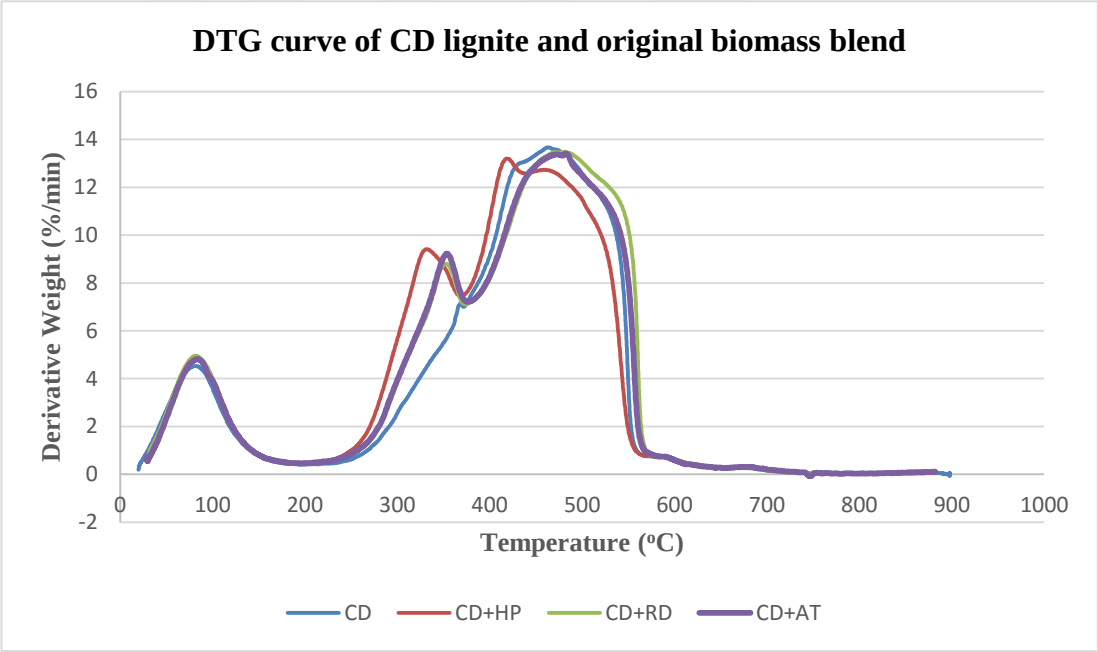

Figure A.50 : DTG curve of CD lignite and original biomass blend.

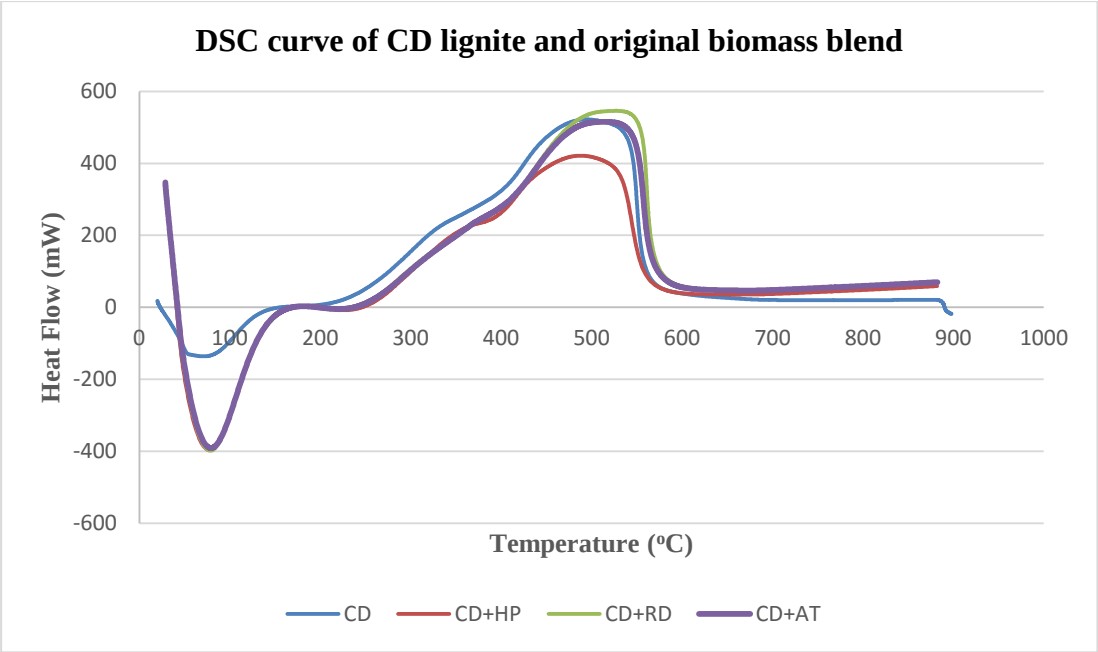

Figure A.51 : DSC curve of CD lignite and original biomass blend.

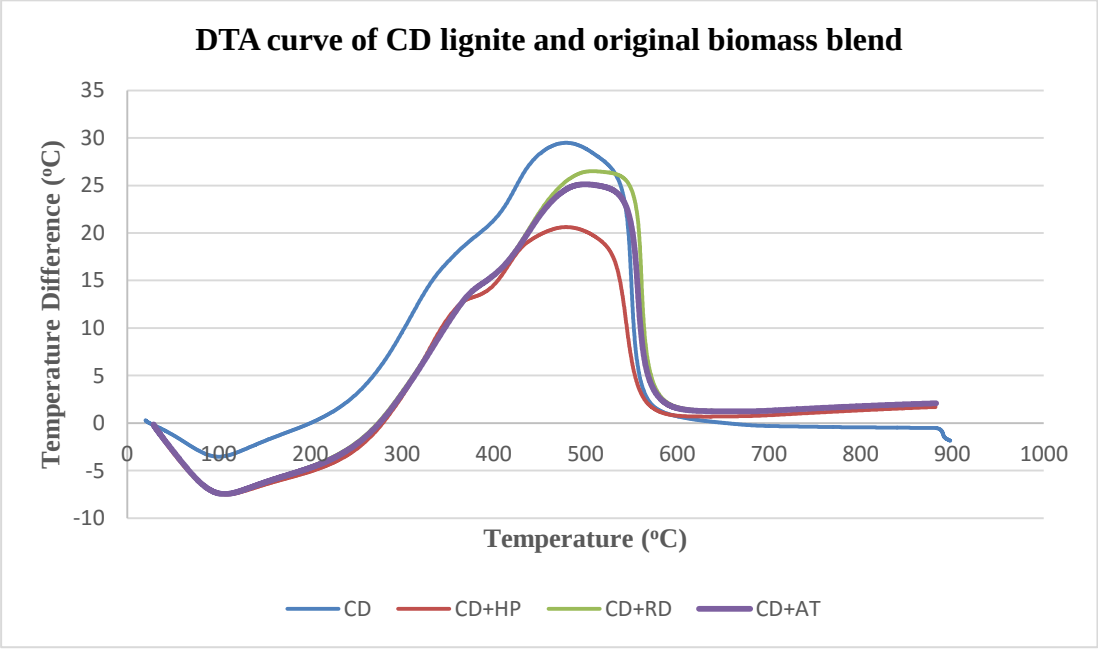

Figure A.52 : DTA curve of CD lignite and original biomass blend.

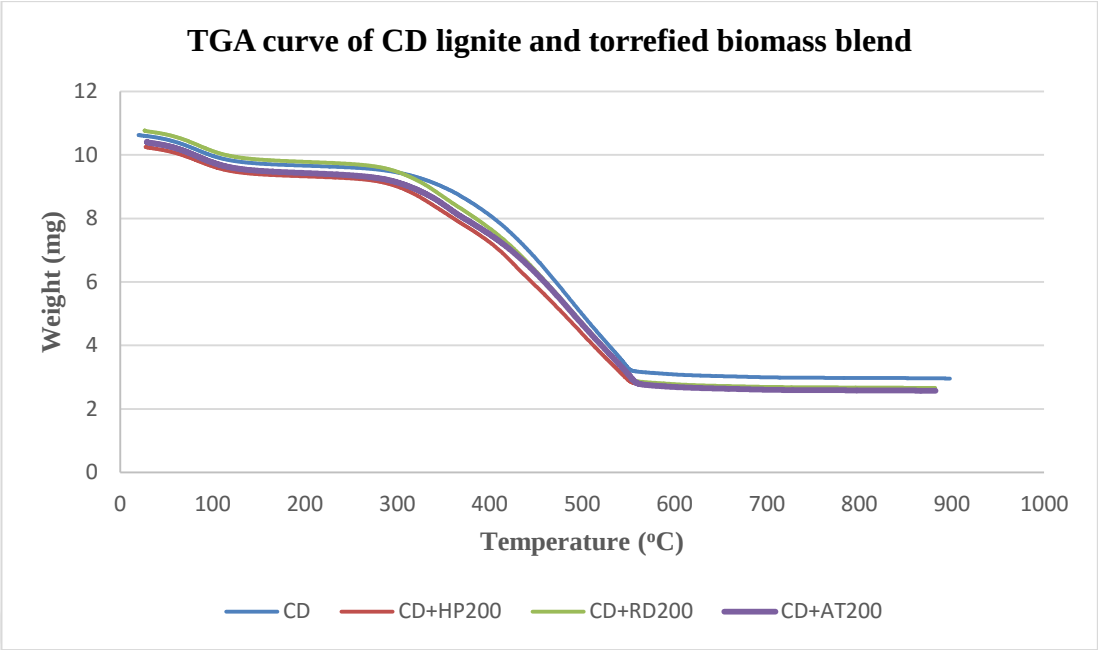

Figure A.53 : TGA curve of CD lignite and torrefied biomass blend.

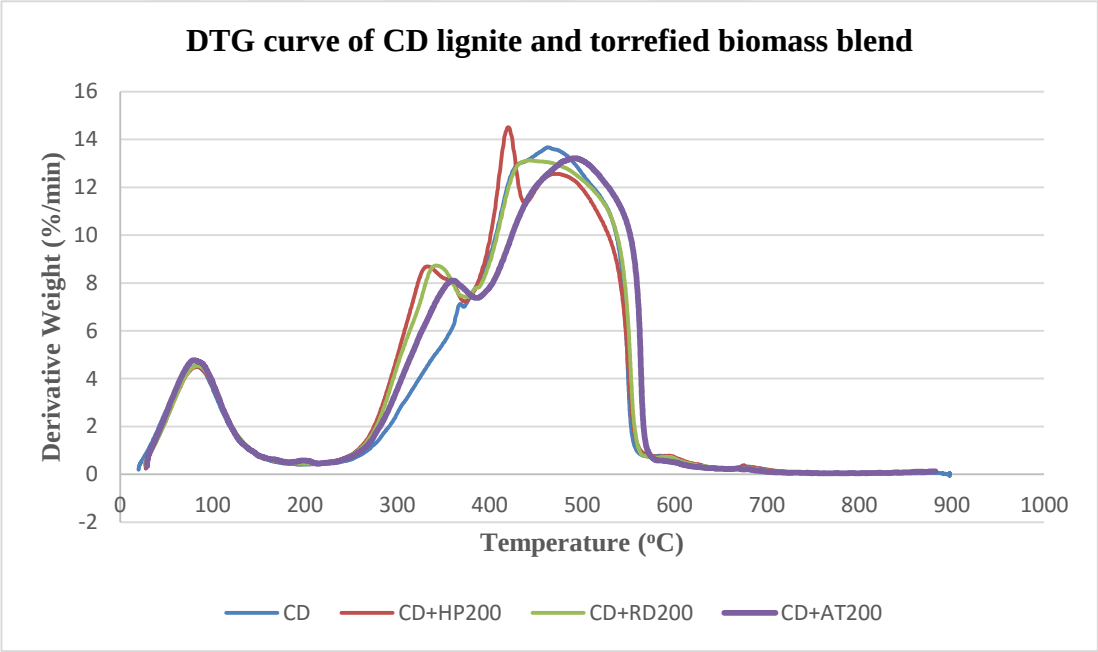

Figure A.54 : DTG curve of CD lignite and torrefied biomass blend.

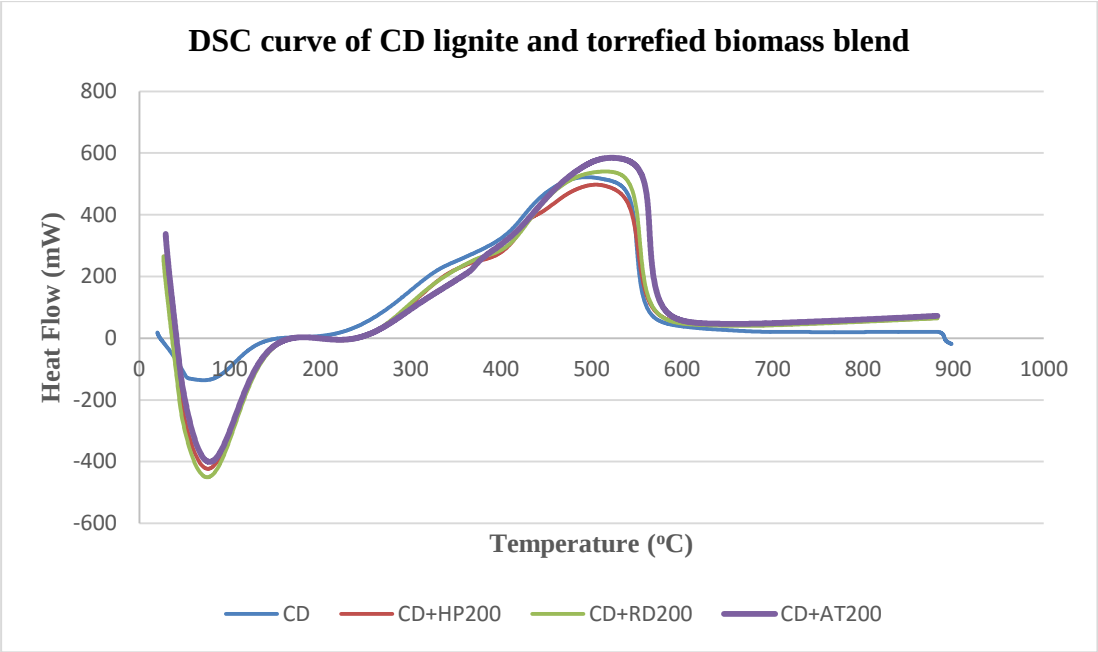

Figure A.55 : DSC curve of CD lignite and torrefied biomass blend.

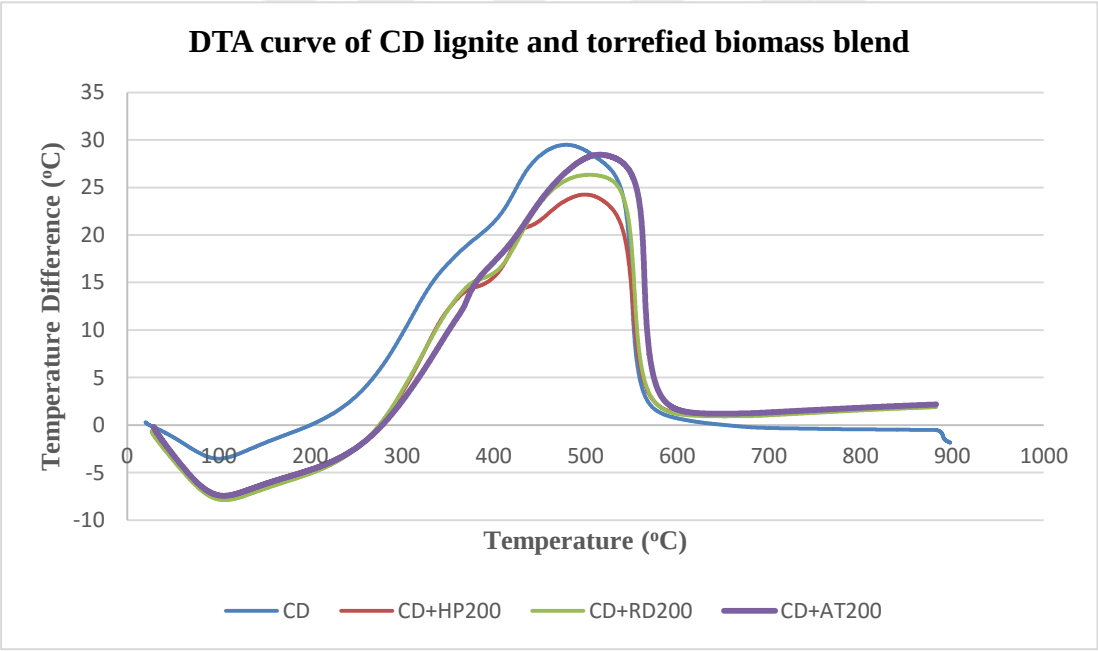

Figure A.56 : DTA curve of CD lignite and torrefied biomass blend.

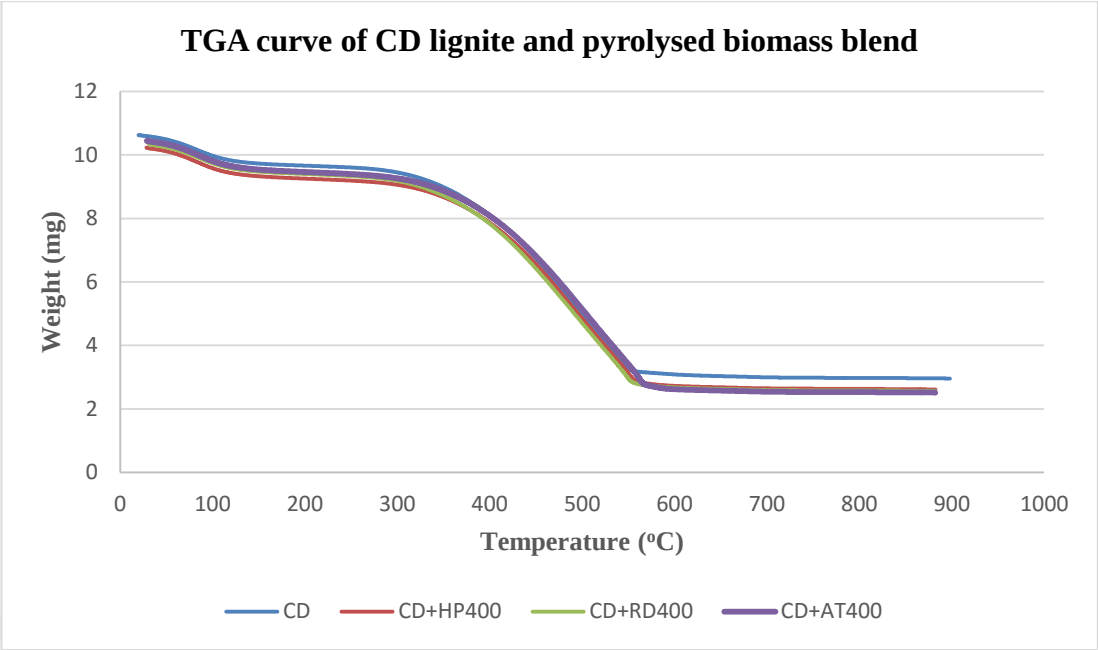

Figure A.57 : TGA curve of CD lignite and pyrolysed biomass blend.

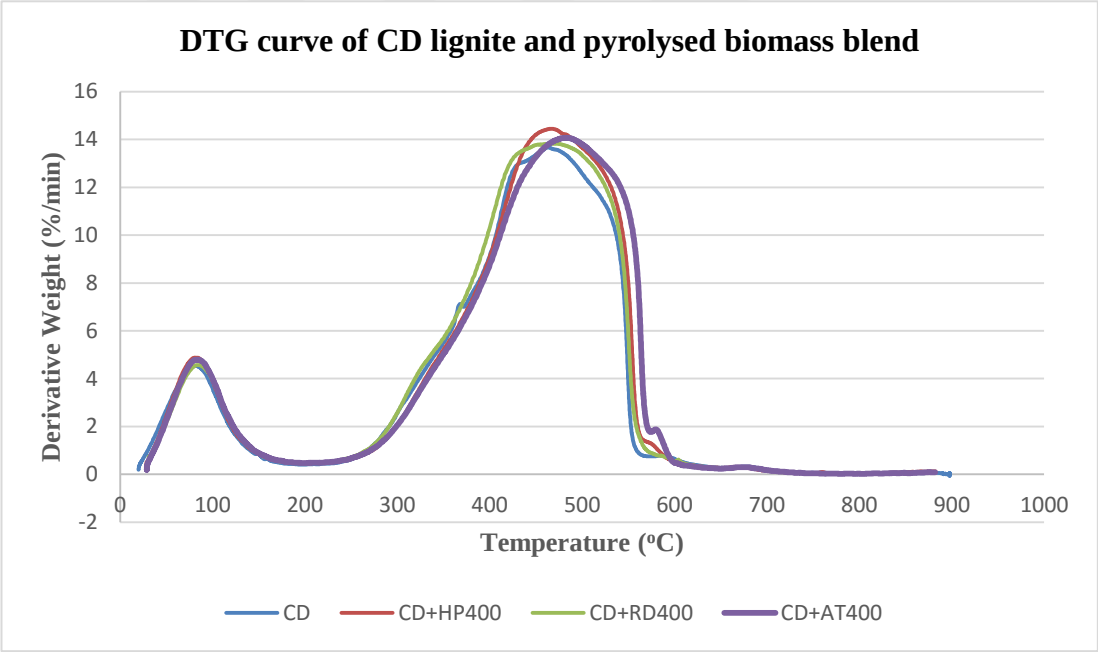

Figure A.58 : DTG curve of CD lignite and pyrolysed biomass blend.

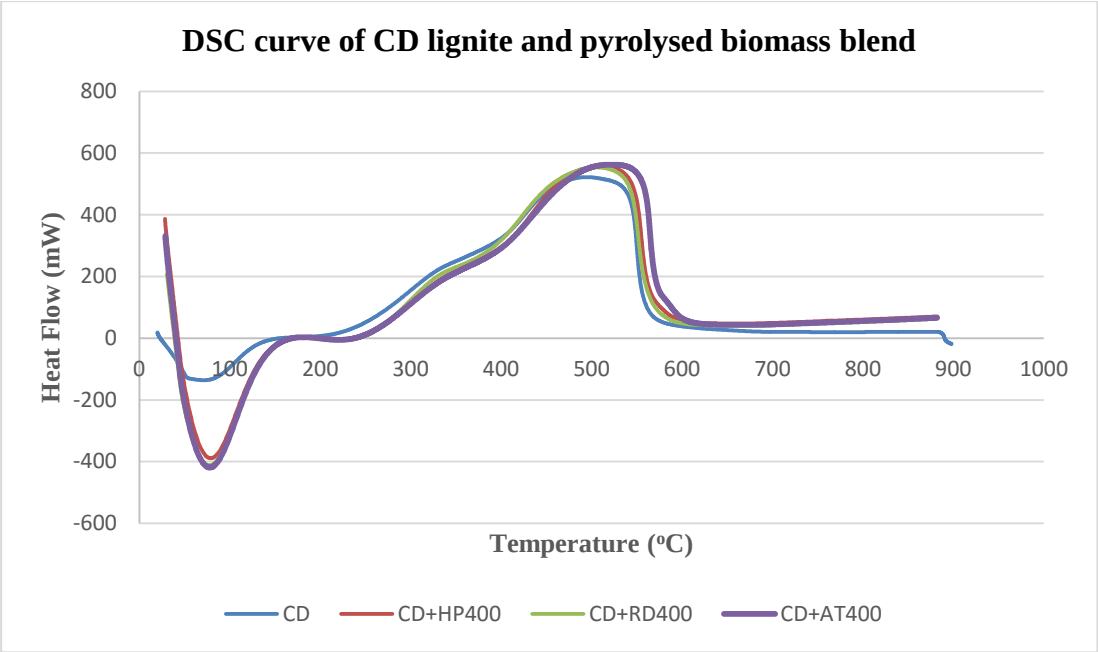

Figure A.59 : DSC curve of CD lignite and pyrolysed biomass blend.

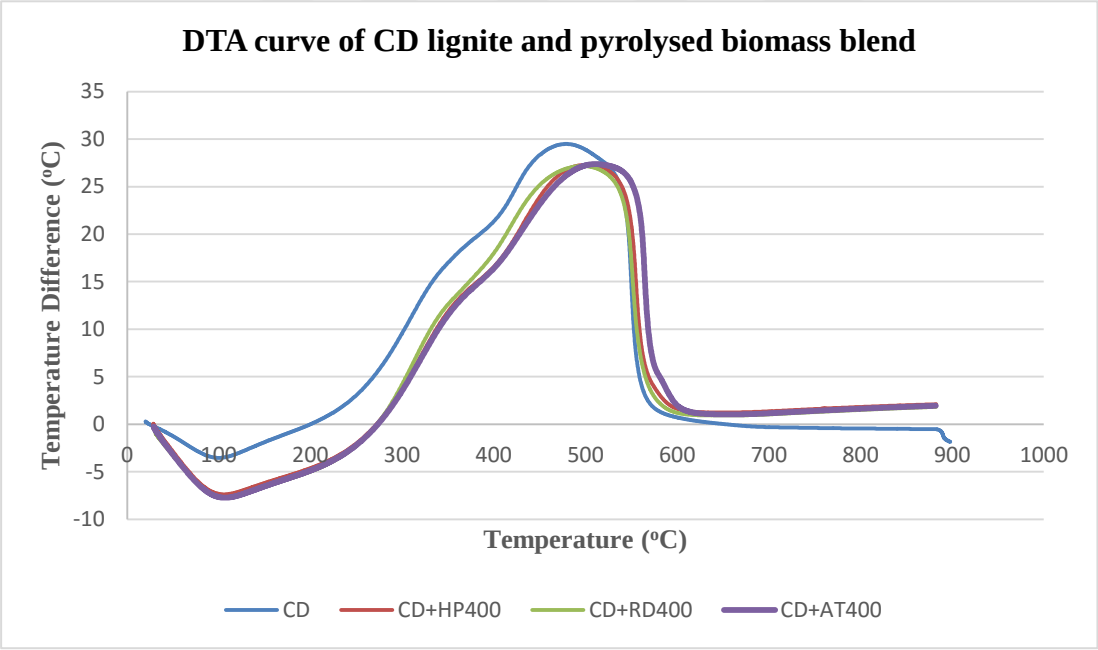

Figure A.60 : DTA curve of CD lignite and pyrolysed biomass blend.

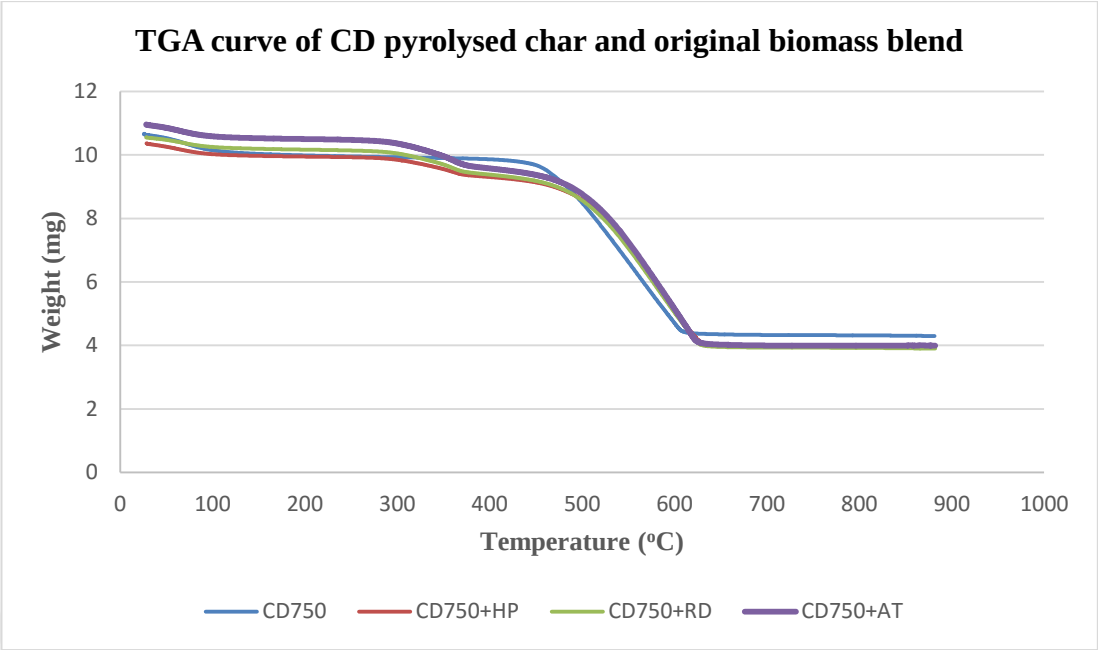

Figure A.61 : TGA curve of CD pyrolysed char and original biomass blend.

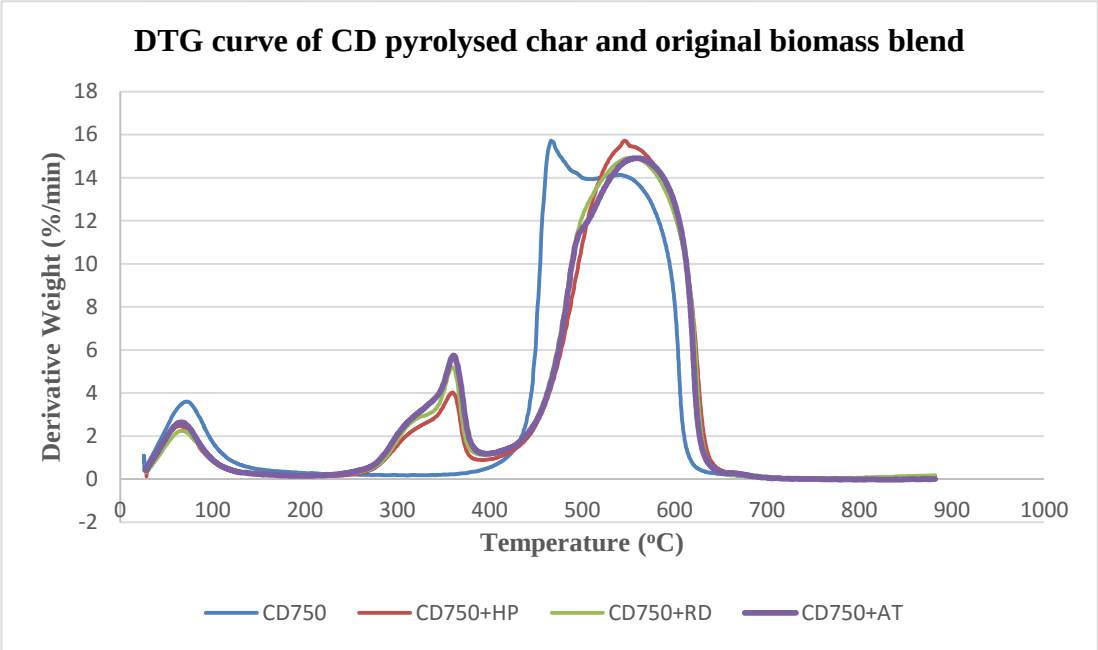

Figure A.62 : DTG curve of CD pyrolysed char and original biomass blend.

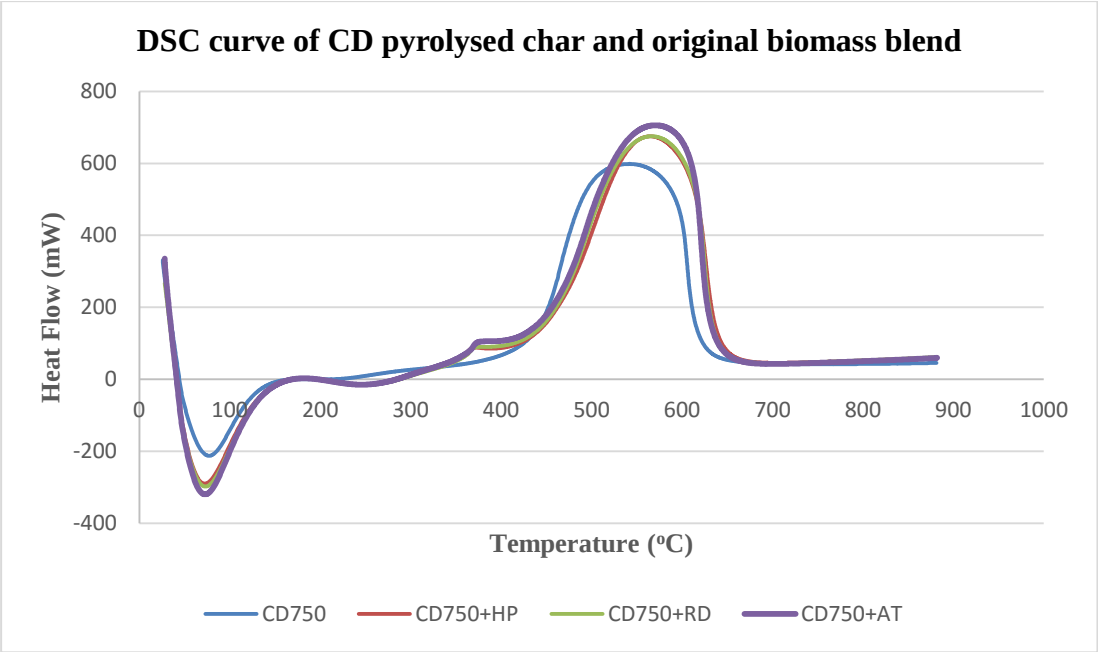

Figure A.63 : DSC curve of CD pyrolysed char and original biomass blend.

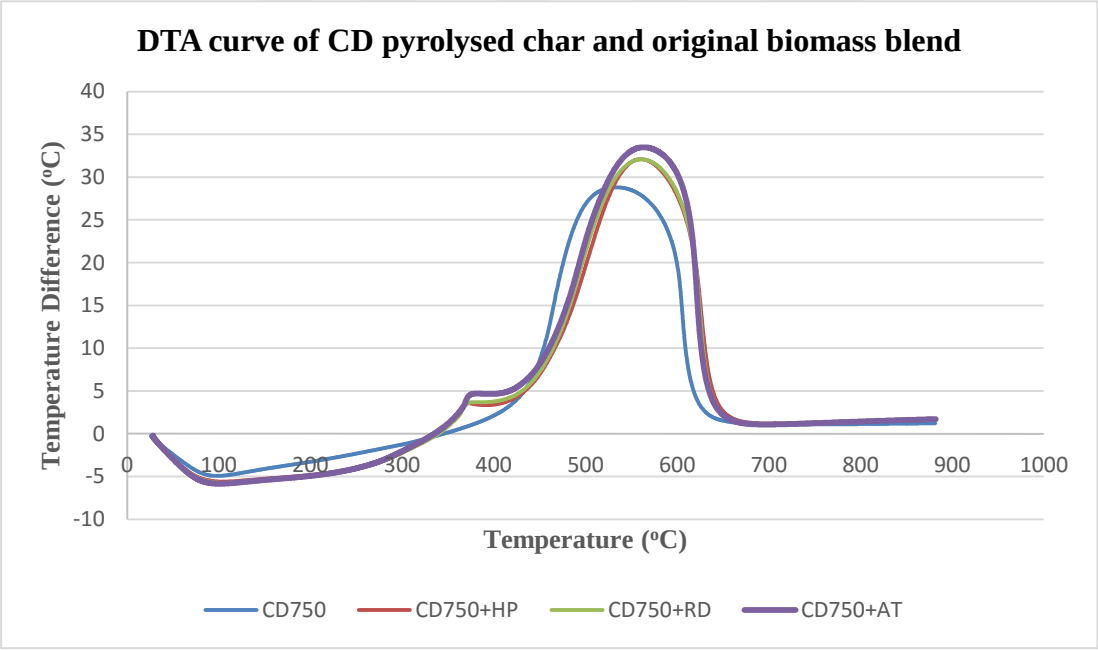

Figure A.64 : DTA curve of CD pyrolysed char and original biomass blend.

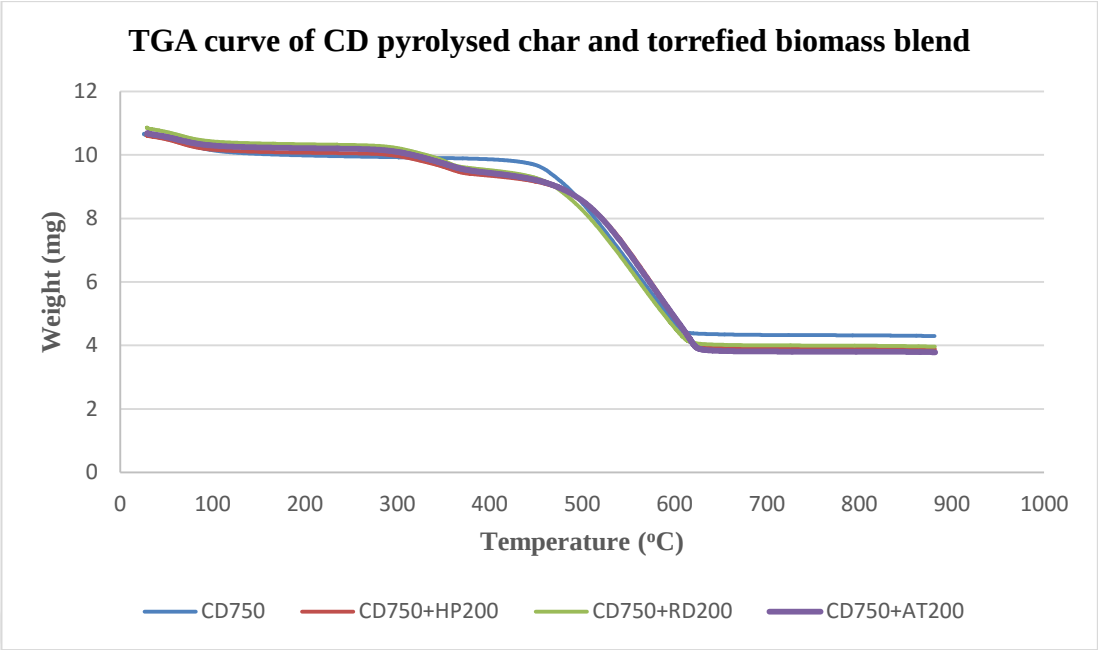

Figure A.65 : TGA curve of CD pyrolysed char and torrefied biomass blend.

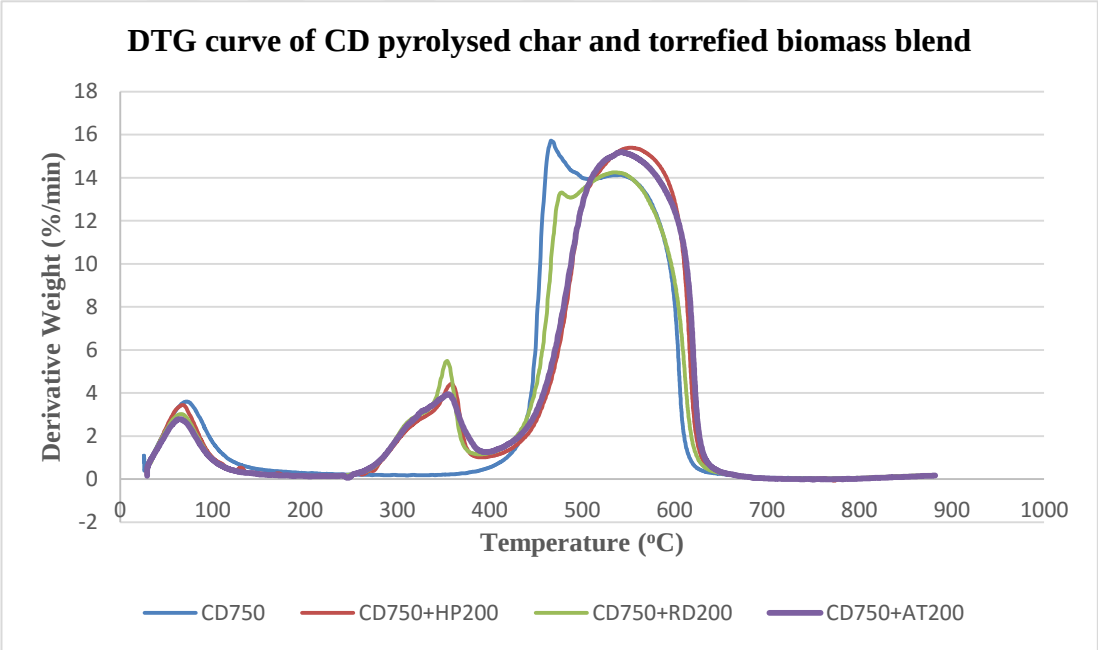

Figure A.66 : DTG curve of CD pyrolysed char and torrefied biomass blend.

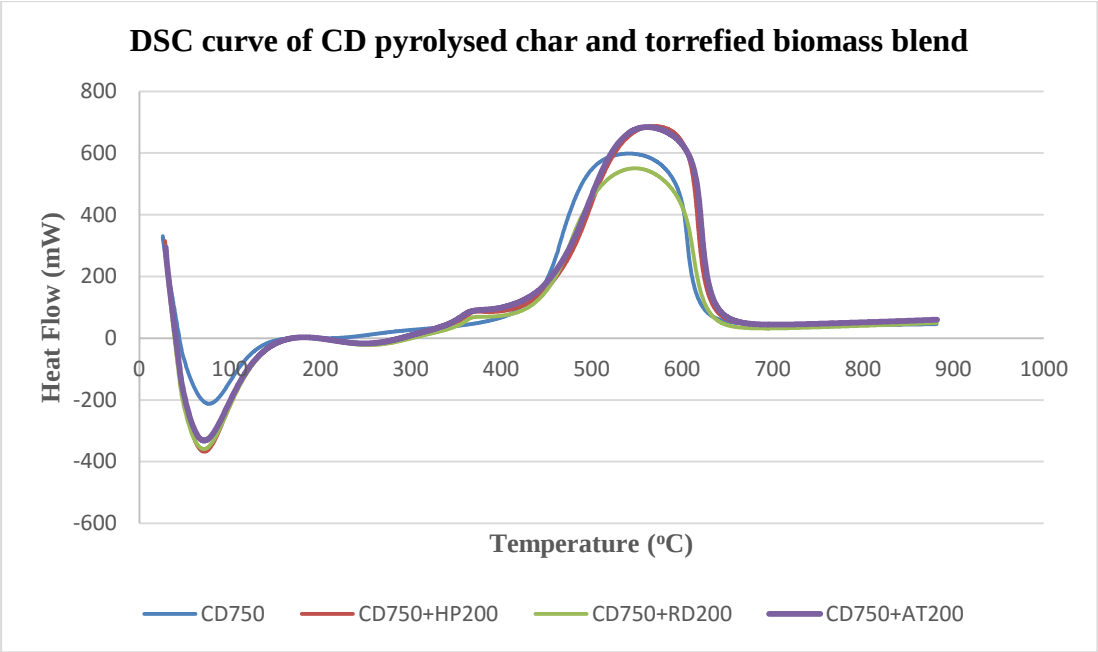

Figure A.67 : DSC curve of CD pyrolysed char and torrefied biomass blend.

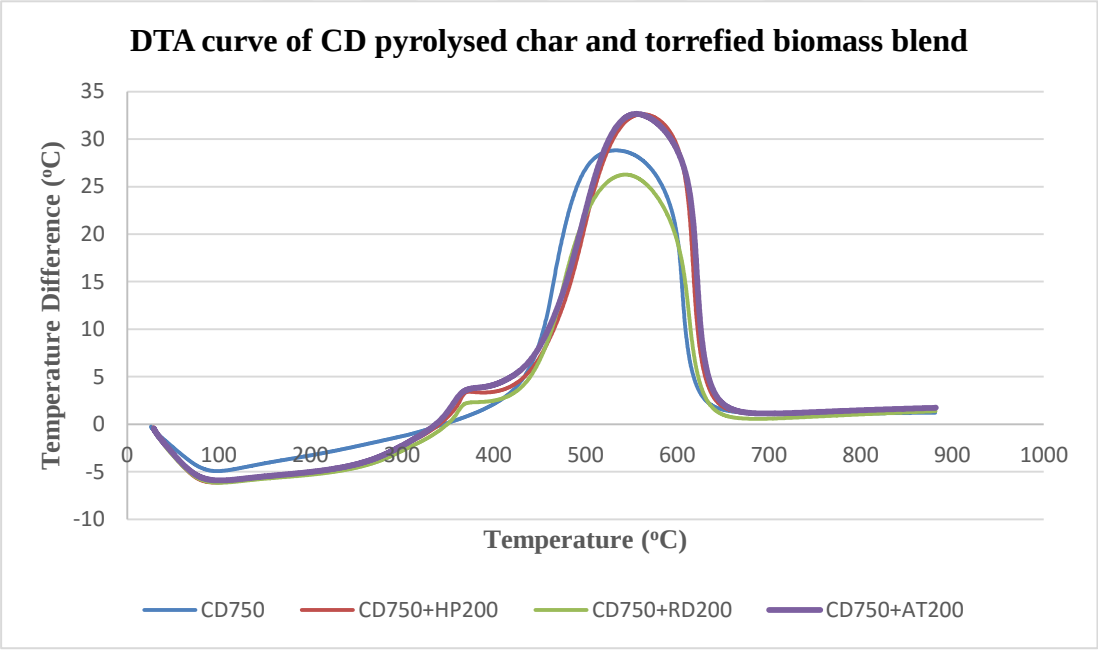

Figure A.68 : DTA curve of CD pyrolysed char and torrefied biomass blend.

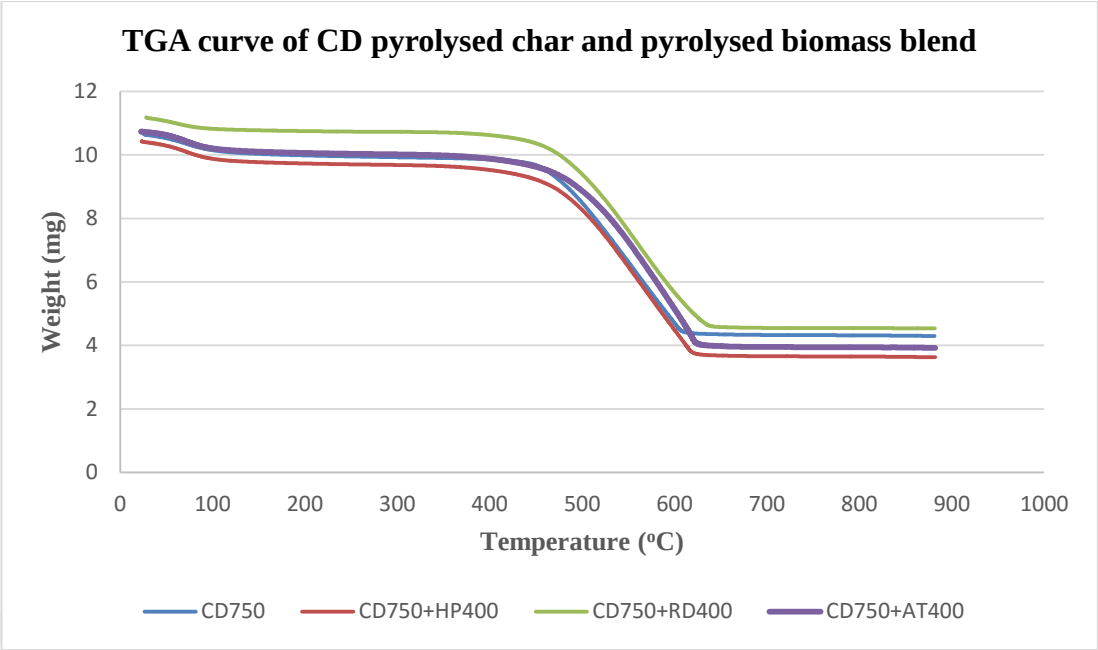

Figure A.69 : TGA curve of CD pyrolysed char and pyrolysed biomass blend.

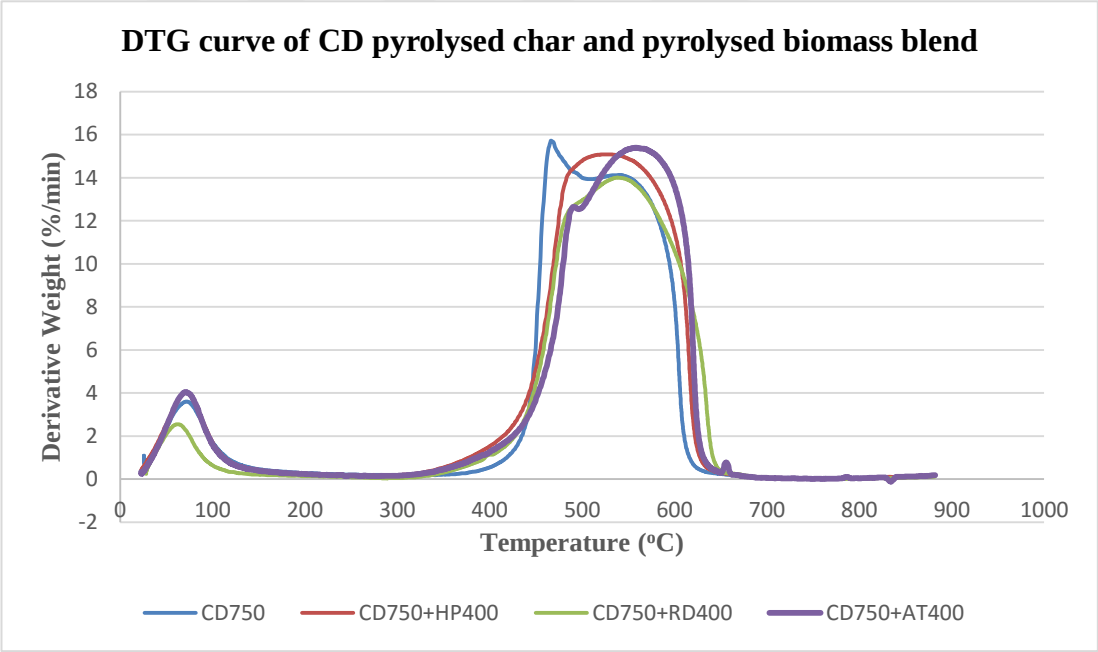

Figure A.70 : DTG curve of CD pyrolysed char and pyrolysed biomass blend.

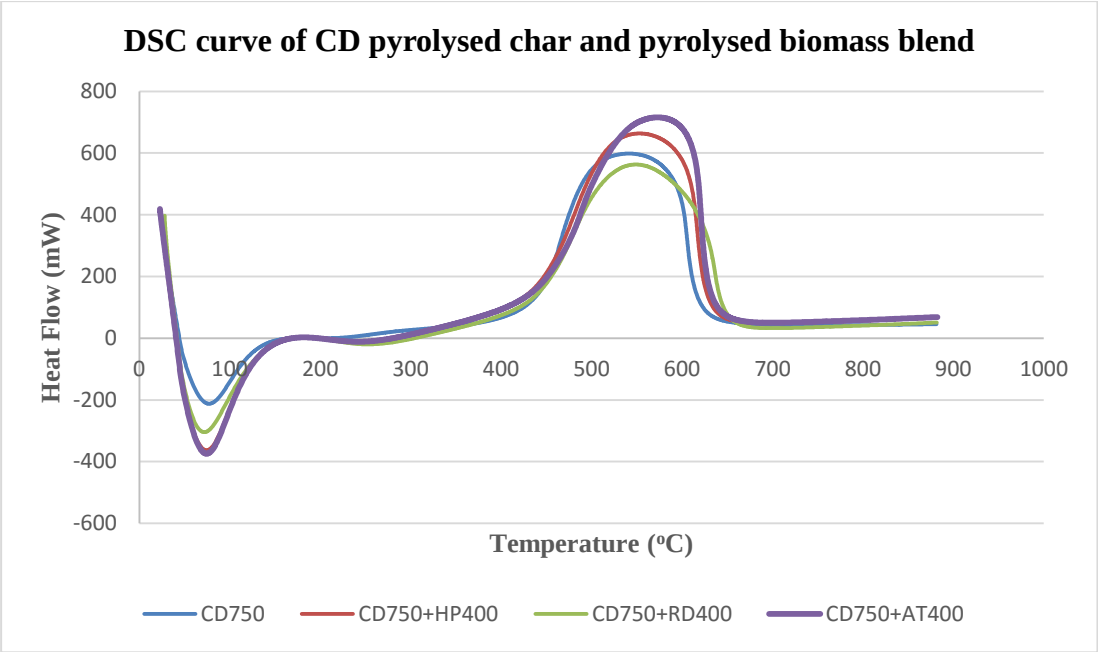

Figure A.71 : DSC curve of CD pyrolysed char and pyrolysed biomass blend.

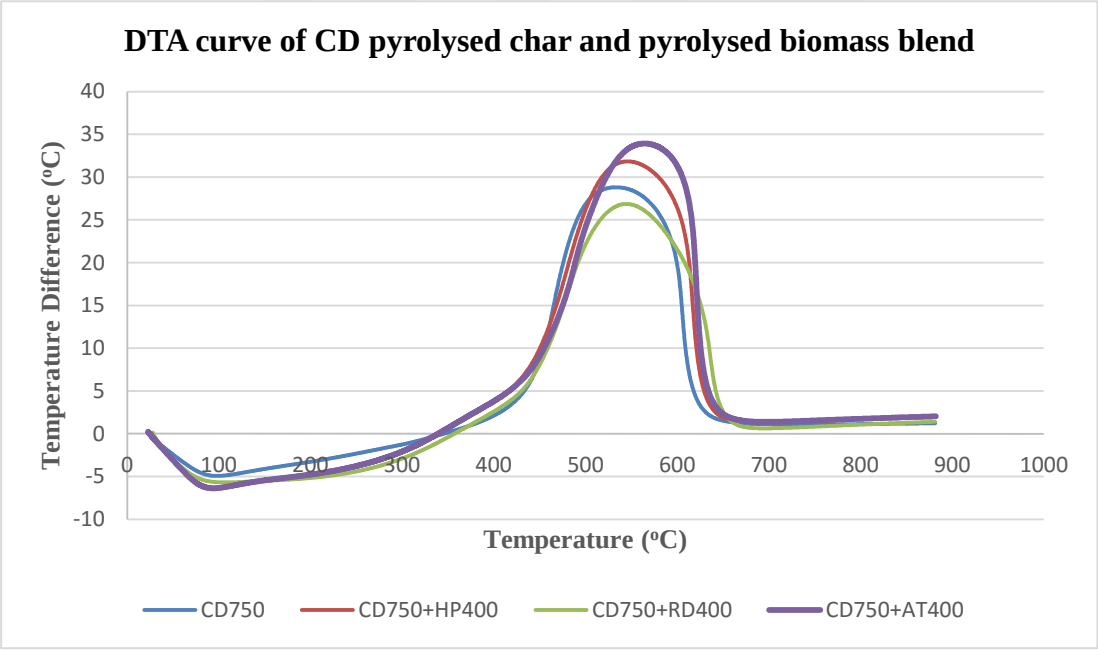

Figure A.72 : DTA curve of CD pyrolysed char and pyrolysed biomass blend.

CURRICULUM VITAE

Name Surname **:** Ayşen ÇALIŞKAN SARIKAYA

Place and Date of Birth **:** BULGARY / 19.12.1990

E-Mail **:** aysen.caliskan@hotmail.com

EDUCATION:

- **B.Sc.** **:** 2014, Istanbul Technical University, Chemical and Metallurgical Engineering Faculty, Chemical Engineering Department